

AD

USAAMRDL TECHNICAL REPORT 72-47

EXPENDABLE MAIN ROTOR BLADE STUDY

By

John A. Longobardi
Everett Fournier

DATA QUALITY INDEXED 4

19960328 088 April 1973

EUSTIS DIRECTORATE
U. S. ARMY AIR MOBILITY RESEARCH AND DEVELOPMENT LABORATORY
FORT EUSTIS, VIRGINIA

CONTRACT DAAJ02-71-C-0046
SIKORSKY AIRCRAFT
DIVISION OF UNITED AIRCRAFT CORPORATION
STRATFORD, CONNECTICUT

Approved for public release;
distribution unlimited.



L1461

DISCLAIMERS

The findings in this report are not to be construed as an official Department of the Army position unless so designated by other authorized documents.

When Government drawings, specifications, or other data are used for any purpose other than in connection with a definitely related Government procurement operation, the United States Government thereby incurs no responsibility nor any obligation whatsoever; and the fact that the Government may have formulated, furnished, or in any way supplied the said drawings, specifications, or other data is not to be regarded by implication or otherwise as in any manner licensing the holder or any other person or corporation, or conveying any rights or permission, to manufacture, use, or sell any patented invention that may in any way be related thereto.

Trade names cited in this report do not constitute an official endorsement or approval of the use of such commercial hardware or software.

DISPOSITION INSTRUCTIONS

Destroy this report when no longer needed. Do not return it to the originator.

DISCLAIMER NOTICE



**THIS DOCUMENT IS BEST
QUALITY AVAILABLE. THE
COPY FURNISHED TO DTIC
CONTAINED A SIGNIFICANT
NUMBER OF PAGES WHICH DO
NOT REPRODUCE LEGIBLY.**



DEPARTMENT OF THE ARMY
U. S. ARMY AIR MOBILITY RESEARCH & DEVELOPMENT LABORATORY
EUSTIS DIRECTORATE
FORT EUSTIS, VIRGINIA 23604

This is one of a number of parallel studies examining various rotor blade design concepts emphasizing reliability and maintainability. Other concepts that have been studied are repairable and sectionalized rotor blade designs. A parallel expendable rotor blade study has been performed by Kaman Aerospace Corporation. These design studies are aimed at achieving considerable improvement in rotor blade R&M characteristics, thereby reducing life-cycle cost. To achieve comparability, all blade designs are required to match UH-1D/H characteristics, and life-cycle cost is compared to that for the UH-1D/H.

This study concentrated on designing a low-cost rotor blade that is more cost effective to scrap than to return for depot level repair. For the 1972 time frame, a blade with an aluminum extruded spar and honeycomb-filled fiberglass afterbody was the most cost effective configuration considered. Because of the predicted trends in material and labor costs together with the anticipated automated processes for composites, an all-composite configuration with a fiberglass spar and preformed carbon and fiberglass afterbody was projected to be the most cost effective for the 1980 time frame.

The cost results, although valid for comparative purposes, cannot be considered on an absolute scale. The blade design selected and the repair procedures arrived at in this study must also be tested under operational conditions, as must the structural integrity of the repaired blade.

The conclusion that field-expendable rotor blade designs, as presented in this Phase I report, are cost effective is supported by the results of the parallel design study, although a different design approach was selected. A Phase II report with comparative radar cross-section measurements for simulated Configurations I, IV, and UH-1 rotor blades is in preparation. The results of this study and other related efforts are being considered in a recently initiated procurement for the design and development of a field-repairable/expendable rotor blade concept.

The program was conducted under the technical management of Philip J. Haselbauer, Technology Applications Division, with engineering support from Joseph H. McGarvey, Military Operations Technology Division.

Task 1F162205A11901
Contract DAAJ02-71-C-0046
USAAMRDL Technical Report 72-47
April 1973

EXPENDABLE MAIN ROTOR BLADE STUDY

Final Report - Phase I

Sikorsky Engineering Report 50748

By

John A. Longobardi
Everett Fournier

Prepared by

Sikorsky Aircraft
Division of United Aircraft Corporation
Stratford, Connecticut

for

EUSTIS DIRECTORATE
U.S. ARMY AIR MOBILITY RESEARCH AND DEVELOPMENT LABORATORY
FORT EUSTIS, VIRGINIA

Approved for public release;
distribution unlimited.

SUMMARY

The report presents results of a design study of expendable main rotor blades for the UH-1H helicopter. The objective of the study was to design blades which could eventually be thrown away after extensive damage rather than be sent back to depot for major overhaul. Unit cost, field repairability, resistance to corrosion and erosion, fatigue strength, and damage tolerance were factors considered for maximum cost effectiveness or lowest life-cycle cost. The study was limited to the UH-1 blade, which requires a structural skin for edgewise rigidity. For an articulated rotor blade, some of the conclusions regarding skin construction and material could be different.

The study included development of reliability, maintainability, and cost-effectiveness models. In addition, the United Aircraft Normal Modes Computer Program was modified to include two-bladed teetering rotor dynamics. The cost model was based upon the present UH-1H aircraft to provide life-cycle cost comparisons with the new blades designed in this study.

More than fifteen blade designs were generated. They included aluminum, steel, and composite blade designs. The study covered two time frames: 1972 and 1980. The results showed that a low-cost aluminum extrusion with a fiberglass composite skin is the most cost effective blade for the 1972 time frame. This blade, which has 30% fewer parts, was estimated to be 20% cheaper and 75% more repairable than the Bell blade. It is estimated that this blade could save \$12 million for a baseline fleet of 1,000 aircraft.

For the 1980 time frame, the Sikorsky "twin beam" all-composite blade has the potential of being twice as repairable as the Bell blade and could save \$26 million for a baseline fleet of 1,000 aircraft. To realize this potential, the costs of carbon must be reduced to \$25 per pound. The technology to automate the manufacture of the blade in one or two pieces must be developed and demonstrated, and the ability to repair the spar and trailing edge with sufficient remaining strength must also be demonstrated. Because of the potential of the twin beam concept and the research and development needed to demonstrate its production suitability, the plan for hardware development is centered on development of this concept.

FOREWORD

This design study for expendable main rotor blades was performed under Contract DAAJ02-71-C-0046 with the Eustis Directorate, U. S. Army Air Mobility Research and Development Laboratory, Ft. Eustis, Virginia, Task 1F162205A11901, and was under the general technical direction of Mr. Philip J. Haselbauer of the Structures Division of USAAMRDL. This expendable main rotor blade study is one of two such studies conducted as follow-on studies to earlier sectionalized and repairable rotor blade advanced design studies. The objective of all these studies was to obtain more cost-effective blade concepts for Army utilization.

Sikorsky's principal participants were Everett F. Fournier of the Reliability and Maintainability Section, Mario J. D'Onofrio and John R. Olson from the System Analysis Section, and William C. Reinfelder of the Rotor System Section. John A. Longobardi, also from the Rotor System Section, was the Team Task Manager. The program was under the general supervision of William F. Paul, Rotor System Section Head.

TABLE OF CONTENTS

	<u>Page</u>
SUMMARY	iii
FOREWORD	v
LIST OF ILLUSTRATIONS	viii
LIST OF TABLES	xiii
LIST OF SYMBOLS	xvi
INTRODUCTION.....	1
DEVELOPMENT OF METHODOLOGY AND DESIGN CONFIGURATIONS	2
ANALYSIS OF DESIGN CONFIGURATIONS	53
DESIGN SELECTION	144
CONCLUSIONS	149
RECOMMENDATIONS	151
LITERATURE CITED	152
APPENDIX I - BLADE CHARACTERISTICS	154
APPENDIX II - RELIABILITY/MAINTAINABILITY DATA.....	158
APPENDIX III - COST-EFFECTIVENESS MODEL	215
APPENDIX IV - UH-1H BLADE DATA.....	234
APPENDIX V - COST EFFECTIVE COMPARISON USING MTBR OF 1063 HOURS	236
APPENDIX VI - PLAN FOR FUTURE HARDWARE EVALUATION	254
DISTRIBUTION	273

LIST OF ILLUSTRATIONS

<u>Figure</u>		<u>Page</u>
1	Impact of Nonrecurring, Shop Hours, Material Cost on Blade Costs	7
2	Cost-Effectiveness Model	9
3	Life-Cycle Blade Logistics	11
4	Material Cost Comparisons	19
5	Configuration I	21
6	"C" Spar Blade	24
7	"C" Spar Blade With Backwall Channel	24
8	UH-1 Root End	28
9	Aluminum Laminates Root End	28
10	Stepped Extrusion Root End	28
11	Solid Aluminum Root End	29
12	Fiberglass Laminates Root End	29
13	Reduced Doubler Root End	29
14	Roll-Formed Schematic	31
15	Roll-Formed Spar	32
16	Configuration II	33
17	Configuration III	37
18	Flatwise and Torsional Stiffness Change with Spar Chord Change	39
19	Configuration IV	41
20	Fabrication of Beam Concept	43

<u>Figure</u>		<u>Page</u>
21	Fiberglass Root End Attachment	45
22	Configuration V	47
23	Pultrusion Schematic	49
24	Configuration VI	51
25	Natural Frequencies, Configuration UH-lH	54
26	Natural Frequencies, Configuration I and VI	55
27	Natural Frequencies, Configuration II	56
28	Natural Frequencies, Configuration III	57
29	Natural Frequencies, Configuration IV and V	58
30	Vibratory Moments, Configuration I, VI and UH-lH....	61
31	Vibratory Moments, Configuration II and UH-lH.....	62
32	Vibratory Moments, Configuration III and UH-lH	63
33	Vibratory Moments, Configuration IV, V and UH-lH ..	64
34	Steady Moments - Typical for All Configurations	65
35	Centrifugal Force vs. Blade Radius	66
36	Weight Distribution	67
37	Flatwise Stiffness Distribution	68
38	Edgewise Stiffness Distribution	69
39	Torsional Stiffness Distribution	70
40	Blade Static Deflection Comparisons	71
41	Blade Flexural Axis Comparisons	72
42	Blade Center of Gravity Comparisons	73

<u>Figure</u>		<u>Page</u>
43	Typical Goodman Diagram	86
44	Stress-Cycle Curve	88
45	Material Strain Allowables	90
46	.50 Caliber Hit Sikorsky Main Blade	95
47	Blade Spar Structural Damage	96
48	Blade Tear Damage	116
49	Blade Tear Damage	116
50	Blade Gash Damage	117
51	Blade Dent Damage	117
52	Impact of Blade Acquisition Cost, 1972 Configurations	127
53	Impact of Blade Acquisition Cost, 1980 Configurations	128
54	Blade Acquisition Cost, 1972 - 1980.....	145
55	Forecast of Material and Labor Costs	146
56	Maximum Torsional Deflection	155
57	Normalized Vibratory Stress	156
58	Rotor Thrust - Blade Twist Curve.....	157
59	Remove Skin and Prepare Overlap Area.....	205
60	Trim Patch to Fit.....	205
61	Prime Patch and Skin	205
62	Prime Patch and Skin	205
63	Fill Edge Separations.....	206

<u>Figure</u>		<u>Page</u>
64	Apply Adhesive and Position Patch	206
65	Apply Adhesive and Position Patch	206
66	Apply Adhesive and Position Patch	206
67	Positioned Patch	207
68	Apply Adhesive	207
69	Apply Adhesive to Overlay and Position Scrim Cloth	207
70	Position Overlay.....	207
71	Install and Inflate Compression Blanket.....	208
72	Finished Patch	208
73	Damaged Blade	210
74	Repair Materials	210
75	Replacement Plug.....	210
76	Plug in Place	210
77	Apply Foam to Cavity.....	211
78	Expanded Foam	211
79	Foam Trimmed and Sanded to Contour.....	211
80	Apply Adhesive to Overlay and Plug	211
81	Apply Overlay - Apply Adhesive to Plug	212
82	Apply Overlay to Plug	212
83	Apply Compression Blanket	212
84	Finished Repair	212
85	UH-1H Mission Environment.....	233

<u>Figure</u>		<u>Page</u>
86	Impact of MTBR Criteria on Cost Effectiveness - Acquisition Cost Sensitivity.....	250
87	Impact of Blade Acquisition Cost - Baseline - 1063 MTBR	251
88	Plan for Future Hardware Evaluation.....	256
89	Outboard Specimen.....	259
90	Inboard Specimen.....	260
91	Stress Level of Operation	262
92	S-N Strength Data.....	262
93	Crack Propagation	262
94	Static Rap Test for Blade Frequency.....	263
95	2000 HP Main Rotor Test Stand	265
96	Rotor Hover Performance Comparison Configuration V vs. Standard Blade.....	266
97	Typical Strain Gaged Blade.....	269

LIST OF TABLES

<u>Table</u>		<u>Page</u>
I	Comparison of Physical Properties.....	74
II	Blade Design Features	75
III	Material Properties	77
IV	Blade Stress in Level Flight Cruise - Configuration UH-1H	81
V	Blade Stress in Level Flight Cruise - Configuration I and VI.....	82
VI	Blade Stress in Level Flight Cruise - Configuration II	83
VII	Blade Stress in Level Flight Cruise - Configuration III.....	84
VIII	Blade Stress in Level Flight Cruise - Configuration IV and V	85
IX	Structural Analysis for Various Modes of Failure/Damage - Configuration I	92
X	Structural Analysis for Various Modes of Failure/Damage - Configuration IV.....	93
XI	Reasons for UH-1D Blade Removal - MTR/MTBR Analysis	103
XII	Reliability Apportionment - Baseline UH-1D Blade	108
XIII	Failure Rate Summary	112
XIV	Blade Repairability and Level of Maintenance	114
XV	Repairability Summary	114
XVI	Aircraft Cost Effectiveness - 1972	124
XVII	Fleet Effective Cost - 1972	124

<u>Table</u>		<u>Page</u>
XVIII	Aircraft Cost Effectiveness - 1980	126
XIX	Fleet Effective Cost - 1980	126
XX	1972 Cost Effectiveness Summary - Baseline	130
XXI	1980 Cost Effectiveness Summary - Baseline.....	131
XXII	1972 Cost Effectiveness Summary - Conf. I	132
XXIII	1980 Cost Effectiveness Summary - Conf. I	133
XXIV	1972 Cost Effectiveness Summary - Conf. II	134
XXV	1980 Cost Effectiveness Summary - Conf. II	135
XXVI	1972 Cost Effectiveness Summary - Conf. III	136
XXVII	1980 Cost Effectiveness Summary - Conf. III.....	137
XXVIII	1972 Cost Effectiveness Summary - Conf. IV.....	138
XXIX	1980 Cost Effectiveness Summary - Conf. V	139
XXX	Cost Effectiveness Summary	140
XXXI	Cost of New Blade to the Army	141
XXXII	Reliability Analysis - Configuration I	159
XXXIII	Repairability Analysis - Configuration I	163
XXXIV	Math Model R/M Input Variables - Configuration I....	167
XXXV	Design Failure Mode and Effect Analysis - Configuration I	168
XXXVI	Reliability Analysis - Configuration II	172
XXXVII	Repairability Analysis - Configuration II	176
XXXVIII	Math Model R/M Impact Variables - Configuration II	180

<u>Table</u>		<u>Page</u>
XXXIX	Design Failure Mode and Effect Analysis - Configuration II	181
XXXX	Reliability Analysis - Configuration IV	185
XXXXI	Repairability Analysis - Configuration IV	189
XXXXII	Math Model R/M Input Vairables - Configuration IV	193
XXXXIII	Design Failure Mode and Effect Analysis - Configuration IV	194
XXXXIV	UH-1 Rotor Blade Design Cost Comparisons	234
XXXXV	Reliability Apportionment - Baseline UH-1 With 1063 Hour MTBR	238
XXXXVI	Reliability Analysis - Configuration V Compared to Baseline UH-1 Blade With 1063 Hour MTBR	240
XXXXVII	Repairability Analysis - Configuration V Compared to Baseline UH-1 Blade With 1063 Hour MTBR	244
XXXXVIII	Math Model R/M Input Variables-Configuration V Compared to Baseline UH-1 Blade With 1063 Hour MTBR	248
XLIX	Cost Effective Summary - 1063 MTBR Baseline Configuration - 1980	252
L	Cost Effective Summary-1063 MTBR Configuration V - 1980	253

LIST OF SYMBOLS

A_b	blade set attrition, sets/FH
A_m	mission availability
B	installed blades per aircraft
B_{att}	blades lost to attrition
B_{dep}	total damaged blades sent to depot
B_{ds}	removed blades sent to direct support
B_{inv}	initial blade spares
B_{repl}	blade replenishment spares
B_{req}	blades requisitioned from inventory
B_{ret}	blades retired from service
B_{ri}	blades removed or installed
B_{sa}	blades lost to scrappage and attrition
BD	total blades damaged
BD_e	blades externally damaged
BD_i	blades inherently damaged
BD_{rem}	damaged blades removed from aircraft
BDS_{dep}	damaged blades sent to depot from direct support
BLCC	blade life-cycle cost, \$
$BLCC_{UH}$	baseline UH-1 blade life-cycle cost, \$
BO_{dep}	damaged blades sent to depot from organizational level

BR_{dep}	damaged blades repaired, depot
BR_{ds}	damaged blades repaired, direct support
BR_{off}	removed blades repaired off aircraft, organizational level
BR_{on}	damaged blades repaired on aircraft
BS	total damaged blades scrapped, all levels
BS_{dep}	damaged blades scrapped, depot
BS_{ds}	damaged blades scrapped, direct support
BS_o	removed blades scrapped, organizational level
b	number of blades
C_T	coefficient of thrust
C_{cont}	blade container cost, \$
C_{fly}	blade contribution to aircraft flyaway cost, \$
C_{fuel}	fuel and oil cost per pound of fuel consumed, \$/lb
C_{inst}	cost of blade installation, organizational level, \$
C_{isp}	blade contribution to initial spares cost, \$
C_m	average mission capability, ton-knots
C_{rem}	cost of blade removal, organizational level, \$
C_{req}	cost to requisition and obtain replacement blades, organizational level, \$

C_{rsp}	blade contribution to replenishment spares cost , \$
C_{xx}	distance between the point under consideration and the chordwise blade neutral axis, in.
C_{yy}	distance between the point under consideration and the neutral axis perpendicular to the chordwise axis, in.
CB_{acq}	single blade acquisition cost, \$
CG	total blade contribution to replenishment GSE cost, all levels , \$
CG_{dep}	replenishment GSE cost, depot level, \$
CG_{ds}	replenishment GSE cost, direct support level, \$
CG_O	replenishment GSE cost, organizational level, \$
CGR_{dep}	replenishment GSE cost per repair, depot level, \$
CGR_{ds}	replenishment GSE cost per repair, direct support level, \$
CGR_{off}	replenishment GSE cost per off-aircraft repair, organizational level, \$
CGR_{on}	replenishment GSE cost per on-aircraft repair, organizational level, \$
CGS_{dep}	GSE support cost per aircraft, depot level, \$
CGS_{ds}	GSE support cost per aircraft, direct support level, \$
CGS_O	GSE support cost per aircraft, organizational level, \$
CI_{dep}	cost of blade receiving and inspection, depot level, \$

CI_{ds}	cost of blade inspection, direct support level, \$
CI_{off}	cost of off-aircraft inspection for blade disposition, organizational level, \$
CI_{on}	cost of on-aircraft inspection for blade repairability, organizational level, \$
CM	total blade contribution to maintenance cost, all levels, \$
CM_{dep}	blade contribution to maintenance cost, depot level, \$
CM_{ds}	blade contribution to maintenance cost, direct support level, \$
CM_O	blade contribution to maintenance cost, organizational level, \$
CMR_{ds}	mean material cost per blade repair, direct support level, \$
CMR_{off}	mean material cost per off-aircraft blade repair, organizational level, \$
CMR_{on}	mean material cost per on-aircraft blade repair, organizational level, \$
CO_{dep}	blade overhaul cost, depot level, \$
CP_{dep}	cost of shipping preparation, depot level, \$
CP_{ds}	cost of shipping preparation, direct support level, \$
CP_O	cost of shipping preparation, organizational level, \$
CPOL	aircraft fuel and oil cost, \$

CPOL _{UH}	baseline UH-1 life-cycle fuel and oil cost, \$
CR _{dep}	cost of blade overhauls, depot level, \$
CR _{ds}	cost of blade repairs, direct support level, \$
CR _{off}	cost of off-aircraft repairs, organizational level, \$
CR _{on}	cost of on-aircraft blade repairs, organizational level, \$
CS _{dep}	cost to dispose of scrap, depot level, \$
CS _{ds}	cost to dispose of scrap, direct support level, \$
CS _o	cost to dispose of scrap, organizational level, \$
CSH _{US}	packaged blade shipping cost from field to CONUS, \$
CSH _{cont}	empty blade container shipping cost from field to CONUS, \$
CSH _{dep}	cost of shipping blades to depot, \$
CSH _{fld}	packaged blade shipping cost from CONUS to field, \$
CSHF _{dep}	cost of shipping overhauled blades to field from depot, \$
CSHP _{dep}	blade shipping preparation cost, depot level, \$
CSHP _{ds}	blade shipping preparation cost, direct support level, \$
CSHP _o	blade shipping preparation cost, organizational level, \$
DH	down hours
DS	depot support

DT	aircraft down hours per flight hour
E_c	modulus of elasticity of the component (material), lb/in. ²
E_{ce}	aircraft cost effectiveness, ton-knots/\$
E_m	mission effectiveness, ton-knots
E_{mUH}	baseline UH-1 mission effectiveness, ton-knots
EA	total axial stiffness, lb
$E_{l_{xx}}$	total flatwise bending stiffness, lb/in. ²
$E_{l_{yy}}$	total edgewise bending stiffness, lb/in. ²
F_A	allowable alternating stress, lb/in. ²
F_E	endurance limit of material at zero steady stress, lb/in. ²
F_{tu}	ultimate tensile strength of material, lb/in. ²
FE_{UH}	baseline UH-1 fleet effectiveness, ton-knots
FEC	fleet effective cost, \$
FF	average mission fuel flow, lb/FH
FH	flight hours
f	stress, lb/in. ²
f_s	combined steady stress, lb/in. ²
f_v	combined vibratory stress, lb/in. ²

GW	gross weight, lb
GSE	ground support equipment
HP	horsepower
In.	inches
K_{inv}	ratio of blade inventory spares to blade life-cycle replenishment spares
KSI	1000 lb/in. ²
L_a	aircraft service life, FH
L_b	blade scheduled retirement life, FH
Lb	pounds
LCC	aircraft life-cycle cost, \$
LCC_{UH}	baseline UH-1 life-cycle cost, \$
LCC_{nv}	UH-1 non-variable life-cycle cost, \$
M	material cost,\$
M_{es}	steady edgewise moment, in-lb.
M_{ev}	vibratory edgewise moment, in.-lb.
M_{fs}	steady flatwise moment, in. -lb.
M_{fv}	vibratory flatwise moment, in. -lb.
M_{inst}	mean maintenance man-hours per blade installation, MMH

M_{rem}	mean maintenance man-hours per blade removal, MMH
M_{req}	mean maintenance man-hours to requisition and obtain a replacement blade, organizational level, MMH
MEK	methyl ethylketone
MI_{dep}	mean maintenance man-hours per blade receiving and inspection, depot level, MMH
MI_{ds}	mean maintenance man-hours per blade inspection, direct support level, MMH
MI_{off}	mean maintenance man-hours per off-aircraft blade inspection, organizational level, MMH
MI_{on}	mean maintenance man-hours per on-aircraft damaged blade inspection, organizational level, MMH
MMH	maintenance man-hours
MR_{ds}	mean maintenance man-hours per blade repair, direct support level, MMH
MR_{off}	mean maintenance man-hours per off-aircraft blade repair, organizational level, MMH
MR_{on}	mean maintenance man-hours per on-aircraft blade repair, organizational level, MMH
MS	margin of safety
MS_{dep}	mean maintenance man-hours per blade scrappage, depot level, MMH
MS_{ds}	mean maintenance man-hours per blade scrappage, direct support level, MMH

MS_O	mean maintenance man-hours per blade scrappage, organizational level, MMH
MTB_a	aircraft mean time between loss of blades to attrition - flight hours
MTB_d	aircraft mean time between inherent or external blade damage - flight hours
MTB_e	blade mean time between external damage, flight hours
MTB_i	blade mean time between inherent damage, flight hours
MTB_s	aircraft mean time between blade scrappage - flight hours
MTB_{sa}	aircraft mean time between scrappage and attrition - flight hours
MTB_{sar}	aircraft mean time between scrappage, attrition, or blade retirement - flight hours
MTBR	mean time between removal, flight hours
MTR	mean time to removal, flight hours
N	fleet size
N_b	total number of blades
N_n	number of cycles required to initiate a fatigue crack at n_n stress level
N_r	revolutions per minute
n_n	number of cycles at a specific stress level
ORG	organization

P_{cf}	centrifugal force, lb
PB_{ds}	percent of damaged and removed blades sent to direct support, %
PBR_{dep}	percent of received blades repaired at depot level, %
PBR_{ds}	percent of received blades repaired at direct support level, %
PBR_{off}	percent of damaged and removed blades repaired at organizational level, %
PBR_{on}	percent of damaged blades repaired on aircraft, %
PBS_{ds}	percent of received blades scrapped at direct support level, %
PBS_o	percent of damaged and removed blades scrapped at organizational level, %
POL	petroleum, oil and lubrication
R	minimum combined stresses/maximum combined stresses
R_{civ}	civilian maintenance personnel labor rate, \$/hr
R_c	recurring costs,\$
R_m	mission reliability
R_{mil}	military maintenance personnel labor rate, \$/hr
R_{non}	non-recurring cost ,\$
R_r	rotor radius , ft

R _s	aircraft mission abort failures per flight hour
r	labor cost , \$/hr
SH	shop-hours for fabrication
SL	sea level
SSE	special support equipment
STD	standard
T _d	average daily downtime , hr /day
T _m	average mission flight time, flight hours
U _a	aircraft annual utilization, flight hours
U _d	average daily utilization , FH/day
V	knot (nautical miles/hr) or velocity (ft/sec)
σ	solidity = % of total blade area/rotor diameter area

INTRODUCTION

The need for redesigning rotor blades for a combat environment is evident from field experience with the UH-1 helicopter. The data show that 30% of all UH-1 blades are scrapped in the field, and 58% are returned to depot for overhaul. However, 40% of the blades are scrapped at overhaul. This means that 70% of the original blades are replaced by new blades. However, of new and repaired blades, only 5% or less ever last 2,000 hours.

In recognition of this, the Eustis Directorate has funded Vertol Division, The Boeing Company, to investigate sectionalized blade concepts which could be disassembled. The damaged sections could be scrapped and replaced. Kaman Aerospace Corporation was funded to investigate methods of making blades more field repairable. Sikorsky was funded to assess the practicality of a field replaceable bonded pocket for the CH-54B, and Sikorsky and Kaman were funded to investigate expendable blade designs.

This report presents Sikorsky's study of expendable blade designs. An expendable blade is defined as a blade with a low enough unit cost that it is more cost effective to throw it away than to send it back to depot. This simple concept of expendability was expanded. In addition to low unit cost, the blade must be damage tolerant to reduce the scrappage rate. Secondly, the blade should be reliable enough to minimize non-combat malfunctions. The blade should also be highly repairable in the field. If these goals are met, the blade would have a lower unit cost than conventional blades and would be continued to be repaired in the field until its useful life is expended and it is finally thrown away. To quantify this, the cost effectiveness of the Bell blade was compared with cost effectiveness of the new designs with and without depot repair. Blades were considered expendable when the cost effectiveness was higher to repair in the field or scrap than to send blades back to depot.

The study was conducted in two time frames, primarily because the cost of labor and materials is estimated to change significantly. In addition, new composite technology which has not been demonstrated could not be considered for near-term applications. An important part of this study is to separate those designs which can be flown early and put into production in the 1970's. There are concepts, particularly the composites, which will have a greater potential but require demonstration of cost, manufacturing, and structural viability.

The report will first describe the methods developed to evaluate expendability; designs of aluminum, steel, and composite blades; and selection of expendable blades. The report also includes a recommended plan for hardware development.

DEVELOPMENT OF METHODOLOGY AND DESIGN CONFIGURATIONS

PROGRAM APPROACH

Several approaches were considered feasible to obtain blades of higher cost effectiveness than the UH-1H blade. One possibility was to simplify the present UH-1H design by reducing the number of components while still maintaining a similar low-cost aluminum extrusion. Savings would result from having fewer parts to fabricate and fewer man-hours for assembly of each blade.

Another possibility was to increase the repairability of the present blade by replacing some of the aluminum with fiberglass components. Studies made by Sikorsky Aircraft and by Kaman Aerospace Corporation, Reference 1, have already shown that fiberglass is not only more repairable than aluminum but that it can be repaired in the field. For example, one utilization would be the substitution of fiberglass for the aluminum trailing edge spline and skin, an area where most blade damage occurs.

Another approach was to investigate an entirely new type of structure, i.e., complete fiberglass blades with their many advantages of higher fatigue life and even higher repairability than the metal blades because of their greater area of repairability. The higher fatigue life of fiberglass also offered the potential of increased aircraft performance not possible with the limited properties of steel and aluminum.

Automation is not only another possibility, it is a necessity if blade cost is to be reduced. The fiberglass design, for example, would be virtually eliminated from contention, pricewise, without some form of automation because individual layup of fiberglass sheets requires considerably more man-hours of assembly time than a metal blade. In this respect, extruded fiberglass shapes and tape laying machines must be strongly considered to minimize fabrication labor. The sheet metal design being considered for study must also be automated to obtain low-cost parts. This may be accomplished by a progressive die sheet metal rolling machine with automatic feed and cutoff.

The approaches above were considered for both the 1972 and 1980 time frames, taking into account the changes in material and labor costs for the two periods.

RELIABILITY AND MAINTAINABILITY METHODOLOGY

The methodology employed to conduct the reliability and maintainability portion of the study consisted of establishing an accurate and statistically valid data base from which a complete reliability and maintainability analysis of the baseline UH-1 main rotor blade was conducted. This analysis then served as the basis for generating reliability and maintainability cost-effectiveness values for use in a mathematical model which combined them with other design factors to determine a baseline cost-effectiveness/life-cycle cost value. Candidate expendable blade designs were then analyzed using the same procedure and compared to the established UH-1 baseline to determine changes in blade life-cycle cost and aircraft cost effectiveness.

Reliability and Maintainability Data Research

All available reliability and maintainability data were collected and reviewed. Collected data were screened to determine applicability to the study in terms of equipment operational environment and similarity to UH-1 blade design. Data originating from sources not representative of UH-1 operational environment or blade design were discarded.

Reliability Data

The primary source of reliability data used as the basis for this study was Reference 2. Initial research and screening of available data sources revealed this document to be the most authoritative and valid source of reliability data relative to the UH-1 main rotor blade in its operational environment.

Maintainability Data

Background UH-1 maintainability data were collected from a variety of sources. Repair limitations for the UH-1 main rotor head were established using References 3 and 4. Maintenance task times were calculated on the basis of the procedures set forth in these publications relative to the UH-1 main rotor blade. Overhaul and restoration task times were developed through Sikorsky overhaul and repair facilities and reference to USAAMRDL furnished values and publications.

Baseline UH-1 Blade Profile

A baseline UH-1 blade reliability and maintainability profile was developed using the assembled data. Specific failure modes were associated with blade component parts, part repairability, repair levels, required

support equipment and related cost factors. These parameters were then used to determine applicable cost variables for inclusion in the math model to establish baseline UH-1 blade life-cycle cost and impact on aircraft cost effectiveness. The math model also developed a list of design sensitivities to provide direction in the design of cost-effective candidate expendable blades.

UH-1H BLADE COST ANALYSIS

The task of producing a more cost-effective rotor blade for the UH-1H aircraft is a challenging one, since the present UH-1H blade is already quite low in initial cost. Low-cost aluminum and steel components are already utilized in the construction of the present UH-1H blade, so changes in material alone will not provide significant cost reduction.

The present UH-1H blade is being fabricated in production for approximately \$15.00 per pound based on cost and weight of \$3000.00 and 200 pounds, respectively. The components are mostly aluminum; they consist of a primary spar extrusion, side doubler plates, root end grip plates, skin, and honeycomb core. Additional parts are steel doubler plates, steel and cobalt abrasion strips and structural adhesive. Since the average cost of the material, including the price of the honeycomb and structural adhesive, is approximately \$2.50 per pound, the remaining \$12.50 per pound for the production blade cost must be the result of recurring costs of processing the material; i.e., man-hours associated with component machining, finishing, forming extrusions, subassembly and assembly operations. Cost must also include amortization of non-recurring cost for design, ground and flight test and manufacturing tooling. In addition, of course, a profit must be realized.

Since the base material for the UH-1H represented a small fraction of total cost, other areas of the blade had to be examined to determine where the greatest costs were incurred. Investigation showed that changes in nonrecurring cost had only a small effect on final blade cost when considering production runs of 10,000 blades, whereas a much greater impact was obtained by changes in recurring costs. The examples below illustrate how changes in nonrecurring and recurring cost affect blade cost. Equation (1) shows the basic parameters associated with blade cost (shown without profit for simplification). Equation (2) incorporates typical values for the UH-1H blade where $R_{non} = \$10^6$, $N = 10,000$, $r = \$25/\text{hr}$, $M = \$500$, and $SH = 96 \text{ hr}$. Equation (3) depicts the change in blade cost by reducing nonrecurring expenses by 25% keeping the other values of Equation (2) constant. Equation (4) shows a 25% reduction in shop hours for fabrication while retaining other values of Equation (2) constant.

$$\text{Blade Cost} = \frac{R_{\text{non}}}{N_b} + R_C = \frac{R_{\text{non}}}{N_b} + M + (SH)(r) \quad (1)$$

where R_{non} = Nonrecurring cost, \$

R_C = Recurring costs = $M + (SH)(r)$, \$

N_b = Total number of blades

r = Labor cost, \$/hr

M = Material cost, \$

SH = Shop-hours for fabrication

$$\text{Blade Cost} = \frac{\$10^6}{10,000} + \$500 + (96 \text{ hr}) (\$25/\text{hr}) = \$3000 \quad (2)$$

$$\text{Blade Cost} = .75(\$10^6) + \$500 + (96 \text{ hr}) (\$25/\text{hr}) = \$2,975 \quad (3)$$

($R_{\text{non}} - 25\%$ reduction)
 $\frac{10,000}{10,000}$

$$\text{Blade Cost} = \frac{\$10^6}{10,000} + \$500 + .75 (96 \text{ hr}) (\$25/\text{hr}) = \$2,400 \quad (4)$$

($SH - 25\%$ reduction)

As shown by Equation (3), for a production run of 10,000 blades, a 25% reduction in nonrecurring costs from \$1,000,000 to \$750,000 reduces the blade cost by approximately \$25.00, which is an insignificant amount. On the other hand, assuming a labor cost at approximately \$25.00 per hour (includes base rate, overhead, etc.), a 25% reduction in shop hours from 96 to 72 hours reduces blade cost by approximately \$600.00 as shown by Equation (4). This represents a recurring to nonrecurring cost factor of 24 to 1, which is significant.

A similar example would show that recurring material cost has higher fluctuation than nonrecurring costs but is small compared to shop hour changes.

$$\text{Blade Cost} = \frac{\$10^6}{10,000} + .75(\$500) + (96 \text{ hr}) (\$25/\text{hr}) = \$2,875 \quad (5)$$

($M - 25\%$ reduction)

Same 25% reduction to reduce material cost (Equation (5)) results in a blade cost of \$2,875 or a savings of \$125 over the base blade of Equation (2). This \$125 is five times greater than that obtained by reducing the nonrecurring cost of Equation (3), but is approximately one-fifth the shop hour cost savings of Equation (4).

Figure 1 shows how Equations (3), (4), and (5) were expanded to show the cost changes (up to 200%) for each parameter. Each curve is a function of one of the three parameters R_{non} , SH or M while the other two parameters remain constant. The specific points of Equations (3), (4) and (5), for a 25% reduction in the base values of R_{non} , SH and M, intercept each curve at .75 along the abscissa.

It is obvious from the slopes of the plots that nonrecurring costs are the least sensitive to change; material costs fluctuate slightly more than recurring costs, while shop hours provide the greatest impact. These slopes can be utilized to determine the changes required to the parameters to control cost. For example, if a base blade costs \$3000 and the price of the material is increased by 100%, i.e., if it doubles from \$500 to \$1,000, the cost of the blade would increase to \$3,500 if all other parameters remain unchanged (this point is shown at the intersection of the M plot and 2.0 on the abscissa). To retain the same base blade cost of \$3000, either the nonrecurring cost or shop hours must be reduced by \$500. Since the slope of R_{non} is virtually a horizontal line, it cannot be used to reduce costs by \$500. The SH slope, however, can be used; Figure 1 shows that \$500 is equivalent to 21% on the SH plot. This shows a 100% M cost increase is offset by a 21% SH decrease.

Summary Conclusions

Several summary conclusions can be made from the above investigation:

1. Amortized nonrecurring costs are extremely low for large production runs and have little effect on final blade cost. Doubling the nonrecurring costs from $\$10^6$ to $\$2 \times 10^6$ adds a mere \$100 to the blade cost.
2. Material cost for the UH-IH is inexpensive because of the utilization of low-cost steel and aluminum. The material is only slightly sensitive to change, i.e., doubling material cost would increase blade cost by less than 20%. This would indicate that some quantities of higher cost material can be utilized to obtain properties of stiffness, strength, low weight, etc., not possible with the present materials. For example, if high cost carbon is judiciously applied in small quantities for torsional and edgewise stiffness

$$\begin{aligned} \text{Constant Values} \\ N_b &= 10,000 \\ r &= \$25/\text{hr} \end{aligned}$$

$$\begin{aligned} \text{Base Values} \\ \text{Blade Cost} &= R_{\text{non}} + M + (\text{SH}) (r) = R_{\text{non}} + M + (\text{SH}) (25) \\ &\quad \frac{1}{N_b} \end{aligned}$$

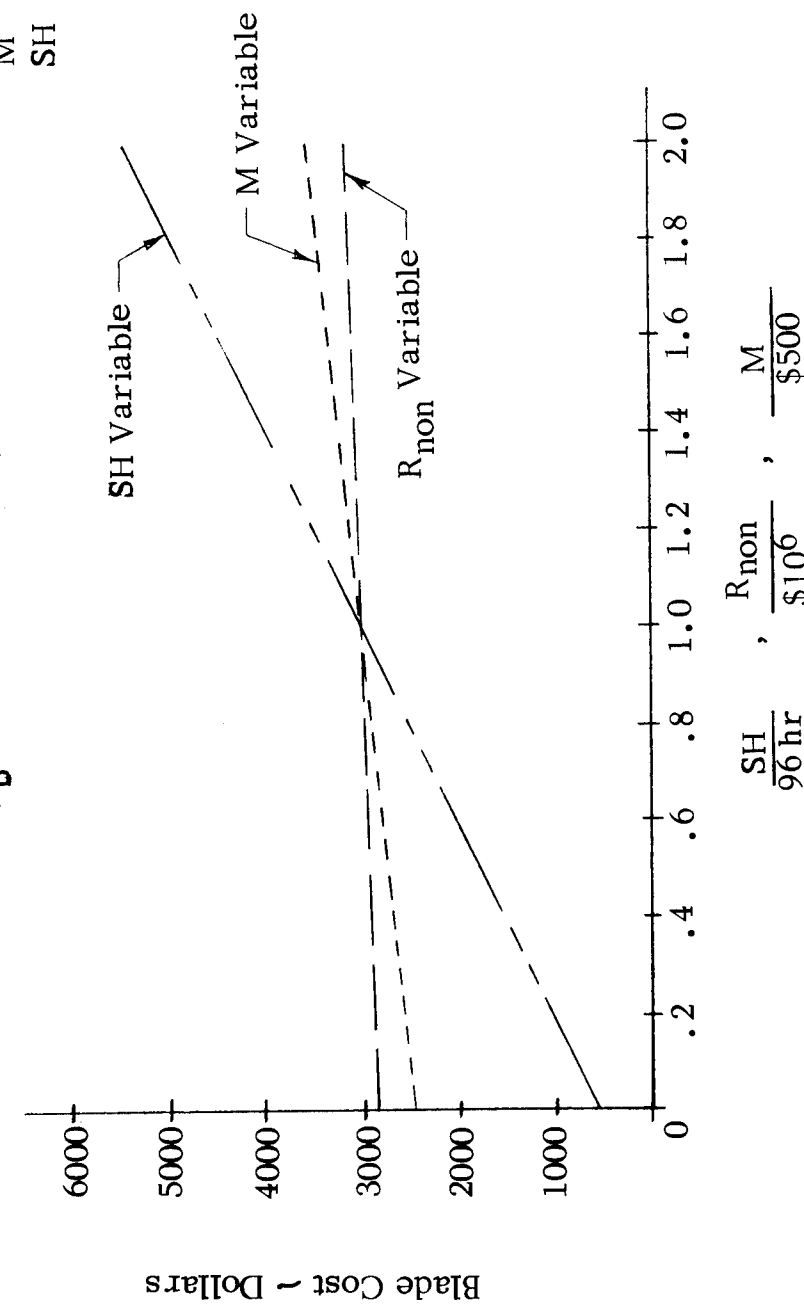


Figure 1. Impact of Nonrecurring, Shop Hours, Material Cost on Blade Costs.

requirements, it should not have a great effect on cost provided carbon decreases in price as forecasted.

3. Shop hour fabrication cost is the most sensitive blade parameter; a change in shop hours magnifies change in blade cost. The most efficient way to reduce blade cost is to minimize number of shop hours. On this basis, automation is the key. Automation also offsets the use of higher cost material as noted in Paragraph 2 above.

COST-EFFECTIVENESS METHODOLOGY

The value of rotor blade design is measured by the relationship of the benefits it contributes to and the costs it imposes on the UH-1 aircraft in Army service. With the exception of a few attributes such as safety and human factors, most system characteristics can be quantified and integrated into an aircraft cost-effectiveness criterion:

$$\text{Cost effectiveness} = \frac{\text{Mission effectiveness}}{\text{Life-cycle cost}} \text{ (ton-knots/mega \$)} \quad (6)$$

A cost-effectiveness model is used to relate rotor blade design characteristics and aircraft cost effectiveness. The general logic of the model is shown in Figure 2. The maintenance burden, including spares requirements, imposed by a rotor blade design on the organizational, direct support and depot levels is the prime blade contribution to aircraft life-cycle cost. This burden, in terms of blade logistics over the aircraft life cycle, is described in Figure 3. A computer model incorporating these analyses was designed and is used to obtain cost effectiveness of the UH-1 equipped with the candidate blade designs. A detailed description of the cost-effectiveness model with equations is presented in Appendix III. A mission analysis program translates UH-1 weight/performance characteristics into mission capability and fuel flow. This program is also described in Appendix III. A MTBR of 914 hours was used for the baseline UH-1 during the study. A comparison of the most cost effective configuration using a MTBR of 1063 hours instead of 914 hours is included in Appendix V. The rationale for the use of ton-knots instead of ton-miles is also included in Appendix V.

Expendability

The evaluation of rotor blade designs depends basically on the aircraft cost-effectiveness criterion. Absolute blade expendability implies that scrappage and replenishment of a damaged blade is always more cost effective than the minimum field level repair. This concept quickly becomes impractical since even the cost of shipping a replenishment blade

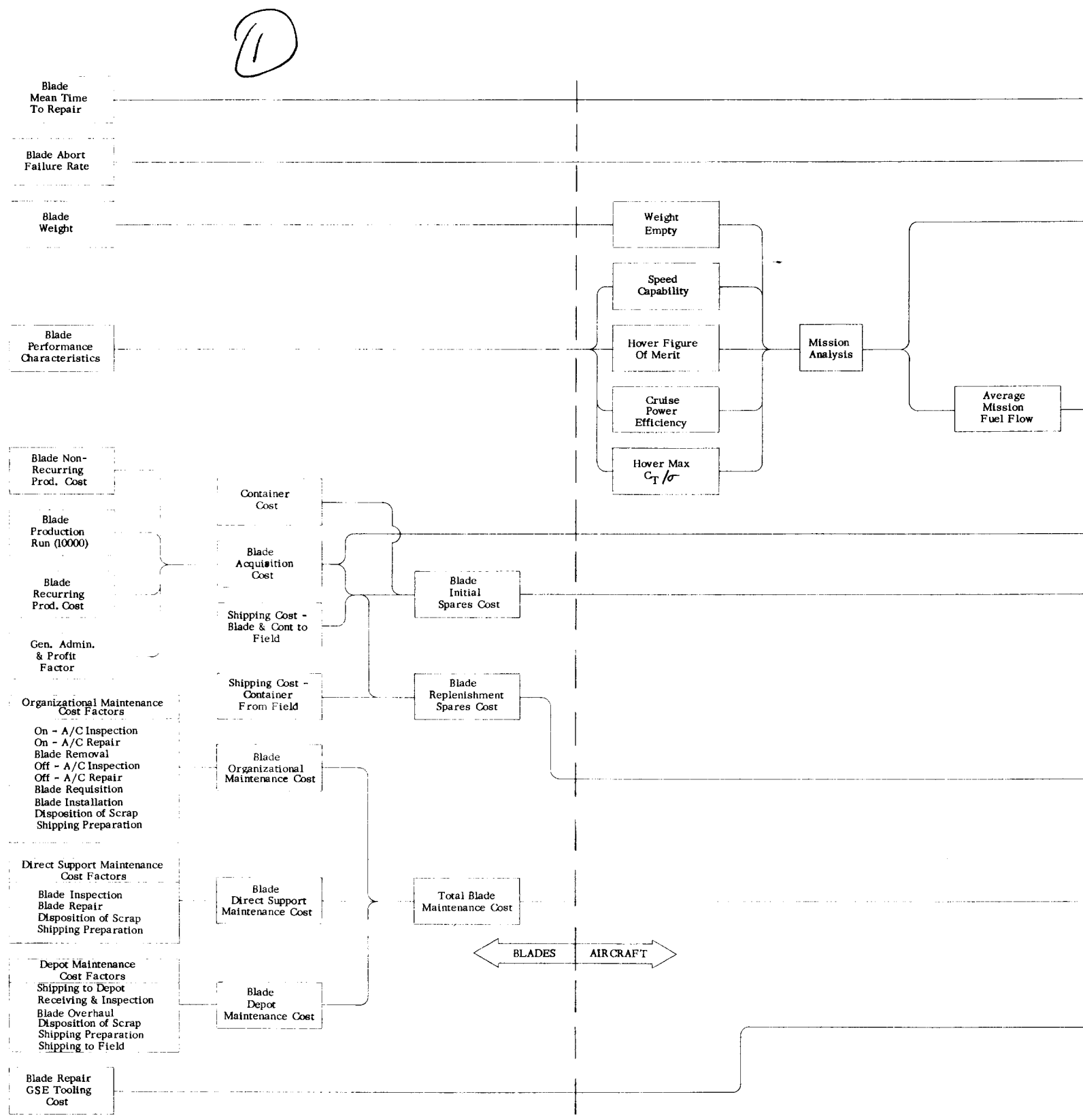
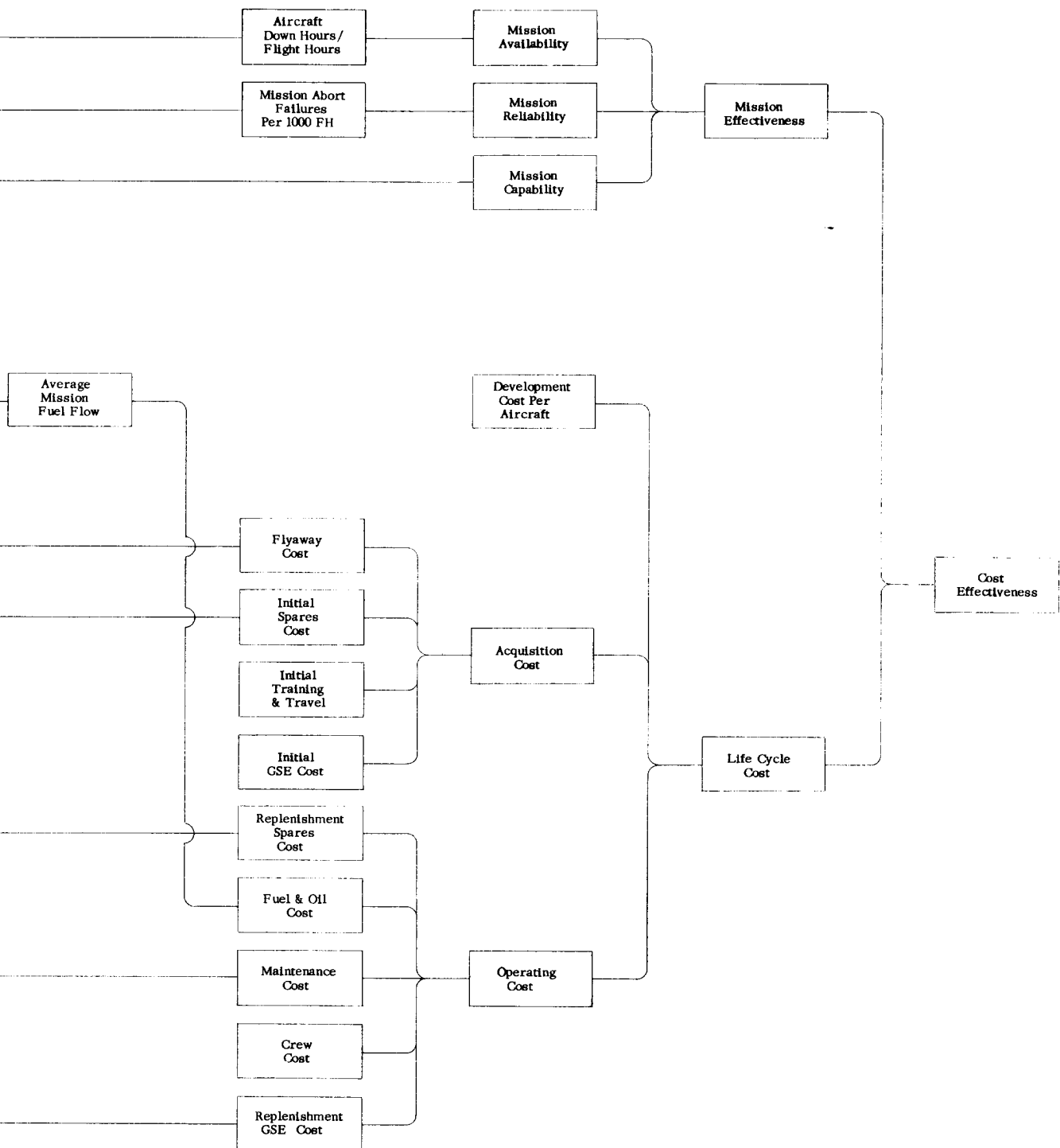


Figure 2. Cost-Effective Model.

(2)



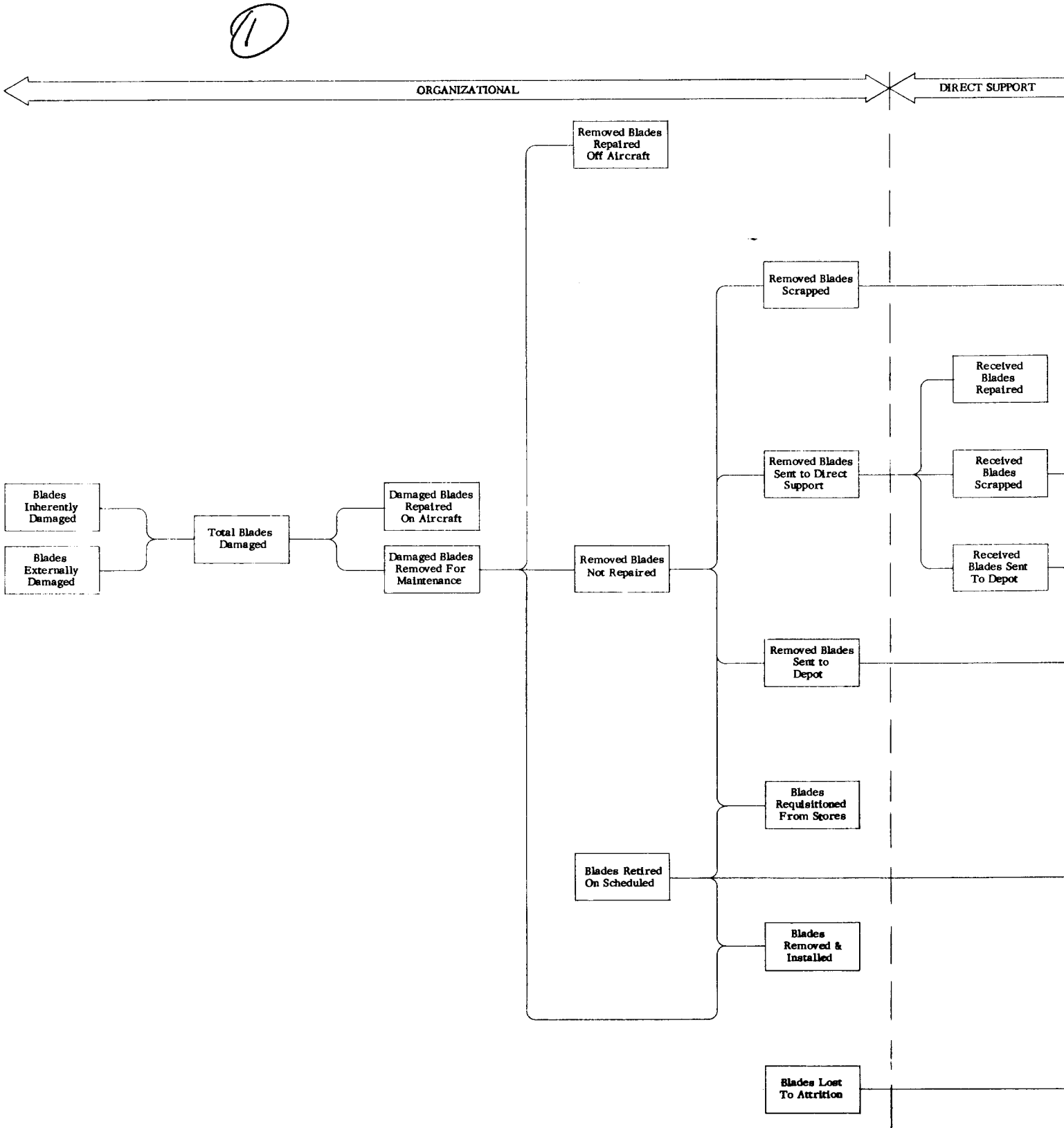
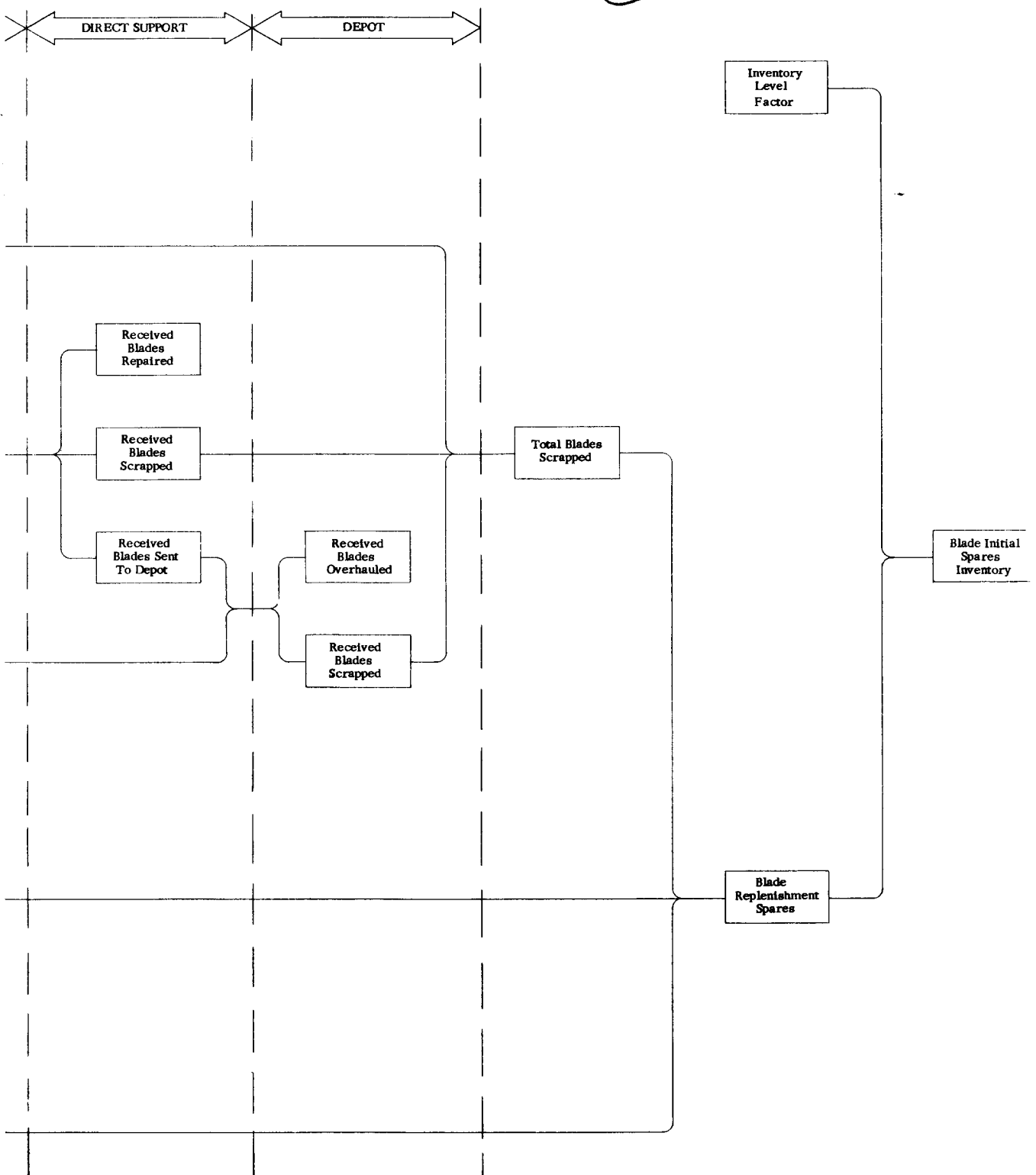


Figure 3. Life-Cycle Blade Logistics.

(2)



can exceed a minor repair cost. A better measure of blade expendability is the degree to which cost effectiveness is enhanced/compromised by the elimination of depot level repair. The cost-effectiveness model is used to analyze the candidate blade designs with and without depot level repair. In the latter case, damaged blades normally sent to depot for overhaul/repair are scrapped at the field level.

Fleet Effective Cost

Fleet effective cost is an equivalent measure of aircraft cost effectiveness on a fleet level. Defining the UH-1 with standard blades as the baseline aircraft, and the UH-1 with any candidate rotor blade design as a candidate aircraft, then for a fleet of N aircraft,

$$\text{Baseline cost effectiveness} = \frac{N \times \text{Baseline effectiveness}}{N \times \text{Baseline life-cycle cost}} \quad (7)$$

or

$$\text{Baseline cost effectiveness} = \frac{\text{Baseline fleet effectiveness}}{\text{Baseline fleet life-cycle cost}} \quad (8)$$

similarly,

$$\text{Candidate cost effectiveness} = \frac{\text{Candidate fleet effectiveness}}{\text{Candidate fleet life-cycle cost}} \quad (9)$$

The change in cost effectiveness can be generated by a change in fleet effectiveness, fleet life-cycle cost, or most frequently, in both. Fleet cost can be made an equivalent cost-effectiveness measure by adjusting fleet size to maintain baseline fleet effectiveness:

$$N' = \frac{\text{Baseline fleet effectiveness}}{\text{Candidate aircraft effectiveness}} \quad (10)$$

and

$$\text{Fleet effective cost} = N' \times \text{Candidate aircraft life-cycle cost} \quad (11)$$

or

$$\text{Fleet effective cost} = \frac{\text{Baseline fleet effectiveness}}{\text{Candidate aircraft cost effectiveness}} \quad (12)$$

Mission Effectiveness

Mission effectiveness is theoretical mission capability degraded by mission abort failures and unavailability. It is the product of mission availability, mission reliability, and mission capability.

Mission Availability

Mission availability is the probability that the aircraft will be available for a mission on demand. Rotor blade designs that increase maintenance burden or mean time to repair will increase aircraft down hours per flight hour and decrease mission availability.

Mission Reliability

Mission reliability is the probability that an available aircraft will be able to avoid a mission abort due to system failure.

Mission Capability

Mission capability is a measure of how well an aircraft can perform its intended missions. It is the mission effectiveness of a perfectly available, perfectly reliable aircraft. For transport aircraft such as the UH-1, mission capability is assumed to be the product of mission payload and mission block speed (productivity) expressed in ton-knots. A change in blade weight will cause a corresponding change in aircraft weight empty. For some missions, this will change mission payload. Changes in blade performance will change aircraft performance characteristics and may affect mission payload, mission speed, or both.

For any given mission, a change in aircraft characteristics may not always produce a change in mission capability. For example, the payload demand for the selected mission may not be limited by the takeoff payload capability of the aircraft. A decrease in weight empty would yield no significant benefit for such a mission. On the other hand, if gross weight limits payload or range capability, reduced weight empty offers a substantial mission payoff. To obtain a realistic evaluation of mission capability, a mission analysis program which simulates 1000 missions while varying payload demand, mission range, operating altitudes and temperatures according to expected probability distributions was used. This program is described in Appendix III.

Life-Cycle Cost

The life-cycle cost of an aircraft is the total cost generated throughout its service life. It is the summation of unit development cost, acquisition cost, and operating cost. Essentially, it is a measure of total user cost.

Unit Development Cost

Unit development cost is the total nonrecurring development cost of the

system amortized over the total number of aircraft procured. It is assumed that the basic nonrecurring costs of the UH-1 aircraft have already been fully amortized. Nonrecurring costs associated with different blade designs are amortized over the specified 10,000 blades to be produced and are included, for convenience, in acquisition cost.

Acquisition Cost

Acquisition cost is the sum of vehicle flyaway cost, initial spares cost, initial training and travel cost, and initial ground support equipment cost.

Vehicle Flyaway Cost

Flyaway cost is the direct cost of the aircraft without spares and includes the acquisition cost of two blades. Blade acquisition cost includes non-recurring investment for engineering design, engineering test, and manufacturing tooling amortized over 10,000 blades and recurring costs for manufacturing labor, materials, and recurring tooling. Material and labor requirements were estimated for the existing blade, and labor rates and overhead factors were adjusted slightly to yield the contractually specified \$3000 blade acquisition cost. These labor rates and overhead factors were used as a basis for evaluating the acquisition costs of the candidate blades.

Initial Spares Cost

Initial spares cost includes the cost of spares in inventory and in the supply pipeline. Blade initial spares are a function of blade replenishment rate and supply pipeline efficiency. It is assumed that blade initial spares are proportional to blade life-cycle replenishment spares. The proportionality factor was adjusted to yield the contractually specified 30% initial spares.

Initial Training and Travel Cost

This cost applies to direct personnel support of the aircraft and is assumed not to vary with blade design.

Initial GSE Cost

This cost covers the initial acquisition cost of ground support equipment and is assumed not to vary with blade design.

Operating Cost

Operating cost is the sum of replenishment spares cost, fuel and oil cost,

maintenance cost, flight crew cost, and replenishment GSE cost. It is the direct cost of operating the aircraft after acquisition for an entire life cycle.

Replenishment Spares Cost

Replenishment spares cost includes the cost of blade replacements demanded by scrappage and scheduled retirement. Blade damage rates, repairability, and retirement life directly impact on replenishment cost.

Fuel and Oil Cost

Fuel and oil cost over the service life of the aircraft is a function of average fuel flow. The impact of blade design on fuel flow is provided by the mission analysis program.

Maintenance Cost

Maintenance cost includes the cost of labor, materials, and shipping on the organizational, direct support, and depot levels. Blade design influences the repair, scrappage, and shipping rates in the blade logistics analysis. In addition, the cost factors such as material cost per repair, overhaul cost, and man-hour burden to repair are affected by blade design.

Flight Crew Cost

This cost is assumed not to vary with blade design.

Replenishment GSE Cost

This cost includes consumable tooling used in blade repair and is affected by the blade repairability scheme.

UH-1 BASELINE COST EFFECTIVENESS

Mission Capability

The mission analysis program described in Appendix III was used to establish the following:

Mission capability	50.344	ton-knots
Average mission fuel flow	533.4419	lb/hr
Average mission time	0.51945	FH

Mission Availability 0.7500

Based on a total of 4.3796 down hours per flight hour.

Mission Reliability 0.99224

Based on 0.015 mission abort failures per flight hour.

Mission Effectiveness 37.466 ton-knots

The product of the above mission parameters.

Ten-Year Life-Cycle Cost Per Aircraft

Baseline UH-1 life-cycle costs were estimated parametrically or assumed as follows:

Unit development cost	\$ 0
Flyaway cost	\$300,000
Initial spares cost	\$100,000
Initial training and travel	\$210,000
Initial GSE cost	\$37,000
Acquisition cost	\$647,000
Replenishment spares cost	\$150,000
Fuel and oil cost	\$53,000
Maintenance cost	\$255,000
Flight crew cost	\$480,000
Replenishment GSE cost	\$ 0
Operating cost	\$938,000
Life-cycle cost	\$1,585,000

Blade Life-Cycle Cost

Baseline blade life-cycle cost consists of the contributions made by blade characteristics to the aircraft life-cycle cost:

Blade contribution to flyaway cost	\$6,000
Blade contribution to initial spares cost	\$1,998
Blade contribution to replenishment spares cost	\$36,202
Blade contribution to maintenance cost	\$4,259
Blade contribution to replenishment GSE cost	0

Baseline blade 10-year life-cycle cost per aircraft \$48,459

Fuel and oil cost for the 10-year aircraft life can be computed on a system level from average fuel flow

Baseline fuel and oil cost = \$53,344

The nonvariable part of UH-1 10-year life-cycle cost becomes

$$LCC_{nv} = 1,585,00 - 48,459 - 53,344 = \$1,483,197 \quad (13)$$

The computation of 10-year life-cycle cost per aircraft for any candidate blade design can now be established:

Candidate life-cycle cost = \$1,483,197
+ Candidate blade life-cycle cost
+ System fuel and oil cost (14)

This specific approach is used in the cost-effectiveness model.

MATERIAL SELECTION

An assessment of the various materials available for rotor blade construction was undertaken at the start of the design study. The candidate materials were compared with respect to the cost per pound and are shown in Figure 4. The more conventional materials, such as aluminum, steel and "E" type fiberglass, are the obvious low-cost materials. Steel and aluminum can be obtained for \$1 per pound; the "E" glass varies in price considerably dependent on its form; the raw spool roving and resin are under \$1 per pound while the cost of preimpregnated "E" glass purchased in a woven cloth or lined ply form may be several times this amount.

Titanium sheet material would be about ten times higher in cost per pound than the conventional metals, aluminum and steel. Titanium usage in an expendable rotor blade can be justified only in very small quantities for blades which require both a high strength and high strain allowable material.

The "S" glass prepreg and woven fabric is five times more expensive per pound than the "E" glass in the same form. Therefore, since "S" glass properties are only 10 - 15 percent better than the considerably less expensive "E" glass, the use of "S" glass would not be cost effective.

The very high modulus to weight ratio materials such as carbon and boron composites are costly at the present time. However, the projected cost of carbon composites shows a very large potential for cost reduction in the late-1970 time frame. Increased usage of carbon composites and

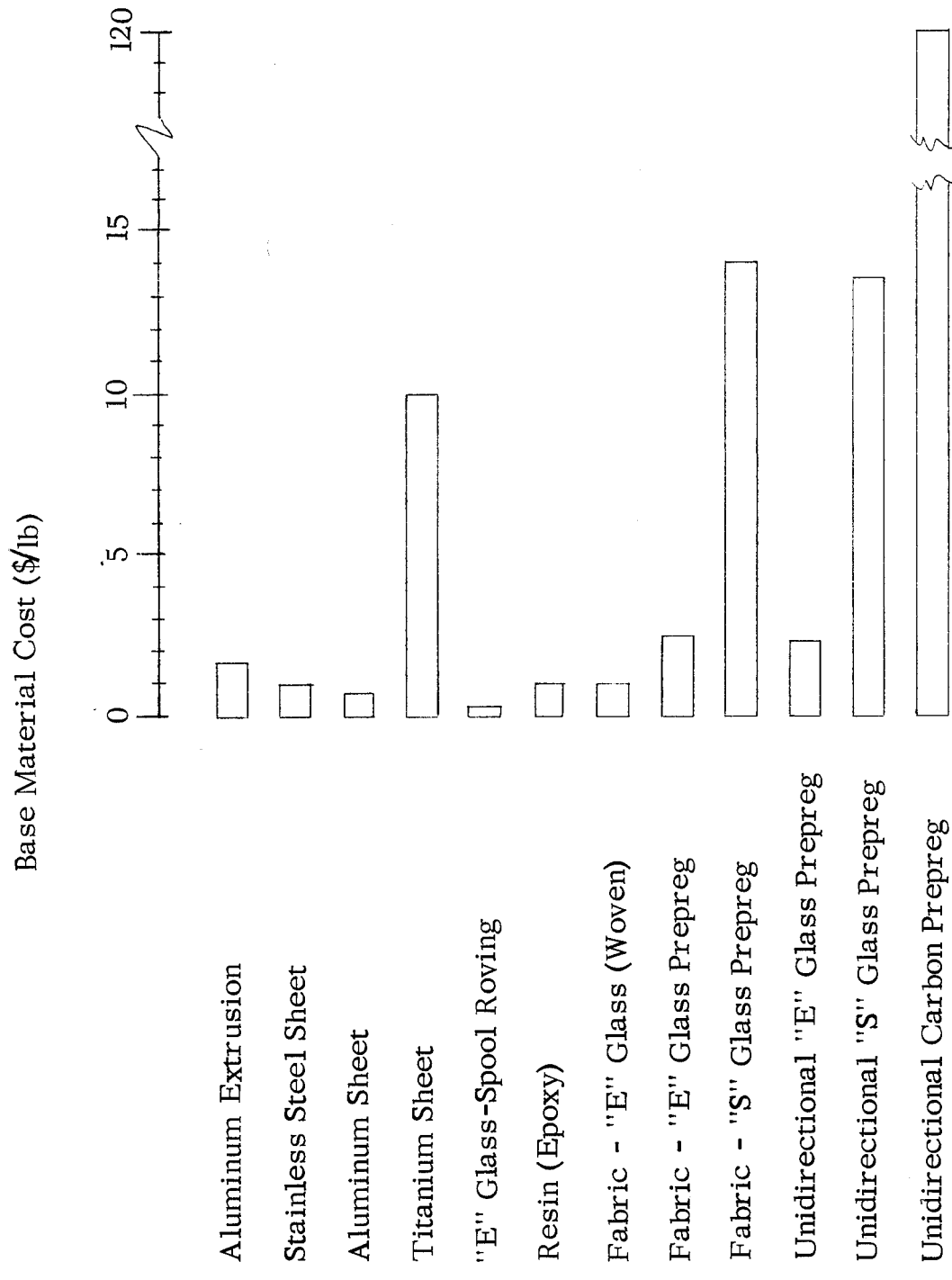


Figure 4. Material Cost Comparisons.

improvements in production methods could result in material costs of \$25.00 per pound. At this price level, a limited amount of carbon can be cost effective in an expendable rotor blade.

DESIGN CONFIGURATIONS

Six basic design concepts are considered in this study: an extruded aluminum spar (Configuration I), a rolled sheet metal blade of stainless steel and aluminum (Configuration II), a composite blade with a "D" shaped fiberglass and carbon spar with a fiberglass skin (Configuration III), a composite twin beam spar blade with a fiberglass spar and a carbon skin (Configuration IV), a composite twin beam spar design (Configuration V) similar to Configuration IV but having an automated pultrusion trailing edge skin, and an aluminum extrusion spar (Configuration VI) similar to Configuration I but also having an automated pultrusion skin. Each concept included many trade-off studies to optimize the design in such areas as spar chord, trailing edge construction and materials. Duplication of the basic UH-IH properties such as weight, stiffness and natural frequencies was the primary design criterion used for each of the design configurations.

CONFIGURATION I - AS-EXTRUDED SPAR

The final version of Configuration I is shown in Figure 5. It consists of a two-piece constant section aluminum spar with fiberglass composite trailing edge skins and spline. The skins are stabilized by a resin treated polyamide paper honeycomb (Nomex). The heavy leading edge of the spar is one of the features of this design. Providing a heavy leading edge in the spar eliminates the need for separate counterweights to mass balance the blade. The sidewalls of the spar were also increased to eliminate the side doublers. The heavy leading edge of the spar also provides increased erosion and foreign object damage tolerance because more material is available to blend out nicks and other damage in the leading edge. In addition, a polyurethane abrasion resistant coating is placed over the leading edge to further reduce erosion. The trailing edge fiberglass skins consist of "E" glass with two-thirds oriented at $\pm 45^\circ$ and one-third oriented at 0° to provide maximum shear strength in the skin for torsional rigidity and to resist the edgewise bending shears. At the trailing edge, a buildup of 0° glass fibers is used in the spline to provide edgewise bending stiffness. A plastic honeycomb was selected for the trailing edge core because it is more damage tolerant and less susceptible to corrosion than metal core.

Configuration I has a total of fifteen less components than the UH-IH. The two-piece spar replaces seven components consisting of two lead-

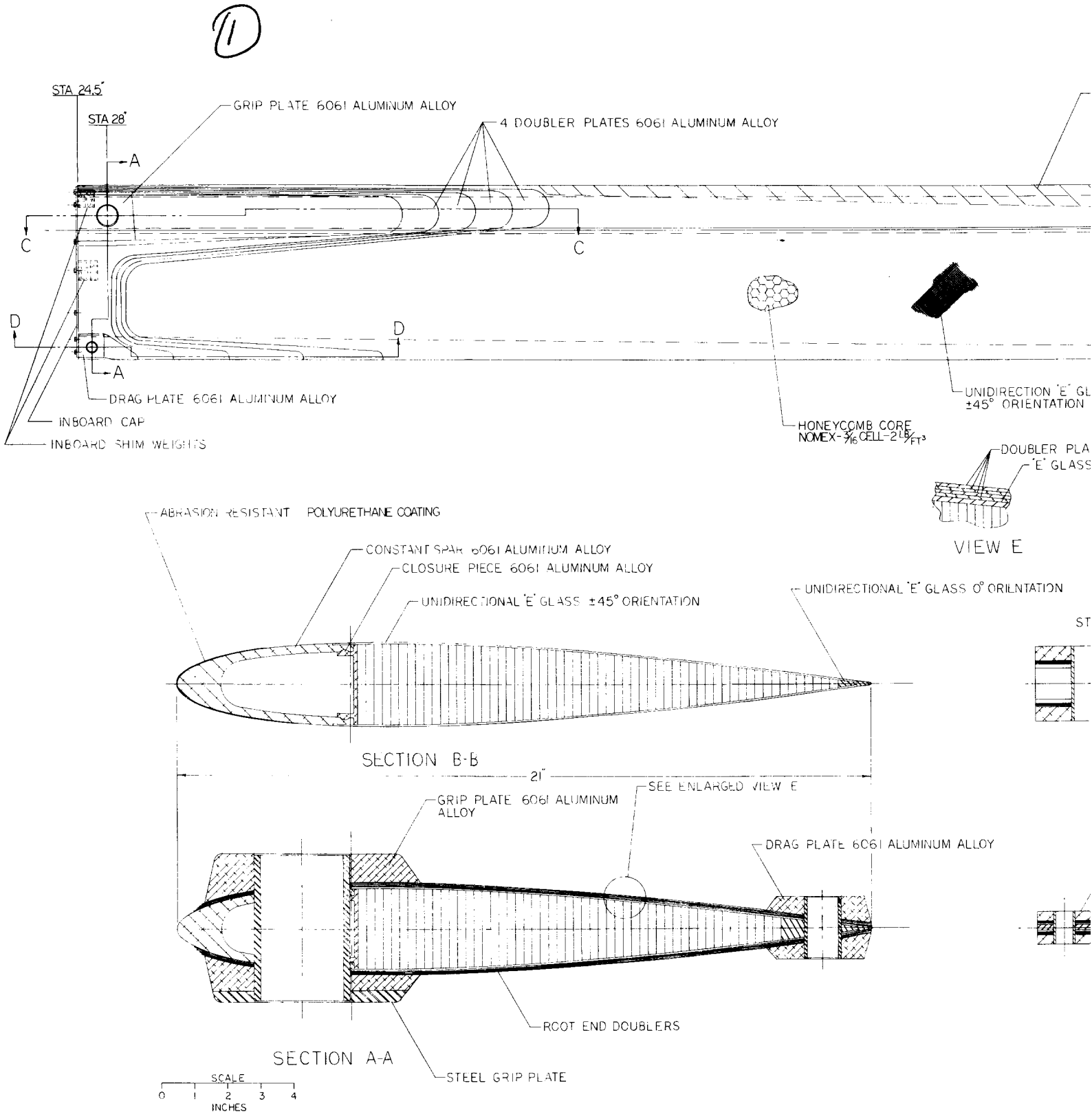
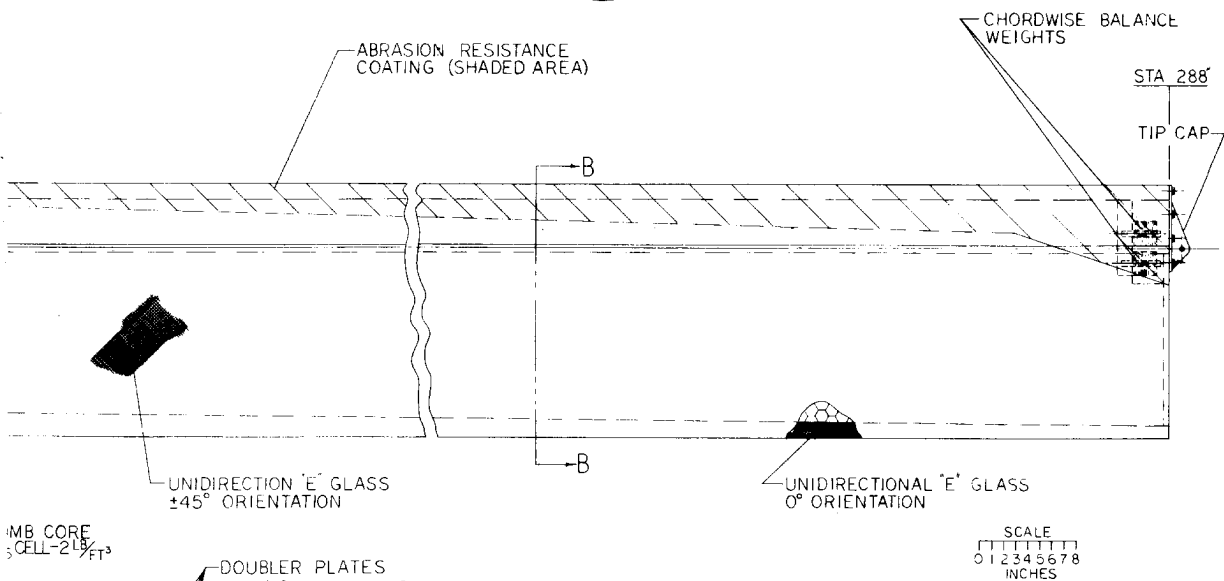


Figure 5. Configuration I.

(1)

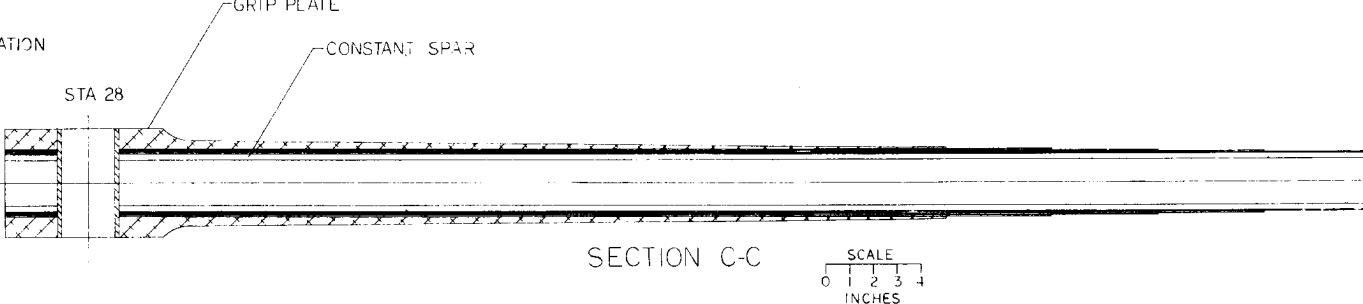


VIEW E

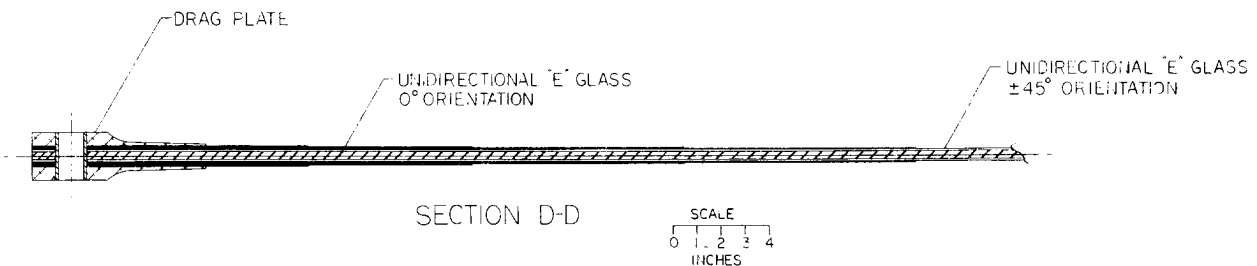
OPTIONAL 'E' GLASS 0° ORIENTATION

GRIP PLATE

CONSTANT SPAR



6061 ALUMINUM ALLOY



(3)

7



/ UNIDIRECTIONAL 'E' GLASS
±45° ORIENTATION

SKORSHY AIRCRAFT, Stratford, Connecticut

PRELIMINARY	
LAYOUT	
DRAWN BY	John A. Lippert
DESIGNED BY	John A. Lippert
STRUCTURE	John A. Lippert
EL. & MECH.	John A. Lippert
FABRICATION	John A. Lippert
DATE DRAWN 12-12-66	
MAKER 100-12-0000	
TITLE - AS EXTRUDED	
ALUMINUM FRAME DESIGN	
(CONFIGURATION E)	
SHEET - 1 - 1	

SD-40

ing edge counterweights, four spar doublers and the present spar. The polyurethane abrasion resistant coating replaces four additional steel and cobalt abrasion strips, and the root end is simplified by the removal of six doubler plates.

This configuration is enhanced over the present UH-IH design by (a) reducing the number of parts, (b) providing an as-extruded, machining-free extrusion and (c) increasing the repairability of the trailing edge by the incorporation of the fiberglass skins. The lower cost of Configuration I coupled with its higher repairability results in more cost-effective blade than the UH-1 for both 1972 and 1980, as shown in Tables XVI and XVIII.

This concept is a simplification of the present UH-IH blade, utilizing an aluminum extrusion as the primary structural member. The first design considered use of an open-ended "C" section with a very thick leading edge whose outer surface formed the contour of the airfoil over the forward 25 percent of the chord. This was combined with a structural trailing edge to form the blade as shown in Figure 6. This blade spar concept facilitates manufacture because the counterweights and side plate doublers are made integral parts of the spar, eliminating the fabrication and handling of separate components.

It was possible to closely match all of the important parameters of the UH-IH blade with the "C" spar except the torsional rigidity which was approximately two-thirds the required amount. Since torsional rigidity is very important in the performance and stability of a blade, it was improved by closing the open end of the "C" spar with an extruded aluminum closure piece across the open legs of the spar (Figure 7). This increased the torsional rigidity to the same level as the UH-IH blade.

Since the open end of the spar required closing the torsional rigidity, a hollow (one-piece) extrusion was investigated as an alternate to the two piece spar extrusion cited above. The study showed that closer tolerances could be held on the open "C" section and it could be assembled as-extruded with a minimum of machining. Tolerances ranged widely on the hollow extrusion because of the difficulty of extruding a spar section having a heavy nose and a thin backwall. The asymmetric hollow extrusion tends to shift the mandrel out of position during the extrusion process, causing poor dimensional control resulting in considerable machining in the final process. The base cost of the hollow section extrusion was double the "C" section; also, because of the additional labor required for machining the hollow extrusion, the total cost was tripled over the "C" section. On this basis, the "C" section with the closure piece was considered the most cost effective for the design. The trailing edge portion of the blade is a structural fairing which completes the

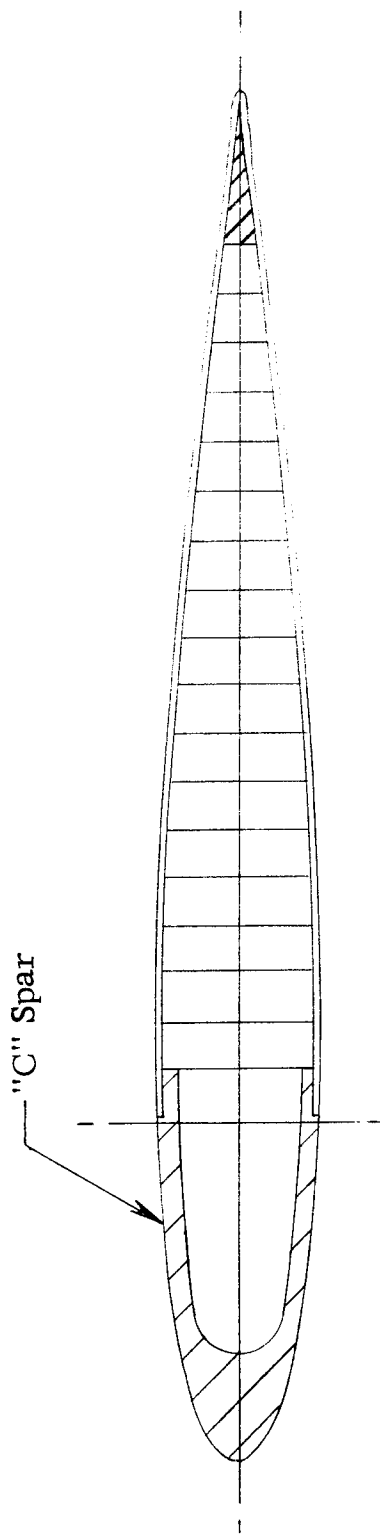


Figure 6. "C" Spar Blade

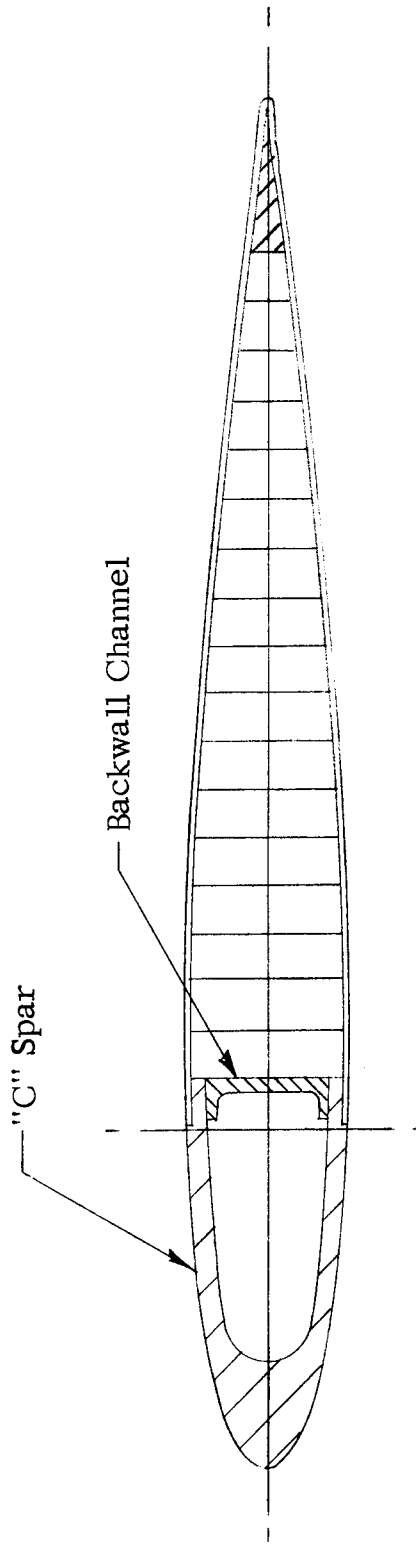


Figure 7. "C" Spar Blade With Backwall Channel.

chordwise airfoil contour aft of the spar. For high repairability and ease of field replacement, segmented pockets approximately 1 foot wide are preferred for the trailing edge. However, the major portion of the blade's inplane stiffness is provided by this trailing edge structure; therefore, it must be continuous and strong as well as light in weight. Various types of construction and materials were considered for supporting and stabilizing the trailing edge skins. A study was made to determine whether a honeycomb core or a rib-type construction would be the most cost effective. The rib-type structure and honeycomb structure were found to weigh about the same amount. However, the close rib spacing required to develop the necessary skin panel strength resulted in higher cost for producing the rib-type structure (Appendix I), since many more parts must be produced and considerably more man-hours are required for assembly. The study also showed that the honeycomb is more repairable than metal or fiberglass ribs because honeycomb can be repaired by simply injecting foam or bonding a new core section in place (see Appendix II).

Foam was another consideration. Foam is desirable in small quantities in areas where it is difficult to assemble or where the shape of the structure is irregular and complicates the machining of the honeycomb. A foam-in-place is ideal for this type of design. The foam also has the advantage of being less expensive than the honeycomb, and its repairability is excellent. However, to obtain the same stability and compressive strength as the honeycomb, a high density foam 25 to 30 pounds heavier than the honeycomb presently used in the blade is required. This increase in weight by itself would not be totally undesirable; it is the additional 50 to 60 pounds of counterweight required in the leading edge to mass balance the blade about the feathering axis which results in a total blade weight increase of 75 to 90 pounds which is not acceptable.

The material for the skin and the trailing edge spline was chosen after evaluating aluminum and fiberglass. Aluminum provided a trailing edge structure that was 8 pounds lighter in total blade weight to produce the same blade stiffness. Cost of the aluminum structure was also somewhat lower than the fiberglass structure. However, when the overall cost effectiveness of the two materials was considered, the fiberglass proved to be more cost effective. Fiberglass provides a higher degree of repairability in the field and also operates at much higher margins of safety than the aluminum. Because of these attributes, more trailing edge damage is repairable in the field and the number of spares required is reduced.

The fiberglass trailing edge structure could be fabricated several ways. One method is by vacuum-injection molding; this is a method of laying

up cloth (without resin) in a half-mold which has the curvature of the airfoil contour. After completion of cloth layup, a mating half-mold is securely fastened and sealed into position. Resin is injected at one end of the mold while a vacuum is drawn on the other end. The amount of resin can be closely controlled to uniformly permeate the cloth to obtain good repeatability of resin content. This method is more applicable for fabricating whole sections or assemblies; for example, a complete trailing edge section containing fiberglass ribs along with the skin or layup of an entire blade. However, for either design, there is a requirement for considerable hand layup and the process does not appear feasible for automation; therefore, it is relatively costly.

Another version would be to automate the skin layup by designing machinery for the application. The skin plies could be produced in a skin mold utilizing automated tape laying equipment; in this process, a machine with the appropriate tape on a roll travels over the required length of the skin mold laying down plies of prepreg. Microswitches to control lateral and longitudinal motion and automatic cutoff and shutdown of the tape and equipment at the completion of tape layup would be designed into the mechanism to obtain complete automation. This present state of the art method was selected for this design.

Filament winding is another method. The filament on a spool is coated with resin as it is wound onto a tooling cylinder whose perimeter and length are equivalent to the dimensions of two side skins of the trailing edge. The process is completely automated so that filament can be wound back and forth, at $\pm 45^\circ$, on the cylinder. After completion of filament winding, while still in the wet layup, the skin is cut in two pieces and laid in skin molds for curing at a specified time and temperature. This process is presently being used very successfully.

The above methods outlined for fabrication of the skin can be applied to the fiberglass spline; however, the spline with its longitudinal "E" glass and constant solid section is adaptable to the pultrusion method. In this process, filaments on spools are dipped in a resin and are pulled through a spline shaped die. Since the filaments are of an indefinite length, the process is a continuous operation fabricating approximately fifteen parts per hour and reducing shop cost to a minimum. The pultrusion process fabricates a constant cross section; however, the spline can be varied in cross section by machining the outboard end to the desired taper.

The study showed that the constant outboard section of the blade accounted for approximately 80% of the total cost; therefore, primary design effort was to reduce cost in this area. However, some investigations were also

made of the blade root end to determine if a more cost-effective design could be obtained by simplifying parts or reducing machining and assembly shop hours.

Figure 8 shows one side of the present UH-1H root end; it consists of a number of thin sheets and one thick forging plate arranged in a stacked fashion to obtain a smooth transition in cross-sectional area, increasing from the constant outboard section to the inboard end of the blade. Figures 9 through 13 show various concepts ranging from a completely laminated built-up section (Figure 9) to a one-piece aluminum die forging (Figure 11). Another was a spar extrusion with an enlarged or upset end (Figure 10) to provide the necessary increase in cross sectional area. Two approaches similar to the present design were: Figure 12, which replaced the aluminum doublers with fiberglass layup while retaining the same grip plate, and Figure 13, which eliminated some of the doublers by extending the grip plate.

Figure 9 removed the need for machining by eliminating the forging, but it was less cost effective because the additional pieces increased (a) the shop hours for assembly, (b) the amount of adhesive required for bonding, and (c) failure modes. The initial cost of the spar extrusion of Figure 10 was found to be costly, and the poor tolerance control on the extrusion required additional machining expense. Figure 11 simplified assembly by replacing all root end components with a one-piece forging on each side. However, experience has shown that it is not good practice to bond thick pieces together because of the need of extremely close tolerances on the mating parts to provide a good bond joint. These close tolerances result in costly fabrication and the possibility of a high rejection rate of out-of-tolerance parts. Figure 12 consists of a layup of fiberglass prepreg molded with a flat surface as shown to facilitate machining and subsequent bonding of the aluminum grip plate. The study showed that simplification of the grip plate did not offset the additional cost of the fiberglass material or the increased assembly time of the fiberglass layup and was therefore less cost effective. Figure 13 is the most similar to the UH-1H design; however, it was simplified by eliminating a total of six doublers while slightly extending the present drag plate. It was shown to be slightly more cost effective than the UH-1H and was selected as the final root end configuration.

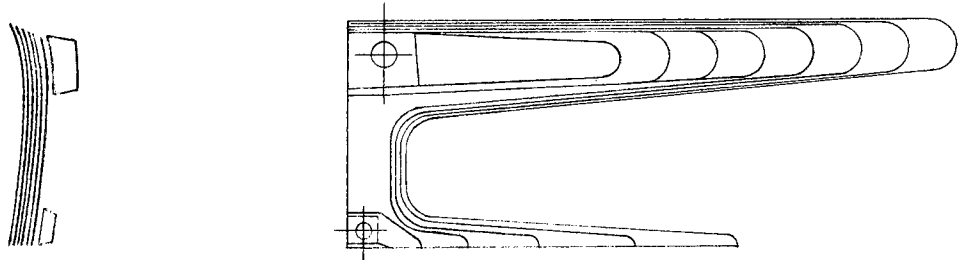


Figure 8. UH-1 Root End.

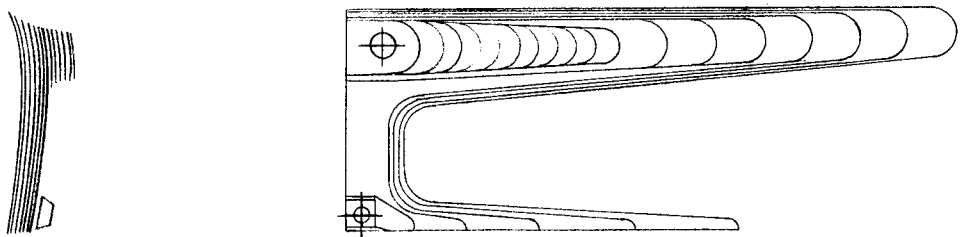


Figure 9. Aluminum Laminates Root End.

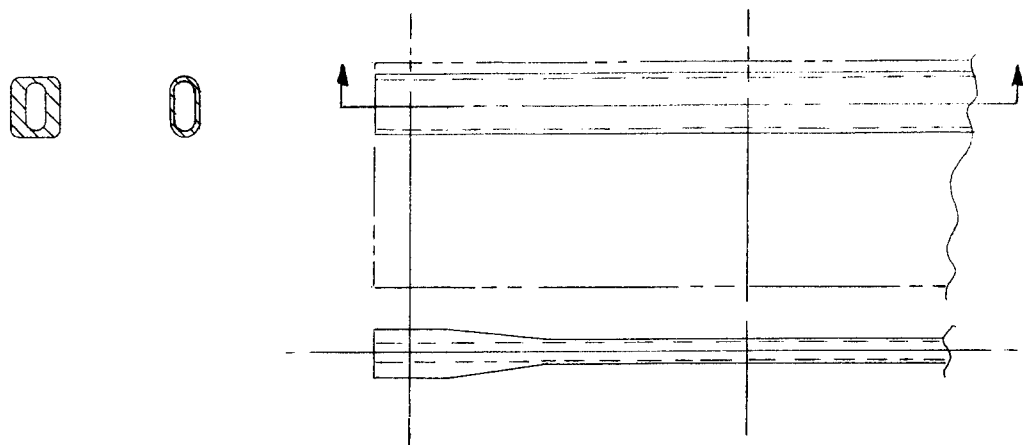


Figure 10. Stepped Extrusion Root End.

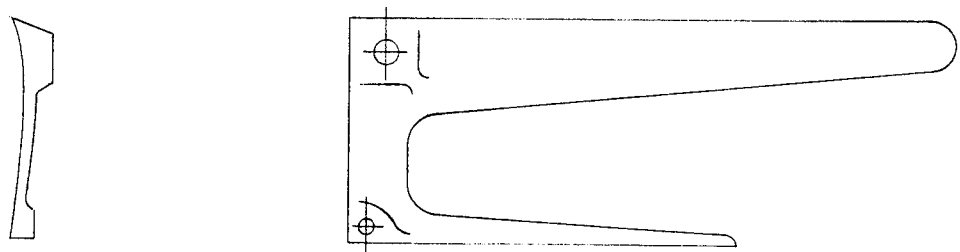


Figure 11. Solid Aluminum Root End.

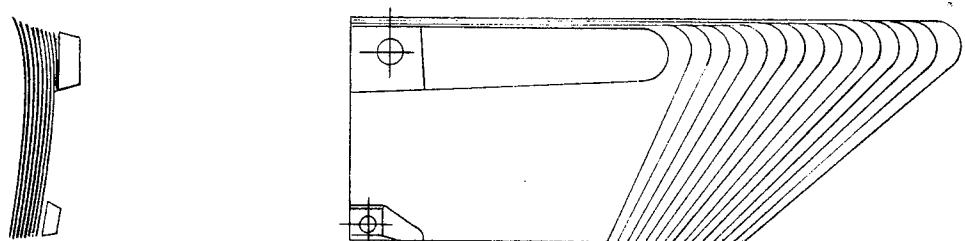


Figure 12. Fiberglass Laminates Root End.

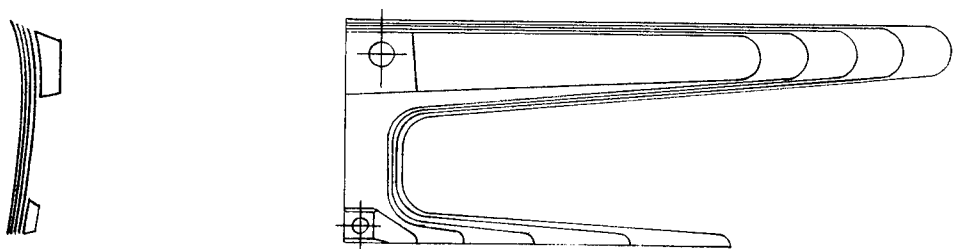


Figure 13. Reduced Doubler Root End.

CONFIGURATION II - SHEET METAL ROLL-FORMED SPAR

Roll-formed stainless steel plate and aluminum sheet are utilized in this concept to build up a bonded spar cross section. The low cost of aluminum and steel sheet material coupled with the opportunity for a highly automated production line are attractive features of this design concept.

Flat plate stock on a continuous roll and of the required thickness is processed through a multiple stage rolling mill. This is a process, as shown in Figure 14, where the material is passed through roll stands, equipped with contoured roller dies, and formed by stages into an ultimate desired shape. The process produces parts which can be held to very close tolerances. After forming, each component is cut to required length with an automatic cutter coordinated to the stage rolls. These cut-off machines can cut formed metal with minimum distortion and in most cases into lengths close enough to specification that no further cutting or trimming is required. This is a high-speed process; the equipment operates at 50 feet per minute producing approximately 100 parts per hour, resulting in extremely low fabrication cost.

After all sections have been formed, the parts are assembled by stacking the three components together after automated tape laying equipment has applied adhesive to the surfaces to be bonded, as shown in Figure 15. Blade twist is built into the spar during the assembly operation; the open-ended sections are easily twisted prior to bonding and are locked in the twisted condition forming a closed tubular structure after adhesive curing.

The steel leading edge of the spar is made sufficiently thick to provide the counterbalancing moment required to balance the outboard portion of the blade without additional balance weights. This feature reduces the number of blade component parts by making leading edge counterweights unnecessary.

Since a trade-off study for Configuration I showed that a combination of fiberglass skin, fiberglass spline, plastic honeycomb and the simplified root end design of Figure 13 were the most cost effective, these concepts were also used for Configuration II, as shown in Figure 16. The combination of roll forming the spar and tape laying of the fiberglass skins resulted in almost a completely automated blade. The cost model study showed this configuration to be slightly less cost effective than Configuration I but more cost effective than the UH-IH blade for both 1972 and 1980, as shown in Tables XVI and XVIII.

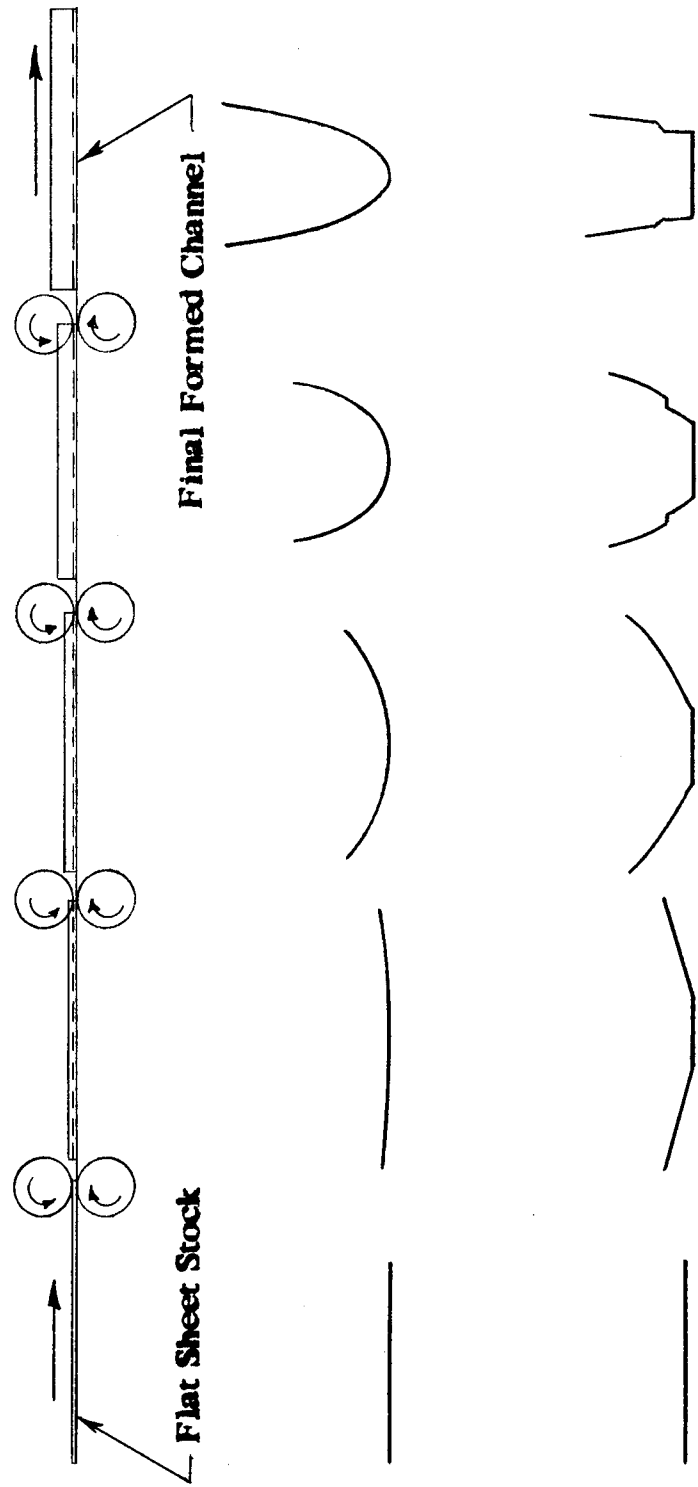


Figure 14. Roll-Formed Schematic.

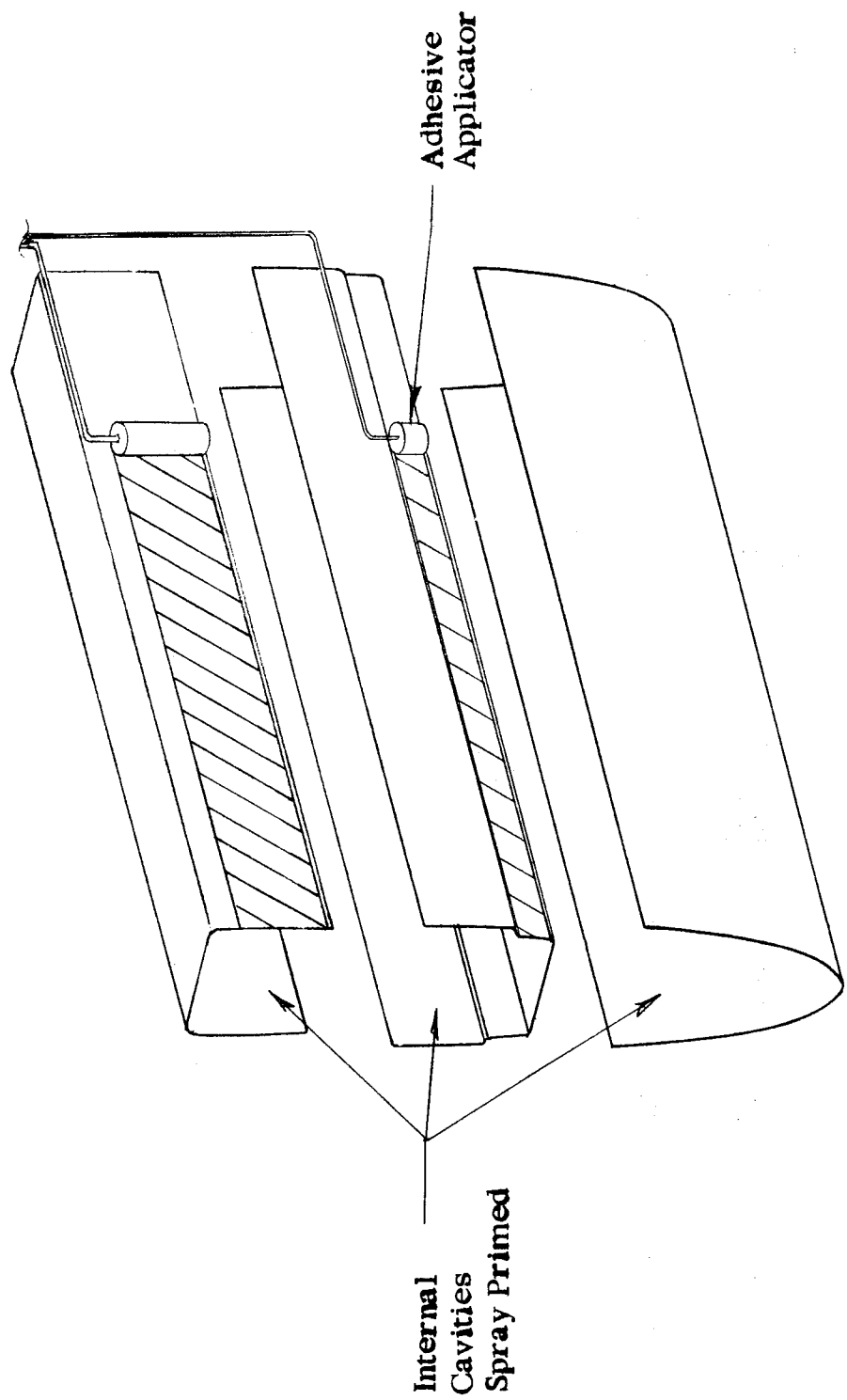


Figure 15. Roll-Formed Spar.

(1)

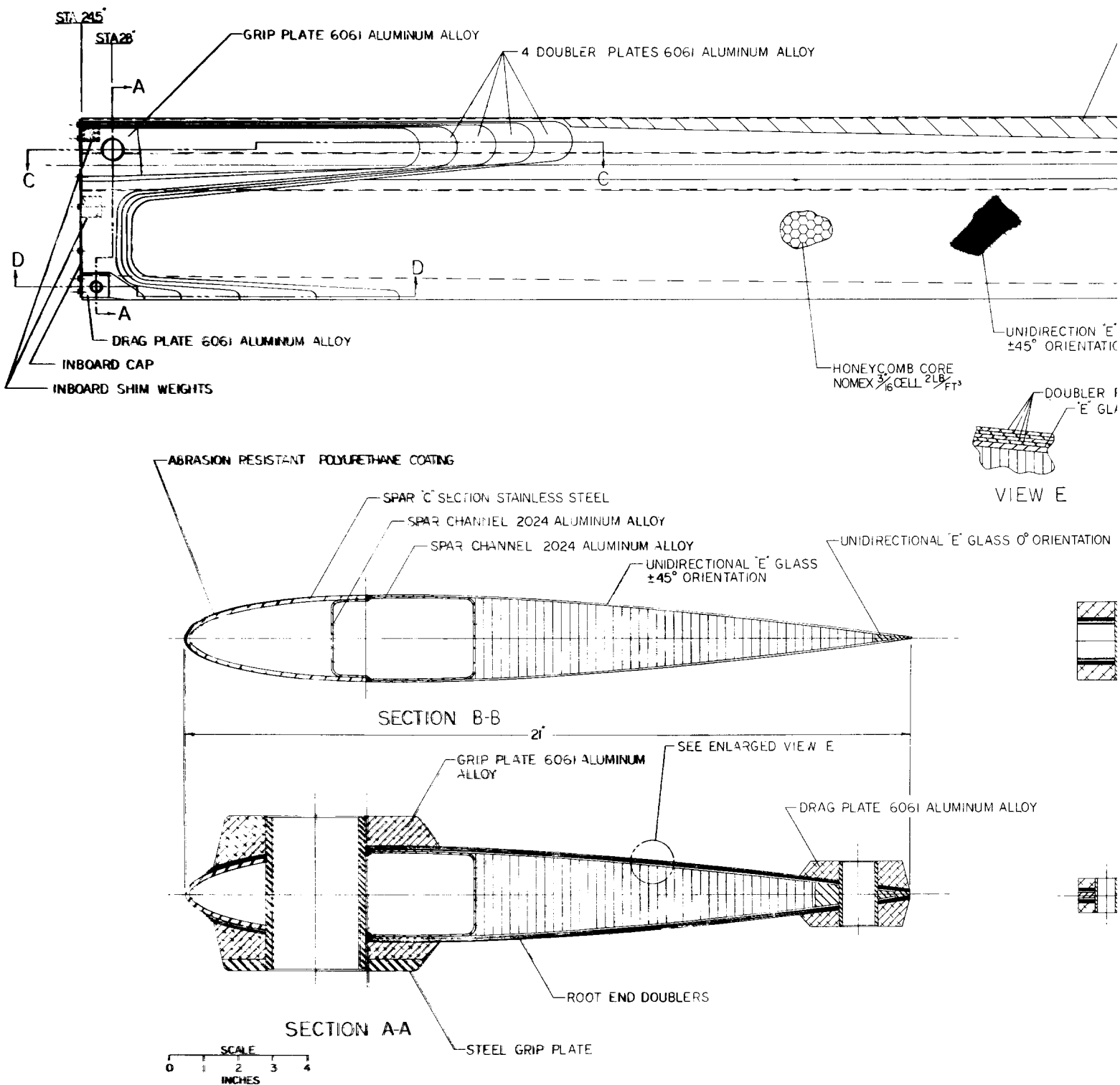
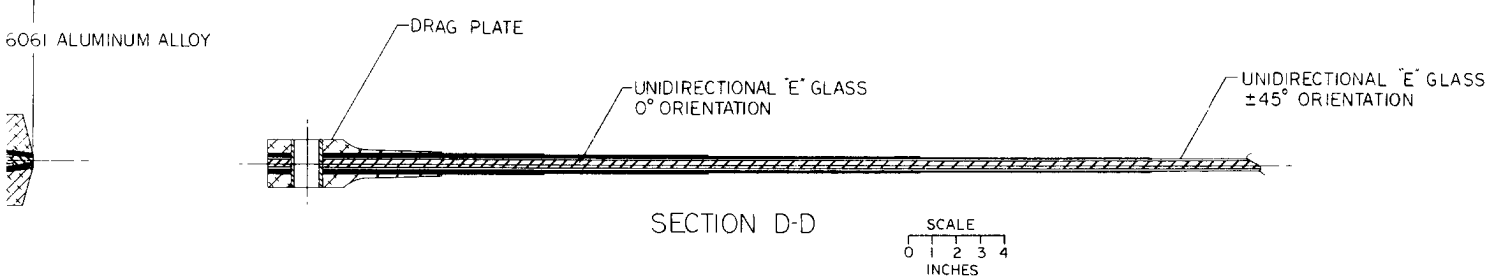
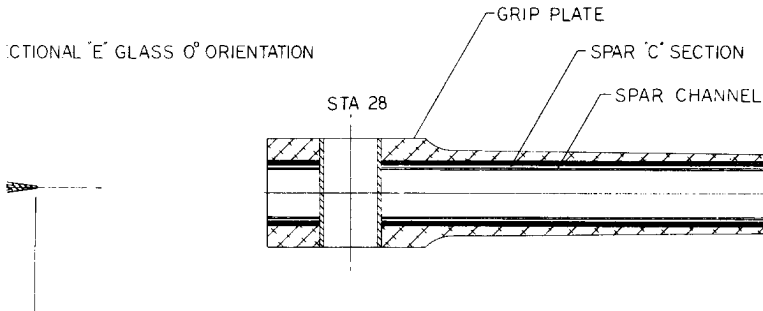
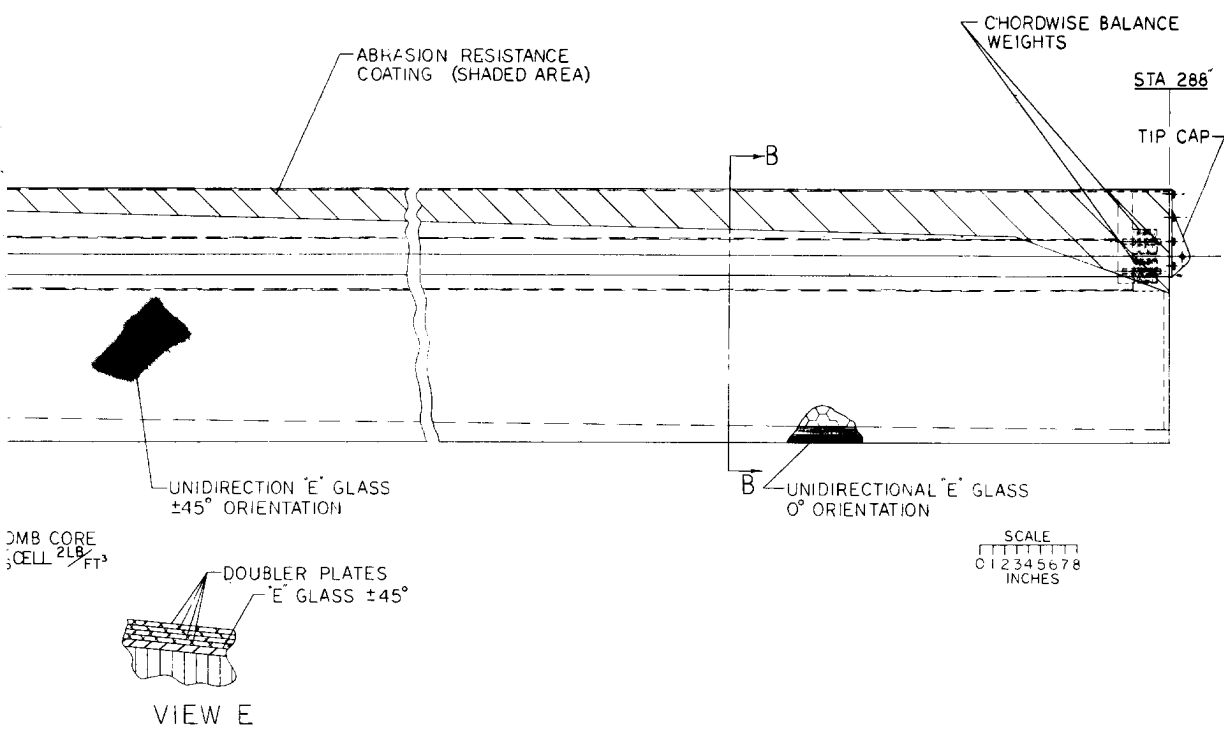


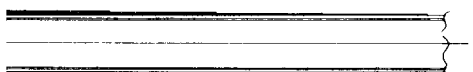
Figure 16. Configuration II.

(2)

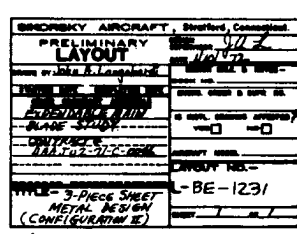


3

7



✓ UNIDIRECTIONAL "E" GLASS
±45° ORIENTATION



CONFIGURATION III - FIBERGLASS TUBULAR SPAR

A "D" shaped tubular type spar made of fiberglass and carbon was considered for Configuration III as shown in Figure 17. The use of a carbon composite in an expendable rotor blade would not seem justifiable in view of the high material cost. However, to provide the required torsional and edgewise stiffness and also to maintain the required weight, a high modulus fiber composite must be used. Projected reductions in the cost of carbon, coupled with improvements in the rotor blade performance capability and the opportunity for a highly automated fabrication technique, should result in a cost-effective solution.

Unidirectionally oriented "E" type fiberglass is the primary spar material since it provides the maximum spanwise stiffness and strength at the minimum per-pound cost. Carbon fibers oriented at $\pm 45^\circ$ to the spanwise axis are wrapped around the fiberglass spar to provide the maximum torsional rigidity. The airfoil contour is completed by a fiberglass skin which encloses the spar and extends to the trailing edge of the blade. A unidirectionally oriented fiberglass spline, located inside of the skin at the trailing edge, is used to increase the inplane stiffness of the blade. Nomex honeycomb core is used to support the skin aft of the spar. A polyurethane coating is applied to the leading edge portion of the skin to provide abrasion protection.

The spar configuration was chosen to provide the maximum torsional rigidity for a minimum weight of material. A tubular type structure is the most efficient member for transmitting torsional loads and was therefore selected for study. The chordwise dimension of the spar was determined by conducting a study to find the most efficient percentage of the blade chord to make the spar. The study showed that both torsional stiffness and the flatwise bending stiffness were a maximum for a given amount of spar cross-sectional area when the spar was 55-60 percent of the blade chord. This is illustrated in Figure 18 which is a plot of spar chord as a percentage of blade chord vs the reduction in stiffness from the peak values obtained at 55-60 percent chord. For our design we used a spar chord of 50 percent, a value close to the peak but which still approximately maintains the mass balance at 25 percent chord without the use of any additional counterweights.

The unique feature of this design concept is the method of producing the spar tube. Present state-of-the-art fabrication techniques for producing a tubular type spar from composites involve a layup of material around a mandrel. The required thickness of material is built up on the mandrel one ply at a time, possibly by automated tape laying equipment. The finished layup is then cured under heat and pressure to produce the finished spar. When a large number of plies are used, the process can

be lengthy even by using tape laying automation.

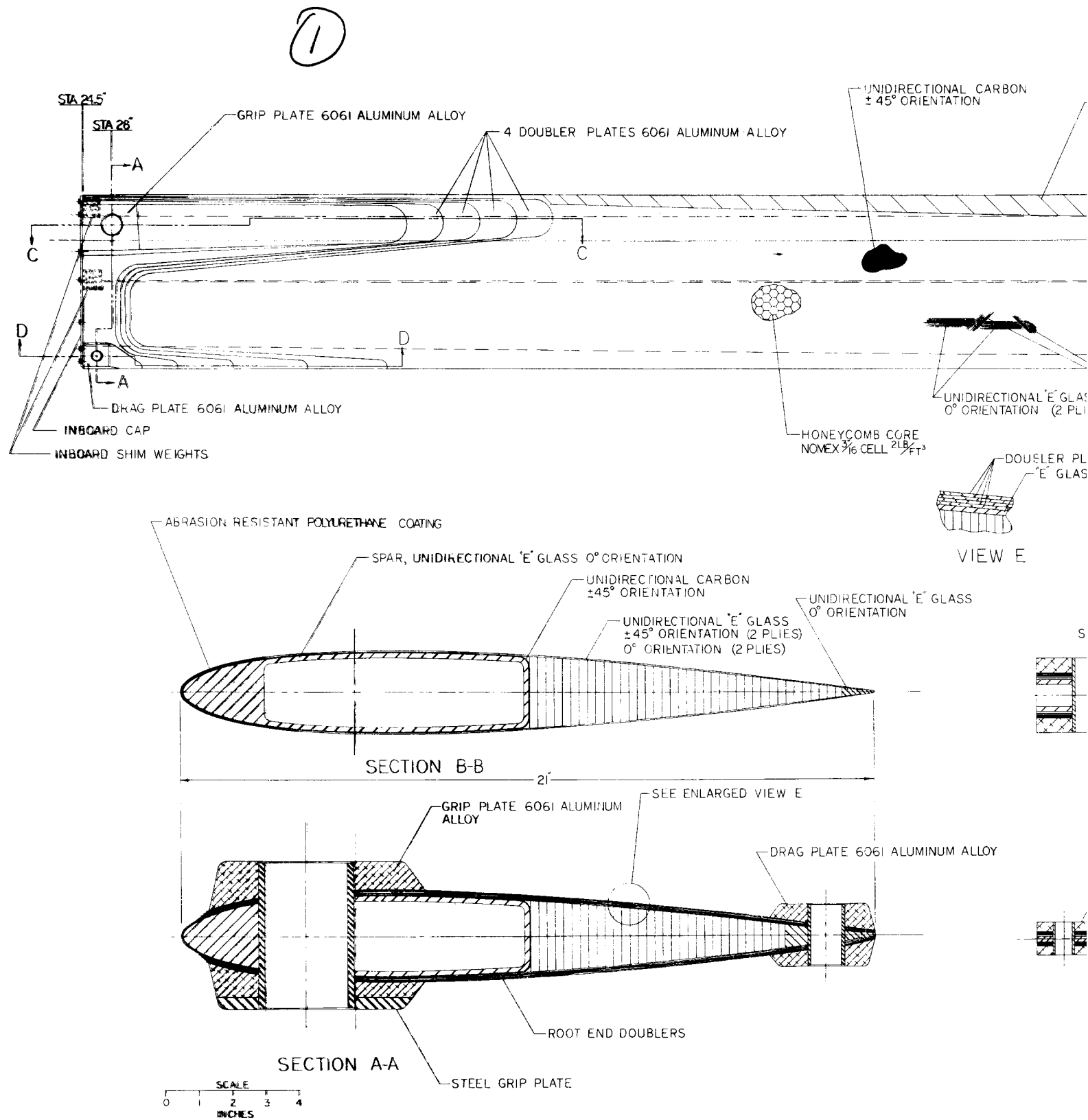
We propose the pultrusion method of producing a hollow composite spar. Because the spar is relatively thick in cross section and composed principally of fibers running axially (a configuration lending itself to the pultrusion technique), the risks involved in pultruding the spar are minimal. However, the control of contour tolerances possible with the pultrusion process for a hollow section is probably not sufficiently accurate at this time to produce a spar to finished dimensions. Also, twist must be molded into the spar since it cannot be warped into the twisted shape after complete curing. The solution to both of these problems is to final form the spar after the extruding process. A closed heated die, made to the final spar contour and including required spar twist, is used to final form the spar. Since it is possible to soften most epoxy resins after they have been partially cured by applying heat, the partially cured spar pultrusion could be placed in the die for the small adjustments in shape and twisting required. An inflatable bag would be placed inside the spar to force it against the die surface while the die was heated and the spar brought to a fully cured condition.

The fiberglass skins and trailing edge spline can be fabricated by the methods outlined for Configuration I. Final assembly of the various components is an adhesive bonding operation, very similar to present blade assembly procedures. A half airfoil section mold is used as the assembly fixture. Components are assembled in the mold with adhesive film between each part. A vacuum is drawn on a pressure bag placed over the blade assembly, and the bonding operation is performed in an autoclave under applied heat and pressure. The root end is a laminated structure similar to those described for Configurations I and II.

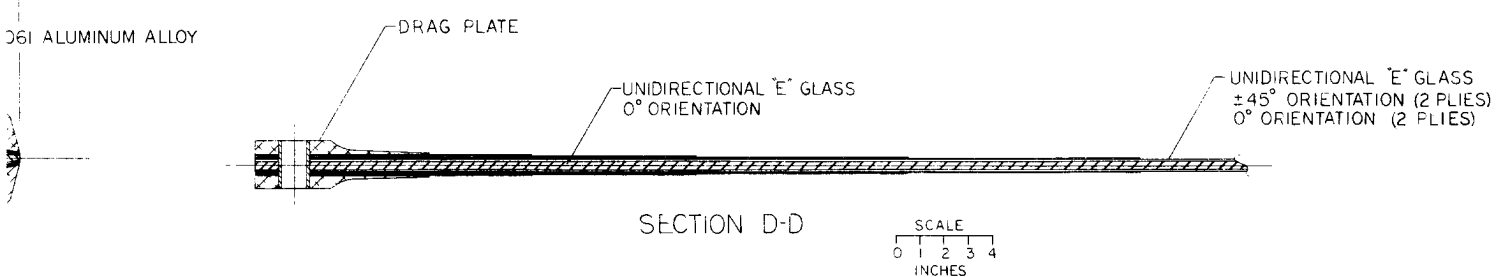
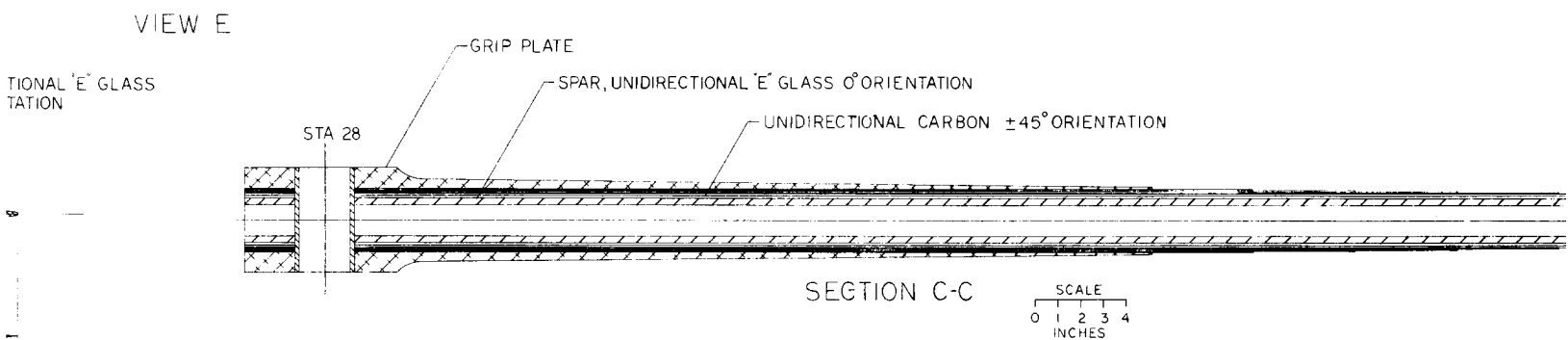
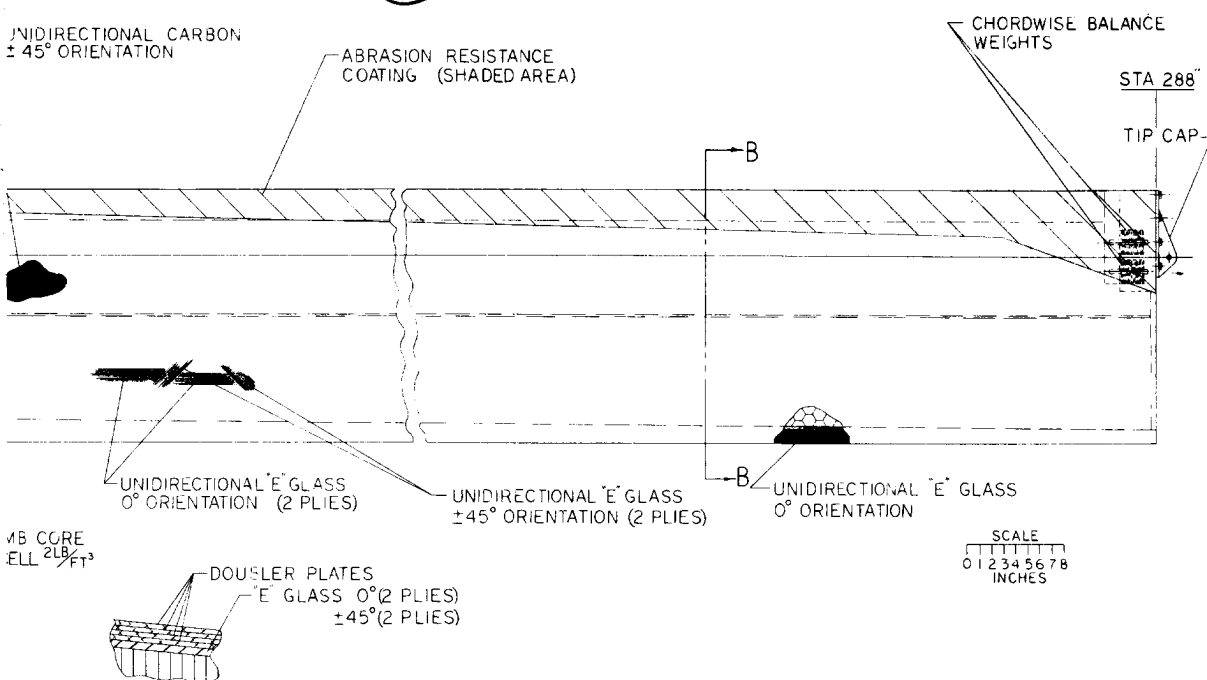
The present high cost of high modulus material for this configuration resulted in a less cost effective (Table XVI) blade than the UH-1 blade for 1972. Reduced carbon prices as forecasted for 1980 indicate that this configuration will be more cost effective than the UH-1H for that time frame, as shown by Table XVIII.

CONFIGURATION IV - FIBERGLASS TWIN BEAM SPAR

A fiberglass twin beam spar (Figure 19) with a full chord width outer carbon skin to form the airfoil contour was investigated as Configuration IV. The twin beam spar is composed of an upper and a lower spar beam separated by a honeycomb core. The spar beams are constructed of "E" type fiberglass oriented at 0°. The material is low in cost and has excellent strain allowable properties which enable the spar to withstand much higher blade deflections without damage than an equivalent metal spar. This "reserve strength" capability of the fiberglass spar provides



(2)



(3)



~ UNIDIRECTIONAL "E" GLASS
±45° ORIENTATION (2 PLIES)
0° ORIENTATION (2 PLIES)

SIKORSKY AIRCRAFT, Stratford, Connecticut	
PRELIMINARY LAYOUT	
DATE 7/17/85	
DRAWN BY John A. Campbell	DESIGNER'S SIGNATURE
DESIGNER'S TITLE	
TELEPHONE NUMBER	
FAX NUMBER	
SOMMERS, R.	
TMA 102-7122-0002	
DRAWING NUMBER	
LAYOUT NO.	
TITLE - 70" SHAPED	
FIBERGLASS SPAR DESIGN	
(CONFIGURATION 3)	
SHEET 1	

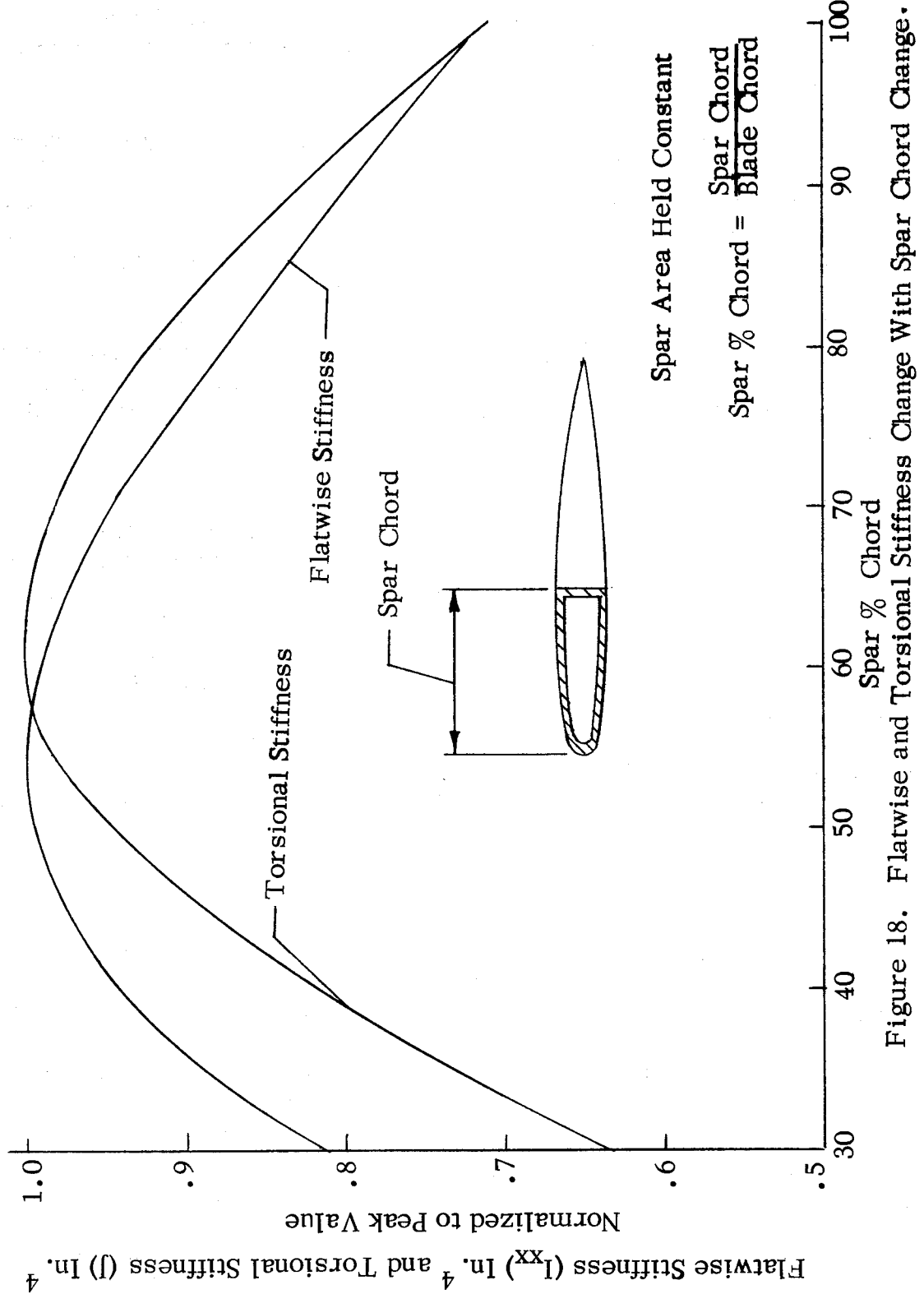


Figure 18. Flatwise and Torsional Stiffness Change With Spar Chord Change.

an increased margin of safety in the event of projectile-induced spar damage. The twin beam concept has the potential of being a fail-safe spar design with redundant load paths, since either spar beam may be severed and the remaining spar beam and skin will carry the centrifugal and bending loads.

The simple design of the spar beam lends itself to a highly automated type of fabrication. The constant cross section of the spar from the tip end to the root end of the blade makes two different construction methods feasible. Automated tape laying machinery can be used to lay the fiber-glass preimpregnated tape into a mold. The layup is then cured in an autoclave producing finished spar beams molded to the required contours. An alternate method of spar fabrication which is even more attractive than the molded spar is the pultrusion process previously mentioned to fabricate the fiberglass spar and spline. The predominantly axial orientation of the spar fibers is particularly well suited to the automated continuous nature of the pultrusion type process and should produce a spar beam of high quality and low cost.

The skin must provide the torsional rigidity for the blade, since both the fiber orientation and configuration of the spar do not provide very much torsional stiffness. Carbon fibers in the skin are oriented at $\pm 45^\circ$, the orientation at which the maximum torsional rigidity will be obtained. One-third of the skin is comprised of unidirectional "E" fiberglass to improve laminate strength properties, based on materials testing at Sikorsky Aircraft. The complete wraparound skin is fabricated by two female molds provided with the blade twist and is split on the chord line so that the upper and lower halves of the skin are molded separately. In this operation, the preimpregnated carbon and fiberglass tapes are laid in the mold by automated tape laying equipment and then cured in an autoclave.

The trailing edge spline and the leading edge skin have carbon fibers oriented at 0° and are both adaptable to the pultrusion process. Both these components would be fabricated in half sections by splitting on the chordline to facilitate subsequent assembly and machining operations.

The blade is assembled in two halves as shown in Figure 20 by placing the previously cured skin, spar beam, leading edge doubler, trailing edge spline and Nomex core into the same skin molds prepared with structural adhesive. Each half of the assembly is bagged and cured in an autoclave and then machined flat on the chordline and finally both halves are bonded together into one assembly. A splice cap is bonded over the leading edge skin to provide a means for shear transfer across the joint.

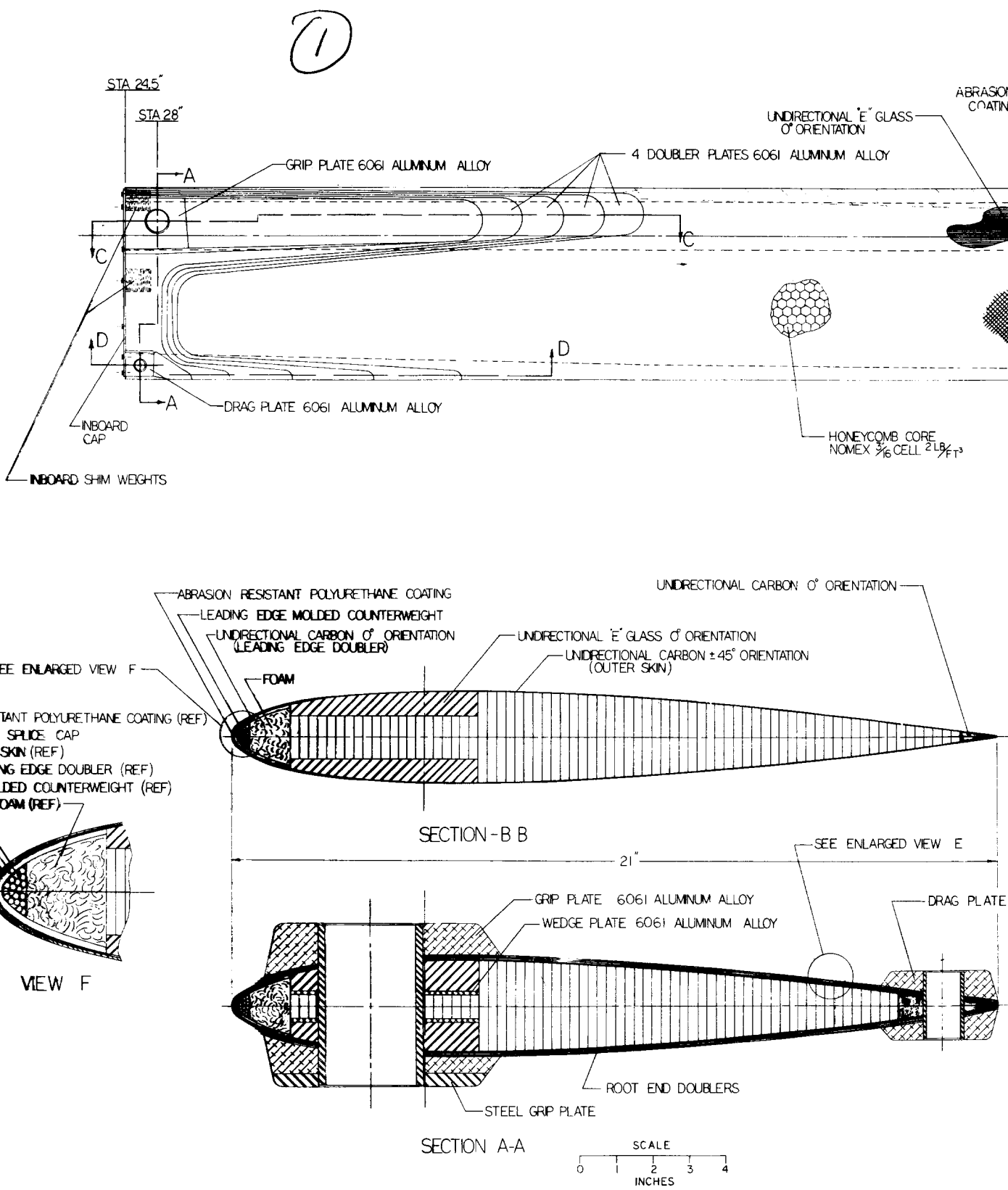
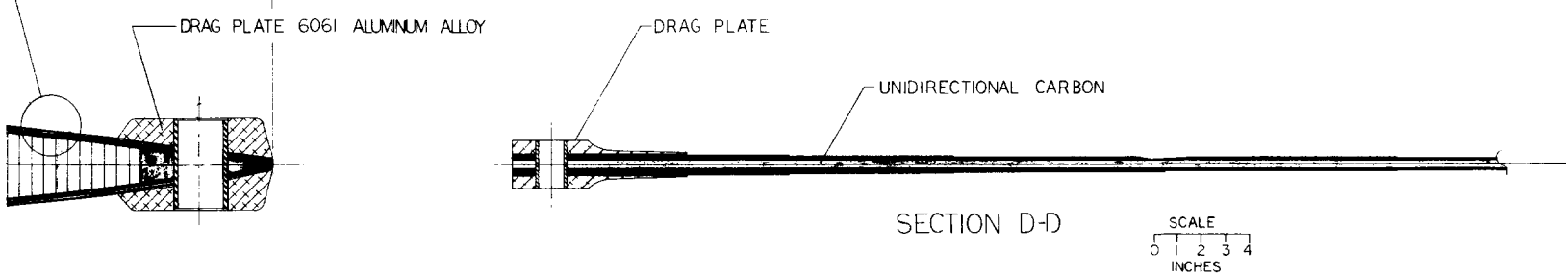
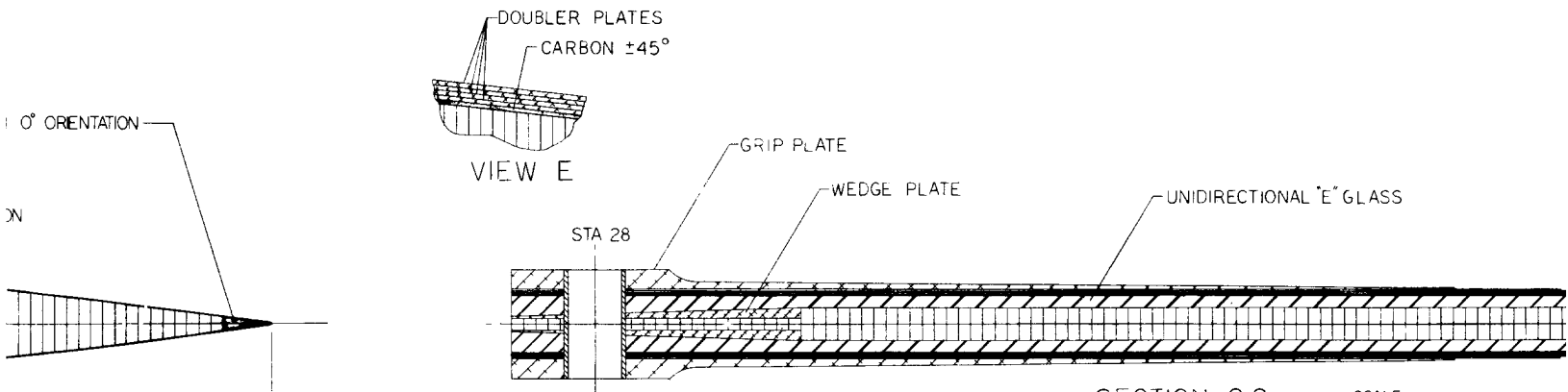
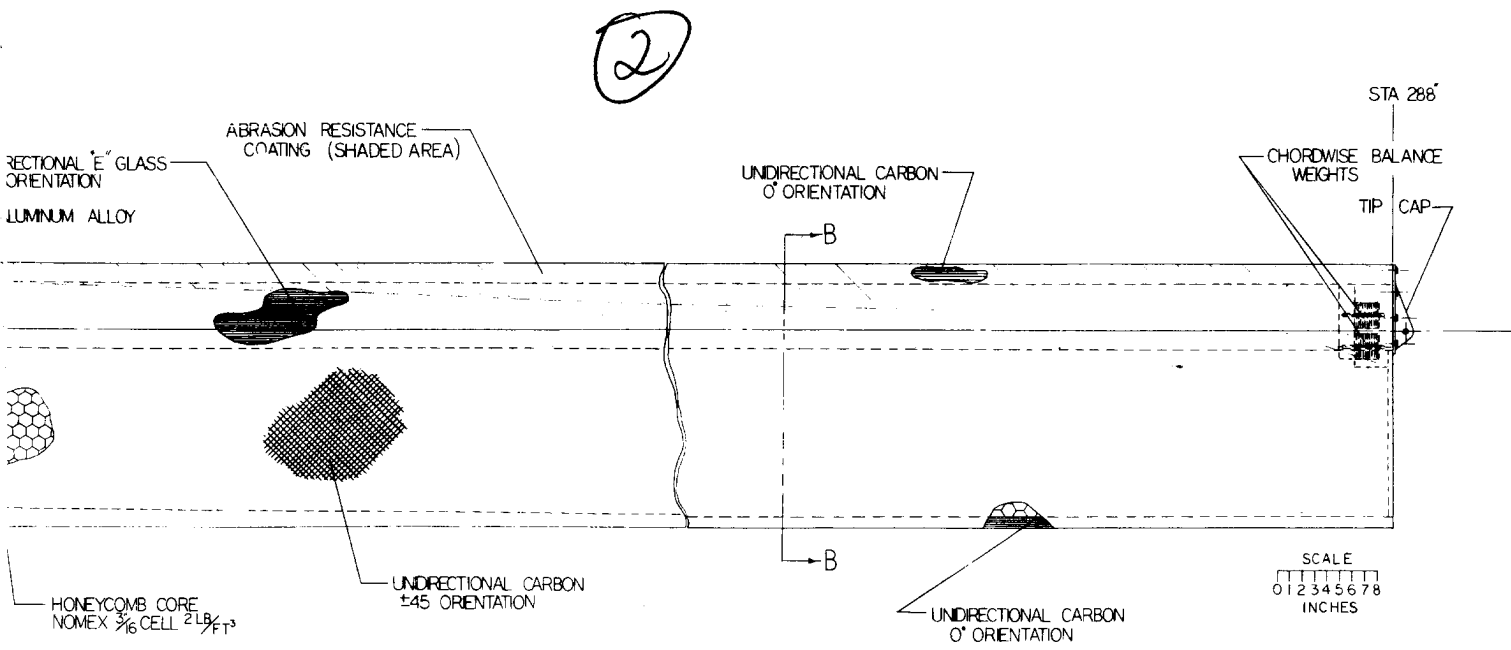
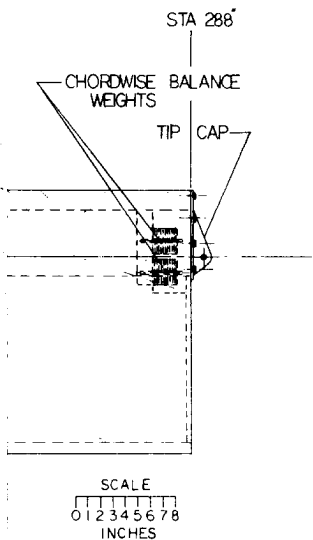
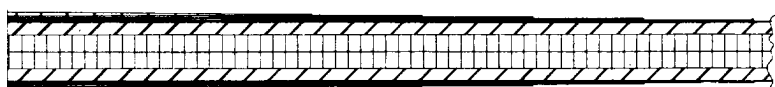


Figure 19. Configuration IV.





UNIDIRECTIONAL "E" GLASS



ION C-C

A scale bar labeled "SCALE" at the top, with tick marks at 0, 1, 2, 3, and 4, and the word "INCHES" at the bottom.



SCALE
1 2 3 4
INCHES

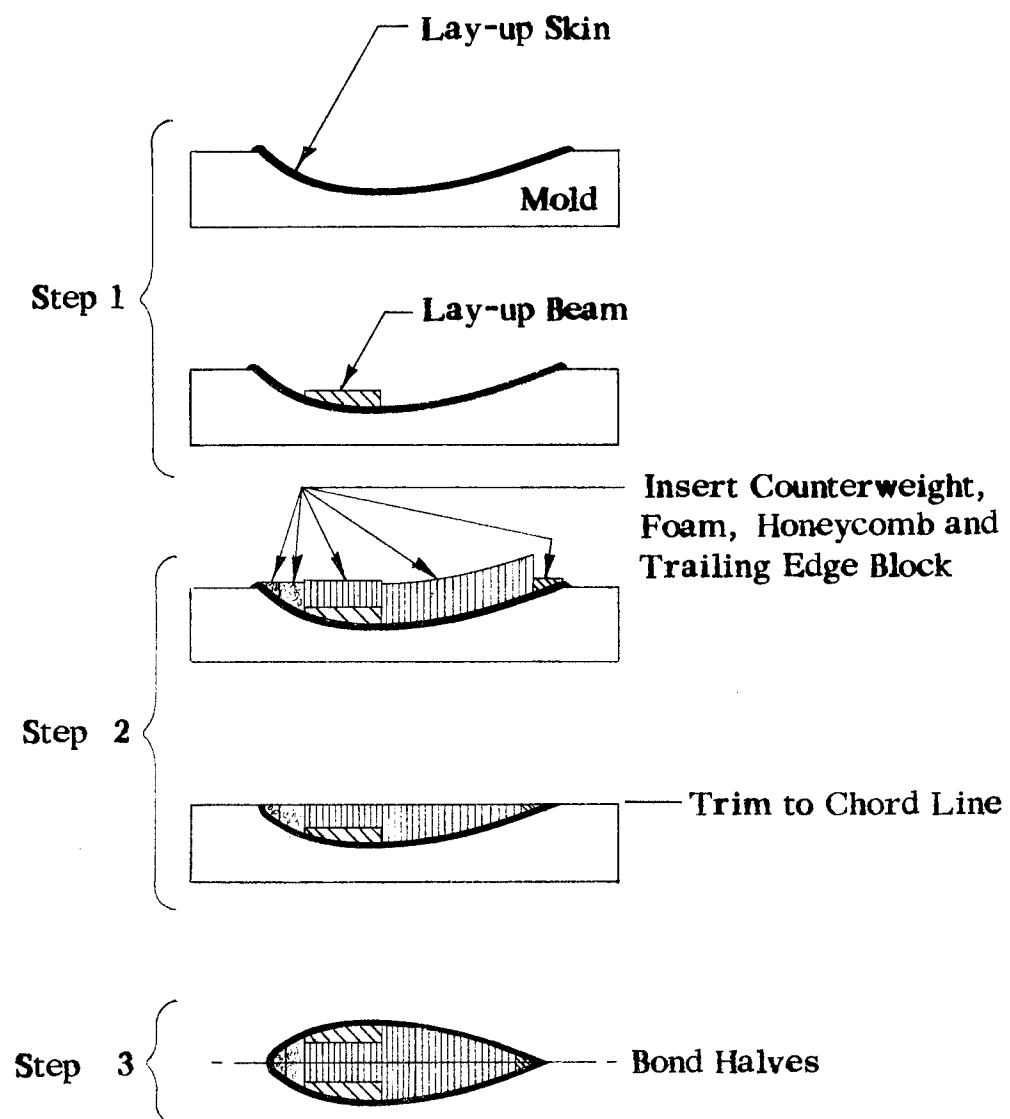


Figure 20. Fabrication of Beam Concept .

The root end buildup for transfer of blade loads to the rotor head is similar to the other configurations. In addition, aluminum wedge plates are bonded to the inside of the spar beams to provide greater bearing and shear tearout strength in the area around the attachment pins. The wedge plates, which are bonded to the spar beams prior to the assembly of the two halves of the blade, form an interlocking taper joint with the root end of the spar beams, as shown in Figure 21. The interlocking tapers provide an additional load transfer path from the spar to the root end attachment that is independent of the primary bonded attachment. The large amount of bond area between the outside doubler plates and the constant section portion of the blade results in low shear stresses in the adhesive. The large cross sectional area of the doublers, coupled with the higher modulus of the aluminum wedge plates, results in most of the spar loads being transferred into these components in the attachment area. These components and attachment fittings then provide the load transfer capability to the rotor head.

The half-mold fabrication principle provides ease of inspection and assembly of the individual components. The open section provides higher quality control because all members are set together in the mold, readily inspectable at a glance. The primary structures such as the spar, leading edge doubler, and trailing edge spline require no internal examination like hollow extrusions or tubes because they are simple, solid sections. The components are placed side by side in the mold without regard to thickness tolerance because each half-assembly is machined flush on the chordline after all components have been arranged in position. Fabricating in this fashion results in excellent dimensional control of the blade aerodynamic contour after machining and final bonding of the two half-molds.

The composite blades of Configurations III and IV offer a significant advantage over metal blades in that they are inherently corrosion free. Except for the aluminum root end, the blade material is nonmetallic.

These blades are field repairable. Composites can be prepared for bonding simply by sanding and cleaning the surface with solvent. This can be done in the field at the direct support level. Bonded metal blades are more costly to repair because they must be removed to a high echelon of maintenance. The metal blade requires cleaning, priming, and bonding under clean, atmospherically controlled conditions.

Configuration IV was found to be less cost effective than the UH-1 blade and Configurations I and II for 1972 because of the high cost of the carbon composite. For the 1980 investigation, this configuration was made cost effective by the reduced cost of the carbon and by fabricating a blade half

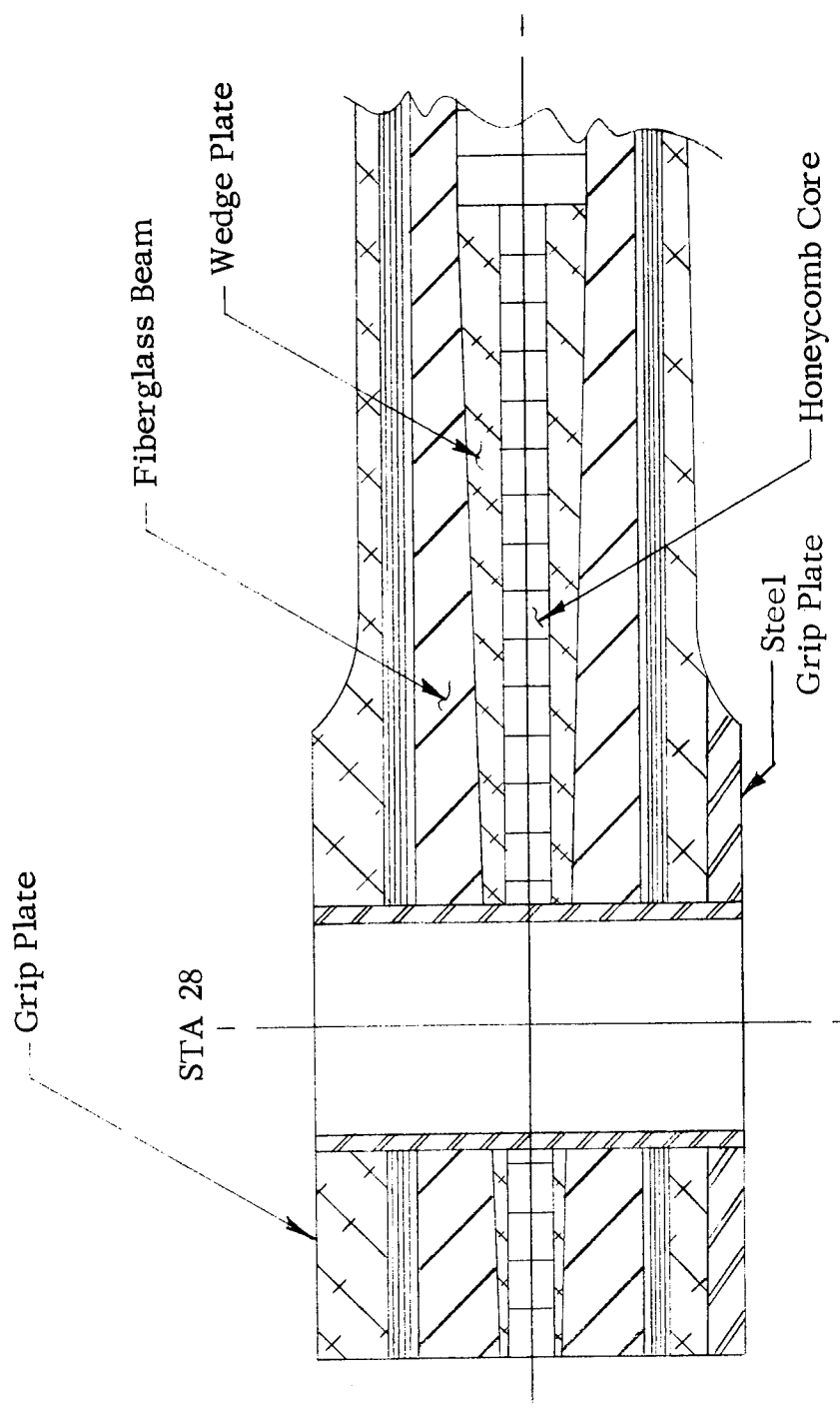


Figure 21. Fiberglass Root End Attachment.

section by the pultrusion process. The blade concept is shown in Configuration V, Figure 22.

CONFIGURATION V, TWIN BEAM FIBERGLASS BY PULTRUSION PROCESS

Configuration V is similar in design to Configuration IV, having all the same attributes; in addition, improvements are made to the trailing edge by eliminating the expensive honeycomb in this portion of the blade and inserting a truss type skin as shown in Figure 22. The truss members consist of outer skin, diagonals and inner skin. The outer skin is still carbon at $\pm 45^\circ$ orientation. The diagonals and inner skin are composed of fiberglass sheets arranged at $\pm 45^\circ$ orientation to provide torsional rigidity and stability to the skin. The inner skin extends the full chord of the blade, enveloping and conforming to the unidirectional carbon fore and aft and the unidirectional fiberglass spar. The components of one-half of the blade thus become one integral part; high and low modulus unidirectional and cross materials are combined in one manufacturing process.

This process is an extension of the simple pultrusion method of fabricating the simple, solid spar and spline sections of the other configurations; it is unique because it combines hollow and solid sections, unidirectional and cross ply and dissimilar materials. Such a complex use of this process has never been demonstrated; therefore, it represents more risk than the more conventional skin and honeycomb layup construction. However, the potential for mass production of a trailing edge structure with an internal system of longitudinal stiffening members, thereby eliminating the cost and assembly associated with honeycomb and skin attachment, represents a sizable reduction in production costs.

Figure 23 shows a schematic of the pultrusion process. The part being fabricated is a simple, hollow, rectangular tube consisting of unidirectional glass between inner and outer layers of a cross-ply material. The shape is obtained by a fixed mandrel extending through a curing die. Fiberglass mat or cross-ply material on a roll is dipped in a resin and then uniformly wrapped around the mandrel by a funneling process as shown. Filament "E" glass roving, also dipped in resin, is evenly distributed over the mat material. A second layer of cross ply or mat is then placed uniformly over the longitudinal filaments. The entire assembly is then slowly drawn through the curing die by a series of rollers bearing against the outer surface of the mat material. The part is essentially cured by the time it exits the die. The complex structure of Configuration V utilizes the same basic principle as above; it is fabricated by a series of triangular mandrels, one for each hollow in the trailing edge, and a die conforming to the blade half section containing the spar, the

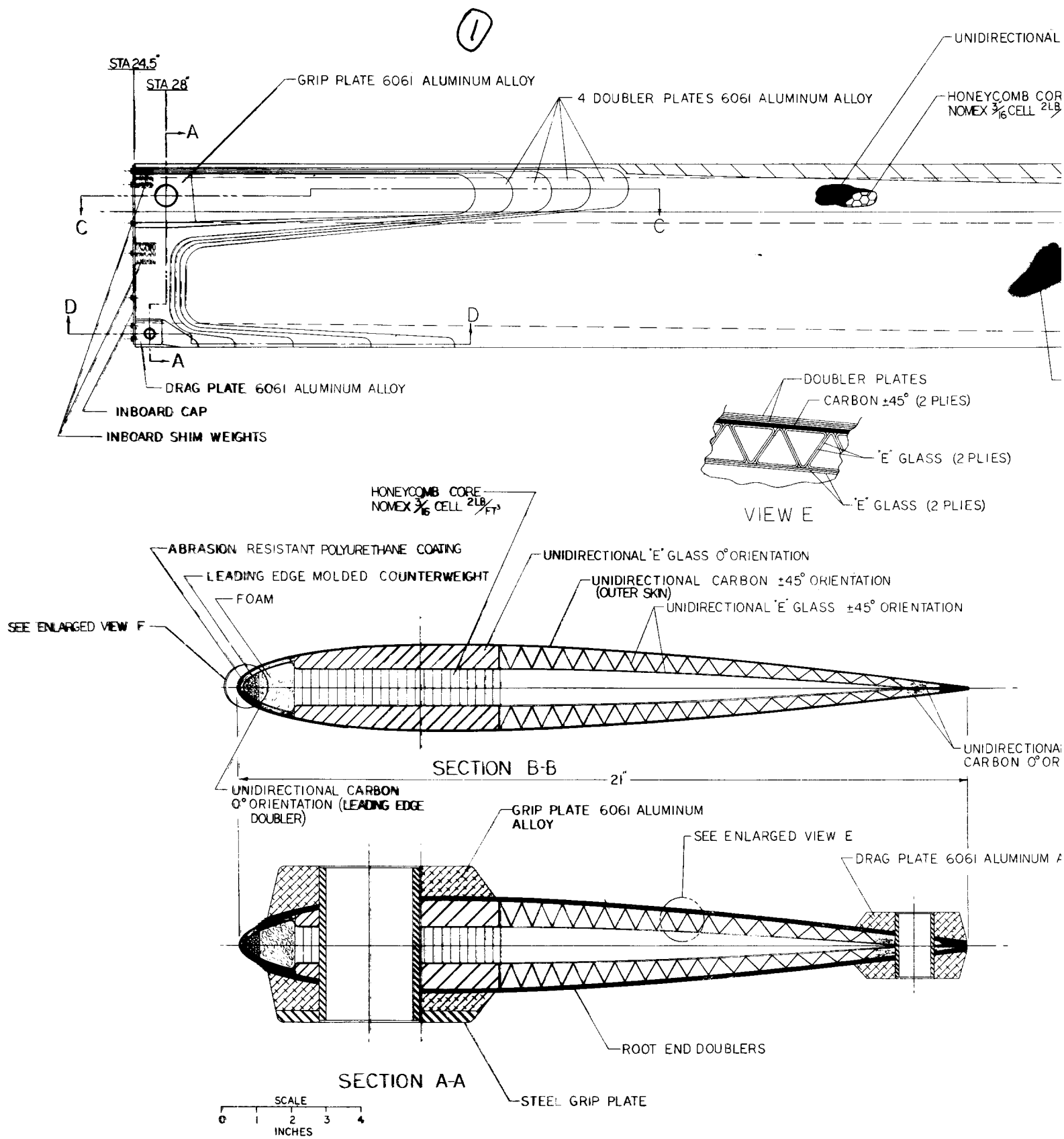
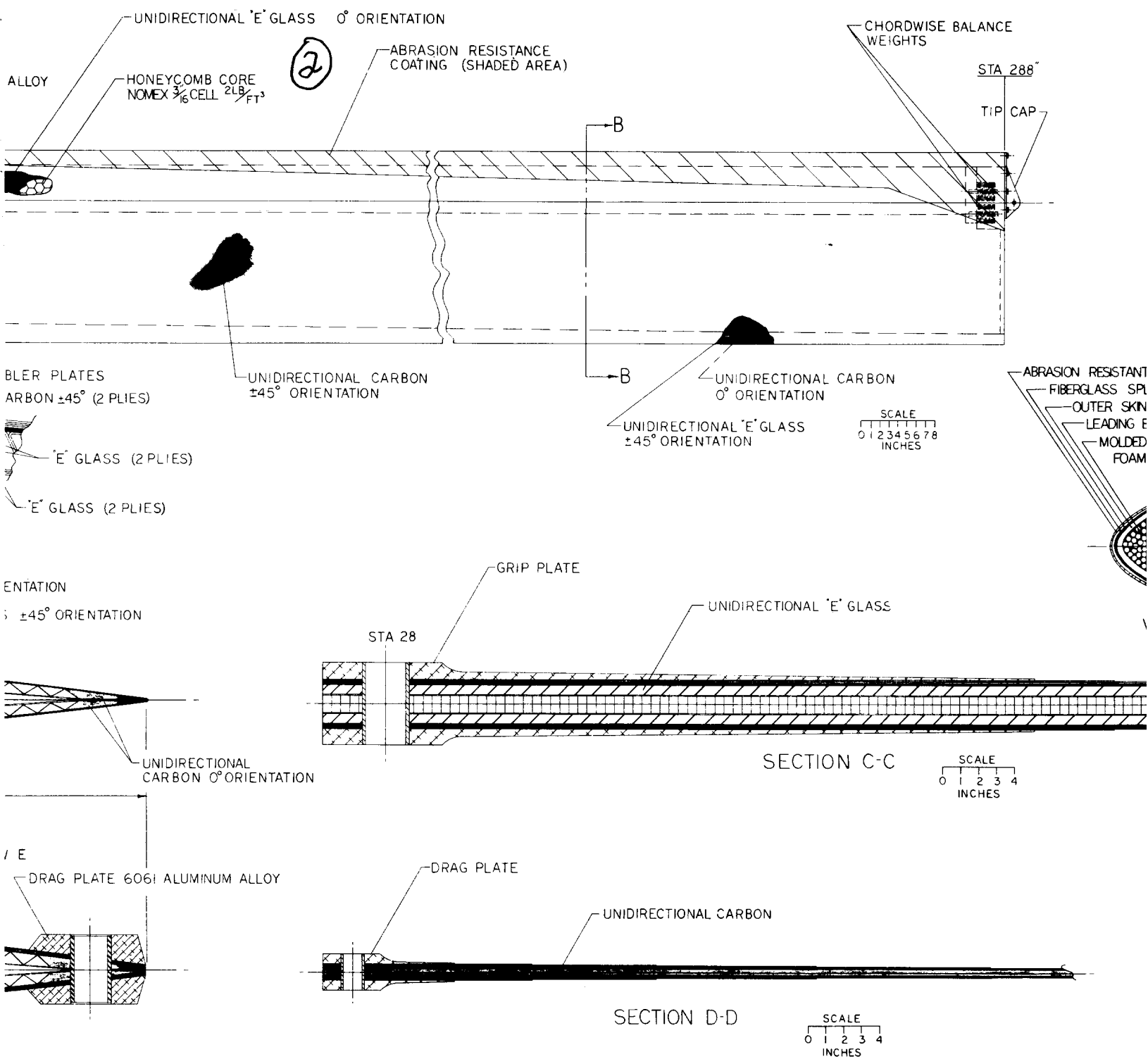
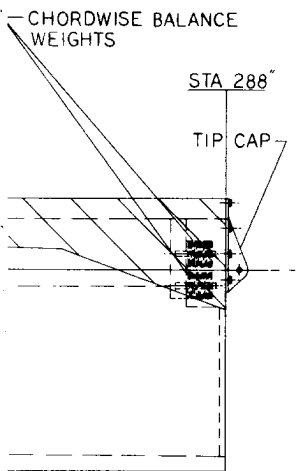
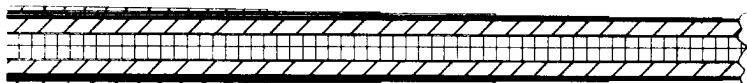
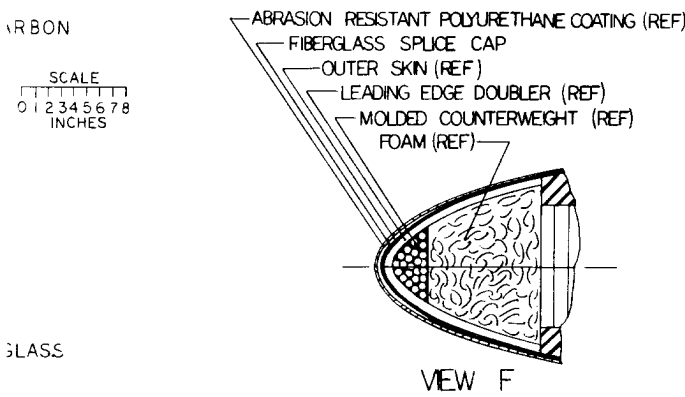


Figure 22. Configuration V.





(3)



C-C

SCALE
0 1 2 3 4
INCHES

E
3 4
S

SUDORESKY AIRCRAFT, Stratford, Connecticut.	
PRELIMINARY LAYOUT	
WINGSPAN	11' 0"
LEADING EDGE LENGTH	10' 0"
LEADING EDGE SPAN	10' 0"
LEADING EDGE WEIGHT	100 LB
LEADING EDGE AREA	100 SQ FT
LEADING EDGE STIFFNESS	1000000 IN-LB
LEADING EDGE STRENGTH	1000000 LB
LEADING EDGE DEFLECTION	1000000 IN
LEADING EDGE SPAN	1000000 IN
LEADING EDGE STIFFNESS	1000000 IN-LB
LEADING EDGE STRENGTH	1000000 LB
LEADING EDGE DEFLECTION	1000000 IN
LEADING EDGE SPAN	1000000 IN
LEADING EDGE STIFFNESS	1000000 IN-LB
LEADING EDGE STRENGTH	1000000 LB
LEADING EDGE DEFLECTION	1000000 IN
TYPE - FIBERGLASS TRUSS BEAM / ALUMINUM SPACERS (CONFIGURATION I)	
- BE - 1234	

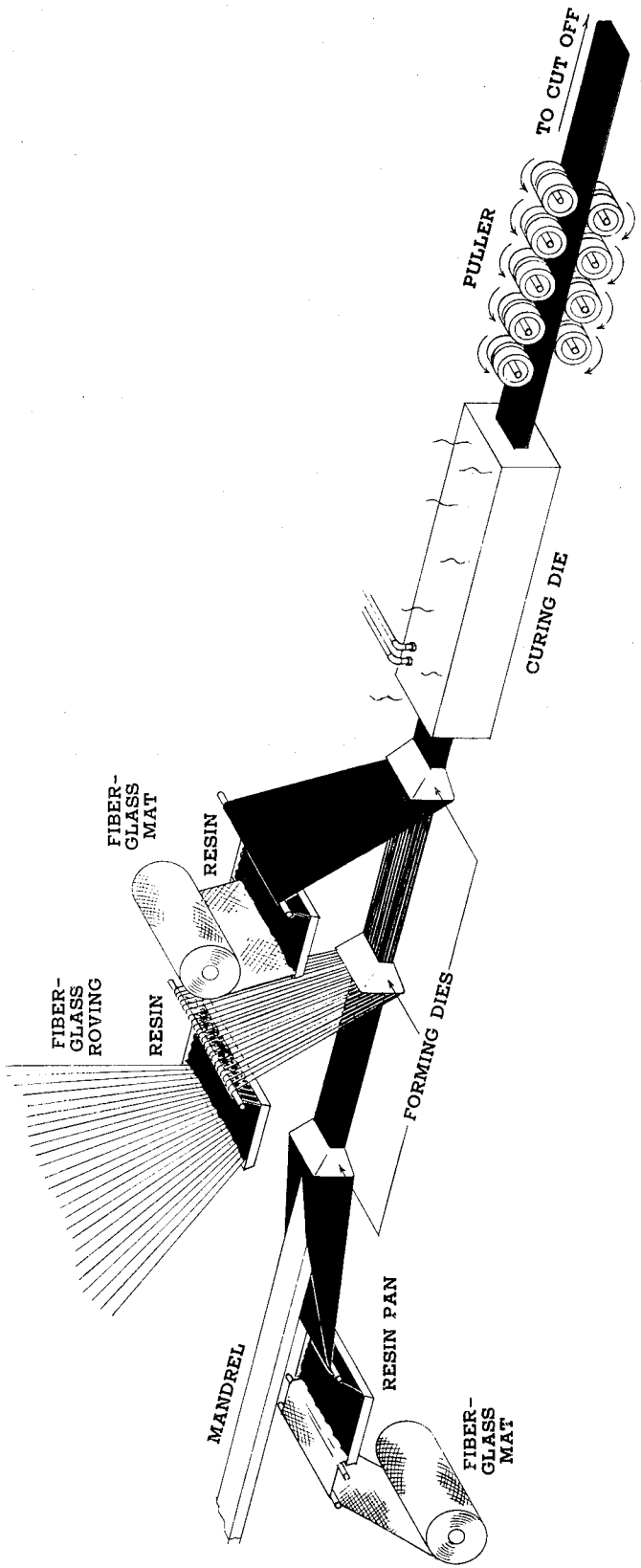


Figure 23. Pultrusion Schematic.

trailing edge truss and carbon leading edge doubler and trailing edge spline. The carbon and "E" glass materials would be arranged to enter the die to produce the section of Configuration V.

CONFIGURATION VI, ALUMINUM SPAR - PULTRUSION TRAILING EDGE

Configuration VI (Figure 24) is a combination of Configurations I and V. The aluminum spar is combined with an automated trailing edge pultrusion. The one-piece construction eliminates separate skins, trailing edge spline and Nomex core. There is a period of development required for this process; however, it is felt it can be accomplished by 1975. To provide structural integrity, the blade is also equipped with Sikorsky's monitoring device BIMR. The blade spar is sealed and pressurized from its root to a point just inboard of the counterweight retaining block. A device to indicate pressure loss visually, by showing red, is installed near the root end, where it is visible from the ground. This method of continual surveillance of the spar provides at a glance a more effective structural inspection than x-ray. Although not shown, this same device is applicable to Configurations I and II.

This design combines all the advantages of the aluminum and fiberglass concepts, resulting in a simplified design and reduced cost.

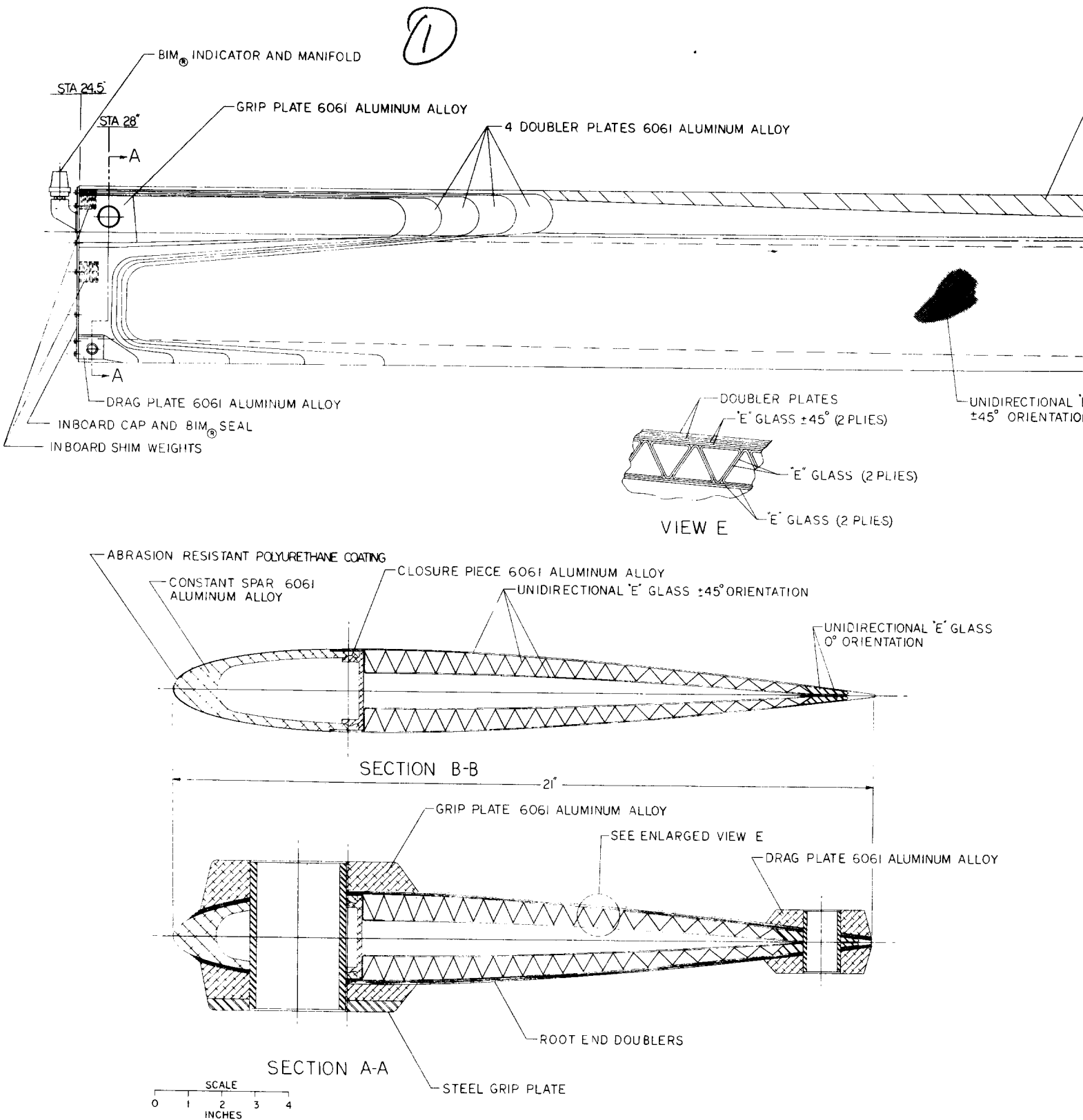
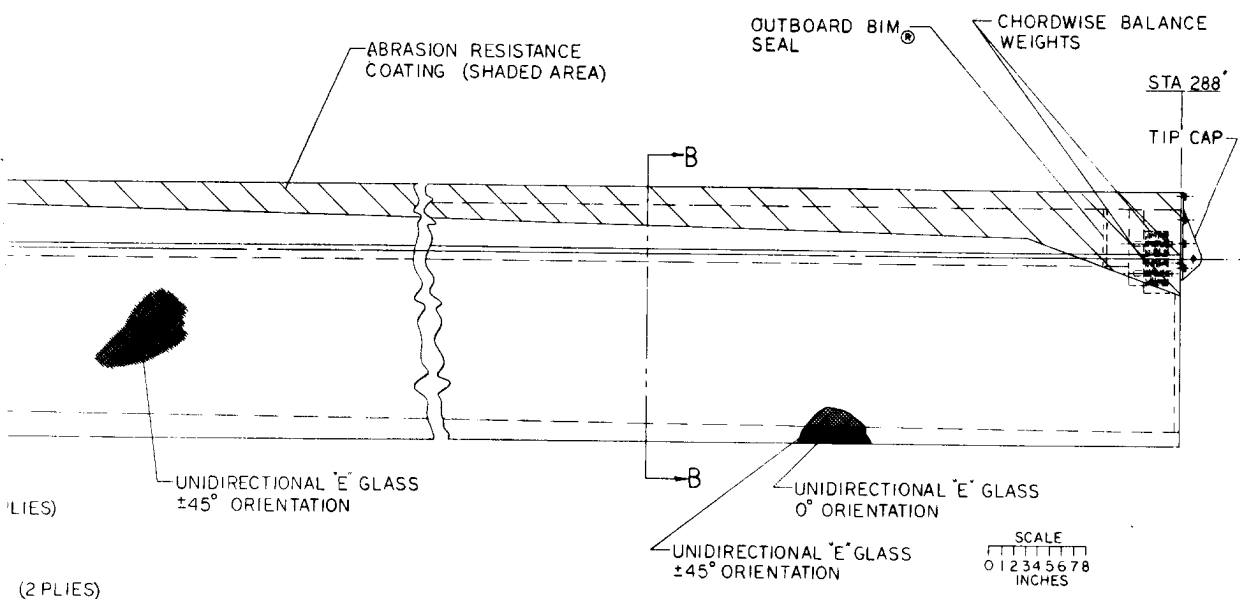


Figure 24. Configuration VI.

(2)



'LIES)

(2 PLIES)

PLIES)

IRECTIONAL "E" GLASS
ORIENTATION

6061 ALUMINUM ALLOY

3

SOKOFSKY AIRCRAFT		Storckford, Connecticut.
PRELIMINARY LAYOUT		
PRINTED BY John A. Lippert		RECEIVED BY R. E. BROWN
DATE 10-10-62		DATE 10-10-62
SHEET 1 OF 1		STYLING SHEET & CRAFT 10
SHEET 1 OF 1		100% SCALE DRAWN APPROVED
SHEET 1 OF 1		WIND - <input type="checkbox"/>
SHEET 1 OF 1		SHADING - <input type="checkbox"/>
SHEET 1 OF 1		LAYOUT NO. -
SHEET 1 OF 1		DATE - 12-35
TITLE - AS-ENTRANCED ALUMINUM SPARE PULTRUSION TEE		
CONF. NUMBER 100-112		

ANALYSIS OF DESIGN CONFIGURATIONS

NATURAL FREQUENCIES

The natural frequency of each design configuration was determined for comparison with a similar calculation for the UH-IH rotor blade. Duplication of the UH-IH frequency characteristics is considered of prime importance in the design of a blade which would be compatible with the UH-IH aircraft. First and second mode flatwise and edgewise frequencies were determined for the appropriate pin ended and cantilevered ended blade root end conditions for the entire range of rotor rotational speeds. For a teetering rotor, the odd-numbered harmonics in the flatwise direction are pin ended and the even numbered are cantilevered ended. Edgewise end restraint is always cantilevered. Since blade torsional response is of prime importance (Appendix I), the first torsional mode frequencies were also determined.

Blade beam bending frequencies are determined using a computer program which considers the blade as a series of uniform rigid beam segments connected by hinges and springs. Segment length, mass and spring stiffnesses are varied along the blade to represent the nonuniform characteristics of the actual blade. A system of nonlinear differential equations describes the forces, motion and acceleration experienced by the segmented blade. The end conditions of the blade are introduced as constraints at the root and tip of the blade. Solution of a determinate system comprised of the differential equations of motion yields the blade bending natural frequencies and modal amplitudes.

The Southwell plots for each of the blade configurations and the UH-IH are presented in Figures 25 to 29. The plots show the close correlation of each design with the UH-IH blade. In particular, the first edgewise mode frequency and the first torsional mode frequency are of prime importance. Separation of the first edgewise mode from the one-per-rev rotor operating speed is essential to preventing any resonance and amplification of in-flight one-per-rev edgewise loadings. Each proposed blade design is at least as far removed from one-per-rev as the basic UH-IH blade.

LOAD DETERMINATION

Evaluation of the structural reliability of each of the four design concepts requires a determination of the bending moments experienced by each of the candidate designs. Since there is very little difference between the mass and stiffness distribution of each design and the basic UH-IH blade, we would expect the blade bending moments to be very similar. As expected, calculation of the blade bending moments for each design at a

(C) = Cantilevered (H) = Hinged

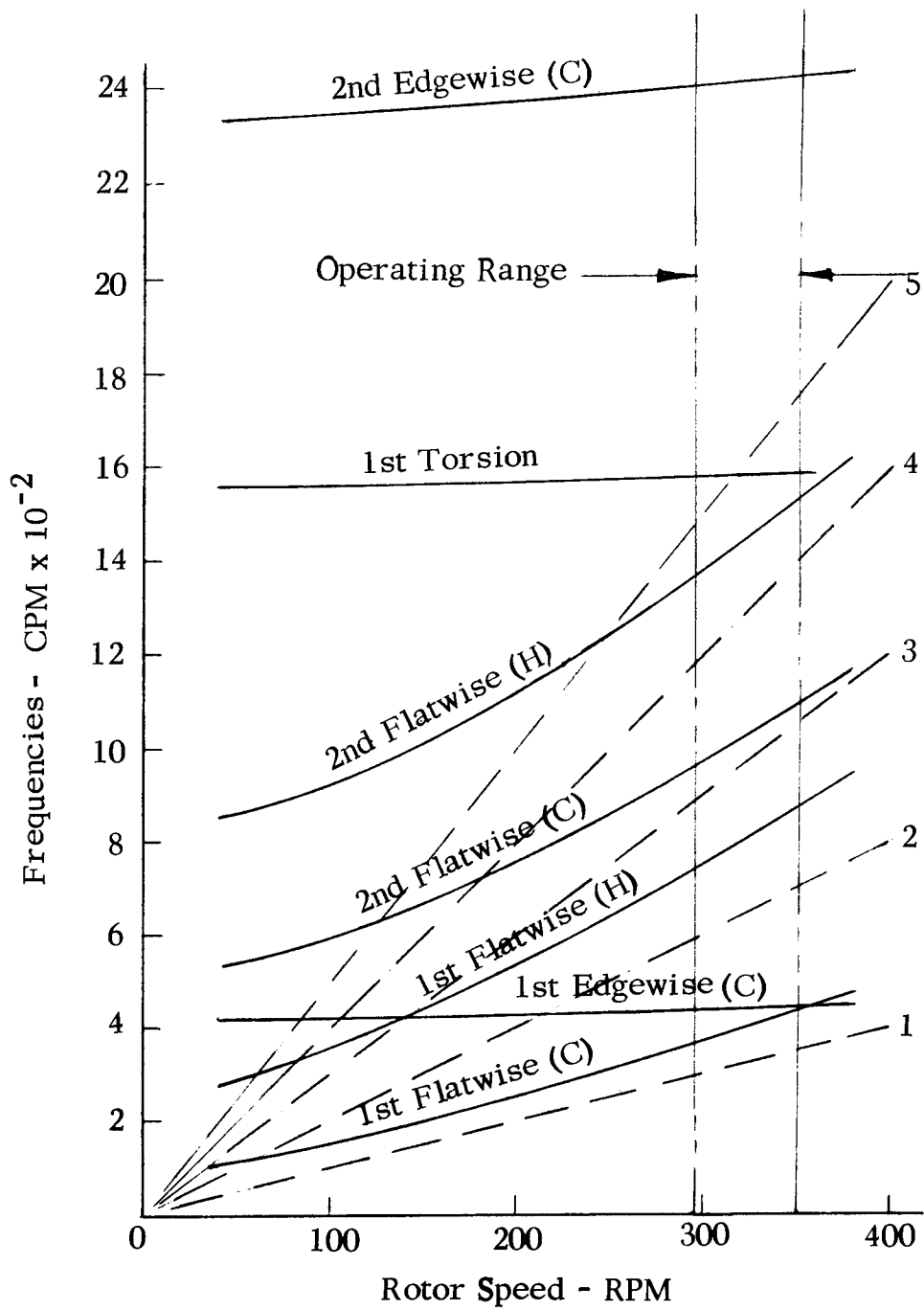


Figure 25. Natural Frequencies, Configuration UH-1H .

(C) = Cantilevered (H) = Hinged

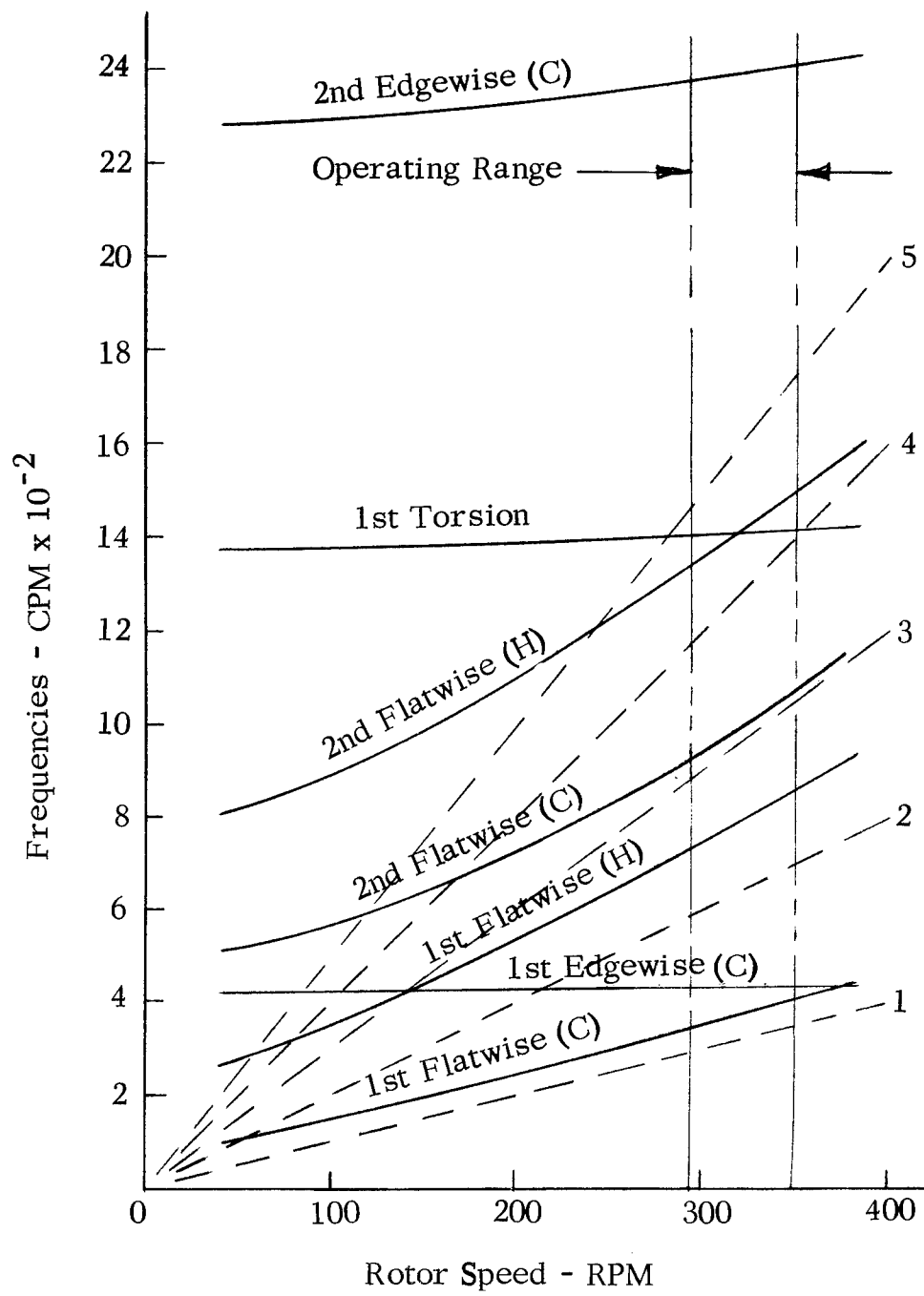


Figure 26. Natural Frequencies, Configuration I and VI.

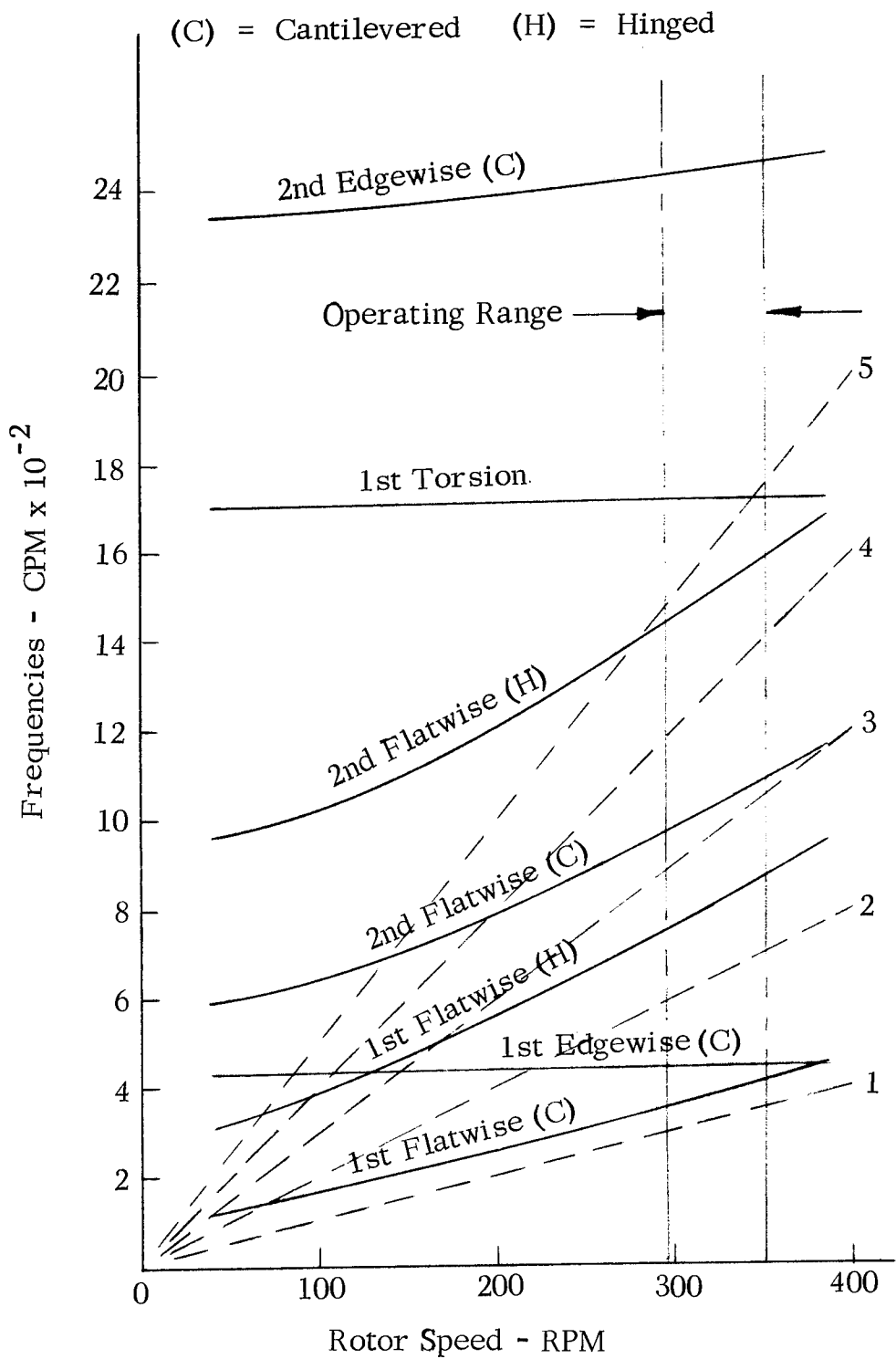


Figure 27. Natural Frequencies, Configuration II.

(C) = Cantilevered (H) = Hinged

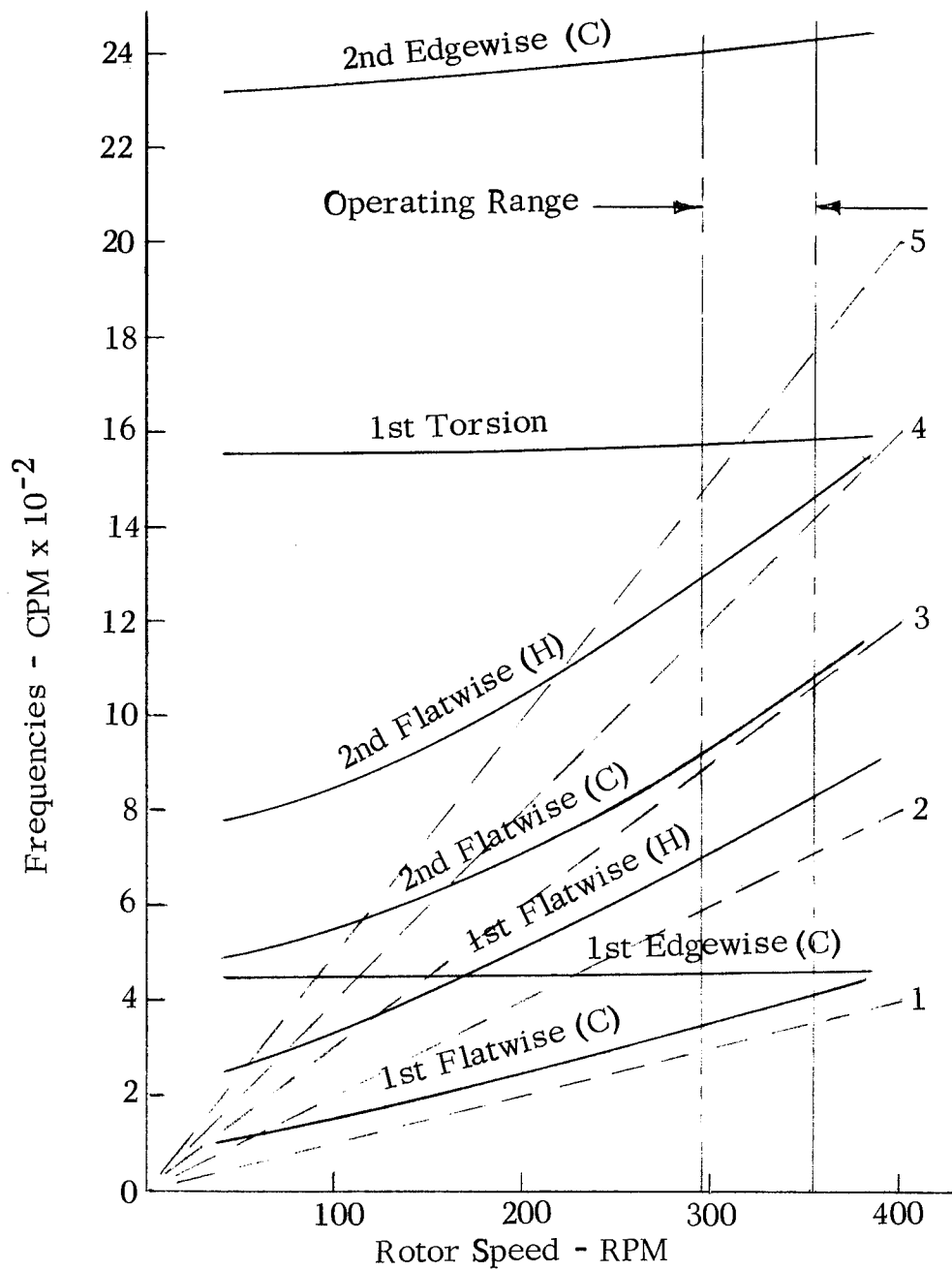


Figure 28. Natural Frequencies, Configuration III.

(C) = Cantilevered (H) = Hinged

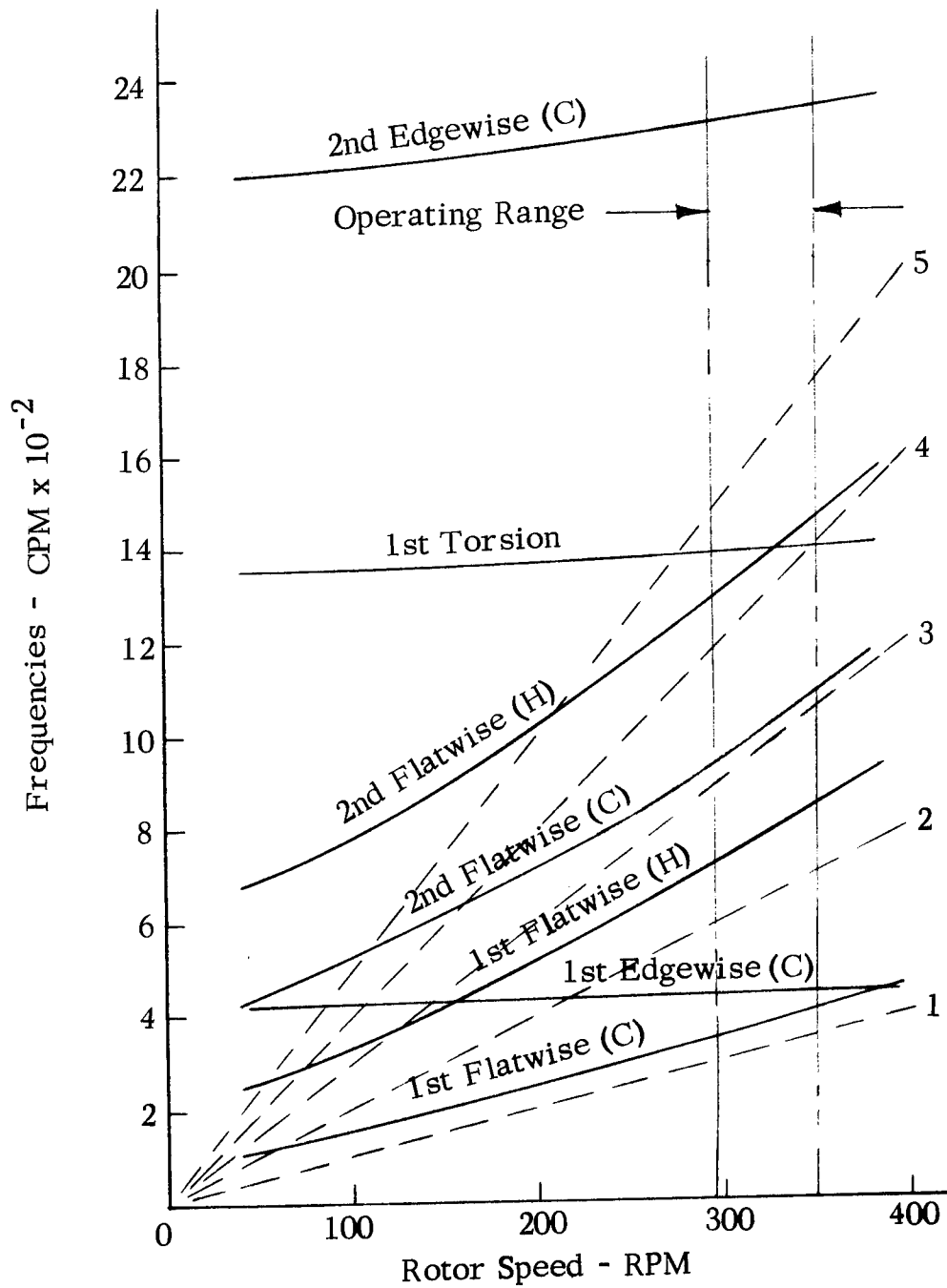


Figure 29. Natural Frequencies, Configuration IV and V.

representative flight condition showed only small differences between designs.

The loads and moments were calculated on a UNIVAC_R 1108 computer, programmed by Sikorsky Aircraft. Two computer programs are available for determining the loads for a teetering rotor, a normal modes analysis and a modified Myklestad analysis. The Sikorsky normal modes transient analysis was modified to make it applicable to teetering rotor blades. In this computer program, blade flatwise, edgewise and torsional elastic deformation are represented by a summation of normal mode responses. The modal equations of motion are integrated numerically to permit rational coupling between airloads and blade response. In order to treat the teetering rotor system program, modifications were made to accommodate the blade mode shapes and natural frequencies characteristic of the two-bladed configuration. The modal excitations of two blades (located 180° apart in azimuth) were combined to give the generalized excitation of the teetering rotor system. Three hinged and three hingeless flatwise modes, one hinged and two hingeless edgewise modes and two torsional modes were retained in the analysis.

Correlation studies of the blade bending moments determined using this program with those obtained from flight test data for the UH-1H aircraft showed poor correlation of the edgewise moments. Computed edgewise moments were much greater than the flight test data and proved to be very sensitive to changes in first mode edgewise frequency. Because of this sensitivity to edgewise frequency and some question as to the actual hub stiffnesses of the UH-1H rotor system (which would directly influence edgewise frequency), we elected not to use the normal modes analysis.

The Myklestad analysis program proved to correlate better with the test data than the normal modes program and was therefore used for the blade bending moment calculations. Good correlation of this program had been previously demonstrated for the UH-1A teetering rotor as reported in Reference 5. The Myklestad analysis is divided into two distinct parts. The first is an aerodynamics analysis to determine air loadings on the blade for a given flight condition. The second part is a dynamic structural analysis which calculates blade response to the air loads by means of a modified Myklestad approach.

The aerodynamic analysis calculates the rotor blade pitch, coning, and tip path plane angles for given flight condition requirements (airspeed, rotor speed, lift, drag, steady hub moments, density altitude). For the aerodynamic analysis, the blade is assumed to be rigid with no flapping. Flexibility effects are handled in the structural analysis. Two-dimensional steady-state airfoil lift, drag, and pitching moment data are used. These include stall and Mach number effects. Air loads are calculated

at small azimuth intervals for chosen blade radial stations. The azimuthal harmonics of the loads are calculated and used in an iteration procedure to trim the rotor to the flight condition requirements. The final converged harmonic distribution of air loads is used in the structural analysis to determine blade response.

The structural analysis is based on a lumped mass Myklestad approach. It is a fully coupled flatwise-edgewise-torsional analysis. Influence coefficients between masses are calculated using blade area moments of inertia and beam theory. The method of solution is to determine the moments, forces, deflections, and slopes at the blade root due to unit displacements and slopes at the blade tip, and due to the applied air loads (corrected by damping loads due to blade deflections) and centrifugal and other effects. The moments, displacements and slopes required to satisfy the root end boundary are then calculated, and the forces, moments, stresses, deflections and slopes at each radial station are calculated using these values.

Blade bending moments were calculated for a typical UH-1H cruise condition in level flight. A velocity of 90 knots, gross weight of 8,500 pounds and a rotor speed of 318 RPM were used for the calculation. Figures 30 to 33 illustrate the vibratory flatwise and edgewise bending moments obtained for each of the design configurations and the UH-1H blade. Figure 34 shows the steady moments typical for all configurations. Centrifugal force of each of the blades is shown in Figure 35. Only one curve is shown for the steady bending moments because it is representative of all the blade configurations.

STRUCTURAL ANALYSIS

The objectives of the structural analysis work on the four design configurations presented in this report are to identify any major structural problem areas and to evaluate the expected fatigue life for the designs under study. All of the work is based on a direct comparison of the designs under study with a similar calculation for the UH-1H rotor blade.

The spanwise distribution of mass and stiffness, used in the determination of the blade loads and stresses, is presented in Figures 36 through 39. Comparisons of spanwise deflection and flexural and center of gravity locations are shown in Figures 40 through 42. Additional comparisons of blade physical properties and design features are shown in Tables I and II.

The properties of the materials under consideration for the configurations are shown in Table III. These properties were obtained from References 6, 7, 8 and 9 and various material property testing conducted by

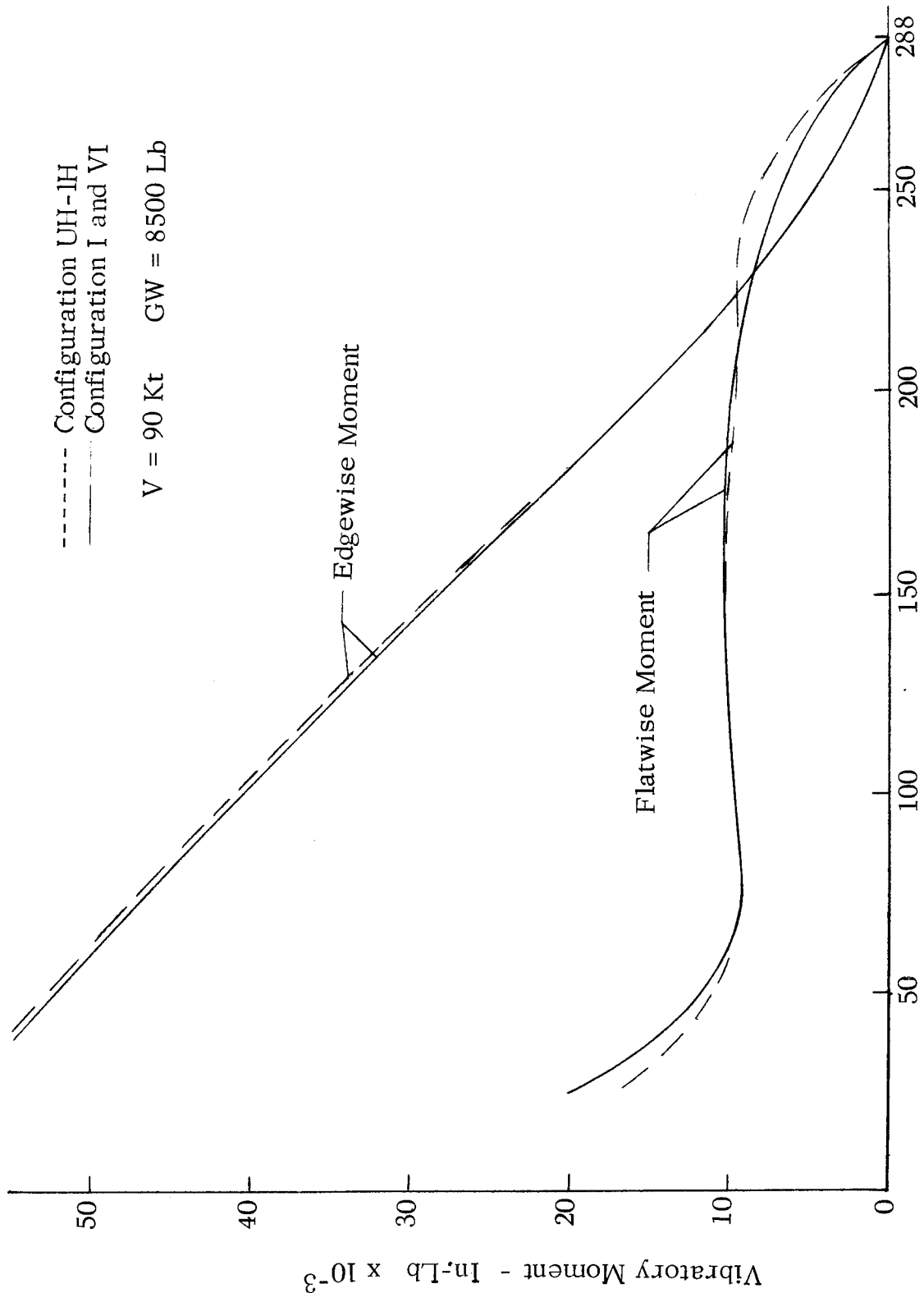


Figure 30. Vibratory Moments, Configuration I, VI and UH-1H.

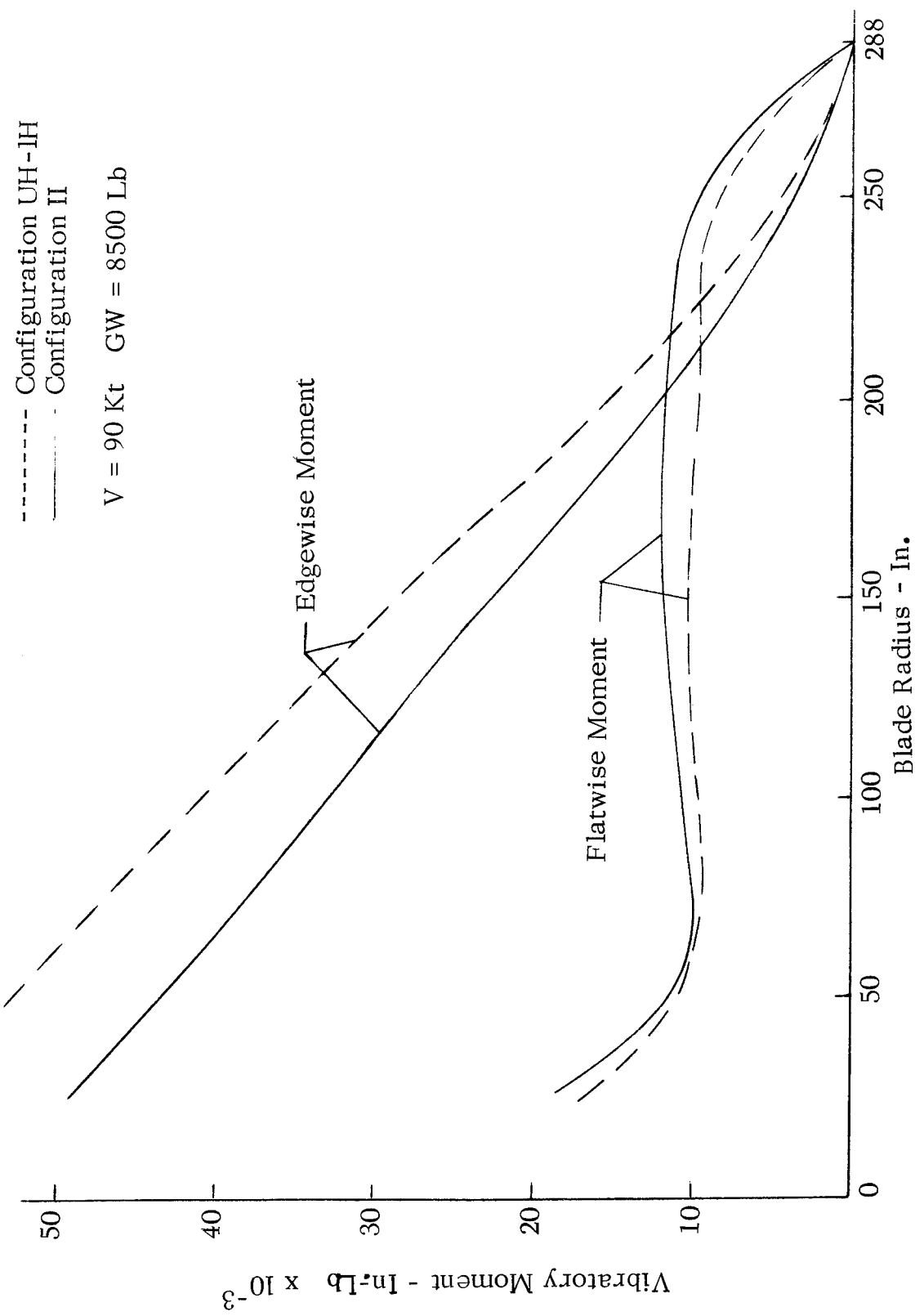


Figure 31. Vibratory Moments, Configuration II and UH-IIH.

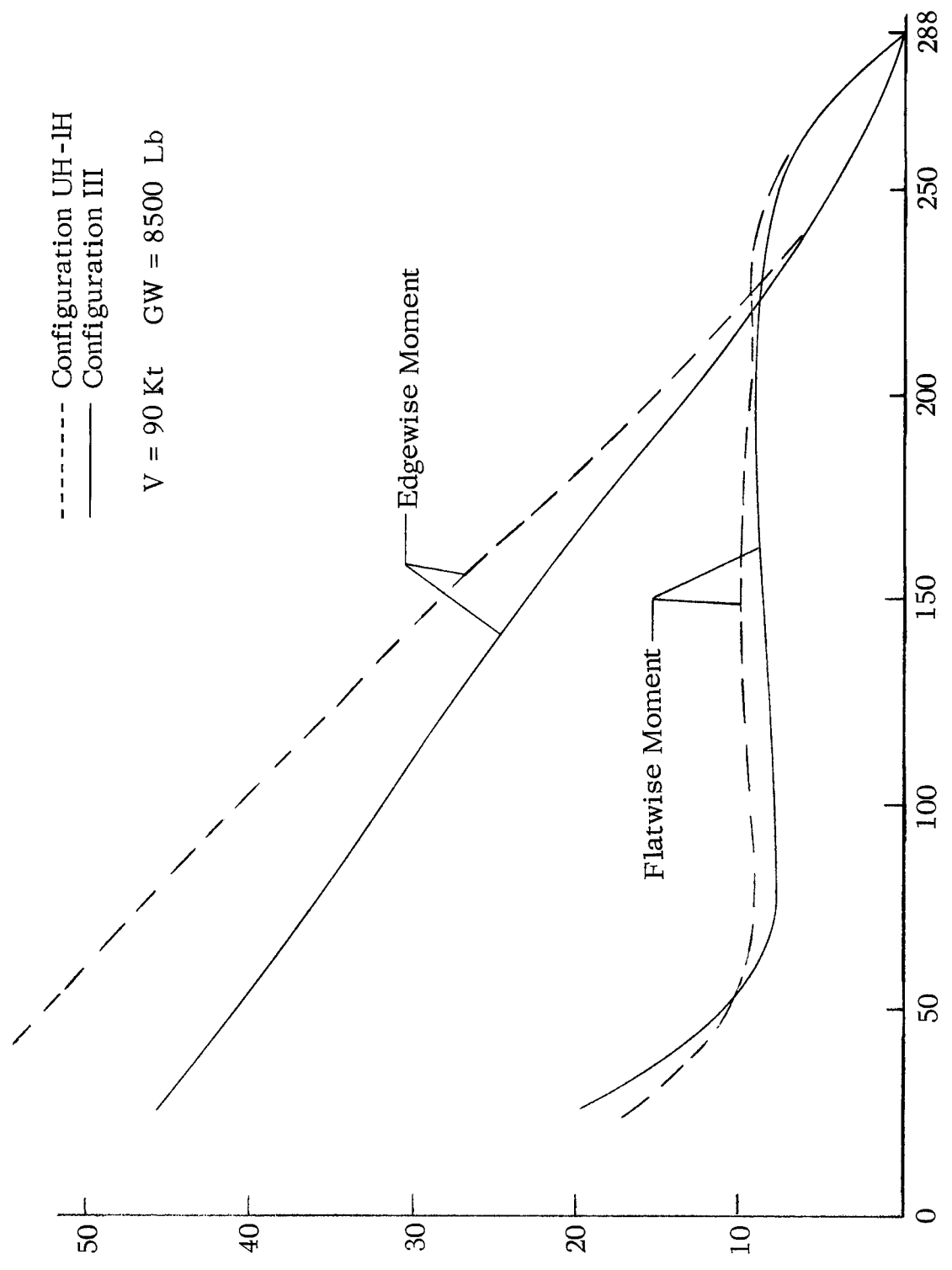


Figure 32. Vibratory Moments, Configuration III and UH-IH.

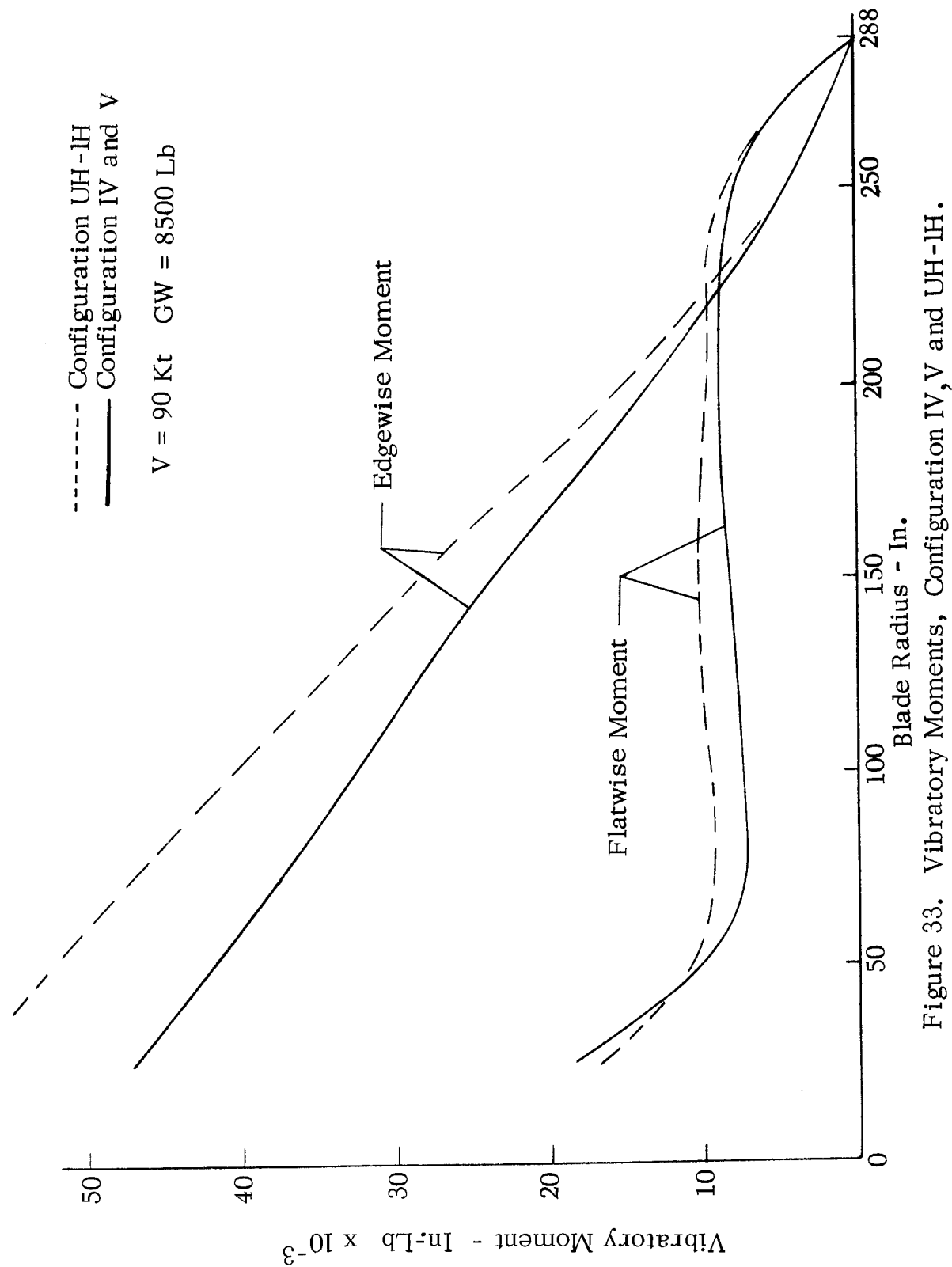


Figure 33. Vibratory Moments, Configuration IV, V and UH-IH.

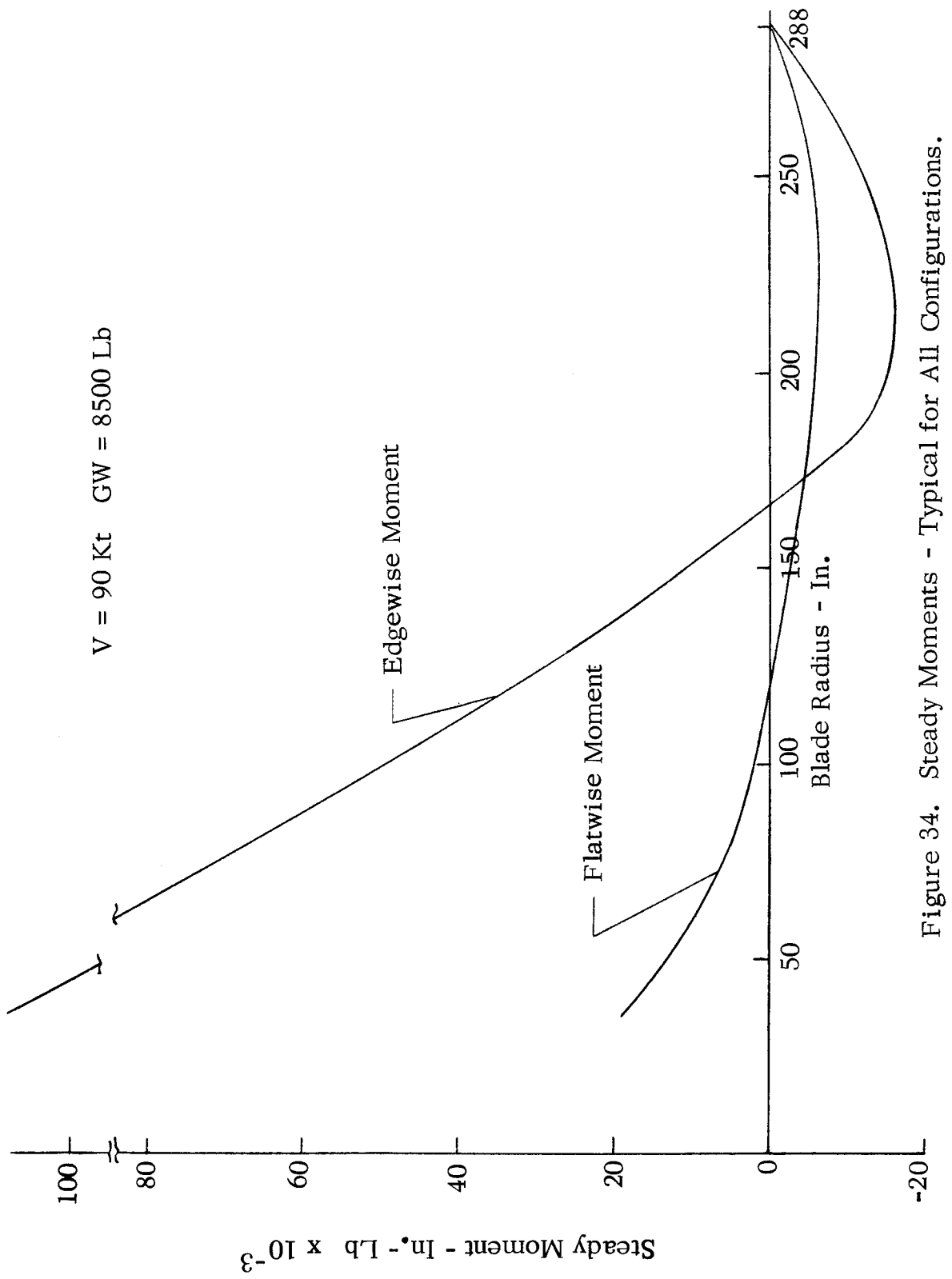


Figure 34. Steady Moments - Typical for All Configurations.

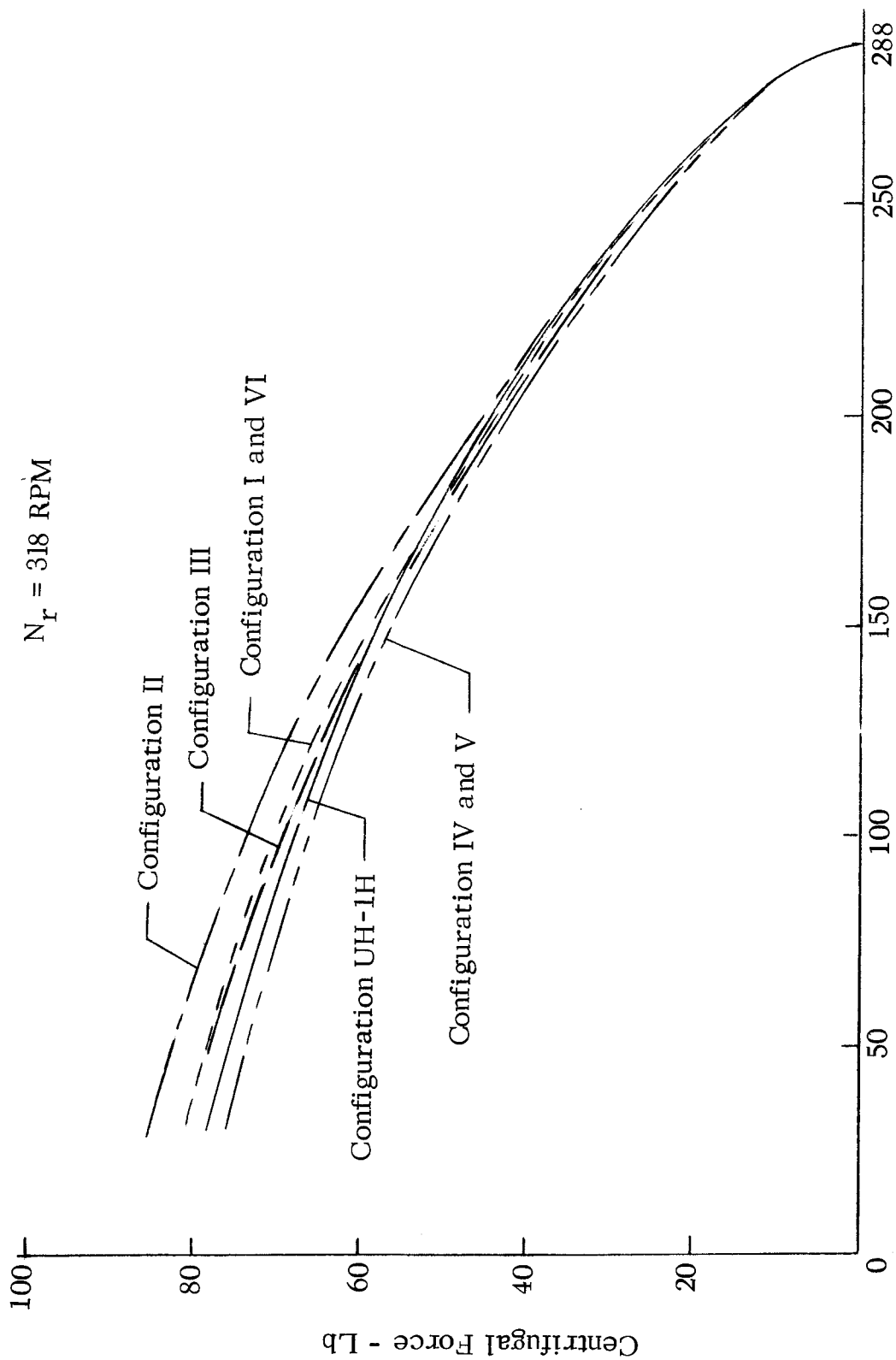


Figure 35. Centrifugal Force vs Blade Radius.

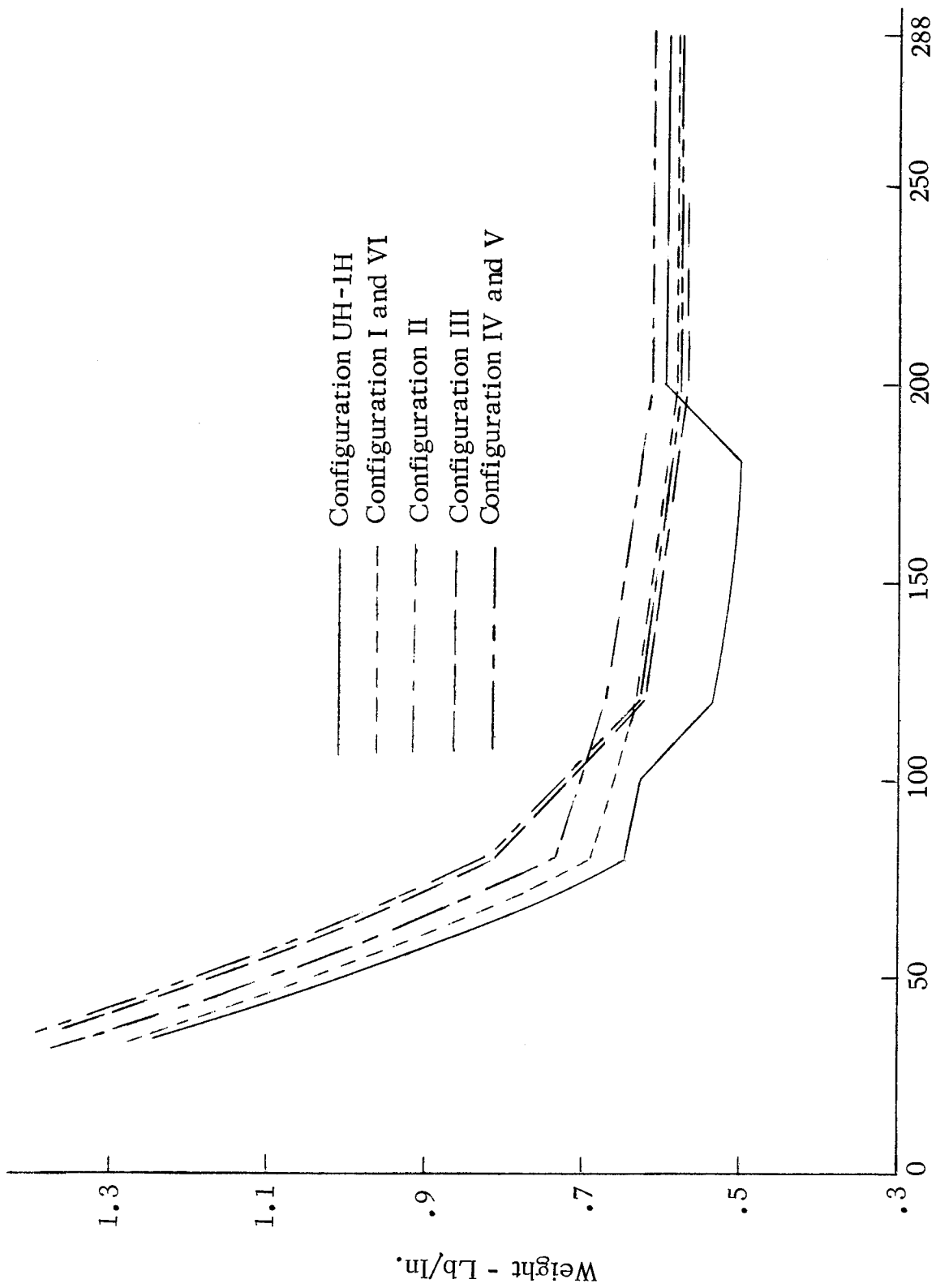


Figure 36. Weight Distribution.

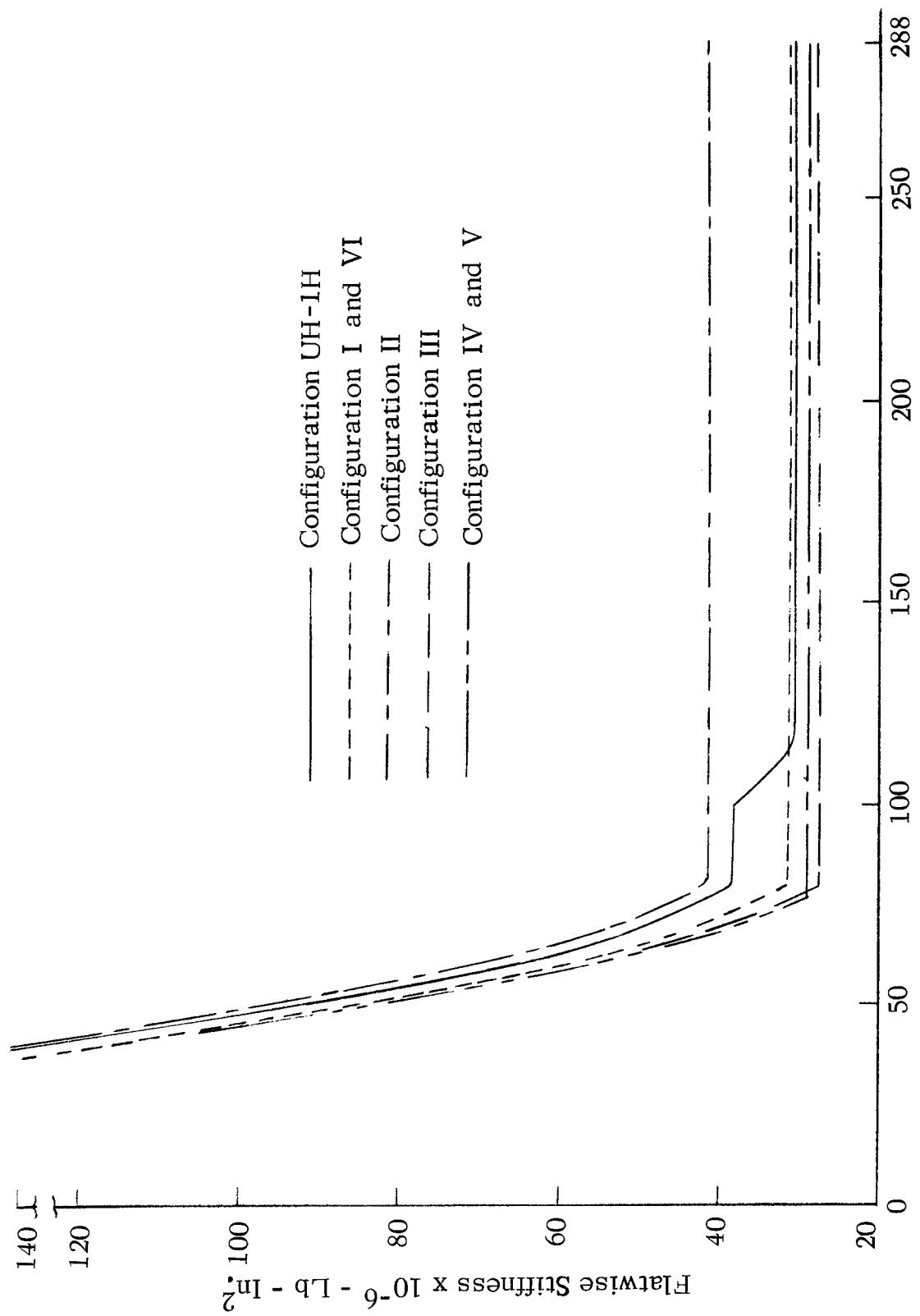


Figure 37. Flatwise Stiffness Distribution.

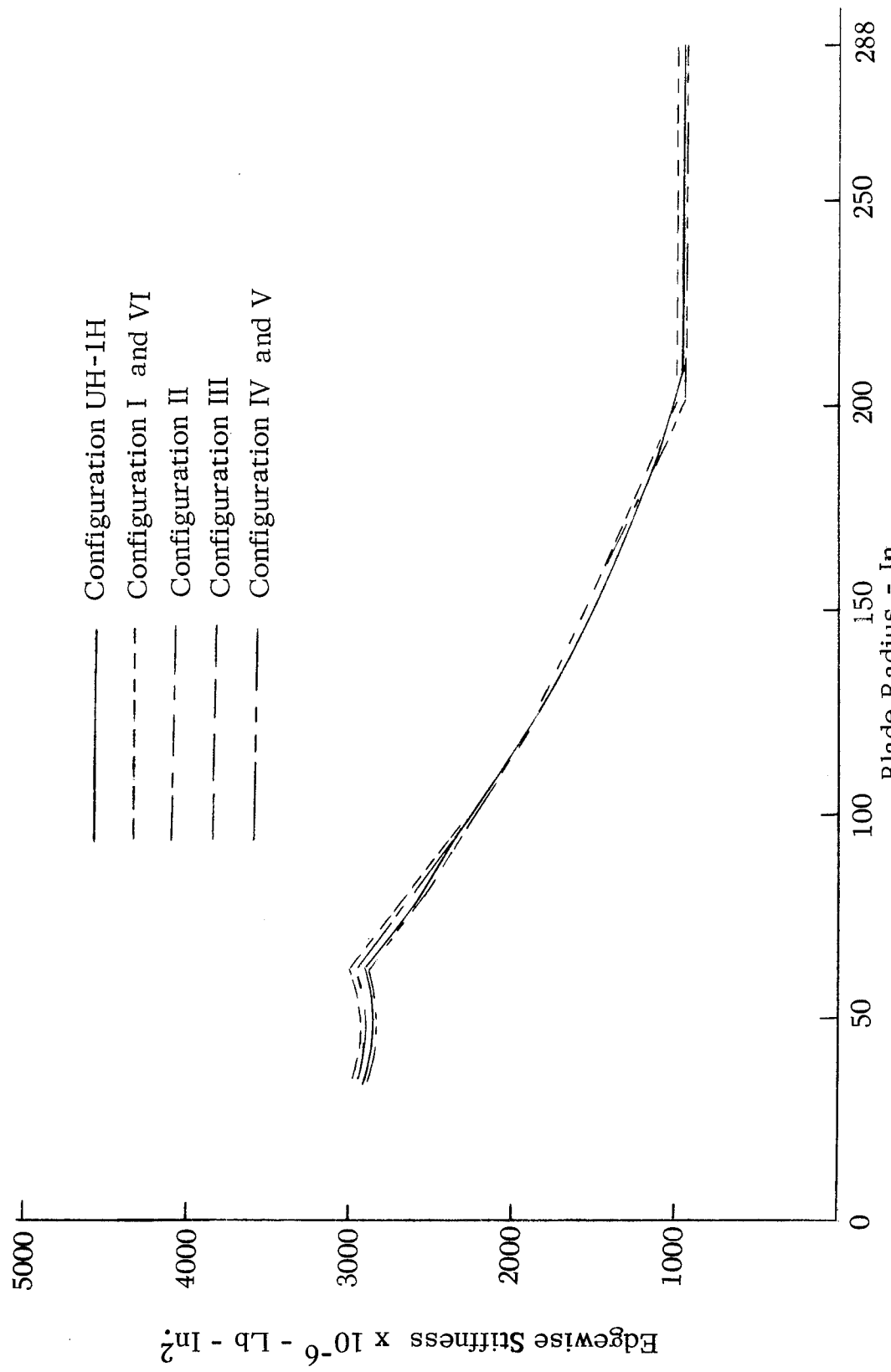


Figure 38. Edgewise Stiffness Distribution.

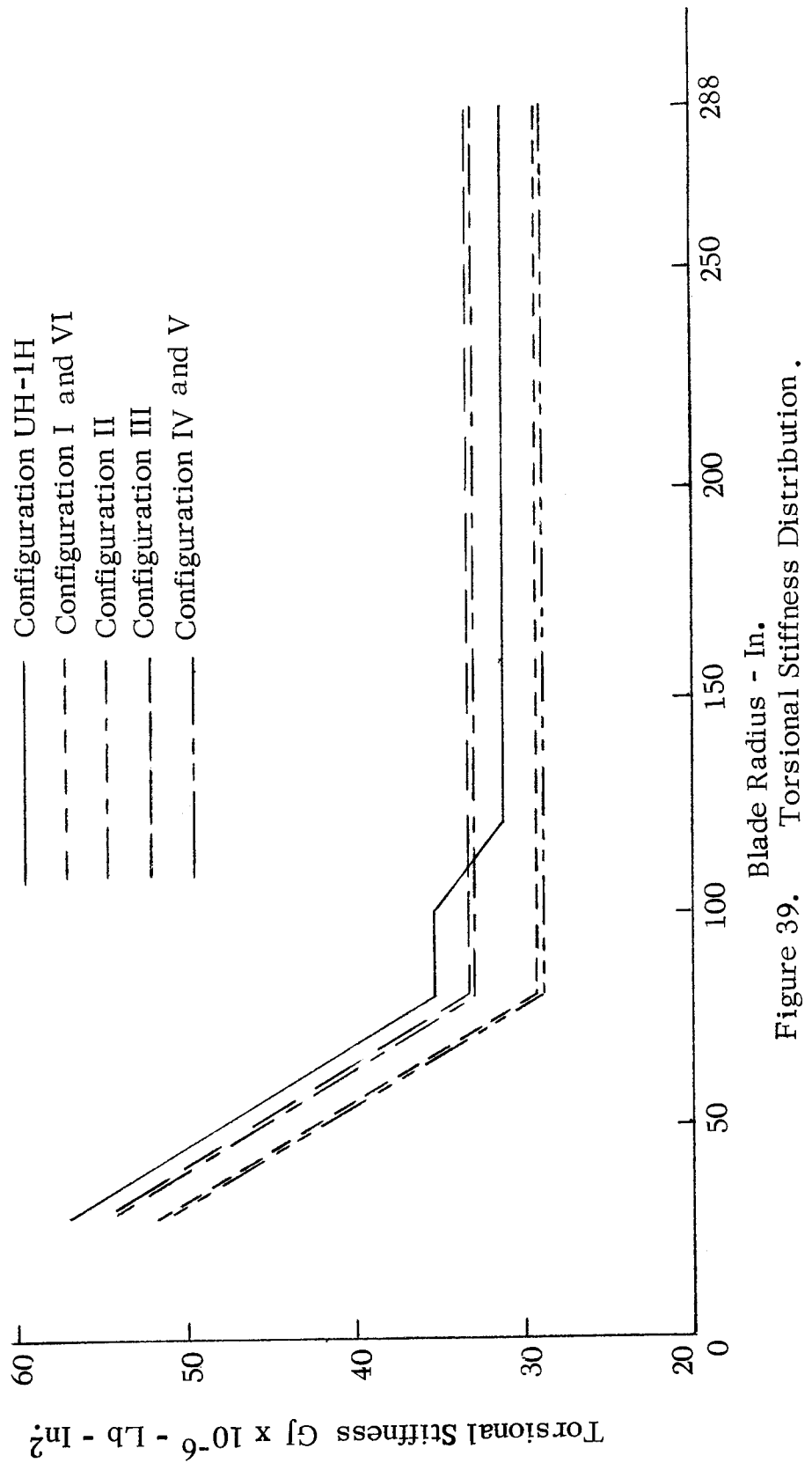


Figure 39. Torsional Stiffness Distribution.

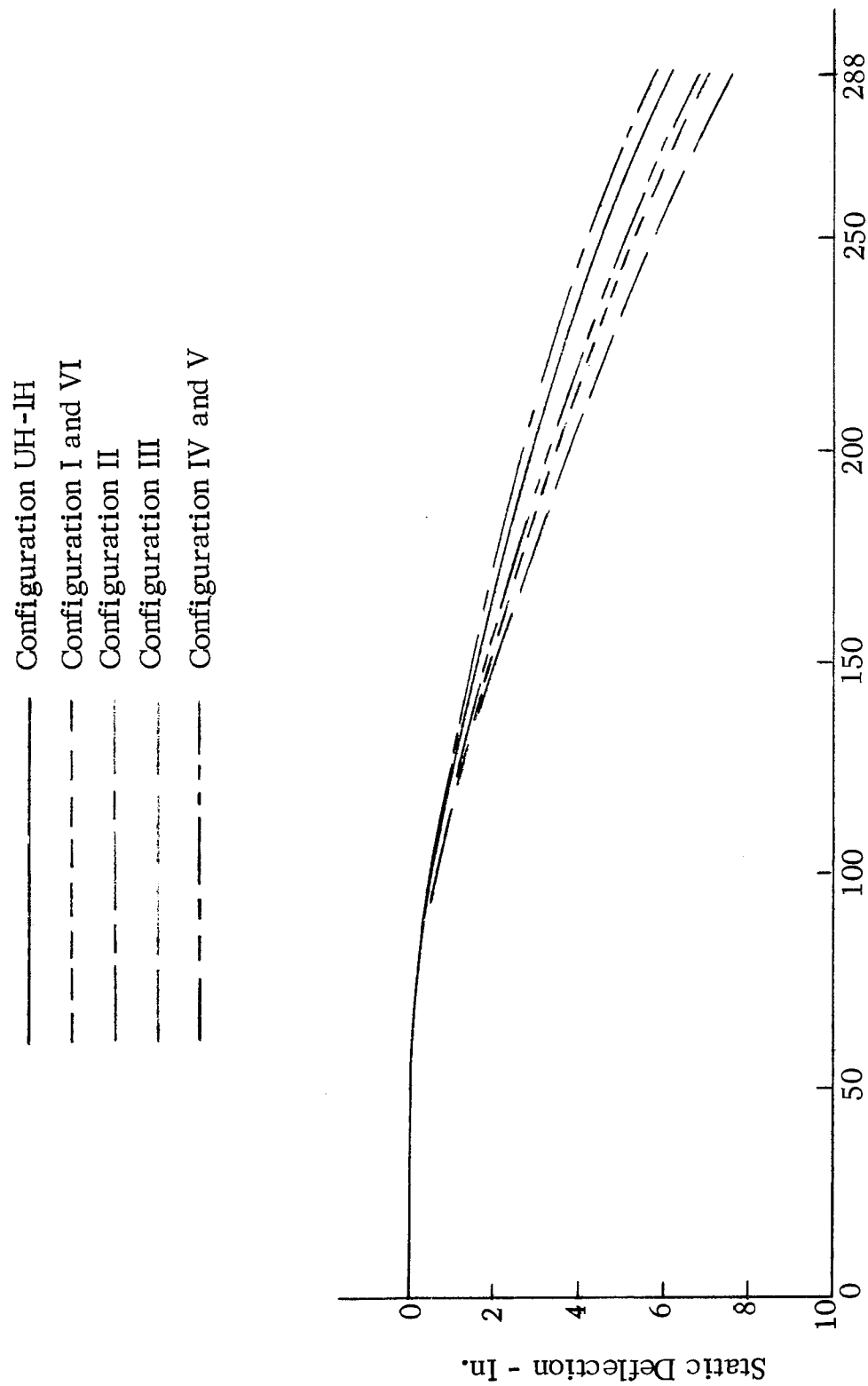


Figure 40. Blade Static Deflection Comparisons.

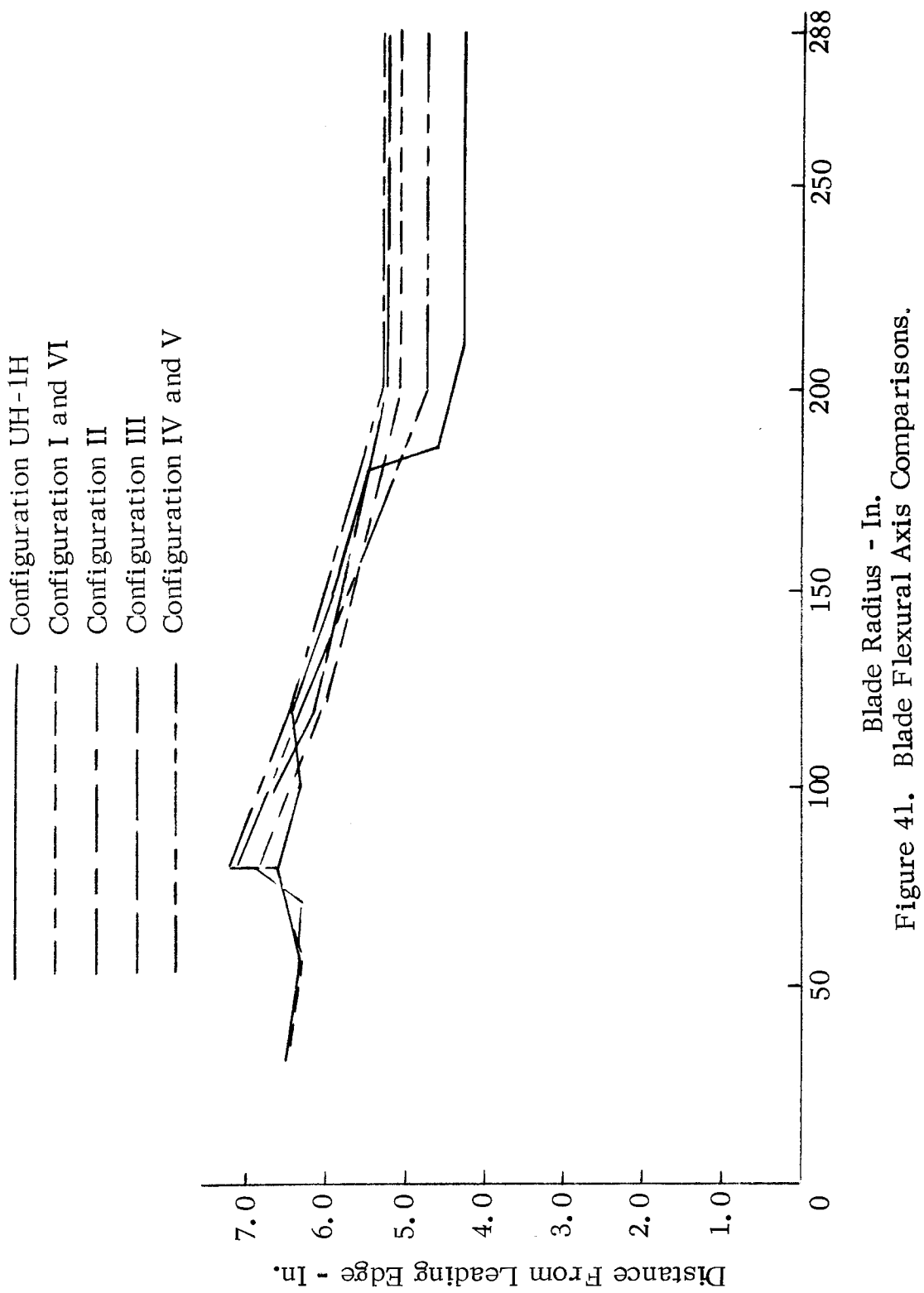


Figure 41. Blade Flexural Axis Comparisons.

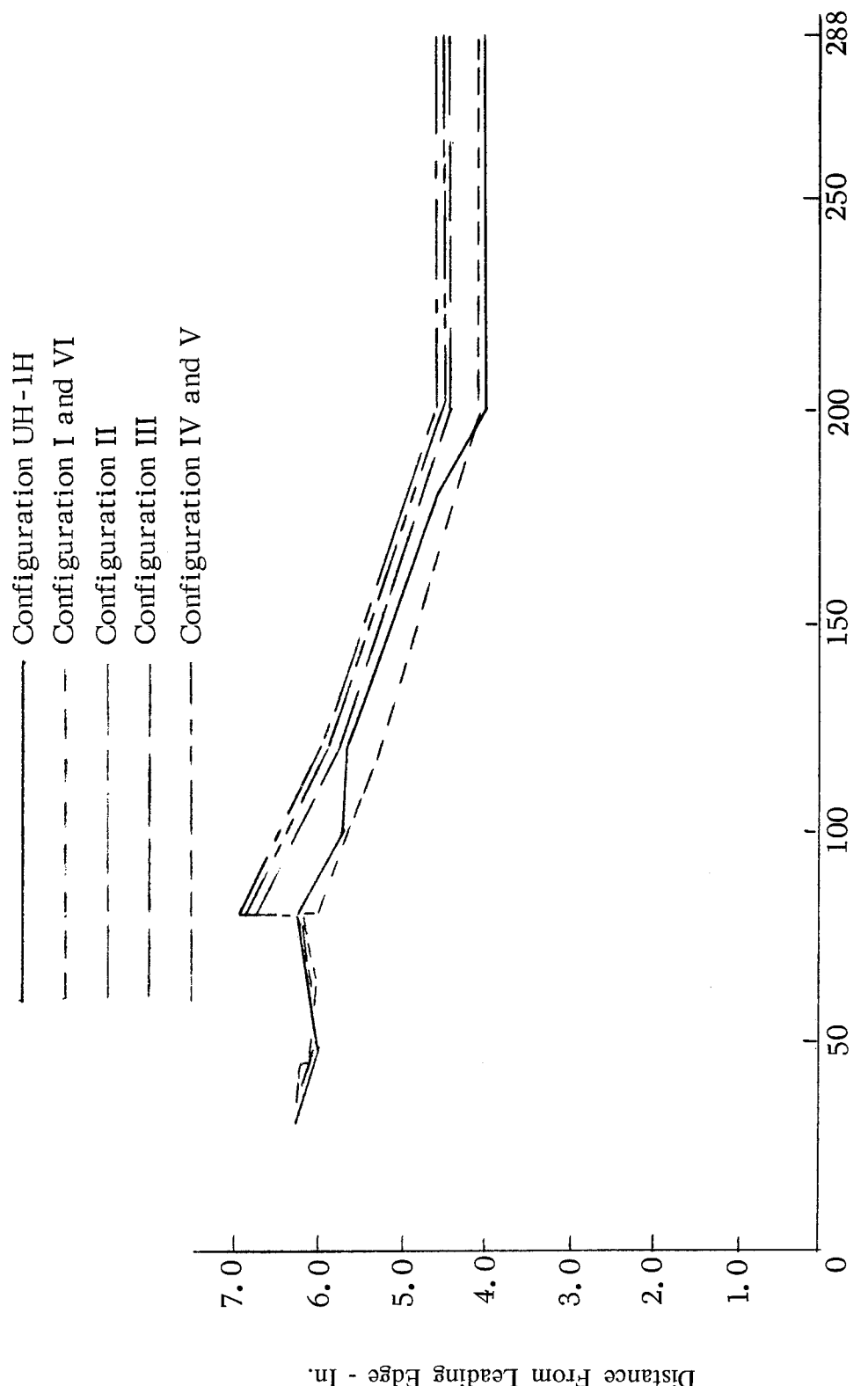


Figure 42. Blade Center of Gravity Comparisons.

TABLE I. COMPARISON OF PHYSICAL PROPERTIES

Configuration	Blade Weight Lb	Moment About Center of Rotation Lb-In.	Spanwise Center of Gravity From Center of Rotation In.	Chordwise Center of Gravity from Leading Edge In.	Flexural Mass Axis from Leading Edge In.	Inertia About Center of Rotation Slug-Ft ²
I, VI	216.35	27403	126.66	5.67	4.85	1076
II	225.34	28841	127.99	5.90	5.35	1135
III	222.14	27594	124.22	5.88	5.25	1067
IV, V	202.30	25597	126.53	5.62	5.33	1012
UH-1	206.62	26131	126.47	5.43	4.94	1039

The blade weight and stiffnesses of VI and V are essentially the same as I and IV respectively.

TABLE II. BLADE DESIGN FEATURES

Configuration	Main Spar		Trailing Edge Section		
	Structure	Balance Weight	Skins	Core	Trailing Edge Spline
I (1)	Extruded Aluminum Alloy 6061-T6	Integral with Extrusion	"E" Glass	Polyamide	
II (1)	Formed Sheets Stainless Steel A1S1-301 Aluminum Alloy 2024-T4	Integral with Stainless Steel Sheet	4 Ply $\pm 45^\circ$ 2 Ply 0°	Paper Honeycomb Nomex	Unidirectional "E" Glass
III (1)	Unidirectional "E" Glass and 2 Ply Carbon $\pm 45^\circ$	Integral with "E" Glass	"E" Glass 2 Ply $\pm 45^\circ$ 2 Ply 0°		(2) (3)
IV (1)	Two Beams of Unidirectional "E" Glass and Unidirectional Carbon in Nose (2)	Molded Weight Hysol EA9320 and Lead Shot	Carbon 2 Ply $\pm 45^\circ$ "E" Glass 1 Ply 0°		Unidirectional Carbon (2) (3)
V (1)(4)				None	Unidirectional Carbon (2)

TABLE II - Continued

Configuration	Main Spar		Trailing Edge Section		
	Structure	Balance Weight	Skins	Core	Trailing Edge Spline
VI (1) (5)	Extruded Aluminum Alloy 6061-T6	Integral with Extrusion	"E" Glass 4 Ply $\pm 45^\circ$ (2)	None	Unidirectional "E" Glass (2)

- (1) Leading edge abrasion resistance polyurethane coating.
- (2) Automated pultrusion process, constant section.
- (3) Machine tapered after pultrusion process.
- (4) One-half blade section fabricated by pultrusion process.
- (5) One-half trailing edge section fabricated in one piece by pultrusion process.

TABLE III. MATERIAL PROPERTIES

Material	Density Lb./In. ³	Modulus of Elasticity Lb./In. ² x 10 ⁻⁶	Modulus of Rigidity Lb./In. ² x 10 ⁻⁶	Ultimate Tensile Strength Lb./In. ²	Ultimate Tensile Strength Lb./In. ²	Endurance Limit (1) Lb./In. ²
2024-T3 Aluminum	.101	10.5	4.0	65, 000	7, 960	(2)
6061-T6 Aluminum	.098	10.0	3.8	38, 000	6, 100	(2)
301 Stainless Steel 1/2 Hard	.286	27.0	11.5	150, 000	23, 100	(3)
1002 E Fiberglass - Unidirectional	.067	5.7	.47	160, 000	12, 500	(4)
1002 E Fiberglass - ±45°	.067	1.5	1.5	11, 900	2, 000	(4)
Carbon Composite - Unidirectional	.057	26.0	.57	110, 000	25, 000	(4)
Carbon Composite - ±45°	.057	2.3	11.8	18, 400	3, 315	(4)

(1) Endurance limit at 10⁸ cycles for zero steady stress (R = -1.0).

(2) Includes a reliability reduction factor of (.61), size effect factor (.75) and surface finish factor of 1.15.

(3) Includes a reliability reduction factor of (.70).

(4) Includes a reliability reduction factor of (.50).

Sikorsky Aircraft. In all cases the working endurance limit stresses shown are reduced from the mean endurance limit by the appropriate probability and size effect factors. All values shown are at a "no steady" stress loading condition ($R = -1.0$).

The stresses in each of the major blade components were calculated at four radial positions on the blade. The four stations selected are radial station 200, 160, 120, and 80 inches. Station 200 is the inboard end of the constant section of the blade; stations 160 and 120 were selected as representative midspan stations; and station 80 is at the outboard end of the root end laminate buildup. At each of these stations, stresses were determined at several locations on the chordwise cross section. These locations include the combined flatwise and edgewise stresses at 10 percent chord, a point of maximum combined stress forward of the 1/4 chord and at the back corner position of the spar where the flatwise stress is generally a maximum. Maximum edgewise bending moment induced stresses occur at the trailing edge in the skin and spline members. At each of these locations, stresses were determined for each of the materials present.

Blade component stresses are determined for the loads shown in Figures 30 to 35 by applying the equation for direct stress, $f = P/A$, and bending stress, $f = Mc/I$ (Reference 10). Because the blade structure in each design is a combination of materials which have different moduli of elasticity, the moduli must be considered in the stress calculation. The equations now become $f = PE_c/EA$ and $F = McE_c/EI$. The effect of the variation in modulus between components is to distribute the load in the structure in proportion to the modulus of each component. Given the same position in the structure, a component made of a high modulus material will carry a higher load and have a higher stress level than the same component made from a lower modulus material. The equations for the calculation of blade stresses are

$$f = f_s + f_v \quad (15)$$

$$f_s = \frac{P_{cf}E_c}{EA} + \frac{M_{fs}C_{yy}E_c}{EI_{xx}} + \frac{M_{es}C_{xx}E_c}{EI_{yy}} \quad (16)$$

$$f_v = \frac{M_{fv}C_{yy}E_c}{EI_{xx}} + \frac{M_{ev}C_{xx}E_c}{EI_{yy}} \quad (17)$$

$$F_A = F_E \left(1 - \frac{f_s}{f_{tu}} \right) \quad (18)$$

where

f = Total stress at a point on the blade cross section, lb/in.²

f_s = Combined steady stress, lb/in.²

f_v = Combined vibratory stress, lb/in.²

P_{cf} = Centrifugal force, lb

M_{fs} = Steady flatwise moment, in.-lb

M_{es} = Steady edgewise moment, in.-lb

M_{fv} = Vibratory flatwise moment, in.-lb

M_{ev} = Vibratory edgewise moment, in. - lb

EI_{xx} = Total flatwise bending stiffness, lb/in.²

EI_{yy} = Total edgewise bending stiffness, lb/in.²

EA = Total axial stiffness, lb

E_c = Modulus of elasticity of the component (material), lb/in.²

C_{xx} = Distance between the point under consideration and the chordwise blade neutral axis, in.

C_{yy} = Distance between the point under consideration and the neutral axis perpendicular to the chordwise axis, in.

F_A = Allowable alternating stress, lb/in.²

F_E = Endurance limit of material at zero steady stress, lb/in.²

F_{tu} = Ultimate tensile strength of material, lb/in.²

For flatwise bending, tension on the bottom side of the beam is considered positive. For edgewise bending, tension on the leading edge of the

beam is considered positive.

The stresses obtained for the 90-knot cruise condition for each of the designs under consideration and the present UH-1H blade are shown in Tables IV to VIII. The allowable alternating stresses shown in the tables are obtained from Goodman diagrams for the appropriate materials. A typical Goodman diagram is shown for 2024T-3 aluminum (Figure 43) to illustrate the relationship between the steady stress level and the allowable vibratory stress. The margins of safety shown in the tables are obtained from the relationship

$$M. S. = F_A/f_v - 1 \quad (19)$$

where

M. S. = Margin of Safety

Fatigue Life Determination

Calculated fatigue life of a rotor blade is a function of the relationship of the stress level in the component to the allowable stress level (endurance limit) of the material of which the component is constructed. If the stress levels in the component were always below the endurance limit stress, then the component would have an infinite life (assuming no externally caused damage such as corrosion, foreign objects, etc.). Design of a component with such low stress levels would be overly conservative however, and would result in a very heavy rotor blade. A typical rotor blade is designed so that the conditions at which the aircraft will spend the major percentage of its operating time will not produce any damaging blade stresses. The effect of those conditions of aircraft operation which produce damaging stresses is evaluated using the Cumulative Damage Theory of Miner (Reference 11). Miner's theory states that a fatigue crack will be initiated when the summation of the increments of fatigue damage equals unity, or

$$\frac{n_1}{N_1} + \frac{n_2}{N_2} + \frac{n_3}{N_3} + \dots + \frac{n_n}{N_n} = 1 \quad (20)$$

where n_n = Number of cycles at a specific stress level

N_n = Number of cycles required to initiate a fatigue crack at that stress level

To calculate the fatigue life of a blade using the cumulative damage theory we first determine the operating spectrum for the aircraft. A spectrum consists of each condition of aircraft operation for the typical mission along with the percentage of total aircraft operating time spent at that

TABLE IV. BLADE STRESS IN LEVEL FLIGHT CRUISE - CONFIGURATION UH-IH

		Blade Station - In.		
		80	120	160
Component Stress				200
Spar Back Corner Stress	14,390 ± 3,108	13,826 ± 4,184	12,867 ± 4,254	11,772 ± 4,157
	7,208	7,249	7,368	7,408
	1.32	.73	.73	.78
Abrasion Strip <u>7-1/2% Chord Stress</u>	38,626 ± 8,315	37,013 ± 10,687	34,167 ± 10,446	29,666 ± 9,405
	15,400	15,750	16,170	17,010
	.85	.47	.55	.81
T E Spline <u>Trailing Edge Stress</u>	4,043 ± 2,753	2,696 ± 2,972	411 ± 3,097	2,654 ± 2,586
	7,050	7,010	7,448	7,478
	1.56	1.36	1.40	1.89
Skin <u>Trailing Edge Stress</u>	4,043 ± 2,753	2,696 ± 2,972	411 ± 3,097	2,654 ± 2,586
	6,485	6,449	6,852	6,880
	1.36	1.17	1.21	1.66

TABLE V. BLADE STRESS IN LEVEL FLIGHT CRUISE - CONFIGURATION I AND VI
 V = 90 Kt GW = 8,500 Lb

Component Stress Lb/In ²	Blade Station - In.		
	80	120	160
Spar (6061-T6 AL) Stress at 10% Chord	10,361 ± 3,445	11,057 ± 3,738	11,964 ± 3,798
F Allow	6,002	5,932	5,890
M S	.74	.59	.55
Spar (6061-T6 AL) Stress at Back Corner	10,803 ± 4,239	11,300 ± 4,356	11,514 ± 4,187
F Allow	5,949	5,914	5,897
M S	.40	.36	.41
Skin (E Glass) Stress at Back Corner	3,132 ± 1,229	3,276 ± 1,263	3,339 ± 1,215
F Allow	4,285	4,285	4,270
M S	2.49	2.39	2.51
Skin (E Glass) Stress at Trailing Edge	3,138 ± 738	3,002 ± 827	4,069 ± 834
F Allow	4,285	4,300	4,205
M S	4.81	4.20	4.04
T E Spline (E Glass) Stress at Trailing Edge	6,169 ± 1,451	5,901 ± 1,625	7,996 ± 1,640
F Allow	11,950	12,000	11,800
M S	7.24	6.38	6.20
			9,027 ± 1,532
			11,750
			6.67

TABLE VI. BLADE STRESS IN LEVEL FLIGHT CRUISE - CONFIGURATION II
 V= 90 Kt GW = 8,500 Lb

Component Stress Lb/In. ²	Blade Station - In.		
	80	120	160
"C" Section (301 S S) Stress at 10% Chord	40,678 ± 8,333	35,295 ± 8,677	32,505 ± 8,918
F Allow	17,500	18,000	18,500
M S	1.10	1.07	1.07
Channel (2024-T4 Alum) Stress at Back Corner	14,367 ± 3,075	12,801 ± 3,532	12,195 ± 3,872
F Allow	6,661	6,771	6,844
M S	1.17	.92	.77
Skin (E Glass) Stress at Back Corner	4,632 ± 1,752	3,820 ± 2,013	3,815 ± 2,207
F Allow	4,175	4,250	4,250
M S	6.18	1.11	.93
Skin (E Glass) Stress at Trailing Edge	4,722 ± 579	4,340 ± 665	3,358 ± 660
F Allow	4,160	4,200	4,250
M S	6.18	5.32	5.44
T E Spline (E Glass) Stress at Trailing Edge	9,281 ± 1,139	8,531 ± 1,307	6,600 ± 1,297
F Allow	11,750	11,750	11,900
M S	9.32	7.99	8.18

TABLE VII. BLADE STRESS IN LEVEL FLIGHT CRUISE - CONFIGURATION III
 $V = 90 \text{ Kt}$ $GW = 8,500 \text{ Lb}$

Component Stress Lb./In. ²	Blade Station - In.		
	80	120	200
Spar <u>Stress at Back Corner</u> of Carbon Laminate	5,196 ± 986	4,963 ± 1,377	4,890 ± 1,540
F Allow	6,000	6,025	6,050
M S	5.09	3.38	2.93
Spar <u>Stress at Back Corner</u> of Fiberglass Laminate	8,605 ± 1,612	8,249 ± 2,249	7,976 ± 2,517
F Allow	11,650	11,700	11,750
M S	6.23	4.20	3.67
Skin (E Glass) <u>Trailing Edge Stress</u>	5,887 ± 725	5,861 ± 835	4,706 ± 861
F Allow	4,065	4,070	4,160
M S	4.61	3.87	3.83
Spline (E Glass) <u>Trailing Edge Stress</u>	9,310 ± 1148	9,283 ± 1,322	7,332 ± 1,363
F Allow	11,600	11,600	11,850
M S	9.10	7.77	7.69

TABLE VIII. BLADE STRESS IN LEVEL FLIGHT CRUISE - CONFIGURATION IV AND V
 $V = 90 \text{ Kt}$ $GW = 8,500 \text{ Lb}$

Component Stress Lb/in. ²	Blade Station - In.		
	80	120	160
Spar (E Glass) Stress at Back Corner	9,020 ± 1,755 11,750 5.70	7,352 ± 1,839 11,850 5.44	7,223 ± 2,105 11,875 4.64
Skin ($\pm 45^\circ$ Carbon) Stress at Back Corner	6,013 ± 1,170 5,950 4.09	4,900 ± 1,226 6,050 3.93	4,823 ± 1,404 6,050 3.31
Skin ($\pm 45^\circ$ Carbon) Stress at Trailing Edge	6,492 ± 725 5,900 7.14	5,792 ± 830 5,975 6.20	4,431 ± 865 6,100 6.05
Skin Doubler (0° Carbon) Stress at 10% Chord	41,547 ± 7,309 18,600 1.54	34,123 ± 7,268 20,000 1.75	30,977 ± 7,812 20,500 1.62
T E Spline (0° Carbon) Stress at Trailing Edge	42,894 ± 4,795 18,250 2.81	38,265 ± 5,491 19,400 2.53	29,271 ± 5,714 20,700 2.62

2024-T3 Aluminum

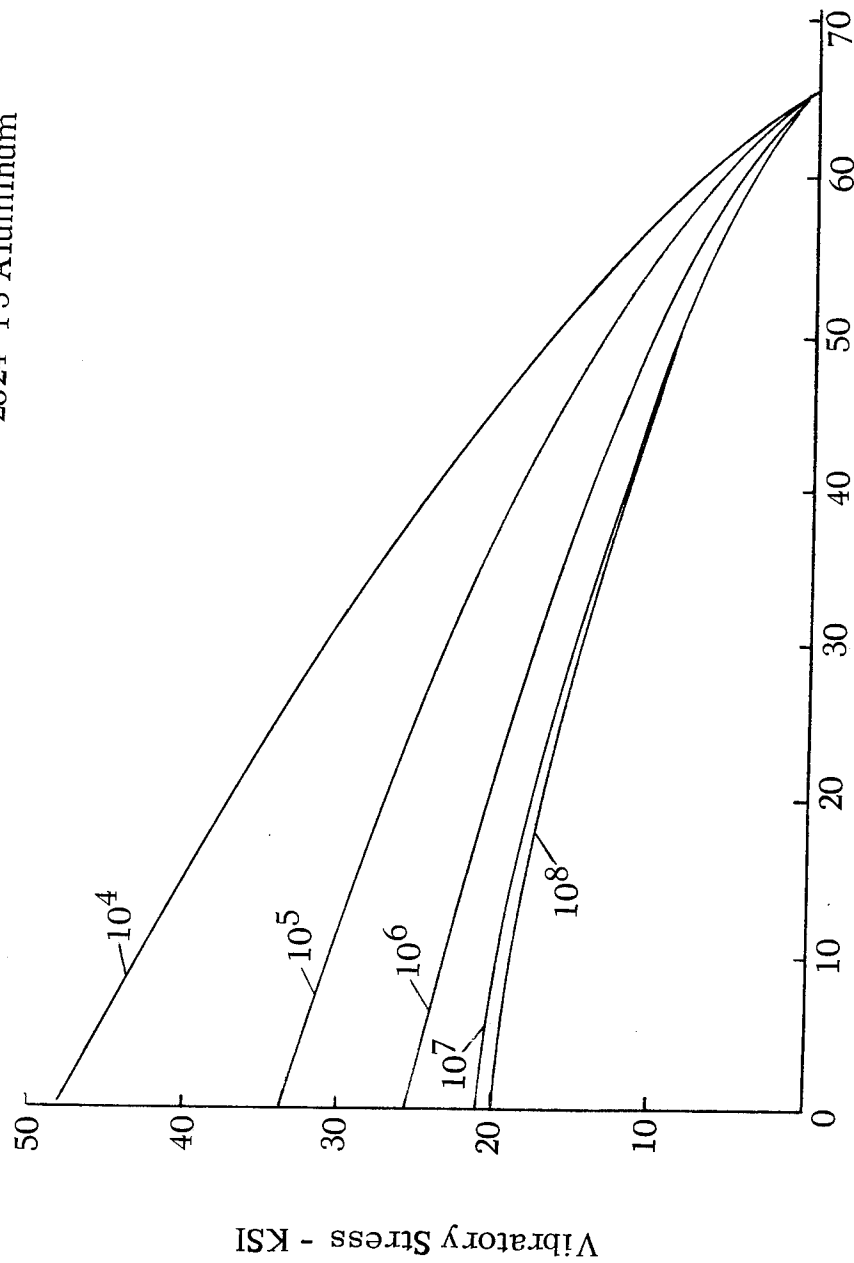


Figure 43. Typical Goodman Diagram.

condition. Blade stresses are determined for each of the operating conditions in the spectrum at a specific location on the blade being analyzed. Each level of blade component stress is then compared with the S-N diagram for the appropriate material.

A point anywhere on the S-N diagram represents the existence of some induced stress for some number of cycles. If the point is on the curve, it represents a failure, or more exactly the probability that a fatigue failure will occur in the number of cycles corresponding to the point. Several points plotted on a sample S-N diagram (Figure 44) illustrate the relation of stress to fatigue life. Point (c) is below the endurance limit and therefore contributes no cumulative damage to the component. Point (a) has an abscissa of 10^2 cycles, while the point on the curve at that ordinate is at 5×10^3 cycles. Thus, point (a) represents the using up of $10^2 / 5 \times 10^3 = .02$ of the fatigue life. Similarly, point (b) represents the using up of $2 \times 10^3 / 5 \times 10^4 = .04$ of the fatigue life. If we assume that these three points represent the stress history of 50 hours of operation, then the three points represent .06 of the life used up in 50 hours of typical operation. The fatigue life based on the cumulative damage theory would then be $50 \text{ hours} / .06 = 833 \text{ hours}$.

Evaluation of the fatigue life of the blade designs under consideration in this study by the previously described method was not attempted. The determination of stresses and the frequency of occurrence in maneuvers, rotor starts and stops and flares are obtainable only from previous testing of similar model aircraft. For this study, it was not deemed necessary to perform a rigorous analysis since a relative comparison with the UH-1H would suffice. Therefore, we chose to calculate only the level flight cruise condition stresses for each proposed design and for the present UH-1H design. By comparing each of these stresses with the material endurance limit stresses and determining their fatigue margins of safety, we obtain a more valid means of comparing designs with each other and the UH-1H blade.

Fatigue margins of safety determined for each of the design configurations are tabulated in Tables IV to VIII. A comparison of fatigue margins shows that all designs are at least as good as the present blade. The metal blade designs including the UH-1H are all very similar in margin; however, the composite blades show significant increases in the fatigue margins of safety. Since the mass and stiffness characteristics of all designs were made similar, the bending deflections would also be similar in magnitude. Therefore, the strain of the material in each blade will also be similar. Then the ability of each blade to resist fatigue damage is only a function of the strain allowable of the material. Strain allowable is defined as the stress at the endurance limit divided by the modulus of elasticity of the material. A bar graph of representative

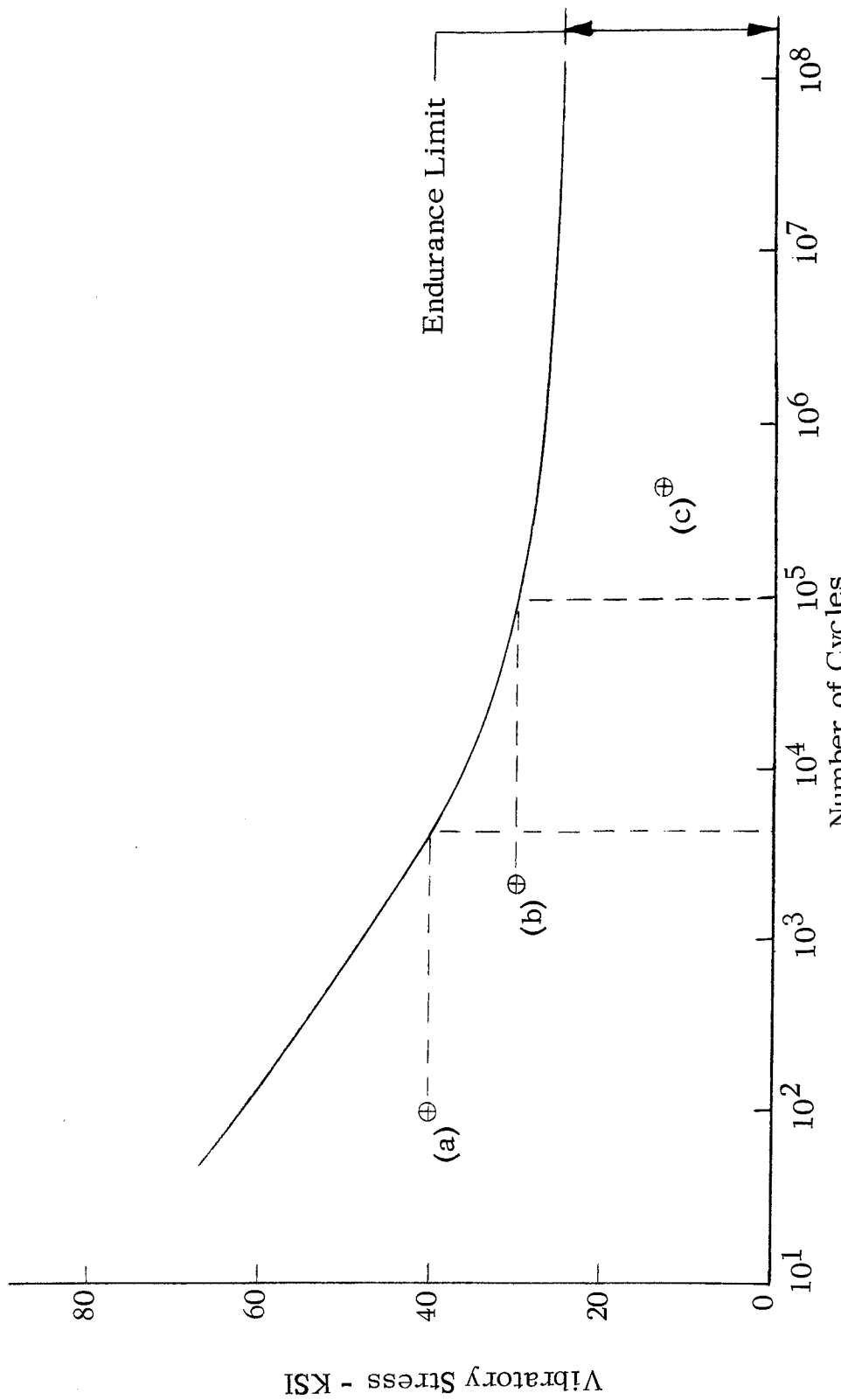


Figure 44. Stress-Cycle Curve.

strain allowables for several typical rotor blade construction materials is shown in Figure 45 (References 12, 13, and 14). The bar graph illustrates very clearly the advantage to be gained in fatigue life using composites.

Because of the close similarity between the fatigue margins of the metal blades and the UH-1H we have assigned the same 2500-hour life as the UH-1H blade to the metal designs. We have assigned an estimated life of 5000 hours to the composite designs, an assumption which we feel is conservative based on the much higher fatigue margins of safety.

SURVIVABILITY ANALYSIS

Since design Configurations I, II and III each had a similar fiberglass trailing edge structure and each of these had a tubular type spar, only Configuration I was subjected to a survivability analysis because it was considered representative of the three designs. Configuration IV consisted of a carbon trailing edge structure and a twin beam type spar and was therefore considered sufficiently different from the other designs to require a separate analysis.

Configurations I and IV were analyzed to determine the amount of damage or component failure the blade structure could withstand before ultimate failure. Various types of damage were considered including the complete separation of the trailing edge spline, cracking of the skin aft of the spar, a combined spline and skin failure and various bullet holes in the spar and other structural members. In each case, the structure was analyzed for loads developed in the 90-knot cruise condition. Two radial stations were considered, one at 80 inches and the other further outboard at 160 inches. The 80-inch location is just outboard of the root end doubler buildup area; at this location the edgewise moments are maximum and the blade cross section is minimum. At 160 inches, the flatwise moments are maximum and the stress levels for the undamaged blade are also maximum.

The blade bending moments calculated for the undamaged blade were also used for the damaged blade analysis. This is because the reduction in blade stiffness associated with the various damage modes will not change the undamaged blade bending moments significantly, since the changes in stiffness occur over only a very small segment of the blade length and therefore will not result in any significant change in curvature of the blade. The internal moments on the structure resulting from the local shifting of the structural centroid (neutral axis) at the damage location are considered in the analysis. For example, removal of structure from the trailing edge of the blade shifts the neutral axis forward locally. Centrif-

Vibratory Strain Allowables at $R = -1.0$

* 2/3 Glass at $\pm 45^\circ$ & 1/3 Glass at 0°
** 2/3 Carbon at $\pm 45^\circ$ & 1/3 Glass at 0°

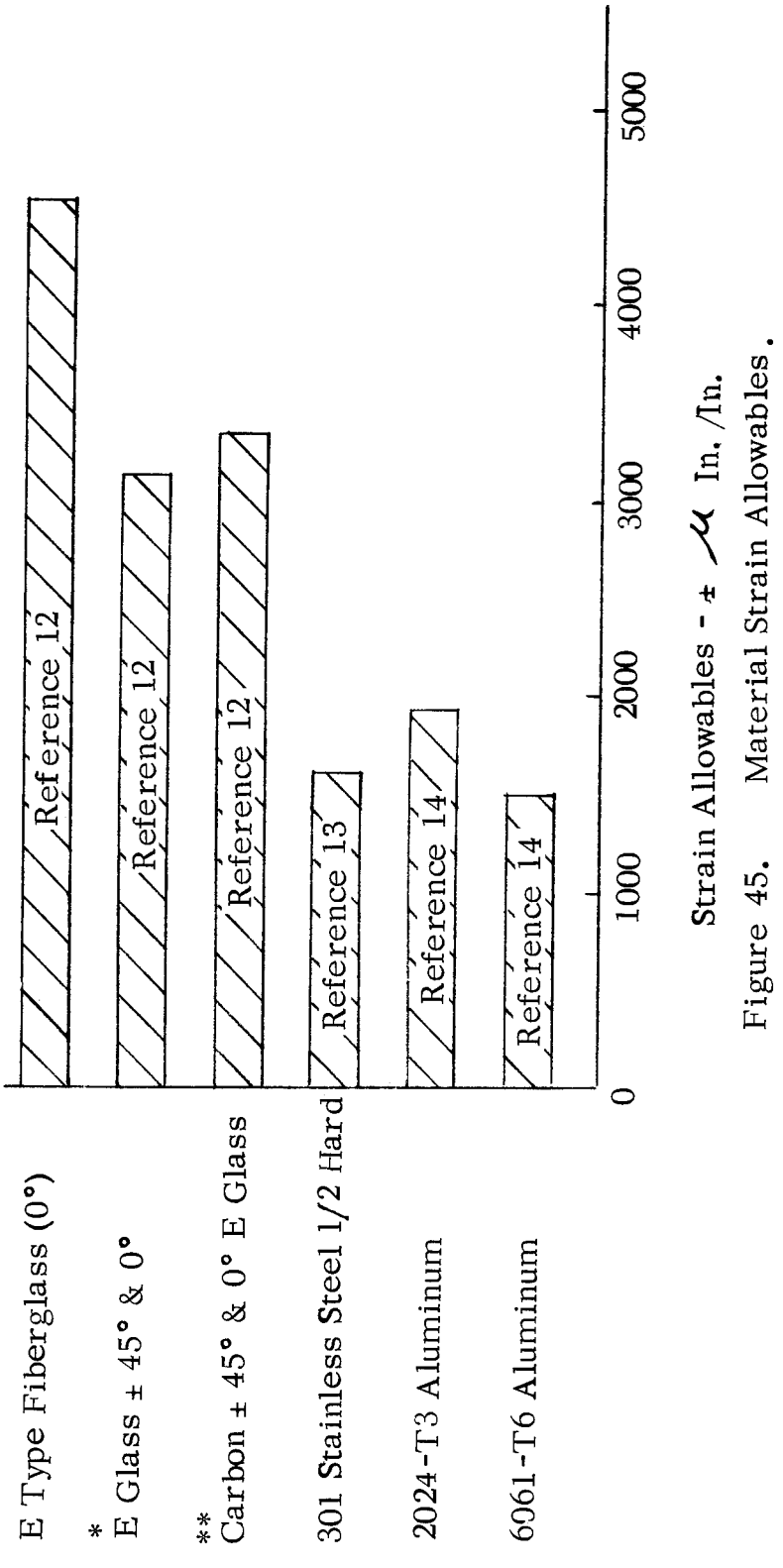


Figure 45. Material Strain Allowables.

ugal force acting through the mass centroid of the blade produces the local internal moment at the point of damage. The moment is the centrifugal force times the offset distance between the mass centroid and the local neutral axis. Dependent on the type of damage and the particular blade configuration, the internal moments can be very significant.

Stresses were calculated at various positions on the remaining undamaged blade components. In general, the trailing edge of the skin is the most highly stressed area of that component. Stresses in the spar are a maximum at the aftmost point on the spar contour. In Tables IX and X, the component stress levels are tabulated for both fatigue stresses and the peak static stress levels. The margins of safety in fatigue are shown as a function of the working endurance limit. Margins of safety for the static stresses are based on the ultimate tensile strength of the materials.

Damage to the trailing edge spline resulting in complete severing of the spline member was considered first. Such damage could result from projectile damage or by a failure of the spline structure. The trailing edge spline provides the major portion of the edgewise stiffness. The percentage of total stiffness contributed by the spline increases from the tip to the root of the blade. For Configuration I, the spline contributes 26% at the tip and 63% at the 80-inch radial station. The spline contributes 61% and 80% at the comparable stations for Configuration IV. Since the spline contributes so much to the edgewise stiffness, it also has a large influence on the neutral axis of the structure. Loss of the spline results in a shift in the neutral axis toward the leading edge of the blade and an internal moment due to centrifugal force which tends to place the trailing edge in tension.

Examination of the tables shows that complete severing of the spline will not result in ultimate failure of the rest of the blade structure for either design concept. The life of the spar in Configuration I would, however, be limited, as would the carbon skin in Configuration IV. Both components would be life limited on the inboard portion of the blade only.

Failure of only the skin aft of the spar reduces the edgewise stiffness and to some degree also the flatwise stiffness. However, the contribution of the skin to the overall blade edgewise stiffness is small compared to the spline. Since the stiffness contribution of the skin is constant over the blade length, the percentage reduction in edgewise stiffness lost will decrease going from the tip to the root. Therefore, in the root end region where the loads are a maximum, the reduction in blade structural properties will be a minimum. Tables IX and X again show the results of the analysis for this failure mode. Both design concepts under consideration have sufficient life to continue flight based on the positive fatigue margins

TABLE IX. STRUCTURAL ANALYSIS FOR VARIOUS MODES OF FAILURE/DAMAGE -
CONFIGURATION I

Failure Mode	Radial Blade Location (In.)	Component	Fatigue Stress (Lb/In. ²)	Fatigue M S	Static Stress (Lb/In. 2)	Ultimate M S
Trailing Edge Spline Separated	160	Spar	14,738 ± 4,899	.14	19,637	.94
	160	Skin	9,706 ± 1,793	1.11	11,499	3.91
	80	Spar	21,352 ± 7,533	*	28,885	.32
	80	Skin	17,123 ± 3,163	.01	20,286	1.79
Skin Aft of Spar Separated	160	Spar	12,632 ± 4,643	.25	17,275	8.26
	160	Spline	8,421 ± 1,687	5.97	10,108	9.88
	80	Spar	14,978 ± 4,124	.35	19,102	.99
	80	Spline	9,356 ± 1,824	5.30	11,180	13.31
Spline and Skin Separated	160	Spar	26,530 ± 7,148	*	33,678	.13
	80	Spar	41,364 ± 8,596	--	49,960	.24
* Life Limited						

TABLE X. STRUCTURAL ANALYSIS FOR VARIOUS MODES OF FAILURE/DAMAGE -
CONFIGURATION IV

Failure Mode	Radial Blade Location (In.)	Component	Fatigue Stress Lb/In. ²	Fatigue M S	Static Stress Lb/In. ²	Ultimate M S
Trailing Edge Spline Separated	160	Spar	10,593 ± 2,389	3.81	12,982	11.32
	160	Skin	16,224 ± 4,120	.24	20,344	2.88
	160	LE Doubler	23,725 ± 10,378	1.07	34,123	2.22
	80	Spar	15,260 ± 3,035	2.71	18,295	7.75
	80	Skin	28,344 ± 6,817	*	35,160	1.25
	80	LE Doubler	51,861 ± 8,571	.84	60,432	.82
	160	Spar	7,760 ± 2,366	5.97	10,126	14.80
	160	Spline	33,425 ± 8,169	1.45	41,594	1.64
	160	LE Doubler	32,587 ± 8,501	1.38	41,088	1.68
	80	Spar	9,830 ± 1,913	4.88	11,743	3.81
	80	Spline	30,765 ± 6,482	2.16	37,247	1.95
	80	LE Doubler	43,288 ± 8,423	1.16	51,711	1.13
Spline Aft of Spar Separated	160	Spar	17,657 ± 4,603	1.42	22,260	6.19
	160	LE Doubler	7,761 ± 14,500	2.29	22,261	3.94
	80	Spar	31,369 ± 5,964	.68	37,333	3.29
	80	LE Doubler-15	083 ± 19,681	.27	-34,764	1.45
* Life Limited						

of safety, and both have high ultimate strength margins of safety as well.

A combined failure of the skin and the trailing edge spline was also considered where all of the structure aft of the spar is eliminated. The spar and the remaining skin provide all of the edgewise stiffness. Flatwise stiffness is not reduced very much since the spline and skin provide very little of the total flatwise stiffness. The neutral axis will be displaced toward the leading edge, further forward than when only the spline was severed. The resultant large edgewise moment thus produced is reacted by large tensile stresses in the trailing edge of the spar. Table IX shows that the spar in Configuration I is life limited over its entire spanwise length. Stresses in the aluminum spar will also exceed the ultimate strength of the spar inboard of approximately midspan of the blade. The very high fatigue and ultimate strengths of the composite spar are evident in Table X. Whereas the aluminum spar stresses would exceed the ultimate, the composite spar and skin doubler will still have a positive margin in fatigue as well as a high ultimate margin of safety.

Ballistic damage to the blade spars in all the design concepts is considered survivable. Service experience with aluminum spar blades has shown that up to .50-caliber bullet holes in various locations on the spar are survivable. Figures 46 and 47 are photos of actual in-flight ballistic damage sustained by Sikorsky main blades. The blade in Figure 46 was actually flown on a subsequent mission after the .50-caliber hole was "repaired" with aluminum foil tape. Although no service experience is available on composite blade spars, we expect that the composite blades will be even more damage tolerant than the present metal ones. The very large amount of reserve strength present in the twin beam composite spar, as shown in the analysis of both the damaged and undamaged rotor blades, makes this very probable.



Figure 46. .50-Caliber Hit Sikorsky Main Blade.

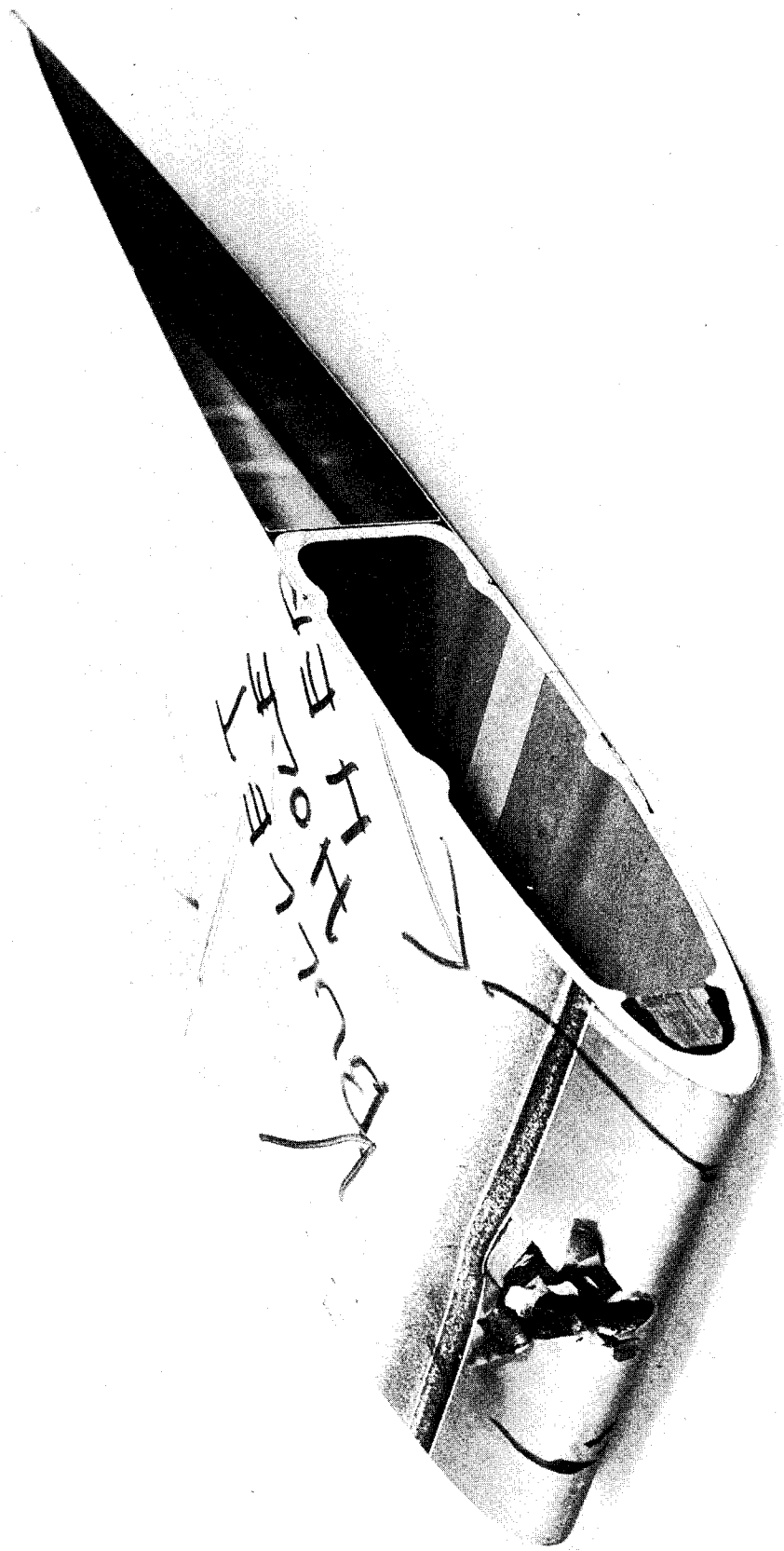


Figure 47. Blade Spar Structural Damage.

RELIABILITY AND MAINTAINABILITY ANALYSIS

Reliability/maintainability participation in the UH-1H expendable blade design effort consisted of assisting in the development of R/M related cost-effectiveness equations and design analysis of baseline and candidate blade designs. A mathematical model was designed to measure UH-1 cost effectiveness when equipped with the current UH-1 blade and comparative cost effectiveness values when equipped with each design candidate expendable blade. Standard nonvariable input values were supplied by the Government for use in the model. Variable input values were developed through reliability, repairability, and maintainability analyses of the baseline UH-1 blade and each candidate blade design. Reliability/maintainability input variables for use in the model are as follows:

<u>Input Variable</u>	<u>Units</u>
1. Aircraft down hours	Down hours/flight hour
2. Aircraft aborting failure rate	Aborting failures/flight hour
3. Blade mean time between inherent failures	Blade hours
4. % damaged blades repaired on aircraft (ORG level)	%
5. % removed blades repaired off aircraft (ORG level)	%
6. % removed blades scrapped (ORG)	%
7. % removed blades sent to direct support level	%
8. % received blades repaired at direct support level	%
9. % received blades scrapped at direct support level	%
10. % received blades repaired at depot level	%
11. MMH/inspection - on aircraft (ORG)	MMH/blade
12. MMH/repair - on aircraft (ORG)	MMH/repair
13. MMH/repair - off aircraft (ORG)	MMH/repair
14. MMH/repair - direct support	MMH/repair
15. GSE cost - on aircraft repair (ORG)	\$/repair
16. GSE cost - off aircraft repair (ORG)	\$/repair
17. GSE support cost (ORG)	\$/aircraft
18. GSE cost per repair - direct support	\$/repair
19. GSE support cost - direct support	\$/aircraft
20. GSE cost per repair - depot	\$/repair

<u>Input Variable</u>	<u>Units</u>
21. GSE support cost - depot	\$/ aircraft
22. Parts/material cost - on aircraft repair - ORG level	\$/ repair
23. Parts/material cost - off aircraft repair-ORG level	\$/ repair
24. Parts/material cost - direct support	\$/ repair
25. Blade overhaul cost - depot	\$/blade

MATH MODEL INPUT VARIABLES - DISCUSSION AND DEFINITION

Aircraft Down Hours

The influence of the baseline UH-1 main rotor blade and of each candidate blade design upon aircraft downtime was estimated and treated as an input variable to the math model for use in measuring changes in aircraft operational availability relative to each blade design. Baseline UH-1 down hours per flight hour were calculated in the following manner:

$$\text{Operational Availability} = \frac{\text{Flying time} + \text{Ready time}}{\text{Total time available}} \quad (21)$$

where operational availability = 75% (value supplied by USAAMRDL)
utilization rate = 41 hours/month/aircraft
time available = 720 hours/month

$$\begin{aligned}
 \text{Flying time} + \text{ready time} &= (720) (.75) = 540 \text{ hours/month} \\
 \text{Total downtime} &= \text{Time available} - (\text{Flying time} + \\
 &\quad \text{ready time}) \\
 &= 720 - 540 \\
 &= 180 \text{ hours/month}
 \end{aligned} \tag{22}$$

$$\text{Down hours/Flight hour} = \frac{\text{Downtime}}{\text{Flying Time}} = \frac{180}{41} = 4.38 \quad (23)$$

The 4.38 down hour per flight hour arrived at above is considered to include supply, administrative, and maintenance downtime and represents the UH-1 DH/FH value used as a baseline value for purposes of this study.

Aircraft Aborting Failure Rate

The aircraft aborting failure rate was originally introduced to the math model to measure variations in mission reliability with changes in main rotor blade designs and resultant impact on cost effectiveness. In

order to effectively use this parameter in the math model a baseline value for the UH-1 aircraft and the UH-1 main rotor blade aborting failure rates was required. The actual values for the UH-1 aircraft proved to be unavailable, and therefore a representative value was estimated for the overall aircraft using Sikorsky in-house aborting failure rate data adjusted to reflect the UH-1 configuration. The estimated value assigned to the UH-1 was .015, or 15 mission aborting failures per 1000 flight hours. Due to the lack of background data relating specifically to UH-1 main rotor blade aborting failure rates and their influence on the overall aircraft aborting failure rate, mission reliability was treated as a constant for all blade designs throughout the study.

Blade Mean Time Between Inherent Failures

The MTBR value assigned to the UH-1 baseline blade for inherent causes was taken directly from Reference 2 and is cited as 3,733 blade hours. The rationale connected with the use of this value is discussed in the following paragraphs.

Blade Retirement Life

Baseline UH-1 blade retirement life was cited as 2500 blade hours in Table XXXXIV. Retirement life values cited for candidate expendable blade designs were based upon load and stress and analyses conducted for each of the proposed designs.

Remove-Repair-Scrap Percentage Values

Math model input values for these parameters were calculated directly from the candidate blade repairability analyses which are presented in Appendix II. Baseline values for the UH-1 blade were furnished by Table XXXXIV.

Maintenance Man-Hour Values

All man-hour input variables to the math model were taken from the maintenance task analyses conducted for each blade repair procedure. Refer to the maintainability analyses presented on page 121 for the methodology used to calculate maintenance man-hour values.

Support Equipment Cost Factors

Support equipment cost factors were computed on the basis of (1) the cost of special support equipment required to support 24 aircraft per site and (2) the cost of special support equipment per repair action. The cost values cited represent only that cost incurred for special support equipment over and above that which is already in existence for the current UH-1 blade. A typical calculation for the cost of support equipment at the direct support level of maintenance follows:

1. Cost of SSE per 24 aircraft = \$15,304.00
2. Frequency of repair at DS level requiring the use of SSE = 3,820 Blade Hours
3. 24 aircraft per site per 10-year life cycle = 240,000 Blade Hours

$$\text{Cost per A/C} = \frac{\text{Cost of SSE per site}}{\text{No. of A/C per site}} = \frac{\$15,304}{24} = \$637.00 \quad (24)$$

$$\begin{aligned} \text{Cost per repair}_{\text{DS}} &= \frac{\text{Cost of SSE per Site}}{(\text{Blade hrs per life cycle } 24 \text{ A/C}) * (\text{Freq repair at DS})} \\ &= \frac{\$15,304.00}{240(10)^3 / 3,820} = \$243.00 \text{ per repair} \end{aligned} \quad (25)$$

Parts/Material Cost

Parts/material cost values were computed on the basis of dollar cost of parts and material per average repair procedure at each level of maintenance. The cost of repair kits containing all required materials for minor and/or extensive repair of fiberglass or carbon skin damage was calculated. Each kit contains required parts as well as materials for accomplishing all fiberglass and carbon repairs. Refer to Appendix II for fiberglass and carbon repair procedures.

Blade Overhaul Costs

Depot level overhaul costs were calculated for each candidate blade design based upon part, material and labor cost estimates. Support equipment cost relative to depot overhaul is not included in the cited values since Table XXXXIV referred this parameter as zero for both the UH-1 and candidate blade designs.

DEVELOPMENT OF RELIABILITY INDEX

Data Source

The presented data was reviewed and the reported failure modes and frequencies were apportioned to the UH-1 component parts. The mean time to removal values quoted in Table D1 of Reference 2 were converted to mean time between removal values for use in determining total inherent and external failure rates for candidate expendable blade designs. Background data relating to the reliability and maintainability of fiberglass skins was taken from contractor experience with the Sikorsky improved rotor blade currently being tested on the CH-53 helicopter, Sikorsky experience with fiberglass fuselage skin panels, service experience with fiberglass propellers, and results of Sikorsky in-house testing relative to the abrasion resistance qualities of fiberglass.

Reliability Values

Table XI is a compilation of published UH-1 main rotor blade mean times to removal due to various failure modes and their conversion to mean times between removal. Mean time to removal is defined as the sum of the times at removal for all blades divided by the number of blades removed, or

$$MTR = \frac{\sum_{i=1}^{n} t_i}{n} \quad (26)$$

where t_i = the total time at removal of the i th blade in hours
 n = the number of blades removed

Reliability data presented in MTR form is not suitable for predicting blade life-cycle failure occurrences or blade life-cycle inventory requirements. Values computed as shown above do not reflect total time generated by the entire blade population. They represent only those hours recorded on removed blades at the time of removal and therefore result in values which are considerably lower than those which should be used for logistics purposes or for determining blade life-cycle cost. In order to account for total blade population and to utilize the published data for prediction purposes the MTR's of Table D-1 of Reference 2 were converted to MTBR's and are reported in Table XI.

Inherent Damage

The established values of Table XI were used to construct a reliability profile of the baseline UH-1 blade. Blade inherent failure modes were determined and quantified in terms of MTBR based upon the number of failure occurrences given in Table XI divided into 6,698,706 total blade hours. This total blade hour value was arrived at by using a representative mean time between removal value of 914 hours, as selected from Table E-1 of Reference 2, multiplied by the total number of occurrences of Table XI. The MTBR values established through the above procedure were then allocated to the component parts of the UH-1 blade. For example,

Table XI indicates that 400 removals took place due to "BONDING SEPARATION".

$$\text{MTBR} = \frac{6,698,706}{400} = 1 \text{ per } 16,747 \text{ blade hours} = .000060$$

(27)

The MTBR value was then allocated to UH-1D blade component parts which are susceptible to "BONDING SEPARATION".

<u>Component Parts</u>	<u>Apportionment</u>
Abrasion Strip Bonding Separation	= .000018
Core to Spar Bonding Separation	= .000004
Skin to Core Bonding Separation	= .000019
Doubler Bonding Separation	= .000004
Trailing Edge Strip to Core S	= .000002
Trim Tab in Bonding	= .000004
Skin to Spar Separation	= .000004
Skin to Trailing Edge Strip Separation	= .000005
	<hr/>
	.000060

Apportionment values were established by reference to various data sources including Sikorsky in-house reliability data relative to main rotor blades. The MTBR values thus established and apportioned for the entire UH-1 blade served as the basis for the evaluation of the inherent failure modes of all candidate blade designs. The established MTBR values were adjusted to compensate for basic differences in candidate blade designs. For example, the UH-1 blade aluminum skin MTBR was established at 43 removals per 10^6 blade hours. This same value was assigned to the skin of our candidate aluminum extruded spar design because there is no basic difference between the two skin designs. However, the same extruded aluminum spar design utilizing a fiberglass

TABLE XI. REASONS FOR UH-1D BLADE REMOVAL-MTR/MTBR ANALYSIS

Reason for Removal	Recorded Number of Removals	Recorded Mean Time To Removal (Blade Hours)	Calculated Mean Time Between Removals (Blade Hours)
Part Cause and External Cause	7,329	441.9	914.0
I. Part Causes	1,795	546.7	3,733
A. Excessive Vibration	436	355.1	15,364
Beyond tolerance	22	443.7	304,487
Excess vibration	144	298.1	46,519
Fluctuates, unstable	5	432.8	1,339,741
Improper adjust	3	895.5	2,232,290
Improper align	1	499.0	6,698,706
Improper track	28	277.9	234,239
Improper weight	4	241.6	1,674,676
Mismatched	28	366.0	234,239
Out of adjust	18	498.9	371,150
Out of position	1	178.0	6,698,706
Out of position	99	401.4	67,663
Unable to adjust	61	367.4	109,815
Unbalanced	17	278.3	394,041
B. Deterioration	585	597.3	11,451
Brittle	7	428.8	956,958
Burst	6	994.0	1,116,451
Cracked	510	585.6	13,135
Deteriorated	58	671.3	115,495
Flaking	4	689.5	1,674,676

TABLE XI - Continued

Reason for Removal	Recorded Number of Removals	Recorded Mean Time To Removal (Blade Hours)	Calculated Mean Time Between Removals (Blade Hours)
I. Part Causes - Continued			
C. Bonding Failure	400	580.8	16,747
Delaminated	107	582.3	62,605
Internal failure	31	530.5	216,087
Loose	15	524.1	446,580
Poor bonding	247	589.6	27,120
D. Excessive Wear			
Brush failure	265	657.4	25,278
Pitted	11	299.7	608,973
Worn	22	563.4	304,487
	232	682.9	28,874
E. Corrosion			
Corroded	109	648.9	61,456
Deposits	64	749.0	104,667
Leaking	6	339.0	1,116,451
Moisture saturation	24	486.0	279,113
	15	599.1	446,580
II. External Causes			
A. Foreign Object Damage	5,534	398.8	1,211
Battle damage	4,721	398.5	1,419
Bent	802	386.8	8,353
Broken	79	409.8	84,794
Buckled	79	426.3	84,794
	39	422.6	181,046

TABLE XI - Continued

Reason for Removal	Recorded Number of Removals	Recorded Mean Time To Removal (Blade Hours)	Calculated Mean Time Between Removals (Blade Hours)
II. External Causes - Continued			
Chipped	24	433.8	279, 113
Collapsed	4	68.6	1, 674, 676
Cut	196	346.5	34.177
Dented	1, 278	437.6	5, 242
Foreign object damage	804	416.5	8, 322
Grooved	11	328.7	608, 973
Nicked	52	406.7	128, 821
Punctured	942	357.8	7, 111
Scored	10	652.0	669, 870
Torn	400	366.8	16, 747
B. Overstressed			
Crash damage	791	400.4	8, 468
Overspeed	173	485.1	38, 721
Overstressed	249	392.6	26, 902
Sudden stoppage	126	297.8	53, 164
Warped	209	412.5	32, 051
	34	330.5	197, 021
C. Heat Damage			
Blistered	17	349.7	394, 042
Burned	10	394.4	669, 870
Heat damage	6	238.4	1, 116, 451
	1	504.0	6, 698, 706

TABLE XI - Continued

Reason for Removal	Recorded Number of Removals	Recorded Mean Time To Removal (Blade Hours)	Calculated Mean Time Between Removals (Blade Hours)
II. External Causes - Continued			
D. Maintenance and Shipping			
Damage	1	106.0	6,698,706
Improperly installed	1	106.0	6,698,706
E. Other	5	583.6	1,339,741
Failure caused by other component failures	5	583.6	1,339,741

skin rather than aluminum exhibits a MTBR for skin problems of 126 removals per 10^6 blade hours. This adjusted value reflects additional failure modes inherent in fiberglass materials as compared to aluminum (see Table XXXII, Appendix II).

External Damage

The frequency of removals caused by external damage is treated as a constant throughout the study as directed by USAAMRDL. The given mean time to removal of 400 hours was converted to a mean time between removal of 1,211 blade hours (excluding no-failure causes and unknown causes). The distribution of UH-1 blade externally caused damage modes is presented in Table XI.

While the external damage rate is a constant value for all blades considered in the study, it is necessary to determine the changes in blade external damage repairability resulting from differences in the inherent design characteristics of each candidate blade. This was accomplished by allocating the MTBR value for external damage to the component parts of each candidate blade design on a percentage basis. For example:

Battle damage - 120 occurrences per 10^6 blade hours for the UH-1 blade. Candidate blade planform is the same as for the UH-1 blade, and therefore it is reasonable to assume that the external damage pattern for the candidate blades will be the same as for the UH-1 blade, and all candidate blades could also be expected to experience 120 incidents of battle damage per 10^6 blade hours. In order to determine how many of these incidents will occur in a given blade component part, the percent of total blade surface area occupied by the part is calculated and multiplied by the battle damage incidence rate of 120 per 10^6 blade hours. This process is repeated for all external damage modes and all component parts until the entire external damage rate (826 occurrences per 10^6 blade hours) is allocated.

The reliability apportionment of the baseline UH-1 blade inherent damage rates is presented in Table XII. External damage rates for the baseline blade are not apportioned since it was not necessary to calculate the degree of repairability of the UH-1 blade. Baseline UH-1 blade repairability was determined from the published data provided by USAAMRDL. External damage rate apportionment for all candidate blade designs is presented in the repairability analysis of Appendix II.

TABLE XII. RELIABILITY APPORTIONMENT-BASELINE UH-1D BLADE

I. Inherent Damage		
Blade Component	Failure Mode	Frequency of Occurrence per 10^6 Blade Hours
1. Spar	A. Bonding separates from core B. Elongation of bushing holes C. Cracks D. Abrasion strip separation E. Corrosion F. Pitted, abraded or eroded abrasion strip	4.0 10.0 14.0 18.0 9.0 <u>12.0</u> 67.0
2. Core	A. Bonding voids B. Water contamination	20.0 <u>10.0</u> 30.0
3. Skin (Aluminum)	A. Unbonded at leading or trailing edge B. Corrosion C. Cracks	9.0 2.0 <u>32.0</u> 43.0
4. Retention Bushings	A. Cracks B. Wear C. Corrosion	10.0 9.0 <u>2.0</u> 21.0
5. Doublers (includes grip and drag plates)	A. Bonding separation B. Corrosion C. Cracks	4.0 2.0 <u>10.0</u> 16.0

TABLE XII - Continued

I. Inherent Damage - Continued

Blade Component	Failure Mode	Frequency of Occurrence per 10^6 Blade Hours
6. Trailing Edge Strip (aluminum)	A. Bonding Separation B. Cracks	2.0 <u>10.0</u> 12.0
7. Trim Tab	A. Loose Rivets B. Unbonded	1.0 <u>4.0</u> 5.0
8. Counterweights	A. Loose B. Corroded	1.0 <u>1.0</u> 2.0
9. General		72.0
Total Inherent Damage		268.0
II. Total External Damage		826.0
III. Total Blade Damage		1,094.0

FAILURE MODE AND EFFECTS ANALYSIS

A failure mode and effects analysis was conducted for each of the candidate blade designs and is presented in Appendix II. Possible failure modes anticipated in the blades' operational environment, their effect upon the blades' functional capability, and probable symptoms and methods of detection were investigated. Specific design features incorporated to minimize and/or reduce the effect of anticipated failure modes are as follows:

Configuration I and VI

1. Use of 6061 aluminum in spar to decrease crack propagation and reduce corrosion.
2. Heavy wall spar to resist external damage and increase field repairability by permitting more extensive blend out procedures.
3. Use of fiberglass skin to increase skin fatigue life and blade field repairability.
4. Attaching point bushings replaceable in the field.
5. Increased bonding area and use of 6061 aluminum in grip pad, drag plate, and doublers provide greater margin of safety, increased crack propagation time and increased corrosion resistance.
6. Use of nonmetallic honeycomb core provides increased elastic memory and reduces effect of external damage on honeycomb (Configuration I only).
7. Trailing edge spline corrosion free and repairable.

Configuration II

1. Three-piece spar construction offers increased redundancy.
2. Stainless steel leading edge provides greater erosion resistance and increased durability.
3. Use of fiberglass skin to increase skin fatigue life and blade field repairability.
4. Attaching point bushings replaceable in the field.
5. Increased bonding area and use of 6061 aluminum in grip pad, drag

plate, and doublers provide greater margin of safety, increased crack propagation time, and increased corrosion resistance.

6. Use of nonmetallic honeycomb core increases elastic memory and reduces effect of external damage on honeycomb core.
7. Trailing edge spline corrosion free and repairable.

Configuration IV and V

1. Twin beam concept provides a potentially fail-safe spar design with redundant load paths. Use of unidirectional fiberglass in beam construction provides greater fatigue life, slow crack propagation, and greater repairability characteristics than other concepts.
2. Leading edge protective coating is field replaceable.
3. Carbon skin increases skin fatigue life and repairability in the field.
4. Attaching point bushings are field replaceable.
5. Increased bonding area and use of 6061 aluminum in grip plate, drag plate, and doublers provide greater safety margin, increased crack propagation time, and increased corrosion resistance.
6. Use of nonmetallic honeycomb core provides increased elastic memory and reduces effect of external damage on honeycomb.
7. Trailing edge spline corrosion free and repairable.

RELIABILITY SUMMARY

The MTBR_T shown in Table XIII for the candidate blade designs reflects removal rates in excess of those attributed to the baseline UH-1 blade. It must be remembered that the influence of design changes upon the external damage rate is not reflected in these values. For this reason the values shown must be considered conservative.

The use of fiberglass skins in all candidate designs is partially responsible for the higher removal rates shown for these blades, since the inherent failure modes of fiberglass appear to be greater than those for a comparable aluminum skin. This is offset, however, by the vast increase in field level repairability which is afforded by the use of fiberglass and the subsequent reduction in the blade scrappage rate. The

TABLE XIII. FAILURE RATE SUMMARY

Blade Design	Mean Time Between Removal			Mean Time To Removal		
	Inherent	External	Total	Inherent	External	Total
Baseline UH-1	3,733	1,211	914	547	400	442
Configuration I and VI	2,680	1,211	833	513	400	436
Configuration II	2,850	1,211	850	502	400	450
Configuration IV and V	1,200	1,211	603	498	400	435

contractor feels that the candidate blade values shown would be substantially higher had the impact of design changes on the external damage rate been a factor in the study. Also, no credit is taken for solving debonding problems. It is fully expected that the mean time between removals of these configurations will be higher than the Bell blade. However, for conservatism, the above hours will be used.

MAINTAINABILITY ANALYSIS

Initial analysis of the cost effectiveness of the baseline UH-1 blade indicated that the poor repairability characteristics inherent in the design and the subsequent high scrappage rate were the primary factors contributing to the high life-cycle cost of the blade. The obvious solution to this problem is to produce a blade with a comparable design life but with a recurring cost so low that repair becomes more costly than replacement. The second best approach is to produce a blade which lends itself to cost effective repair by increasing the repair incidence of failure modes which formerly caused the blade to be scrapped or returned to depot.

The maintainability portion of this study deals with the second of these solutions.

Candidate Blade Repairability

The extensive use of fiberglass in all three candidate blade designs makes possible significant increases in repairability with respect to the baseline blade. Extensive repair of large blade areas can be accomplished by the use of prefabricated blade sections and prestocked

repair kits containing all required repair materials. Bonding agents which are room temperature curable eliminate the need for expensive and cumbersome heat treating equipment, thereby providing increased latitude in assigning repair levels and enhancing unit self-sufficiency in the field. Blade inspection procedures above and beyond those which are currently in use should not be required. Existing balancing and tracking equipment will be compatible with all candidate blades; however, balancing technique and procedure may become more significant in view of the extensive field repairs now possible.

Repairability Analysis

Each candidate blade design was subjected to a repairability evaluation based upon the failure mode and effects analysis previously conducted. Repairability analyses are presented in Appendix II. A scrap versus repair decision was made for each failure mode based upon the following general criteria.

Scrapage Causes

1. Extensive deformation of spar wall or leading edge.
2. Cracked or punctured spar.
3. Extensive bonding separation of spar closure piece or core to spar bond.
4. Externally caused skin damage which extends into spar wall, transition doublers or trailing edge spline.
5. Extensive bonding separation or cracks in trailing edge spline.
6. Extensive delamination or bonding separation of grip doublers, drag link doublers, or transition doublers.
7. Extensive damage at root end attaching points.
8. Overstress conditions such as overspeed, warpage, or other blade deformation.

The causes for scrapage cited above are general in nature and vary depending upon individual candidate blade design. The twin beam spar concept, for example, can tolerate greater damage and exhibits a greater degree of repairability with respect to spar damage than do the other

candidates. Refer to the repairability analyses of Appendix II for candidate blade scrap/repair description.

Level of Repair Decision

Level of repair decisions were made concurrently with the scrap/repair decision for each candidate blade. Repair levels were assigned on the basis of feasibility in terms of aircraft downtime, degree of skill required, and support equipment and facilities required. All fiberglass repair procedures are designated as direct support level repair procedures and are considered to be within the capabilities of the average aircraft rotor and propeller repairman (MO 68 E 20). Individual training in repair technique and procedure will be required. Tables XIV and XV summarize candidate and baseline blade repairability and levels of maintenance.

TABLE XIV. BLADE REPAIRABILITY AND LEVEL OF MAINTENANCE

Blade Design	% Repairable			% Scrap			Total	
	ORG	D S	Depot	ORG	D S	Depot	Repair	Scrap
Baseline UH-1	0	12%	19%	0	30%	39%	31%	69%
Configuration I and VI	6%	44%	4%	33%	11%	2%	54%	46%
Configuration II	5%	44%	4%	33%	12%	2%	53%	47%
Configuration IV and V	1%	74%	2%	13%	8%	2%	77%	23%

TABLE XV. REPAIRABILITY SUMMARY

Blade Design	Blades per Million Hours			Percent of Removed Blades Repaired
	Removed	Repaired	Scrapped	
Baseline UH-1	1094	339	755	31%
Configuration I and VI	1201	646	555	54%
Configuration II	1177	624	553	53%
Configuration IV and V	1659	1288	371	77%

Repair Procedures (Refer to Appendix II for detailed procedures.) Eight repair procedures which can be considered peculiar to the candidate blade designs are outlined in the following pages. These procedures will be used to repair blade damage in the field which previously would have caused the blade to be scrapped or returned to the depot for extensive repair. Figures 48 through 51 illustrate types of damage which are not now field repairable. General repair procedures such as corrosion removal and treatment, repair of loose or missing hardware, etc., are considered standard or commonplace and are not included.

Allowable field repair procedures peculiar to candidate blade designs are as follows:

1. Leading edge polyurethane coating restoration (Configuration IV)
2. Leading edge repair (Configuration IV)
3. Leading edge blend repair (Configuration I)
4. Twin beam repair (Configuration IV)
5. Fiberglass skin repair - patch (Configurations I, II & IV)
6. Fiberglass skin repair - plug (Configurations I, II, & IV)
7. Attaching point bushing replacement (Configurations I, II, & IV)
8. Fiberglass trailing edge spline repair (Configurations I, II, & IV)

Blade Leading Edge Polyurethane Coating Repair - The polyurethane coating used to protect the leading edge of the blade can be restored in the field as required. Repair capability covers the full range of restoration from repair of minor pitting to complete stripping and reapplication of the coating to the entire leading edge surface. The materials required to accomplish the full range of restoration can be supplied in kit form. No special support equipment is required and no special skill or experience is required.

Leading Edge Carbon Repair - Damage to the leading edge of the "twin beam" spar configuration such as dents, gauges or penetration is repairable in the field provided the damage is not extensive enough to have penetrated to the twin beam and honeycomb core. Prefabricated sections of leading edge consisting of 6-inch, prescarfed, ready-to-install nose blocks can be supplied in kit form. The repair procedure will consist of cutting out the damaged area and replacing it with the part provided in the kit. A scarfing tool provided by the manufacturer will be available for reworking the leading edge adjacent to the cutout section for mating with the prefabricated replacement. A simple fixture will be required to apply pressure to the replacement insert during the bonding cure period. This fixture can be supplied by the manufacturer or fabricated locally. This repair procedure should be accomplished in a sheltered area and will require a degree of skill acquired through special training which can be given in the field.

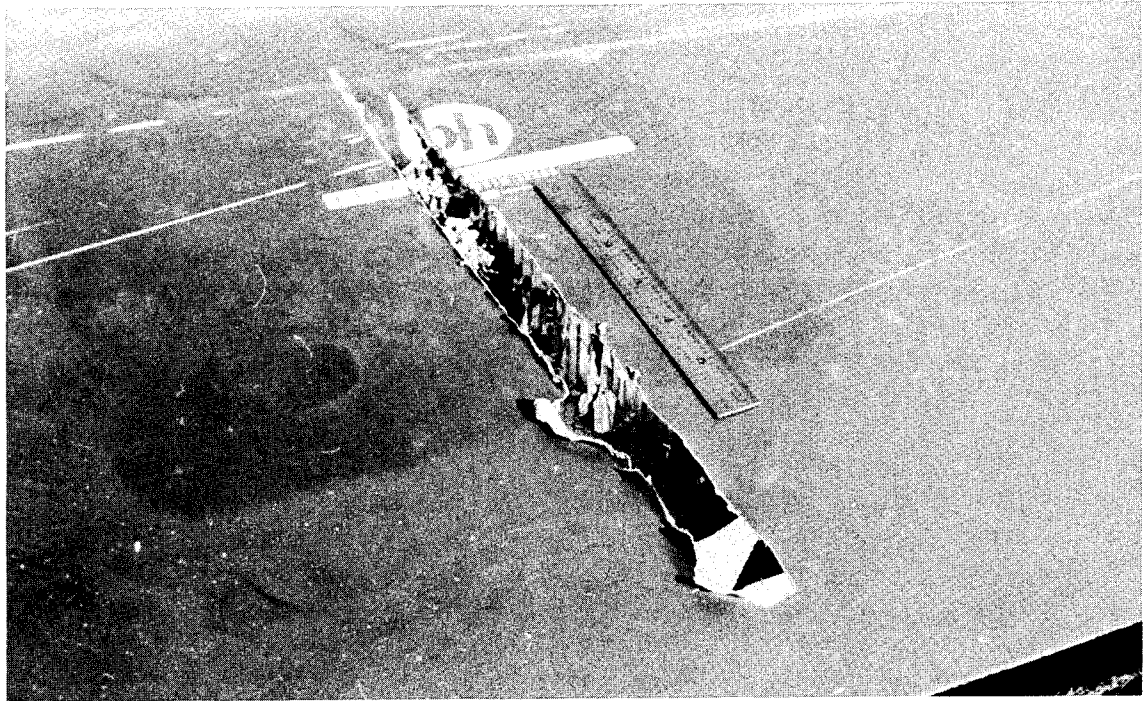


Figure 48. Blade Tear Damage.

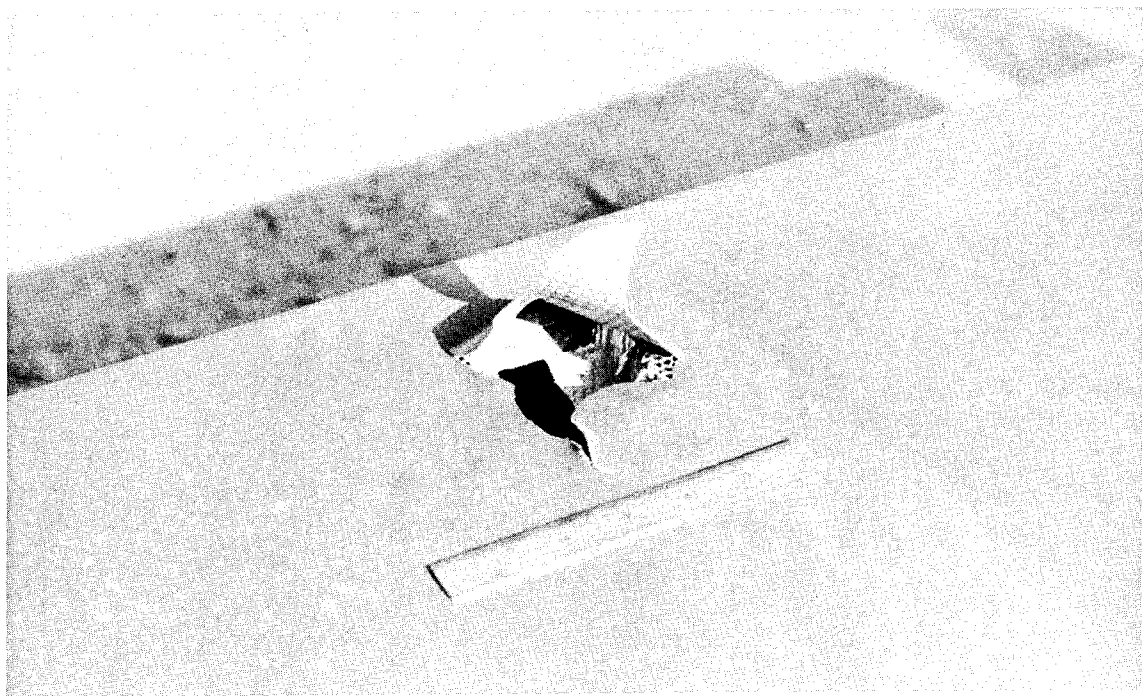


Figure 49. Blade Tear Damage.

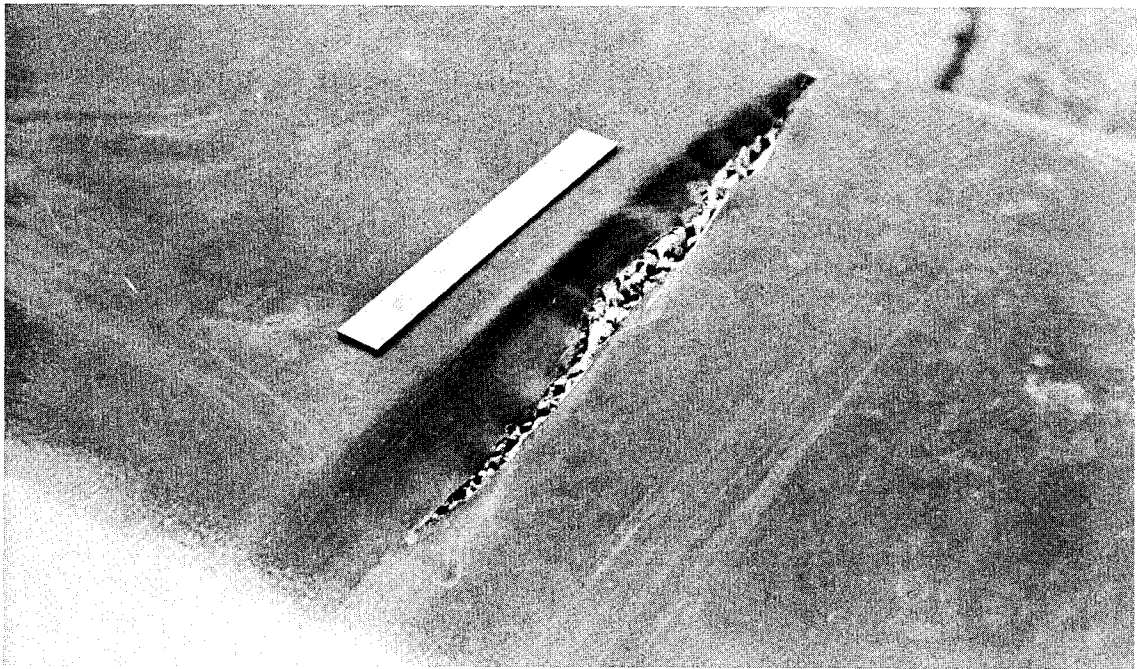


Figure 50. Blade Gash Damage.

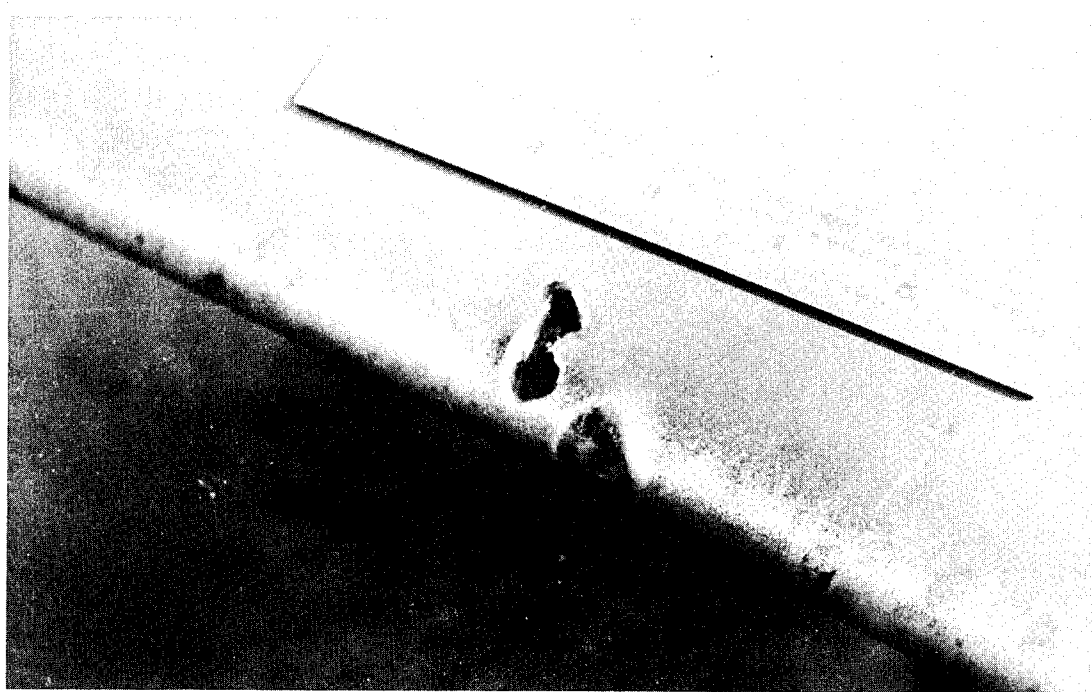


Figure 51. Blade Dent Damage.

Leading Edge Blend Repair - This repair procedure will allow rework of the extruded aluminum spar leading edge to blend out damage resulting from external causes up to 1/4 inch in depth. The repair technique is standard for this type of repair and requires no additional skill beyond that of a trained metal working technician. No special support equipment or facilities are required.

Fiberglass Skin Repair - Patch - Fiberglass skin damage such as abrasion, delamination, bonding separation, crazing and blisters can be repaired by simply removing and replacing the affected area. Repairs of this type are not limited by size of affected area and have been successfully accomplished and flight tested at Sikorsky Aircraft. This procedure, with variations, is also applicable to external damage which penetrates the skin and extends into the honeycomb core. The repair procedure illustrated in Appendix II(Figure 59 through 72)was actually performed on a recent flight test article to repair extensive skin to honeycomb bonding separation which occurred as a result of damage to the trailing edge caused by contact with a foreign object. All required materials, including skin patches up to 1 square foot in area, can be furnished in kit form. Skin material required for patches exceeding 1 square foot can be supplied in bulk form. The repair should be performed in a sheltered area free from environmental influence and requires the use of support equipment in the form of a compression blanket. A high degree of skill is not required; however, training in the repair technique will be necessary.

Fiberglass Skin Repair - Plug - This procedure is used in conjunction with the patching procedure to repair damage which extends through the skin and either penetrates the entire blade or causes extensive damage to a large volume of honeycomb core. Prefabricated skin/core sections of standard or varying sizes can be furnished in kit form to replace damaged sections of the skin and core. Figures 73 through 84 of Appendix II illustrate this type of repair. As with the patching procedure, this repair should be performed in an area free of environmental influence and will require the use of a compression blanket. Again, training in the repair technique will be required.

Attaching Point Bushing Replacement - Removal and replacement of worn attaching point bushings can be accomplished in the field through the use of a dual bushing arrangement. Standard techniques for pressing out and inserting steel bushings can be utilized. Skill levels above and beyond those which are presently available will not be required.

Twin Beam Repair - Damage to the unidirectional fiberglass twin beam is also repairable in the field. Foreign object damage which penetrates the skin and enters the beam can be repaired by removing the damaged

skin and beam section and replacing with tapered unidirectional pre-molded patches. A router and a router template, which would be furnished by Sikorsky Aircraft, will be required to accomplish the repair. No exotic special support equipment is required. Training in the repair technique will be necessary although a great deal of skill is not required. This repair should be accomplished in a sheltered area free from environmental influence.

Trailing Edge Spline Repair - Damaged sections of the trailing edge spline can be repaired in a manner similar to that used for the carbon leading edges. Prefabricated, prescarfed sections of trailing edge spline can be supplied. The repair is accomplished by removing the damaged section and replacing it with the prefabricated replacement. Bonding and compression techniques similar to those used in the patch and plug repair procedures will be utilized.

Repair Kit - A single repair kit containing all the required materials for the fiberglass and carbon repairs detailed in Appendix II can be assembled. Repair kit contents will be as follows:

- a. 1-square foot fiberglass or carbon skin panels
- b. 1-square-foot fiberglass or carbon skin/honeycomb core prefabricated sections
- c. 6-inch prefabricated, prescarfed leading edge nose blocks
- d. 6-inch prefabricated, prescarfed trailing edge spline sections
- e. 180-240 grit sand paper
- f. MEK solvent
- g. Adhesive stripper
- h. Cotton and rubber gloves
- i. Masking tape
- j. Mixing cup, wooden spatula, serrated spreader
- k. Teflon film
- l. Nose template
- m. Scrim cloth
- n. Scarfing tools

Inspection Procedures

Inspection procedures adequate to detect each mode of failure to which the candidate blades are susceptible will be similar to those which are currently in use for the UH-1 blade. In addition, tolerance checks can be performed at predetermined points along the blade span to check for subsurface delamination and bonding separation of the twin beam. Skin defects and skin to core bonding separation will be detectable visually and by tapping and pressure procedures.

Balance and Tracking Procedures

All Sikorsky blades are interchangeable individually or as a set. Any of the six configurations in the report can also be made to be interchangeable. Interchangeability would commence by closely controlling the weight and mass distribution of the blade components during the fabrication stage. The dimensions and tolerances of the component parts of the blade would be held to specified limits so that each blade at final assembly would fall within a specified spanwise moment tolerance. The spar mass distribution would be controlled during the fabrication stage by checking its weight and spar moment. The trailing edge spline weight would be especially controlled because of its extreme location from the chordwise center of gravity. The trailing edge skins are thin and should represent no problem because they are light and would have very little fluctuation in weight. The counterweight package (whether integral or molded) would be determined during the design phase and checked out during assembly of the first few blades. Any changes would be minor and would be done at this time. Static balance is performed on a balance stand with a master blade. The spanwise moment of each blade is matched by inserting tip weights just inboard of the tip cap. By closely controlling weight as described above, the spanwise moments of Table I (which are approximately 27,000 in.- lb.) could be held to ± 6 in.- lb. per blade which is extremely close for balance. Aerodynamic and dynamic balancing is accomplished on the Sikorsky 2000 hp main rotor test stand by adjusting the blade pitching moment and track characteristics to those of a master blade. Aerodynamic balancing consists of adjusting external trailing edge trim tabs to match the blade pitching moments at low angles of attack. Dynamic balancing entails matching the blade pitching moments and track at high collective pitch angles by chordwise adjustments to the blade tip and root end weights. The blade pitch moments are obtained by measuring the steady loads in the rotor head rotating control rods modified by the addition of force load cells. Track measurements are obtained using a Chicago Aerial Electronic Blade Tracker.

Because the blade pitching moment and track characteristics are matched on a whirl stand, no further adjustments are required to the blades when they are installed on an aircraft. Only two installation adjustments are required - rotor trammelling and tracking. The rotor assembly is mounted on a fixture for alignment of the blade tips by adjustment at the rotor head drag struts. Tracking is accomplished after rotor installation. Any suitable tracking device such as the Chicago Aerial Electronic Blade Tracker, the Chadwick-Helmut Strobex Tracker, or a flag, may be used. The only adjustments required are to the rotating push-pull rods to put the blades in track at normal rotor speed and a moderate pitch angle.

Since the blade pitching moment and track characteristics have been

previously matched on the whirl stand, they will stay in track throughout the rotor speed, power and airspeed range of the helicopter and no further trim tab or chordwise balance weight adjustments are necessary.

Maintenance Man Hour Per Flight Hour

The maintenance man hour per flight hour values cited below represent the estimated MMH/FH at the organizational and direct support levels of maintenance. The values include inspection, diagnosis, repair, and checkout time. Cure time and time to secure replacement parts and materials are not included. The values are obtained by determining the weighted average man-hours to repair at each maintenance level and dividing by the frequency at which the repair actions occur.

MMH/FH

Configuration I

Organizational Level

A. Inspect/repair on aircraft	.0002
B. Inspect/remove and replace/disposition	<u>.0195</u>
Total ORG	.0197

Direct Support Level

A. Inspect and repair	.0040
B. Disposition (scrap or return to depot)	<u>.0006</u>
Total Direct Support	.0046

$$\text{Total Configuration I MMH/FH} = .0243$$

MMH/FH

Configuration II

Organizational Level

A. Inspect/repair on aircraft	.0001
B. Inspect/remove and replace/disposition	<u>.0194</u>
Total ORG	.0195

Configuration II - Continued MMH/FH

Direct Support Level

A. Inspect and repair	.0047
B. Disposition (scrap or return to depot)	<u>.0006</u>

Total Direct Support .0053

Total Configuration II MMH/FH = .0248

MMH/FH

Configuration IV

Organizational Level

A. Inspect and repair on aircraft	.0000
B. Inspect/remove and replace	<u>.0292</u>

Total ORG .0292

Direct Support Level

A. Inspect and repair	.0189
B. Disposition (scrap or return to depot)	<u>.0006</u>

Total Direct Support .0195

Total Configuration IV MMH/FH = .0487

Man-Hour Allocation-Allowable Field Repairs

Active Man-Hrs

1. Leading edge polyurethane coating restoration	
touch-up	1.5
full restoration	8.0
2. Leading edge repair-composite	8.0
3. Leading edge blend repair-aluminum	1.5
4. Twin beam repair	16.0
5. Fiberglass skin repair-patch	8.0
6. Fiberglass skin repair-plug	16.0
7. Attaching point bushing replacement	6.0
8. Fiberglass trailing edge spline repair	8.0

COST-EFFECTIVENESS ANALYSIS

The cost-effectiveness model is used to evaluate the cost effectiveness of the UH-1 aircraft equipped with the baseline blade and each of the candidate rotor blade designs. As shown by Table XVI, Configurations I and II both yield more cost effective aircraft than the baseline blade ; Configuration I has a slight edge. Configurations III and IV are less cost effective than the baseline blade. The cost effectiveness differences seem relatively small until translated into an equivalent dollar measure. This measure, fleet effective cost, is defined as the fleet life-cycle cost of N' aircraft equipped with a candidate rotor system design where N' is fleet size adjusted to maintain the fleet effectiveness of 1,000 UH-1 aircraft equipped with the baseline blade. In this manner, any difference in aircraft mission effectiveness can be translated into an equivalent fleet life-cycle-cost increment.

As shown by Table XVII, the cost differences on a fleet basis are significant. For example, the most cost effective design, Configuration I, can save over \$ 12 million for a baseline fleet of 1,000 aircraft. Similarly, half of this saving is available for a 500 aircraft fleet and 50% more can be saved for a 1,500 aircraft fleet.

None of the blade configurations are truly expendable, since none become more cost effective with the elimination of depot repair. In all cases, the cost of replenishing the system with additional spare blades is greater than the cost savings realized by eliminating depot repair costs. However, both Configurations I and II can be treated as expendable and still be significantly more cost effective than the baseline configuration. For example, Configuration I saves \$12.09 million over the baseline configuration. If depot level repair is eliminated, \$11.64 million is still saved. Some considerations beyond the scope of this cost effectiveness analysis can possibly make this direction worthwhile. For example, if near-expendability can be achieved on a number of aircraft components, it may be possible to reduce the extent of depot facilities required or the indirect burdens of maintenance management.

The relatively low cost effectiveness of Configurations III and IV is due primarily to the use of high cost advanced technology materials. Since materials currently used in blade manufacture tend to increase in cost with time and advanced technology materials tend to decrease, the relative value of these rotor blade designs may shift in future applications. Each configuration is reanalyzed for the 1980 time period using the following assumptions:

1. The UH-1 aircraft is assumed to exist as the baseline vehicle in 1980 at no change in cost other than that generated by the blades.

TABLE XVI. AIRCRAFT COST EFFECTIVENESS-1972 (TON-KNOTS/MEGADOLLAR)

Rotor Blade Design	With Depot Repair	Without Depot Repair
UH-1 Configuration I	23.638	23.601
Configuration II	23.820	23.813
Configuration III	23.798	23.790
Configuration IV	23.363	23.269
	23.550	23.529

TABLE XVII. FLEET EFFECTIVE COST-1972 (MEGADOLLAR)

Rotor Blade Design	With Depot Repair	Without Depot Repair
UH-1 Configuration I	1585.00	1587.47
Configuration II	1572.91	1573.36
Configuration III	1574.35	1574.85
Configuration IV	1603.62	1610.11
	1590.92	1592.35

2. Engineering, manufacturing, and maintenance labor rates, including overheads, are assumed to increase by 50% relative to the 1972 time period.
3. The costs of aluminum and steel are assumed to increase by 30% due primarily to increased labor costs in the materials supply industries.
4. In opposition to the cost increase in (3), unit cost savings due to increased material production and availability are applied to the acquisition cost of advanced technology materials.
5. A decrease in manufacturing labor time is applied to configurations with advanced technology materials to account for learning of advanced manufacturing techniques.
6. Configuration IV is slightly modified for 1980 and re-identified as Configuration V.

With these assumptions, the cost effectiveness analysis yields the values shown in Tables XVIII and XIX for 1980.

For the 1980 time period, Configurations III and V have joined Configurations I and II in providing greater aircraft cost effectiveness than the baseline blade. Configuration V displaces Configuration I as the most cost effective blade design. The fleet effective cost saving of Configuration I over the baseline is almost \$17 million, which is more pronounced than in 1972. The most cost effective blade for 1980, Configuration V , rises from a penalty of almost \$6 million in 1972 to a saving of \$26.22 million in 1980. In addition, \$25.66 million of this saving is retained with the elimination of depot level repair, making it very nearly expendable.

All blade design characteristics have some impact on aircraft cost effectiveness. Of these, the most important are:

1. Blade scheduled retirement life.
2. Blade mean time between inherent damage.
3. Blade repairability.
4. Blade acquisition cost.

Significant changes in cost effectiveness are caused by variations in blade scheduled retirement life, blade mean time between inherent damage below 2,000 flight hours, and blade repairability. But blade acquisition cost has, by far, the greatest impact on cost effectiveness. This sensitivity is illustrated in Figures 52 and 53 for the baseline and the most cost effective blade configurations for the 1972 and 1980 time period.

TABLE XVIII. AIRCRAFT COST EFFECTIVENESS - 1980 (TON-KNOTS/MEGADOLLAR)

Rotor Blade Design	With Depot Repair	Without Depot Repair
UH-1 Configuration	23.370	23.313
Configuration I	23.617	23.607
Configuration II	23.583	23.572
Configuration III	23.506	23.442
Configuration V	23.758	23.748

TABLE XIX. FLEET EFFECTIVE COST - 1980 (MEGADOLLAR)

Rotor Blade Design	With Depot Repair	Without Depot Repair
UH-1 Configuration	1603.20	1607.08
Configuration I	1586.39	1587.09
Configuration II	1588.66	1589.43
Configuration III	1593.91	1598.23
Configuration V	1576.98	1577.64

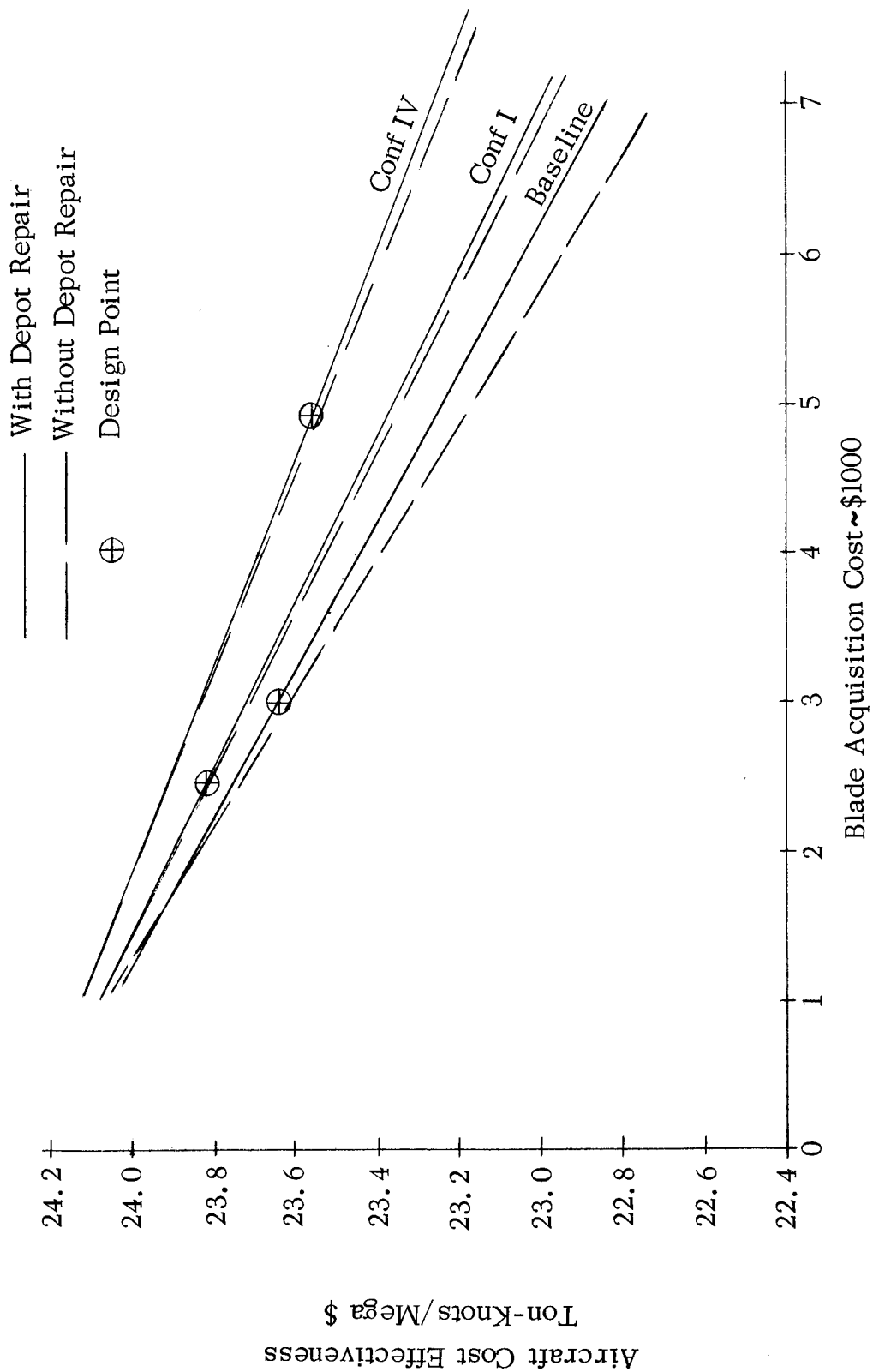


Figure 52. Impact of Blade Acquisition Cost, 1972 Configurations.

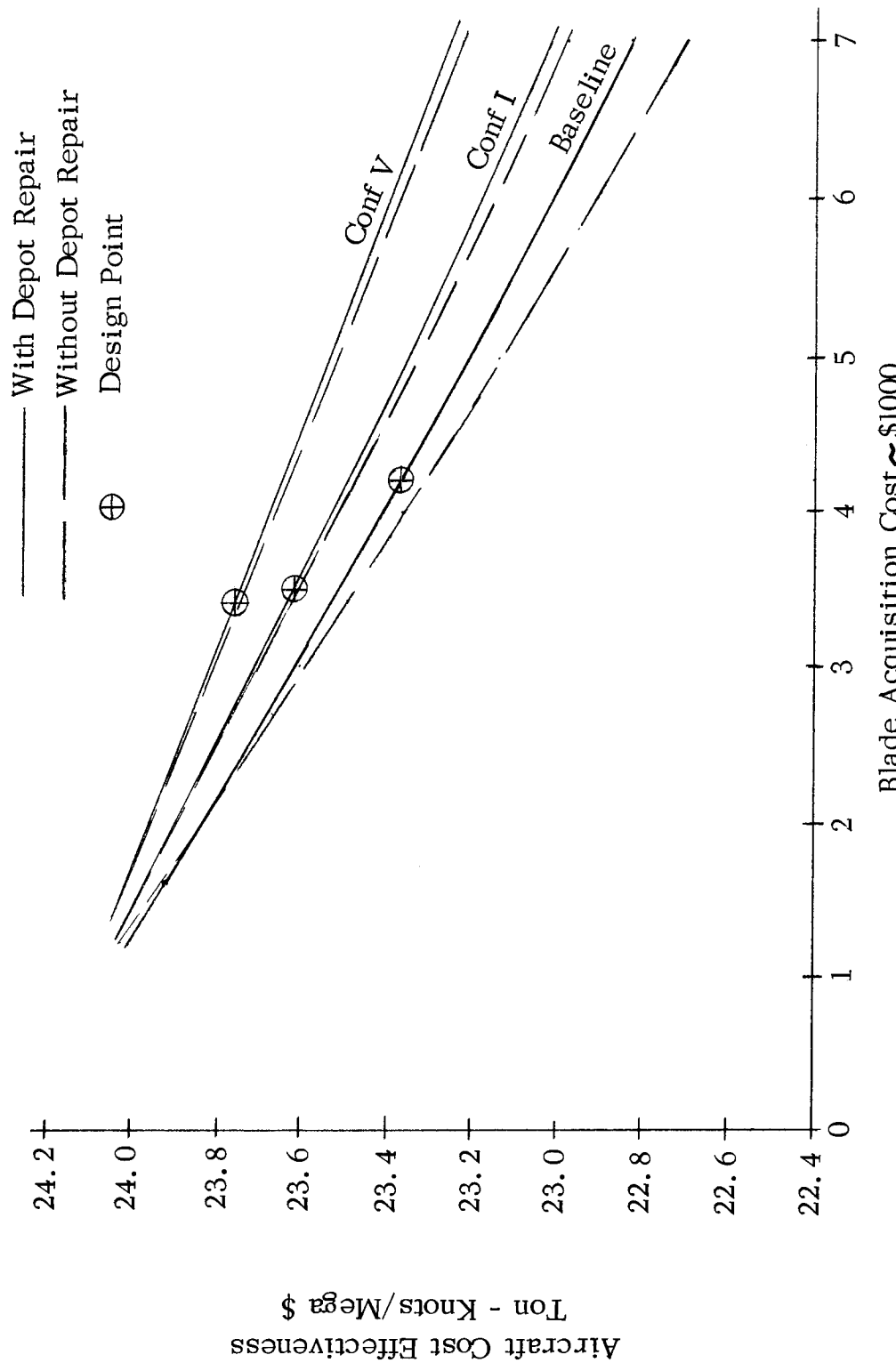


Figure 53. Impact of Blade Acquisition Cost, 1980 Configurations.

These trends were obtained by varying blade acquisition cost in the cost-effectiveness model while holding all other blade design characteristics constant. The space between one configuration trend line and another is due to differences in blade design parameters other than blade acquisition cost. Blade repairability is the major contributor. Both Configurations I and IV would be more cost effective if all blades had the same acquisition cost. The inherent advantage of Configuration I over the baseline is further enhanced by its lower acquisition cost for both time periods. The relatively high acquisition cost of advanced technology Configuration IV for 1972 overpowers its inherent repairability advantage, making it less cost effective than the baseline. With the major reduction in blade acquisition cost available for 1980, this configuration becomes the most cost effective 1980 design.

With the exception of blade acquisition cost, variations in blade design characteristics do not produce blade expendability. Depot level expendability is achieved when the elimination of depot level repair does not incur a cost-effectiveness penalty (Figures 52 and 53). To achieve this, the acquisition cost of the baseline blade would have to be reduced to about \$1,700 for 1972 and \$2,200 for 1980. Configurations I and IV would have to be reduced to about \$1,500 for either time period. Since these derivative trends assume that all other design characteristics remain constant, the expendability break-even points become invalid if design changes made to reduce blade acquisition also change those other characteristics.

Tables XX through XXIX present cost-effectiveness summary tables for each configuration, followed by a discussion of each configuration's key cost-effectiveness parameters. All of the candidate configurations are a few pounds heavier than the baseline and yield a slight decrease in aircraft mission effectiveness. The greatest impact on cost effectiveness derives from blade life-cycle cost. The prime contributor to this cost is blade acquisition cost since it impacts directly on blade contributions to flyaway cost, initial spares cost, and replenishment spares cost. Blade mean time between inherent damage provides damage rate or the number of blades damaged over an aircraft life cycle. Blade repairability determines the number of damaged blades that are repaired and scrapped at the various maintenance levels. An increase in blade repairability or blade scheduled retirement life decreases the number of replenishment spares required and therefore, decreases blade replenishment cost. All of the candidate blade designs require more consumable tooling than the baseline. This contribution to replenishment GSE cost is treated as an increment over the baseline configuration, which is assumed at zero.

Tables XXX and XXXI summarize the blade life-cycle costs and the cost of the new blade to the Army.

TABLE XX. COST EFFECTIVENESS SUMMARY,
BASELINE CONFIGURATION - 1972

Aircraft Mission Effectiveness	37.466	ton-knots
Aircraft Life-Cycle Cost	\$ 1,585,000	
Aircraft Cost Effectiveness	23.638	ton-knots/megadollar
Fleet Effective Cost	\$ 1,585.00	megadollar
Fleet size adjusted to maintain fleet effectiveness of 1,000 base- line UH-1 aircraft		
Life Cycle Fuel and Oil Cost	\$ 53,344	
<u>Blade Contribution To:</u>		
Flyaway cost	\$ 6,000	
Initial spares cost	\$ 1,998	
Replenishment spares cost	\$ 36,202	
Organizational level maintenance cost	\$ 634	
Direct support level maintenance cost	\$ 554	
Depot level maintenance cost	\$ 3,071	
Replenishment GSE cost	\$ 0	
Blade Life-Cycle Cost	\$ 48,459	
<u>Life-Cycle Blades:</u>		
Damaged	10.94	Blades
Repaired at the organizational level	0	"
Repaired at the direct support level	1.31	"
Repaired at the depot level	2.03	"
Retired on schedule	0.81	"
Replenished by new spares	11.40	"
<u>Expendability:</u>		
Scraping blades normally sent to depot for overhaul yields the following:		
Aircraft cost effectiveness	23.601	ton-knots/megadollar
Fleet effective cost	1587.47	megadollar

TABLE XXI. COST EFFECTIVENESS SUMMARY,
BASELINE CONFIGURATION - 1980

Aircraft Mission Effectiveness	37.466	ton-knots
Aircraft Life-Cycle Cost	\$ 1,603, 200	
Aircraft Cost Effectiveness	23.370	ton-knots/mega- dollar
Fleet Effective Cost	\$ 1,603 . 20	megadollar
Fleet size adjusted to maintain fleet effectiveness of 1,000 base- line UH-1 aircraft		
Life-Cycle Fuel and Oil Cost	\$ 53, 34 4	
<u>Blade Contribution To:</u>		
Flyaway cost	\$ 8,417	
Initial spares cost	\$ 2,771	
Replenishment spares cost	\$ 49,979	
Organizational level maintenance cost	\$ 951	
Direct support level maintenance cost	\$ 608	
Depot level maintenance cost	\$ 3,930	
Replenishment GSE cost	\$ 0	
Blade Life-Cycle Cost	\$ 66,656	
<u>Life-Cycle Blades:</u>		
Damaged	10.94	Blades
Repaired at the organizational level	0	"
Repaired at the direct support level	1.31	"
Repaired at the depot level	2.03	"
Retired on schedule	0.81	"
Replenished by new spares	11.40	"
<u>Expendability</u>		
Scraping blades normally sent to depot for overhaul yields the following:		
Aircraft cost effectiveness	23.313	ton-knots/megadollar
Fleet effective cost	1607.08	megadollar

TABLE XXII. COST EFFECTIVENESS SUMMARY,
CONFIGURATION I - 1972

Aircraft Mission Effectiveness	37.437	ton-knots
Aircraft Life-Cycle Cost	\$1,571,690	
Aircraft Cost Effectiveness	23.820	ton-knots/megadollar
Fleet Effective Cost	\$1,572.91	megadollar
Fleet size adjusted to maintain fleet effectiveness of 1,000 base- line UH-1 aircraft		
Life-Cycle Fuel and Oil Cost	\$ 53,334	
<u>Blade Contribution To:</u>		
Flyaway cost	\$ 4,969	
Initial spares cost	\$ 1,442	
Replenishment spares cost	\$ 25,886	
Organizational level maintenance cost	\$ 693	
Direct support level maintenance cost	\$ 260	
Depot level maintenance cost	\$ 569	
Replenishment GSE cost	\$ 1,336	
Blade Life-Cycle Cost	\$ 35,155	
<u>Life-Cycle Blades:</u>		
Damaged	11.99	Blades
Repaired at the organizational level	0.72	"
Repaired at the direct support level	5.20	"
Repaired at the depot level	0.47	"
Retired on schedule	1.13	"
Replenished by new spares	9.73	"
<u>Expendability:</u>		
Scraping blades normally sent to depot for overhaul yields the following:		
Aircraft cost effectiveness	23.813	ton-knots/megadollar
Fleet effective cost	1573.36	megadollar

TABLE XXIII. COST EFFECTIVENESS SUMMARY,
CONFIGURATION I - 1980

Aircraft Mission Effectiveness	37.437	ton-knots
Aircraft Life-Cycle Cost	\$ 1,585,160	
Aircraft Cost Effectiveness	23.617	ton-knots/megadollar
Fleet Effective Cost	\$ 1,586.39	megadollar
Fleet size adjusted to maintain fleet effectiveness of 1,000 base- line UH-1 aircraft		
Life-Cycle Fuel and Oil Cost	\$ 53,384	
Blade Contribution To:		
Flyaway cost	\$ 6,999	
Initial spares cost	\$ 2,003	
Replenishment spares cost	\$ 35,765	
Organizational level maintenance cost	\$ 1,039	
Direct support level maintenance cost	\$ 348	
Depot level maintenance cost	\$ 734	
Replenishment GSE cost	\$ 1,737	
Blade Life-Cycle Cost	\$ 48,625	
Life-Cycle Blades:		
Damaged	11.99	Blades
Repaired at the organizational level	0.72	"
Repaired at the direct support level	5.20	"
Repaired at the depot level	0.47	"
Retired on schedule	1.13	"
Replenished by new spares	9.73	"
Expendability:		
Scraping blades normally sent to depot for overhaul yields the following:		
Aircraft cost effectiveness	23.607	ton-knots/megadollar
Fleet effective cost	1587.09	megadollar

TABLE XXIV. COST EFFECTIVENESS SUMMARY,
CONFIGURATION II - 1972

Aircraft Mission Effectiveness	37.442	ton-knots
Aircraft Life-Cycle Cost	\$ 1,573,340	
Aircraft Cost Effectiveness	23.798	ton-knots/megadollar
Fleet Effective Cost	\$ 1,574.35	megadollar
Fleet size adjusted to maintain fleet effectiveness of 1,000 base- line UH-1 aircraft		
Life-Cycle Fuel and Oil Cost	\$ 53,336	
<u>Blade Contribution To:</u>		
Flyaway cost	\$ 5,163	
Initial spares cost	\$ 1,500	
Replenishment spares cost	\$ 26,989	
Organizational level maintenance cost	\$ 698	
Direct support level maintenance cost	\$ 248	
Depot level maintenance cost	\$ 576	
Replenishment GSE cost	\$ 1,633	
Blade Life-Cycle Cost	\$ 36,807	
<u>Life-Cycle Blades:</u>		
Damaged	11.77	Blades
Repaired at the organizational level	0.35	"
Repaired at the direct support level	5.27	"
Repaired at the depot level	0.47	"
Retired on schedule	1.12	"
Replenished by new spares	9.79	"
<u>Expendability:</u>		
Scraping blades normally sent to depot for overhaul yields the following:		
Aircraft cost effectiveness	23.790	ton-knots/megadollar
Fleet effective cost	1574.85	megadollar

TABLE XXV. COST EFFECTIVENESS SUMMARY,
CONFIGURATION II - 1980

Aircraft Mission Effectiveness	37.442	ton-knots
Aircraft Life-Cycle Cost	\$ 1,587,640	
Aircraft Cost Effectiveness	23.583	ton-knots/megadollar
Fleet Effective Cost	\$ 1,588.66	megadollar
Fleet size adjusted to maintain fleet effectiveness of 1,000 base- line UH-1 aircraft		
Life-Cycle Fuel and Oil Cost	\$ 53,336	
<u>Blade Contribution To:</u>		
Flyaway cost	\$ 7,302	
Initial spares cost	\$ 2,093	
Replenishment spares cost	\$ 37,463	
Organizational level maintenance cost	\$ 1,047	
Direct support level maintenance cost	\$ 334	
Depot level maintenance cost	\$ 744	
Replenishment GSE cost	\$ 2,123	
Blade Life-Cycle Cost	\$ 51,106	
<u>Life-Cycle Blades:</u>		
Damaged	11.77	Blades
Repaired at the organizational level	0.35	"
Repaired at the direct support level	5.27	"
Repaired at the depot level	0.47	"
Retired on schedule	1.12	"
Replenished by new spares	9.79	"
<u>Expendability:</u>		
Scraping blades normally sent to depot for overhaul yields the following:		
Aircraft cost effectiveness	23.572	ton-knots/megadollar
Fleet effective cost	1589.43	megadollar

TABLE XXVI. COST EFFECTIVENESS SUMMARY,
CONFIGURATION III - 1972

Aircraft Mission Effectiveness	37.451	ton-knots
Aircraft Life-Cycle Cost	\$1,602,970	
Aircraft Cost Effectiveness	23.363	ton-knots/megadollar
Fleet Effective Cost	\$1,603.62	megadollar
Fleet size adjusted to maintain fleet effectiveness of 1,000 base- line UH-1 aircraft		
Life-Cycle Fuel and Oil Cost	\$ 53,339	
<u>Blade Contribution To:</u>		
Flyaway cost	\$ 9,363	
Initial spares cost	\$ 2,727	
Replenishment spares cost	\$ 50,212	
Organizational level maintenance cost	\$ 653	
Direct support level maintenance cost	\$ 317	
Depot level maintenance cost	\$ 2,130	
Replenishment GSE cost	\$ 1,033	
Blade Life-Cycle Cost	\$ 66,435	
<u>Life-Cycle Blades:</u>		
Damaged	11.85	Blades
Repaired at the organizational level	0.24	"
Repaired at the direct support level	2.58	"
Repaired at the depot level	1.75	"
Retired on schedule	0.06	"
Replenished by new spares	10.34	"
<u>Expendability:</u>		
Scraping blades normally sent to depot for overhaul yields the following:		
Aircraft cost effectiveness	23.269	ton-knots/megadollar
Fleet effective cost	1610.11	megadollar

TABLE XXVII. COST EFFECTIVENESS SUMMARY,
CONFIGURATION III - 1980

Aircraft Mission Effectiveness	37.451	ton-knots
Aircraft Life-Cycle Cost	\$1,593,270	
Aircraft Cost Effectiveness	23.506	ton-knots/megadollar
Fleet Effective Cost	\$1,593.91	megadollar
Fleet size adjusted to maintain fleet effectiveness of 1,000 base- line UH-1 aircraft		
Life-Cycle Fuel and Oil Cost	\$ 53,339	
<u>Blade Contribution To:</u>		
Flyaway cost	\$ 7,646	
Initial spares cost	\$ 2,303	
Replenishment spares cost	\$ 41,337	
Organizational level maintenance cost	\$ 980	
Direct support level maintenance cost	\$ 371	
Depot level maintenance cost	\$ 2,750	
Replenishment GSE cost	\$ 1,342	
Blade Life-Cycle Cost	\$ 56,729	
<u>Life-Cycle Blades:</u>		
Damaged	11.85	Blades
Repaired at the organizational level	0.24	"
Repaired at the direct support level	2.58	"
Repaired at the depot level	1.75	"
Retired on schedule	0.06	"
Replenished by new spares	10.34	"
<u>Expendability:</u>		
Scraping blades normally sent to depot for overhaul yields the following:		
Aircraft cost effectiveness	23.442	ton-knots/megadollar
Fleet effective cost	1598.23	megadollar

TABLE XXVIII. COST EFFECTIVENESS SUMMARY,
CONFIGURATION IV - 1972

Aircraft Mission Effectiveness	37.431	ton-knots
Aircraft Life-Cycle Cost	\$1,589,450	
Aircraft Cost Effectiveness	23.550	ton-knots/megadollar
Fleet Effective Cost	\$1,590.92	megadollar
Fleet size adjusted to maintain fleet effectiveness of 1,000 base- line UH-1 aircraft		
Life-Cycle Fuel and Oil Cost	\$ 53,336	
<u>Blade Contribution To:</u>		
Flyaway cost	\$ 9,939	
Initial spares cost	\$ 1,985	
Replenishment spares cost	\$ 36,613	
Organizational level maintenance cost	\$ 922	
Direct support level maintenance cost	\$ 1,306	
Depot level maintenance cost	\$ 490	
Replenishment GSE cost	\$ 1,660	
Blade Life-Cycle Cost	\$ 52,915	
<u>Life-Cycle Blades:</u>		
Damaged	16.59	Blades
Repaired at the organizational level	0.15	"
Repaired at the direct support level	12.16	"
Repaired at the depot level	0.39	"
Retired on schedule	0.23	"
Replenished by new spares	7.12	"
<u>Expendability:</u>		
Scraping blades normally sent to depot for overhaul yields the following:		
Aircraft cost effectiveness	23.529	ton-knots/megadollar
Fleet effective cost	1592.35	megadollar

TABLE XXIX. COST EFFECTIVENESS SUMMARY,
CONFIGURATION V - 1980

Aircraft Mission Effectiveness	37.431	ton-knots
Aircraft Life-Cycle Cost	\$1,575,520	
Aircraft Cost Effectiveness	23.758	ton-knots/megadollar
Fleet Effective Cost	\$1,576.98	megadollar
Fleet size adjusted to maintain fleet effectiveness of 1,000 base- line UH-1 aircraft		
Life-Cycle Fuel and Oil Cost	\$ 53,336	
<u>Blade Contribution To:</u>		
Flyaway cost	\$ 6,668	
Initial spares cost	\$ 1,402	
Replenishment spares cost	\$ 24,973	
Organizational level maintenance cost	\$ 1,382	
Direct support level maintenance cost	\$ 1,773	
Depot level maintenance cost	\$ 631	
Replenishment GSE cost	\$ 2,158	
Blade Life-Cycle Cost	\$ 38,987	
<u>Life-Cycle Blades:</u>		
Damaged	16.59	Blades
Repaired at the organizational level	0.15	"
Repaired at the direct support level	12.16	"
Repaired at the depot level	0.39	"
Retired on schedule	0.23	"
Replenished by new spares	7.12	"
<u>Expendability:</u>		
Scraping blades normally sent to depot for overhaul yields the following:		
Aircraft cost effectiveness	23.748	ton-knots/megadollar
Fleet effective cost	1577.64	megadollar

TABLE XXX. COST EFFECTIVENESS SUMMARY

Blade Design	Blade Life-Cycle Cost/Aircraft	
	1972	1980
Baseline UH-1	\$48,459 (1) \$50,925 (2)	\$66,656 (1) \$70,540 (2)
Configuration I	\$35,155 (1) \$35,607 (2)	\$48,625 (1) \$49,320 (2)
Configuration II	\$36,807 (1) \$37,307 (2)	\$51,106 (1) \$51,877 (2)
Configuration III	\$66,435 (1) \$72,922 (2)	\$56,729 (1) \$61,050 (2)
Configuration IV	\$52,915 (1) \$54,340 (2)	
Configuration V		\$38,987 (1) \$39,649 (2)

(1) Includes depot repair
 (2) Eliminates depot repair

TABLE XXXI. COST OF NEW BLADES TO THE ARMY

Blade Design	1972 Time Frame			1980 Time Frame		
	Recurring Production Cost	Amortized RDT & E Cost	G&A, OH & Profit Cost	Recurring Production Cost	Amortized RDT & E Cost	G&A, OH & Profit Cost
	Cost/Unit	Cost to Army	Cost/Unit	Cost to Army	Cost/Unit	Cost/Unit
Baseline UH-1	\$2143	\$84	\$773	\$3000	\$3007	\$118
Configuration I	\$1760	\$84	\$640	\$2484	\$2480	\$118
Configuration II	\$1826	\$90	\$665	\$2581	\$2585	\$125
Configuration III	\$3360	\$115	\$1206	\$4681	\$2680	\$158
Configuration IV	\$3594	\$95	\$1280	\$4969		\$985
Configuration V					\$2343	\$132
						\$859
						\$3334

SIGNIFICANT CONFIGURATION FEATURES

Baseline Configuration

Mission effectiveness is established for the baseline aircraft using the mission analysis program. The \$3,000 Bell blade acquisition cost impacts directly on flyaway cost, initial spares cost, and replenishment spares cost. This configuration's low repairability results in high blade scrappage and consequently, high blade spares requirements. The limited field repairability, in particular, places a large burden on depot level blade maintenance. 1980 labor rates and material costs increase all blade life-cycle cost contributions and further decrease cost effectiveness.

Configuration I

This configuration has greater repairability, particularly on a field level, which significantly reduces spares requirements. Blade acquisition cost is less than for the baseline, directly reducing flyaway cost. Taken with the reduced spares requirement, it provides a major reduction in spares cost. Even with an increase in replenishment GSE cost, this overall life-cycle cost reduction provides the aircraft with a major increase in cost effectiveness. All blade life-cycle costs increase for the 1980 time period, but the advantage over the baseline blade is retained. This is the most cost effective blade design for the 1972 time period.

Configuration II

This configuration is more cost effective than the baseline for both 1972 and 1980. Its damage rate and repairability are roughly comparable to Configuration I, but it has a higher blade acquisition cost and hence, yields a slightly lower aircraft cost effectiveness.

Configuration III

The repairability of this configuration is better than the baseline but poorer than Configurations I and II. The damage rate is roughly comparable to Configurations I and II; but with less repairability, blade spares requirements fall between these configurations and the baseline. For 1972, the high blade acquisition cost generated by the use of advanced technology materials makes this configuration less cost effective than the baseline. For 1980, the lower blade acquisition cost is reflected in a marked reduction in blade life-cycle cost. For this time period, this blade design becomes more cost effective than the baseline.

Configuration IV (1972) and V (1980)

This configuration exhibits the highest damage rate and the best repairability of all blade configurations. Blade repairability is so superior, however, that the combined effect produces the lowest spares requirement. Repair costs remain moderate since 97% of repairs occur on the field maintenance level. The use of expensive advanced technology material results in the largest 1972 blade acquisition cost of any configuration with a corresponding blade life-cycle cost penalty. For the 1972 time period, this penalty reduces cost effectiveness below that of Configurations I, II, and the baseline. The better blade repairability provides a cost effectiveness advantage over Configuration III. With its low spares requirement, this configuration is the most sensitive to reduction in blade acquisition cost. With the application of the lower 1980 blade acquisition cost, blade life-cycle cost and aircraft life-cycle cost are greatly reduced, making this the most cost effective 1980 blade configuration.

Configuration VI

This configuration is simply an extension of Configuration I having all the same features at the basic design. The automated pultrusion process has been added for the trailing edge and should reduce manufacturing cost. A complete analysis was not performed for this configuration. However, it is felt that the pultrusion process could be productionized for this configuration by 1975 if development were to start by 1972.

DESIGN SELECTION

RATIONALE

Selection of the most cost effective rotor blade design from the four candidate concepts discussed in this report was difficult since each design offered some improvements over the present UH-1 blade. These improvements were in the areas of reduced acquisition cost, improved repairability, potential for highly automated production, and improved rotor system performance. Design Configuration V, which is the twin beam composite blade with the truss-type trailing edge, was finally chosen as the prime candidate for 1980 based on the cost effectiveness studies shown in Table XVIII and Figure 54 and by a comparative evaluation of the various blade attributes.

The acquisition costs of the four designs under consideration were compared for 1972 and 1980. The aluminum extruded spar with a fiberglass trailing edge (Configuration I) had the lowest cost for 1972. The roll-formed sheet metal spar and fiberglass trailing edge (Configuration II) was slightly more costly than the aluminum spar design. Even though the production of the spar channel sections of stainless steel and aluminum of Configuration II was highly automated, it was more costly to bond and assemble than the two-piece aluminum extrusion of Configuration I. The twin beam spar, Configuration IV, and the "D" shaped tubular spar composite, Configuration III, are both considerably more expensive in 1972 than the metal spar blades because of the high cost of carbon and the need for high automation.

The costs of all four candidate designs were projected for the 1980 time frame and are shown in Figure 54 along with the 1972 blade costs. The figure shows that both metal spar blades are expected to increase substantially in cost by 1980. Both the material and labor rate costs are expected to increase as shown by Figure 55, while the fabrication time will remain about the same because there is little room for increasing the manufacturing technology (automation) for these metals. The composite blades, however, have vast areas for potential improvements in manufacturing. The methods to extrude a composite half section of a blade will be developed in the next several years, a process which will save on labor and also reduce the amount of wasted material common to present composite production. This type of operation would also utilize low-cost forms of the raw composite materials, such as spool roving, mat and liquid resin, thereby reducing the costs further. In addition, the cost of the composite materials, in particular carbon fiber, is expected to reduce substantially in the next few years. Increased use of composite materials, coupled with improvements in the manufacturing methods for the basic materials is expected to reduce carbon composite prices to

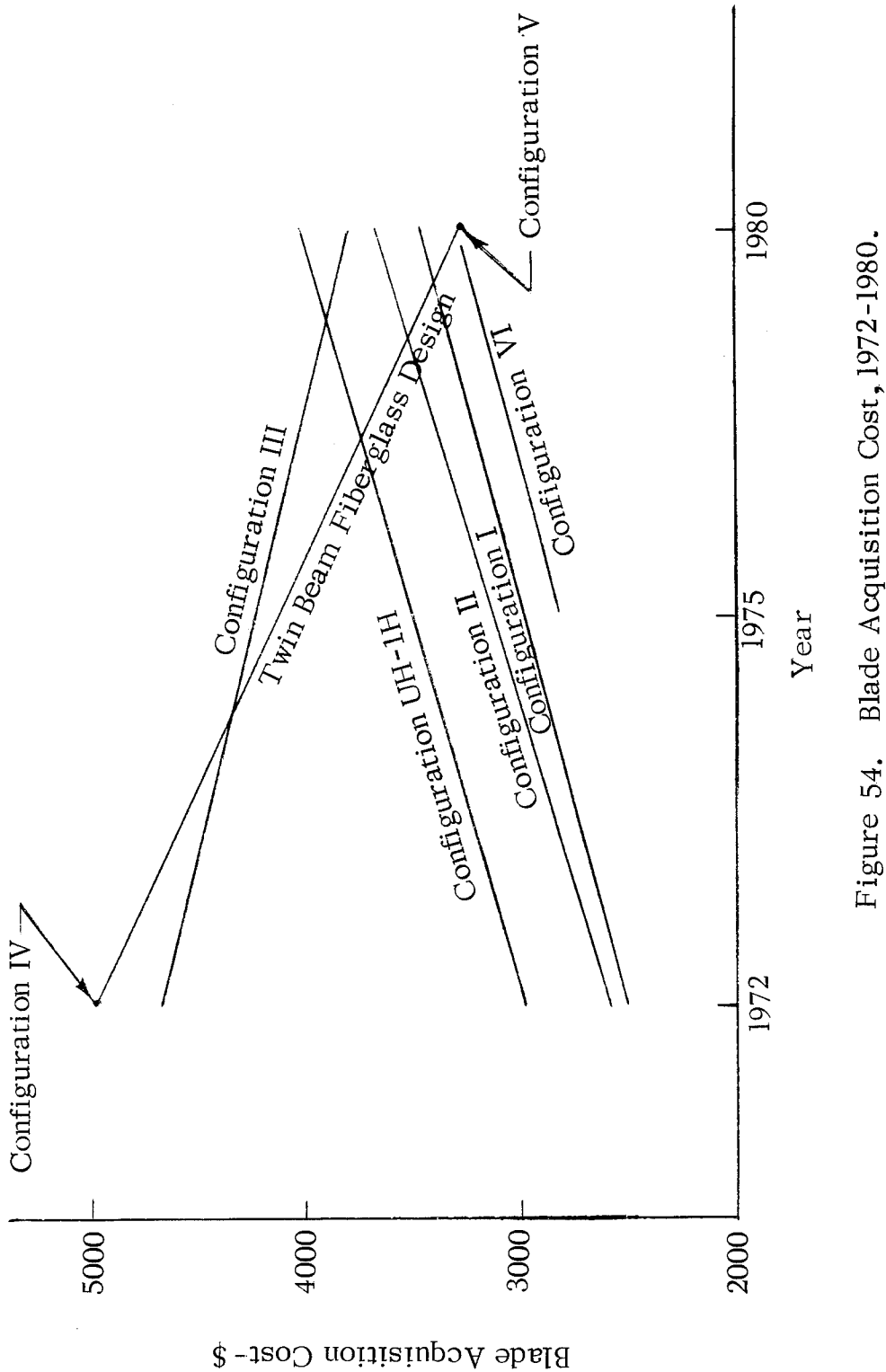
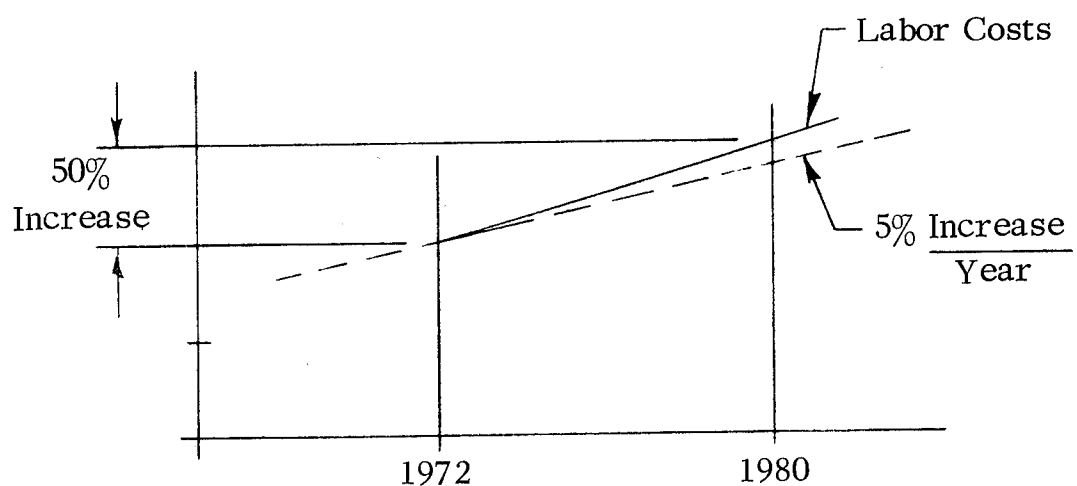


Figure 54. Blade Acquisition Cost, 1972-1980.

Labor Rate Trends



Material Rate Trends

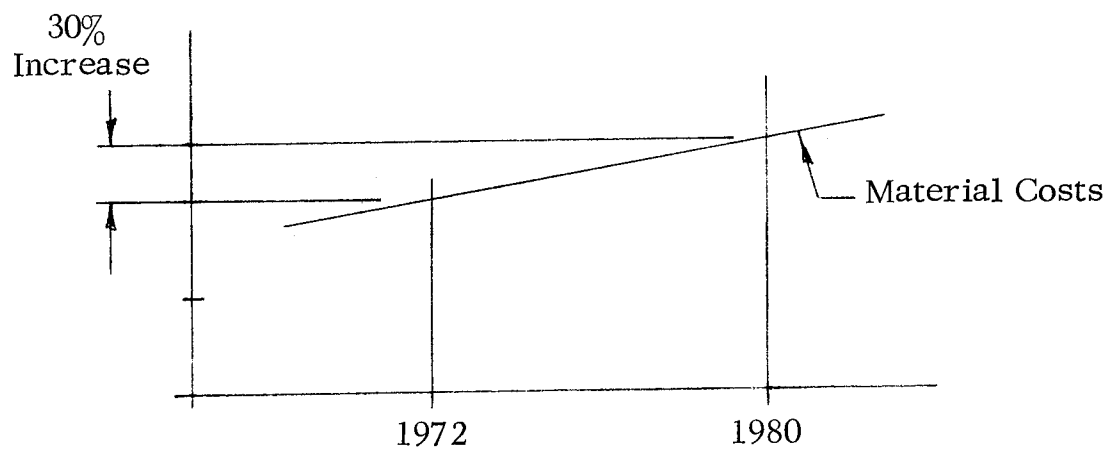


Figure 55. Forecast of Material and Labor Costs.

\$25.00 per pound. Such reductions in material and labor costs are expected to reduce the composite blade prices below those of the metal spar designs by 1980.

Of the two composite blade designs, the twin beam spar concept will offer the greatest potential for automated production because of its unique simple two-half construction. The solid cross section of the spar with its very simple, almost rectangular shape will be very easy to extrude. The trailing edge truss section will also be extrudable, after development, resulting in an entire half section of the blade being fabricated as one part. Making the blade in two halves eliminates the operations of fabricating and assembling a separate skin, spar, spline, etc., for each half section. The two halves are twisted, requiring very little torque, and are assembled in separate precision-made contoured molds having the blade twist. The blade thickness tolerance buildup is eliminated when the two halves are machined off to a flat mating surface on the chordline joint face and then bonded into one assembly.

The repairability of each design was also considered in the selection of the prime candidate. Both of the metal spar designs have highly repairable fiberglass trailing edge pockets. The fiberglass material has a low notch sensitivity and can therefore tolerate a large amount of damage and repair. The metal spars can tolerate only very minor damage and repair since the metals are much more notch sensitive. Projectile type damage which punctures the metal spar would not be repairable because of the high stress concentrations produced around the discontinuity in the structure. Strain allowables of the metals used for the spar are considerably lower than the fiberglass strain allowables, which means that at a given blade loading condition, the fiberglass will be operating at a much higher margin of safety than the metals. Since the margins of safety of the fiberglass components are higher, it follows that they will be more tolerant of repaired damage than a similar metal part.

Repairability of the composite blades will be better than for either of the metal spar designs because some repair of the spars is possible. Trailing edge repairability of the all composite blades will be about the same as for the metal spar blades, since the trailing edge construction of all the designs is very similar. The fiberglass spars both have a high margin of safety and low notch sensitivity, making repair of even projectile type damage possible. The twin beam spars are more repairable than the tubular type spar because of the very simple configuration. Damaged portions of the spar can be routed out and replaced with a bonded-in pre-molded repair section. The damaged honeycomb core would be filled with a room temperature curing foam. The repair procedures are described in Appendix II.

Evaluation of the growth potential of the four candidate designs considered the capability of each design to be used at higher aircraft speeds and also to increase hovering performance by the increasing of blade twist. Increases in blade twist will produce improved hover performance as described in Appendix I, but will also increase blade vibratory stress levels. Both the aluminum extruded spar and the roll-formed stainless steel and aluminum spars are operating at close to their vibratory stress limits. Very little increase in aircraft speed or blade twist can be tolerated in either of these designs; therefore, there is little growth potential. The composite blades, because of their much higher strain allowable materials, have a very large potential for future growth. Either blade twist or aircraft speed can be substantially increased, or a combination of both, without overstressing the blade.

CONCLUSIONS

The following conclusions are based upon a study of over 15 blade designs which are interchangeable with the UH-1 blade. The conclusions pertain to structural skin designs which are limited to the UH-1 requirement for edgewise rigidity. The conclusions could be quite different for blades with nonstructural pockets which are used extensively in articulated rotors.

A. 1972 Time Frame - Configuration I

The aluminum spar blade with a fiberglass and honeycomb cover is the optimum expendable blade configuration for the 1972 time frame. This blade requires very little development and could be retrofitted immediately. The blade has 30% fewer parts than the Bell blade. It uses 6061 aluminum spars instead of 2024 aluminum for superior corrosion characteristics. The spar has a 1.3-inch-thick leading edge for erosion protection. The blade is 54% repairable compared with 31% for the Bell blade. Its life-cycle costs could result in a \$12 million savings. The steel blade was slightly more expensive, and the composite blade material costs in this time frame were prohibitive.

B. 1975 Time Frame - Configuration VI

An aluminum spar with an automated advanced composite cover was considered to be the optimum expendable blade for this time frame. Essentially, this is a composite blade with an aluminum spar. Because 70% of the blade costs are associated with the cover assembly, the use of the pultrusion method of manufacturing a one-piece fiber-glass cover offers tremendous savings potential. It is considered that this technology can be demonstrated by 1975. The aluminum spar is the same as that defined in Section A.

C. 1980 Time Frame - Configuration V

The all composite Sikorsky twin beam design can potentially be the optimum expendable blade for the 1980 time frame. For this potential to be realized, the cost of carbon or boron must be reduced to \$25 a pound. The ability to withstand damage without shattering or delaminating extensively must be demonstrated. The ability to repair the structural spar and trailing edges without significantly affecting its strength must be demonstrated. Finally, the pultrusion or other automated methods of fabricating the blade in one or

two pieces with contour and weight control must be demonstrated. It is considered that this technology must be proven prior to committing to production. There is sufficient time to develop this technology, and the twin beam concept should greatly simplify the development task.

RECOMMENDATIONS

It is recommended that the pultrusion process of manufacturing a one-piece composite cover be developed. It is applicable to the aluminum spar concept for 1975 and the twin beam composite blade concept for 1980. In addition, it is recommended that a program be undertaken to develop the twin beam concept and demonstrate the needed technology as early as possible. It is conceivable that this concept could be available much sooner than 1980. To explore this, it is recommended that the twin beam design be manufactured, fatigue tested, whirled and flown. In parallel, the pultrusion development should be expanded to include the entire blade.

LITERATURE CITED

1. DESIGN STUDY OF REPAIRABLE MAIN ROTOR BLADES, Kaman Aerospace Report R-928, April 1971.
2. Carr, P. V., and Hensley, O. L., UH-1 and AH-1 HELICOPTER MAIN ROTOR BLADE FAILURE AND SCRAP RATE DATA ANALYSIS, Bell Helicopter Company, USAAVLabs Technical Report 71-9, Eustis Directorate, U. S. Army Air Mobility Research and Development Laboratory, Fort Eustis, Virginia, January 1971, AD 881132L.
3. ORGANIZATIONAL MAINTENANCE MANUAL - ARMY UH-1D HELICOPTER, Army TM-55-1520-210-20.
4. DIRECT SUPPORT AND DEPOT MAINTENANCE MANUAL, Army TM-55-1520-35.
5. Carlson, R. G., and Hilzinger, K. D., ANALYSIS AND CORRELATION OF HELICOPTER ROTOR BLADE RESPONSE IN A VARIABLE INFLOW ENVIRONMENT, Sikorsky Aircraft Div., USAAML Technical Report 65-51, U. S. Army Aviation Materiel Laboratories, Fort Eustis, Virginia, 1965, AD 622412.
6. MIL-HDBK-5 METALLIC MATERIAL AND ELEMENTS FOR AEROSPACE VEHICLE STRUCTURES, Department of Defense, Washington, D. C.
7. Bell, W. J., and Benham, P. P., THE EFFECT OF MEAN STRESS ON FATIGUE STRENGTH OF PLAIN AND NOTCHED STAINLESS STEEL SHEET IN THE RANGE FROM 10 TO 10^8 CYCLES, Symposium On Fatigue Tests of Aircraft Structures, ASTM STP 338, 1963, pp 25 - 46.
8. MIL-HDBK-17A PLASTICS FOR AEROSPACE VEHICLES, PART I, REINFORCED PLASTICS, Department of Defense, Washington, D. C., January 1971.
9. STATIC AND FATIGUE TEST PROPERTIES FOR WOVEN AND NONWOVEN S-GLASS FIBERS, Boeing Vertol Co., USAAVLabs Technical Report 69-9, U. S. Army Aviation Materiel Laboratories, Fort Eustis, Virginia, April 1969, AD 688971.
10. Roark, Raymond J., FORMULAS FOR STRESS AND STRAIN, New York, New York, McGraw-Hill Book Co., Inc., 1954.

11. Miner, M. A., CUMULATIVE DAMAGE IN FATIGUE, Journal of Applied Mechanics, 1945.
12. CHARACTERIZATION OF BORON, GRAPHITE AND GLASS FILAMENT/ORGANIC MATRIX COMPOSITE MATERIALS, Sikorsky Aircraft Engineering Report SER-50644, January 1970.
13. MATERIALS PROPERTY HANDBOOK VOL. II STEELS, AGARD (1/2 Hard 150/110), March 1966.
14. ENGINEERING MATERIALS MANUAL, Sikorsky Aircraft, 1972.
15. UH-1D HORSEPOWER REQUIREMENTS STUDY, CORG Memo 185, June 1965.
16. COMBAT OPERATIONAL FLIGHT PROFILES ON THE UH-1G, AH-1G, AND UH-1H HELICOPTERS, AHS Forum, June 1970.
17. FY 71 DETAIL SPECIFICATION 205-947-135, March 2, 1970.
18. CATEGORY II PERFORMANCE TESTING OF THE YUH-1D WITH A 48 FOOT ROTOR, FTC-TDR-64-27.

APPENDIX I BLADE CHARACTERISTICS

EFFECT OF TORSIONAL STIFFNESS ON BLADE STRESS AND TORSIONAL DEFLECTION

A study was made to determine the effect of varying the torsional rigidity on various blade parameters. The UH-IH rotor blade was used as the base for the study. Torsional stiffness of the UH-IH blade was both increased and decreased to observe the effect on blade stress and blade torsional deflection. The blade stiffness was varied by the same percentage from root to tip of the blade in each case studied. It was observed that the torsional deflection and blade stress were directly related to each other; as deflection began to rise rapidly when the stiffness fell to approximately 50% of the base value, the stress also began to rise rapidly. The relationship between torsional deflection in degrees and the percentage of the UH-IH torsional stiffness is shown in Figure 56. Vibratory stress normalized to the UH-IH stress at the UH-IH stiffness is plotted vs. the varying UH-IH torsional stiffness in Figure 57. In all cases, the study was conducted at a forward velocity of 110 knots and a gross weight of 3500 pounds. The study has shown that reduction in torsional stiffness of up to 50% of the UH-IH is possible without serious problems; however, for a blade with increased forward speed potential, the torsional stiffness must be kept at a high level.

EFFECT OF BLADE TWIST ON HOVER PERFORMANCE

A study was made to determine the improvements which can be made in rotor hovering performance by varying the blade twist. The Sikorsky Rotor Hover Performance Analysis which is programmed for a UNIVAC computer was used for the calculations. The UH-IH rotor system was used as the model for these calculations. Because the basic UH-IH blade loading is not very high ($C_T/\bar{C} = .0854$), the performance gains were relatively small. About 50 pounds of additional thrust was obtained for each additional degree of blade twist at 990 horsepower delivered to the rotor. Figure 58 illustrates the improvement in rotor thrust vs blade twist.

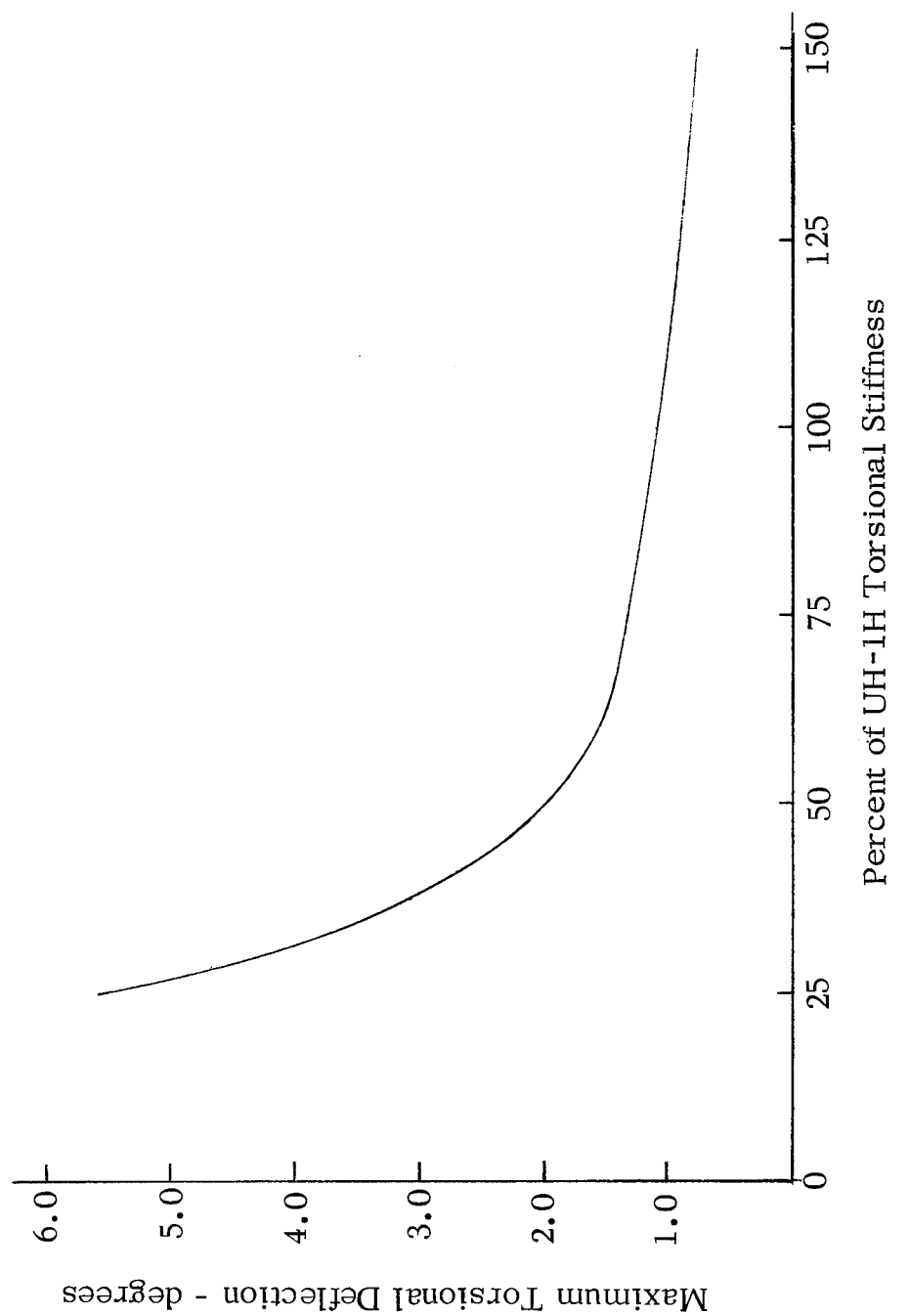


Figure 56. Maximum Torsional Deflection.

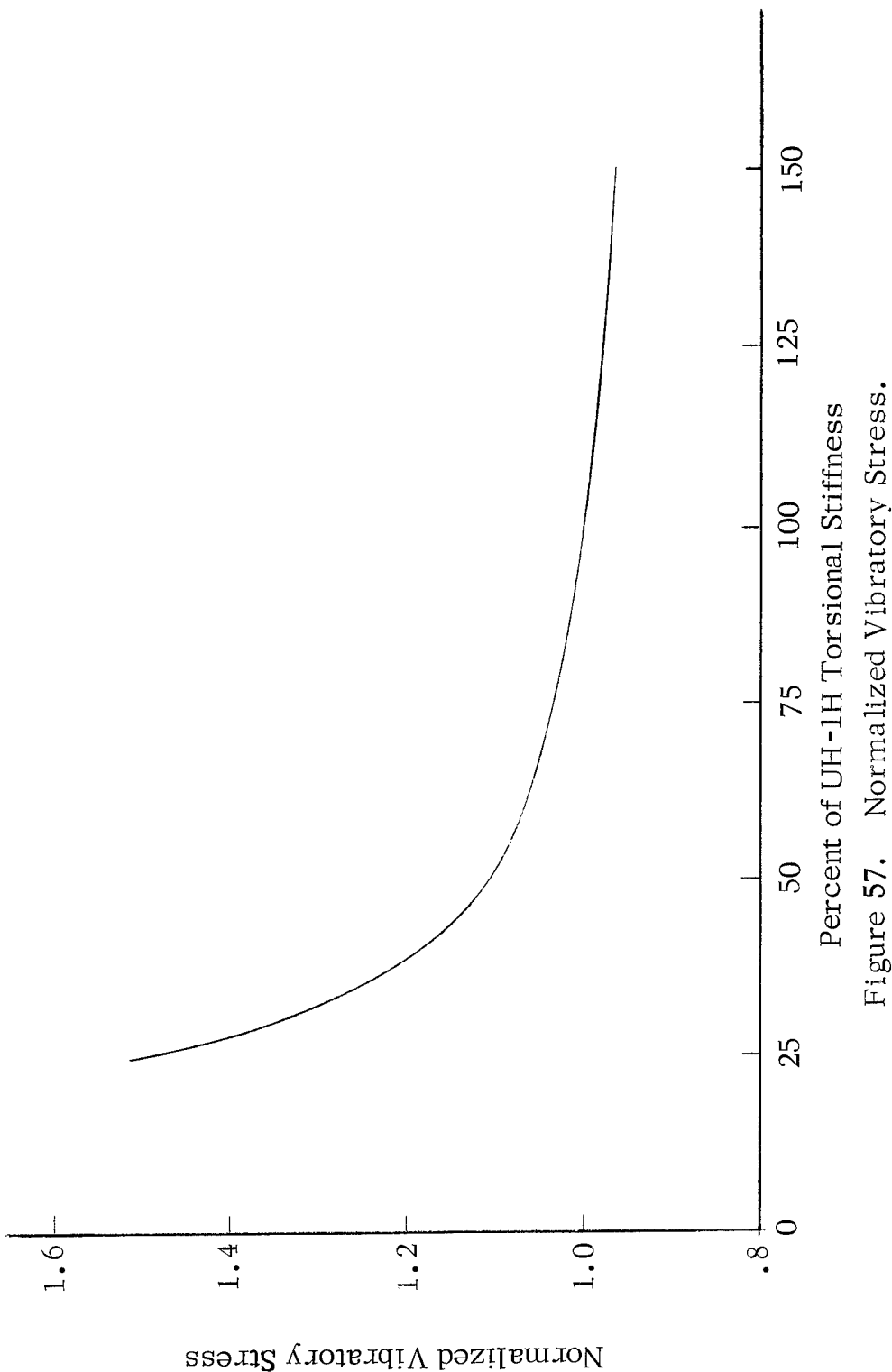


Figure 57. Normalized Vibratory Stress.

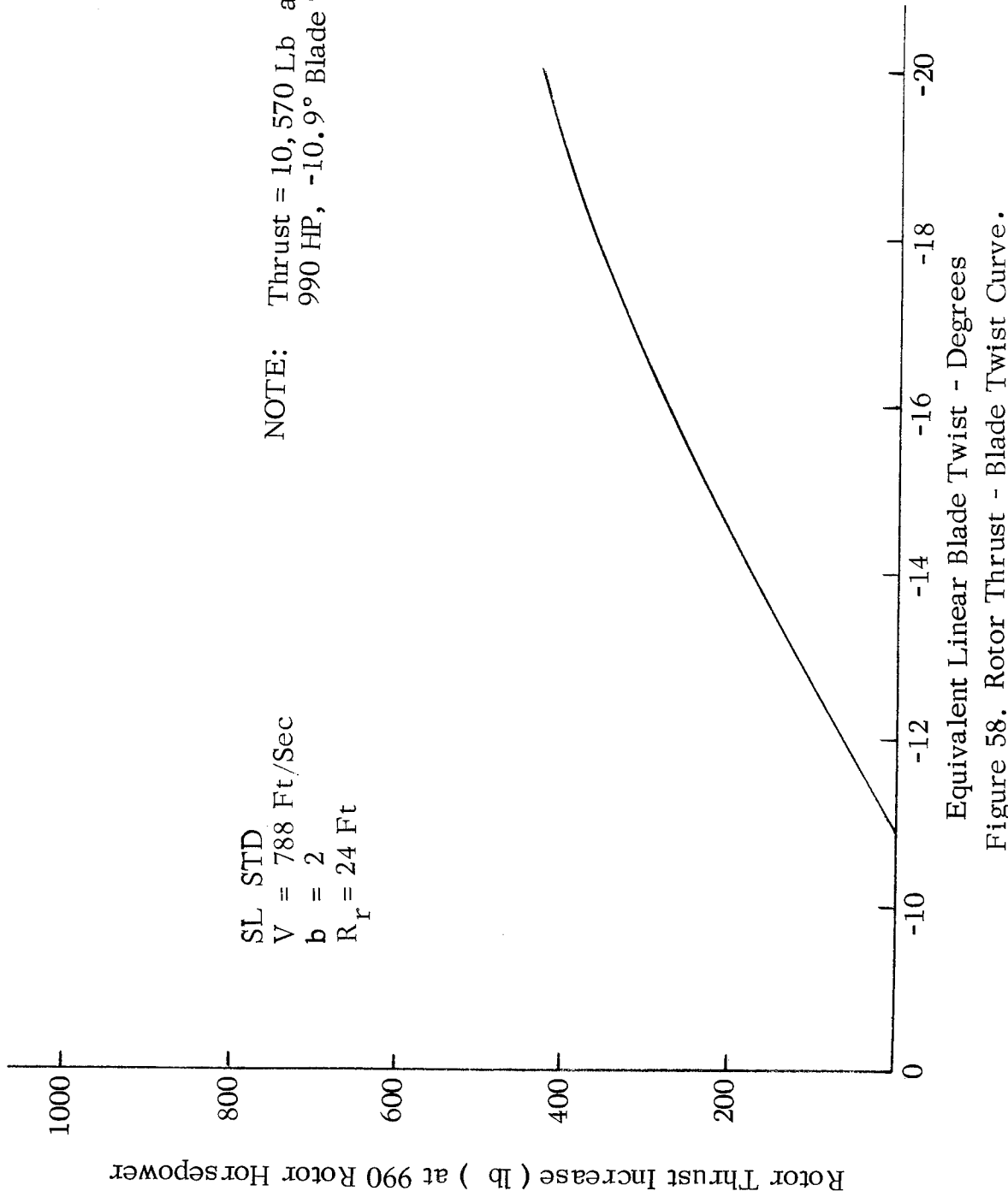


Figure 58. Rotor Thrust - Blade Twist Curve.

APPENDIX II

RELIABILITY/MAINTAINABILITY DATA

Appendix II includes the Reliability/Maintainability data referred to in the body of this report. It consists of Configurations I, II, and IV Reliability Analyses, Repairability Analyses, Math Model R/M Input Variables, Failure Mode and Effects Analysis and Repair Procedures.

TABLE XXXII. RELIABILITY ANALYSIS - CONFIGURATION I

Component	Mode	Inherent Causes					
		Occurrences Per 10 ⁶ Blade Hours					
1. Spar (Aluminum Extrusion)	1. Bonding separation (spar-to-core)	4.0					
	2. Leading edge erosion	36.0					
	3. Corrosion	12.0					
	4. Elongation of bushing holes	15.0					
	5. Crack	13.0					
	6. Spar closure piece bonding separation	2.0					
2. Core - (Aluminum Honeycomb)	1. Bonding separation (core-to-skin)	21.0					
	2. Water contamination	10.0					
3. Skin (Fiberglass)	1. Bonding separation (skin-to-spar)	15.0					
	2. Abrasion	27.0					
	3. Blisters	29.0					
	4. Crazing	17.0					
	5. Delamination	38.0					
4. Attaching Point Bushings	1. Cracks	10.0					
	2. Wear	9.0					
	3. Corrosion	3.0					
5. Doublers, Grip and Drag Plate	1. Bonding separation	4.0					
	2. Corrosion	3.0					
	3. Cracks	15.0					

TABLE XXXII. (Continued)

Component	Mode	Occurrences Per 10 ⁶ Blade Hours	
		1.	2.
6. Trailing Edge Spline	1. Bonding separation 2. Cracks	13.0 2.0	
7. Trim Tab	1. Loose rivets 2. Bond separation	1.0 4.0	
8. Counterweights	1. Loose 2. Corroded	1.0 2.0	
9. General	Excess vibration, out of adjustment, unbalance	69.0	
	Total Inherent	375.0	
	Externally Caused		
1. Spar	1. Battle damage 2. Chipped 3. Dented 4. Foreign object damage 5. Punctured 6. Scored 7. Grooved 8. Nicked	40.0 4.0 64.0 39.0 47.0 1.0 1.0 8.0	

TABLE XXXII. (Continued)

Component	Mode	Occurrences Per 10 ⁶ Blade Hours
2. Skin	1. Battle damage 2. Bent 3. Broken 4. Buckled 5. Collapsed 6. Cut 7. Dented 8. Foreign object damage 9. Punctured 10. Torn	68.0 12.0 12.0 1.0 1.0 29.0 110.0 68.0 80.0 59.0
3. T. E. Spline	1. Battle damage 2. Dented 3. Foreign object damage 4. Punctured	12.0 17.0 13.0 14.0
4. General	Overstressed, warped, sudden stop, overspeed	126.0
	Total External	826.0
	Total Blade	1201.0

TABLE XXXII. (Continued)

Mean Time Between Removals	
Total Inherent = 375 Maint. Actions Per 10^6 Blade Hours	
MTBRI = 2,680 Hours	
Total External = 826 Maint. Actions Per 10^6 Blade Hours	
MTBRE = 1,211 Hours	
Total Blade = 1201 Maint. Actions Per 10^6 Blade Hours	
MTBRT = 833 Hours	
Mean Time To Removal	
Total Blade MTR = 436 Blade Hours	
Total Inherent MTR = 513 Blade Hours	
Total External MTR = 400 Blade Hours	

TABLE XXXII. REPAIRABILITY ANALYSIS - CONFIGURATION I

Blade Component	Reason for Removal	Blade Removals - Inherent Causes		Maint Actions Per 10 ⁶ Blade Hours	Depot Level
		Org Level	DS Level		
1. Spar	1. Bonding separation	4.0		36.0	15.0
	2. Leading edge erosion			12.0	
	3. Corrosion				
	4. Elongation of bushing holes				
	5. Crack		13.0		
	6. Spar closure piece bonding separation		2.0		
2. Core	1. Bonding separation			21.0	5.0
	2. Water contamination			5.0	
3. Skin	1. Bonding separation			15.0	5.0
	2. Abrasion			27.0	
	3. Blisters			29.0	
	4. Crazing			17.0	
	5. Delamination			38.0	
4. Attaching Point Bushings	1. Cracks			10.0	3.0
	2. Wear			9.0	
	3. Corrosion			3.0	
5. Doublers, Grip and Drag Plate	1. Bonding separation			4.0	15.0
	2. Corrosion				
	3. Cracks				

TABLE XXXIII. Continued

Blade Component	Reason for Removal	Blade Removals - Inherent Causes					
		Maint	Actions Per 10 ⁶	Blade Hours	DS Level	Depot Level	Scrap Repair
		Org Level	Scrap Repair	Repair			
6. T.E. Spline	1. Bonding separation 2. Cracks		13.0 2.0				
7. Trim Tab	1. Loose rivets 2. Bond separation			1.0 4.0			
8. Weights	1. Loose 2. Corroded			1.0 2.0			
9. General	Excess vibration, out of adjust, unbalance	21.0	8.0		27.0	13.0	
	Total Inherent	55.0	67.0	5.0	174.0	27.0	47.0

TABLE XXXIII. (Continued)

Blade Component	Reason for Removal	Blade Removals - External Causes					
		Maint	Actions Per	10	6	Blade Hours	
		Org Level	DS Level	Depot Level	Scrap Repair	Scrap Repair	Scrap Repair
1. Spar	1. Battle damage 2. Chipped 3. Dented 4. Foreign object damage 5. Punctured 6. Scored 7. Grooved 8. Nicked	40.0	4.0	64.0	15.0	24.0	
2. Skin	1. Battle damage 2. Bent 3. Broken 4. Buckled 5. Collapsed 6. Cut 7. Dented 8. Foreign object damage 9. Punctured 10. Torn	14.0	54.0	12.0	12.0	1.0	
3. T.E. Spline	1. Battle damage 2. Dented 3. Foreign object damage 4. Punctured	12.0	17.0	13.0	14.0		

TABLE XXXIII. (Continued)

Blade Component	Reason for Removal	Blade Removals - External Causes	Maint	Actions Per 10 ⁶	Blade Hours
			Org Level	D S Level	Depot Level
4. General	Overstressed, warped, overspeed, sudden stop	126.0			
	Total External	334.0	12.0	134.0	346.0
				--	--
	Total Blade - 54% Repairable	389.0	79.0	139.0	520.0
				27.0	47.0

TABLE XXXIV. MATH MODEL R/M INPUT VARIABLES - CONFIGURATION I

Variable	Value
1. Aircraft Down Hours	
2. Aircraft Aborting Failure Rate	
3. Blade Mean Time Between Inherent Failures	
4. Blade Retirement Life	
5. % Damage Repaired On Aircraft (ORG)	
6. % Damage Repaired Off Aircraft (ORG)	
7. % Removed Blades Scrapped (ORG)	
8. % Removed Blades Sent to Direct Support	
9. % Received Blades Repaired (Direct Support)	
10. % Received Blades Scrapped (Direct Support)	
11. % Received Blades Repaired at Depot	
12. Maintenance Man-Hours per Inspection on Aircraft (ORG)	.25 Maint. Man-Hours
13. Maintenance Man-Hours per Repair on Aircraft (ORG)	1.0 Maint. Man-Hours
14. Maintenance Man-Hours per Repair at Direct Support	3.9 Maint. Man-Hours
15. GSE Cost per Repair (Direct Support)	\$134.25 per repair
16. GSE Cost per Aircraft (Direct Support)	\$637.66 per aircraft
17. Parts/Material Cost (Direct Support)	\$15.60 per repair
18. Blade Overhaul Cost - Depot	\$822.00 per blade

TABLE XXXV. DESIGN FAILURE MODE AND EFFECT ANALYSIS - CONFIGURATION I

Nomenclature	Function	Possible Failure Modes in Anticipated Environment	Effect of Failure Upon Assembly Function	Probable Symptom and Method of Detection
Spar (6061 Aluminum)	Primary Structural member	<u>Inherent:</u>		
		1. Leading edge erosion	1. No mission effect. Progressive deterioration if uncontrolled.	1. Possible blade unbalance. Detectable visually.
		2. Corrosion	2. Progressive deterioration if undetected. Possible source of fatigue cracks.	2. Corroded appearance. Detect visually.
		3. Elongation of bushing holes at blade attachment points	3. Vibration will cause blade removal prior to any effect on structural capability.	3. Noise and vibration. Detectable by inspection.
		4. Crack	4. Possible fracture if allowed to propagate.	4. Possible vibration. Visual inspection.
		5. Spar closure piece bonding separation	5. No effect for localized separation. Deterioration in structural capability if widespread.	5. Possible out of contour detectable by visual inspection. Possible vibration.
		<u>External:</u>		
		1. Punctured	1. Up to .50 cal. No effect.	1. Visual detection.
		2. Gashed or torn	2. Degradation in structural capability depending on size location.	2. Visual detection.
		3. Dented	3. Minor dents, no effect. Large dents, possible stress concentration and deterioration in structural integrity.	3. Possible vibration, visual detection.
		4. Scratched	4. No effect	4. Visual detection.
		5. Fractured	5. Loss of blade	5. Loss of control.
Honeycomb Core	Provide stability for skin panel	<u>Inherent:</u>		
		1. Skin to core bonding separation	1. No effect for small areas. Possible deterioration in stiffness for large areas.	1. Buckled skin detectable by visual inspection or coin tapping. Possible noise or vibration.
		2. Water contamination	2. Vibration due to blade unbalance.	2. Blade unbalance, leakage or seepage

TABLE XXXV. (Continued)

Nomenclature	Function	Possible Failure Modes in Anticipated Environment	Effect of Failure Upon Assembly Function	Probable Symptom and Method of Detection
Honeycomb Core (continued)	Provide stability for skin panel	<u>External:</u> 1. Punctured, bent, cut or crushed	1. No effect for small areas. Deterioration in stiffness characteristics for large areas.	1. Possible noise and vibration. Detectable visually
Skin Fiberglass	Provide airfoil surface contour and edgewise bending stiffness	<u>Inherent:</u> 1. Bonding Separation A. Skin to spar B. Skin to T.E. spline 2. Blisters 3. Abrasion 4. Crazing 5. Delamination	1. No effect for small areas; large areas may reduce blade stiffness. 2. No effect for small areas if repaired. Progressive deterioration of skin laminates if undetected. 3. Progressive deterioration of skin laminates if undetected. 4. Same as 3 above. 5. Progressive deterioration and possible loss of skin strength if undetected.	1. Visual detection and by coin tapping. 2. Visual detection. 3. Visual detection. 4. Visual detection 5. Visual detection
Attaching Point Bushings	Provide bearing surface for mounting bolts	<u>External:</u> 1. Punctured, cut, torn, dented, scratched	1. No effect for small areas; large areas reduce blade strength.	1. Probable noise and vibration. Detectable visually
		<u>Inherent:</u> 1. Crack 2. Wear 3. Corrosion	1. No effect. 2. Performance deterioration 3. No effect	1. Visual inspection. 2. Noise and vibration. Detected visually. 3. Visual inspection.
		<u>External:</u> 1. Battle damage	1. Mission abort to loss of blade, depending upon type and degree of damage.	1. Noise, vibration, loss of control. Visual inspection.

TABLE XXXV. (Continued)

Nomenclature	Function	Possible Failure Modes in Anticipated Environment	Effect of Failure Upon Assembly Function	Probable Symptom and Method of Detection
External Built-up Doublers (Aluminum)	Provide greater cross-sectional area at root end attaching points	<u>Inherent:</u> <ol style="list-style-type: none"> 1. Bonding separation 2. Cracks 3. Corrosion <u>External:</u> <ol style="list-style-type: none"> 1. Scratched, punctured, dented, cut, torn 	<ol style="list-style-type: none"> 1. Progressive deterioration if undetected. 2. Deterioration of structural capability. 3. Possible origin of fatigue cracks if undetected <ol style="list-style-type: none"> 1. Deterioration of functional capability. 	<ol style="list-style-type: none"> 1. Visual detection or coin tap inspection. 2. Visual inspection. 3. Visual inspection. <ol style="list-style-type: none"> 1. Visual inspection.
Trailing Edge Spline	Provide edgewise blade stiffness	<u>Inherent:</u> <ol style="list-style-type: none"> 1. Bonding separation <u>External:</u> <ol style="list-style-type: none"> 1. Scratched, dented, crushed, punctured, cut, torn 	<ol style="list-style-type: none"> 1. No effect for separation under 6 inches. Greater than 6 inches will cause deterioration of edgewise stiffness characteristics. 2. Crack <ol style="list-style-type: none"> 1. Deterioration or loss of edgewise stiffness characteristics depending upon degree and location. 	<ol style="list-style-type: none"> 1. Possible out of contour. Visual or coin tap inspection. <ol style="list-style-type: none"> 2. Possible vibration. Visual inspection. <ol style="list-style-type: none"> 1. Detect visually.
Trim Tab	Blade track adjustment	<u>Inherent:</u> <ol style="list-style-type: none"> 1. Loose rivets 2. Bonding separation <u>External:</u> <ol style="list-style-type: none"> 1. Bent, cracked, punctured 	<ol style="list-style-type: none"> 1. Possible loss of blade track. 2. Possible loss of blade track. <ol style="list-style-type: none"> 1. Possible loss of blade track. 	<ol style="list-style-type: none"> 1. Noise, vibration. Visual detection. 2. Noise, vibration. Visual detection. <ol style="list-style-type: none"> 1. Noise, vibration. Visual detection.
Counterweights Spanwise and Chordwise Balance	Balance blade	<u>Inherent:</u> <ol style="list-style-type: none"> 1. Loose 2. Corroded 	<ol style="list-style-type: none"> 1. No effect 2. No effect 	<ol style="list-style-type: none"> 1. Visual inspection. 2. Visual inspection.

TABLE XXXV. (Continued)

Nomenclature	Function	Possible Failure Modes in Anticipated Environment	Effect of Failure Upon Assembly Function	Probable Symptom and Method of Detection
Counterweights, Spanwise and Chordwise Balance (continued)	Balance blade	<u>External:</u> 1. Battle damage	1. Loss of blade balance if weights are separated.	1. Vibration; visual inspection.
Grip Pad and Drag Plate	Transfer blade leads to rotor head	<u>Inherent:</u> 1. Bonding separation 2. Cracks 3. Corrosion	1. Deterioration in structural integrity if undetected. 2. Same as 1 above. 3. Possible source of fatigue cracks.	1. Visual inspection. 2. Visual inspection. 3. Visual inspection.
		<u>External:</u> 1. Scratched, gouged, punctured, cut, torn	1. Deterioration in structural integrity depending on extent of damage.	1. Visual inspection.

TABLE XXXVI. RELIABILITY ANALYSIS - CONFIGURATION II

Component	Mode	Inherent Causes					Occurrences Per 10 ⁶ Blade Hours
1. Spar		1. Bonding separation				4.0	
		2. Abrasion, pitted, eroded				12.0	
		3. Corrosion				14.0	
		4. Elongation of bushing holes				15.0	
		5. Crack				13.0	
2. Core		1. Bonding separation				21.0	
		2. Water contamination				10.0	
3. Skin		1. Unbonded				15.0	
		2. Abrasion				27.0	
		3. Blisters				29.0	
		4. Crazing				17.0	
		5. Delamination				38.0	
4. Attach Point Bushings		1. Cracks				10.0	
		2. Wear				9.0	
		3. Corrosion				3.0	
5. Doublers, Grip and Drag Plates		1. Bonding separation				4.0	
		2. Corrosion				3.0	
		3. Cracks				15.0	

TABLE XXXVI. (Continued)

Component	Mode	Inherent Causes		Occurrences Per 10^6 Blade Hours
6. T. E. Spline		1. Bonding separation 2. Cracks		13.0 2.0
7. Trim Tab		1. Loose rivets 2. Unbonded		1.0 4.0
8. Counterweights		1. Loose 2. Corroded		1.0 2.0
9. General		Excess vibration, out of adjustment, unbalance		69.0
		Total Inherent		351.0

TABLE XXXVI. (Continued)

Component	Mode	External Causes	
			Occurrences Per 10 ⁶ Blade Hours
1. Spar		1. Battle damage 2. Chipped 3. Dented 4. Foreign object damage 5. Punctured 6. Scored 7. Grooved 8. Nicked	40.0 4.0 64.0 39.0 47.0 1.0 1.0 8.0
2. Skin		1. Battle damage 2. Bent 3. Broken 4. Buckled 5. Collapsed 6. Cut 7. Dented 8. Foreign object damage 9. Punctured 10. Torn	68.0 12.0 12.0 1.0 1.0 29.0 110.0 68.0 80.0 59.0
3. T. E. Spline		1. Battle damage 2. Dented 3. Foreign object damage	12.0 17.0 14.0

TABLE XXXVI. (Continued)

External Causes		Occurrences Per 10 ⁶ Blade Hours
Component	Mode	
4. General	Overstressed, warped, sudden stop, overspeed, other	126.0
	Total External	826.0
	Total Blade	1177.0
Mean Time Between Removals		
Total Inherent = 351 Maintenance Actions Per 10 ⁶ Blade Hours		
MTBRI = 2,850 Hours		
Total External = 826 Maintenance Actions Per 10 ⁶ Blade Hours		
MTBRE = 1,211 Hours		
Total Blade = 1177 Maintenance Actions Per 10 ⁶ Blade Hours		
MTBRT = 850 Hours		
Mean Time To Removal		
Total Blade MTR = 450 Hours		
Total Inherent MTR = 502 Hours		
Total External MTR = 400 Hours		

TABLE XXXVII. REPAIRABILITY ANALYSIS - CONFIGURATION II

Blade Component	Reason for Removal	Blade Removals - Inherent Causes		Maint	Actions Per	10^6	Blade Hours
		Org Level	D S Level	Scrap	Repair	Scrap	Repair
1. Spar	1. Bonding separation 2. Abrasion, pitted, eroded 3. Corrosion 4. Elongation of bushing holes 5. Crack	4.0		12.0			
				14.0			
					13.0		
2. Core	1. Bonding 2. Water contamination			5.0		21.0	
						5.0	
3. Skin	1. Unbonded 2. Abrasion 3. Blisters 4. Crazing 5. Delamination					15.0	
						27.0	
						29.0	
						17.0	
						38.0	
4. Attaching Point Bushings	1. Cracks 2. Wear 3. Corrosion					10.0	
						9.0	
						3.0	
5. Doublers, Grip and Drag Plates	1. Bonding separation 2. Corrosion 3. Cracks					4.0	
					3.0		
						15.0	

TABLE XXXVII. (Continued)

Blade Component	Reason for Removal	Blade Removals - Inherent Causes			
		Maint	Actions Per	10 6	Blade Hours
		Org Level	DS Level	Depot Level	Scrap Repair Scrap Repair
6. T. E. Spline	1. Bonding separation 2. Cracks		2.0		
			13.0		
7. Trim Tab	1. Loose rivets 2. Unbonded		1.0		
			4.0		
8. Counterweights	1. Loose 2. Corroded		1.0		
			2.0		
9. General	Excess vibration, out of adjustment, unbalance	21.0	8.0		
				27.0	13.0
	Total Inherent	53.0	45.0	5.0	174.0 27.0 47.0

TABLE XXXVII. (Continued)

Blade Component	Reason for Removal	Blade Removals - External Causes					
		Maint Actions Per Org Level	10 ⁶ Blade Hours	DS Level	Depot Level	Scrap Repair	Scrap Repair
1. Spar	1. Battle damage	40.0					
	2. Chipped		4.0				
	3. Dented	64.0					
	4. Foreign object damage		15.0	24.0			
	5. Punctured	47.0					
	6. Scored			1.0			
	7. Grooved				1.0		
	8. Nicked		8.0				
						14.0	54.0
						12.0	
2. Skin	1. Battle damage					12.0	
	2. Bent					12.0	
	3. Broken					1.0	
	4. Buckled					1.0	
	5. Collapsed					11.0	18.0
	6. Cut					23.0	87.0
	7. Dented					29.0	39.0
	8. Foreign object damage					17.0	63.0
	9. Punctured					25.0	34.0
	10. Torn						
3. T.E. Spline	1. Battle damage		12.0				
	2. Dented		17.0				
	3. Foreign object damage		13.0				
	4. Punctured		14.0				

TABLE XXXVII. (Continued)

Blade Component	Reason for Removal	Blade Removals - External Causes			Depot Level Scrap Repair Scrap Repair
		Maint	Actions per 10 ⁶	Blade Hours	
		Org Level	D S Level	Repair	
4. General	Overstressed, warped, sudden stop, overspeed		126.0		
	Total External	334.0	12.0	134.0	346.0 - -
	Total Blade = 53% Repairable	387.0	57.0	139.0	520.0 27.0 47.0

TABLE XXXVIII. MATH MODEL R/M INPUT VARIABLES - CONFIGURATION II

Variable	Value
1. Aircraft Down Hours	4.3802 Down Hours Per Flight Hour
2. Aircraft Aborting Failure Rate	.015 Aborting Failures Per Flight Hour
3. Blade Mean Time Between Inherent Failures	2,850 Blade Hours
4. Blade Retirement Life	2,500 Blade Hours
5. % Damage Repaired On Aircraft (Org.)	6.0 Percent
6. % Damage Repaired Off Aircraft (Org.)	0.0 Percent
7. % Removed Blades Scrapped (Org.)	35.0 Percent
8. % Removed Blades Sent to Direct Support	65.0 Percent
9. % Removed Blades Repaired at Direct Support	71.0 Percent
10. % Received Blades Scrapped at Direct Support	19.0 Percent
11. % Received Blades Repaired at Depot	64.0 Percent
12. Maintenance Man-Hours Per Inspection (On-Aircraft, Org.)	.25 Maintenance Man-Hours
13. Maintenance Man-Hours Per Repair (On-Aircraft, Org.)	1.0 Maintenance Man-Hours
14. Maintenance Man-Hours Per Blade Repair (Direct Support)	4.25 Maintenance Man-Hours
15. GSE Cost Per Repair (Direct Support)	\$189.00 Per Repair
16. GSE Cost Per Aircraft (Direct Support)	\$637.66 Per Aircraft
17. Parts/Material Cost (Direct Support)	\$11.20 Per Repair
18. Blade Overhaul Cost (Depot)	\$822.00 Per Blade

TABLE XXXIX. DESIGN FAILURE MODE AND EFFECTS ANALYSIS - CONFIGURATION II

Nomenclature	Function	Possible Failure Modes in Anticipated Environment	Effect of Failure Upon Assembly Function	Probable Symptoms and Method of Detection
Spar (Stainless Steel & Aluminum)	Primary structural member	Inherent:		
		1. Leading edge erosion, pitting	1. No mission effect. Progressive deterioration if uncontrolled.	1. Detect visually.
		2. Corrosion	2. Progressive deterioration if undetected. Possible source of fatigue cracks.	2. Corroded appearance; detect visually.
		3. Elongation of bushing holes at blade attachment points	3. Vibration will cause blade removal prior to any effect on structural capability.	3. Noise and vibration; detectable by visual inspection.
		4. Crack	4. Possible fracture if allowed to propagate.	4. Possible vibration; visual inspection.
		5. Bonding separation	5. No effect for small unbonded areas. Deterioration in structural capability if allowed to progress.	5. Detectable visually or by coin tap.
		<u>External:</u>		
		1. Punctured	L. Up to .50 cal., no effect.	1. Visual detection.
		2. Gashed or torn	2. Degradation of structural capability depending upon size and location.	2. Visual detection.
		3. Dented	3. Minor dents, no effect. Large dents, 3. Possible vibration. Visual detection. possible stress concentration and deterioration in structural integrity.	
		4. Scratched	4. Possible stress concentration and source of crack, depending upon depth and location.	4. Visual detection.
		5. Fractured	5. Loss of blade.	5. Loss of control.

TABLE XXXIX. (Continued)

Nonnomenclature	Function	Possible Failure Modes in Anticipated Environment	Effect of Failure Upon Assembly Function	Probable Symptoms and Method of Detection
Honeycomb Core for skin panel	Provide stability	<u>Inherent:</u> 1. Skin to core bonding separation 2. Core to spar bonding separation 3. Water contamination	1. No effect for small areas. Possible deterioration in stiffness for large areas. 2. No effect for small areas. Large areas may reduce blade stiffness. 3. Vibration due to blade unbalance.	1. Buckled skin. Detect by visual inspection or coin tap. 2. Buckled skin. Detect by visual inspection. 3. Blade unbalance, leakage or seepage.
	<u>External:</u>	 1. Punctured, bent, cut or crushed	1. No effect for small areas; deterioration in stiffness characteristics for large areas.	1. Possible noise and vibration. Detect visually.
Skin (Fiberglass)	Provide airfoil surface contour and edgewise bending stiffness	<u>Inherent:</u> 1. Bonding separation A. Skin to spar beam B. Skin to T.E. spline 2. Blisters	1. No effect for small areas. Large areas may reduce blade stiffness. 2. No effect for small areas if repaired. Progressive deterioration of skin laminates if undetected. 3. Abrasion 4. Crazing 5. Delamination	1. Visual detection and coin tap. 2. Visual detection. 3. Visual detection. 4. Same as 3 above. 5. Progressive deterioration and possible loss of skin strength if undetected.
	<u>External:</u>	 1. Punctured, cut, torn, dented, scratched	1. No effect for small areas. Large areas reduce blade strength.	1. Probable noise and vibration. Detect visually.

TABLE XXXIX. (Continued)

Nomenclature	Function	Possible Failure Modes in Anticipated Environment	Effects of Failure on Assembly Function	Probable Symptoms and Method of Detection
Attaching Point Bushings	Provide bearing surface for mounting bolts	<u>Inherent:</u> <ul style="list-style-type: none"> 1. Crack 2. Wear 3. Corrosion <u>External:</u> <ul style="list-style-type: none"> 1. Battle damage 	<ul style="list-style-type: none"> 1. No effect. 2. Performance deterioration. 3. No effect. <ul style="list-style-type: none"> 1. Mission abort to loss of blade, depending upon type and degree of damage. 	<ul style="list-style-type: none"> 1. Visual inspection. 2. Noise and vibration. Detect visually. 3. Visual inspection. <ul style="list-style-type: none"> 1. Noise, vibration loss of control. 2. Visual inspection.
External Built-Up Doublers	Provide greater cross-sectional area at root end attaching points	<u>Inherent:</u> <ul style="list-style-type: none"> 1. Bonding separation 2. Cracks 3. Corrosion <u>External:</u> <ul style="list-style-type: none"> 1. Scratched, punctured, dented, cut, torn 	<ul style="list-style-type: none"> 1. Progressive deterioration if undetected. 2. Deterioration of structural capability if allowed to propagate. 3. Possible origin of fatigue cracks if undetected. <ul style="list-style-type: none"> 1. Deterioration of functional capability. 	<ul style="list-style-type: none"> 1. Visual detection or coin tap inspection. 2. Visual inspection. 3. Visual inspection. <ul style="list-style-type: none"> 1. Visual inspection.
Trailing Edge Spline	Provide edgewise blade stiffness	<u>Inherent:</u> <ul style="list-style-type: none"> 1. Bonding separation 2. Crack <u>External:</u> <ul style="list-style-type: none"> 1. Scratched, dented, crushed, punctured, cut, torn 	<ul style="list-style-type: none"> 1. No effect for separation under 6 inches. Greater than 6 inches will cause deterioration of edgewise stiffness characteristics. 2. Loss of edgewise stiffness if allowed to propagate. <ul style="list-style-type: none"> 1. Deterioration of edgewise stiffness characteristics depending upon degree and location. 	<ul style="list-style-type: none"> 1. Possible out of contour. Visual or coin tap inspection. 2. Possible vibration. <ul style="list-style-type: none"> 1. Noise, vibration. Detect visually.

TABLE XXXIX. (Continued)

Nomenclature	Function	Possible Failure Modes in Anticipated Environment	Effects of Failure on Assembly Function	Probable Symptoms and Method of Detection
Trim Tab	Blade track adjustments	<u>Inherent:</u> 1. Loose rivets 2. Bonding separation	1. Possible loss of blade track. 2. Possible loss of blade track.	1. Noise; vibration. Visual detection. 2. Noise; vibration. Visual detection.
		<u>External:</u> 1. Bent, cracked, punctured	1. Possible loss of blade track.	1. Noise; vibration. Visual detection.
Counterweights - Spanwise and Chordwise Balance	Balance blade	<u>Inherent:</u> 1. Loose 2. Corroded	1. No effect. 2. No effect.	1. Visual inspection. 2. Visual inspection.
		<u>External:</u> 1. Battle damage	1. Loss of blade balance if weights are separated.	1. Vibration, visual inspection.
Grip Pad and Drag Plate	Transfer blade leads to rotor head	<u>Inherent:</u> 1. Bonding separation 2. Cracks 3. Corrosion	1. Deterioration in structural integrity if undetected. 2. Same as 1 above. 3. Possible source of fatigue cracks.	1. Visual inspection. 2. Visual inspection. 3. Visual inspection.
		<u>External:</u> 1. Scratched, gouged, punctured, cut, torn	1. Deterioration in structural integrity depending upon extent of damage.	1. Visual inspection.

TABLE XXXX. RELIABILITY ANALYSIS - CONFIGURATION IV

Component	Mode	Inherent Causes		Occurrences Per 10 ⁶ Blade Hours
		1.	2.	
1. Leading Edge Structure	1. Erosion and pitting of protective coating			440.0
2. Spar-Twin Beam (Unidirectional "E" Glass)	1. Bonding separation 2. Crack 3. Delamination; crazing of "E" glass			48.0 2.0 4.0
3. Honeycomb Core (Nomex)	1. Water contamination 2. Bonding separation			10.0 27.0
4. Skin (Carbon)	1. Abrasion 2. Delamination 3. Crazing 4. Blisters 5. Bonding separation			18.0 36.0 40.0 24.0 50.0
5. Attaching Point Bushings	1. Cracks 2. Wear 3. Corrosion			10.0 9.0 3.0
6. Doublers; Grip and Drag Plate	1. Bonding separation 2. Cracks 3. Corrosion			4.0 15.0 7.0

TABLE XXXX. (Continued)

Component	Mode	Inherent Causes	
		Occurrences Per 10 ⁶	Blade Hours
7. Trailing Edge Spline		1. Cracks 2. Bonding separation 3. Delamination	2.0 2.0 5.0
8. Trim Tab		1. Loose rivets 2. Bonding separation	1.0 4.0
9. Counterweights		1. Loose 2. Corroded	1.0 2.0
10. General		1. Excess vibration, out of adjustment, unbalance	69.0
		Total Inherent	833.0
		Externally Caused	
1. Leading Edge Structure		1. Battle damage 2. Chipped 3. Dented 4. Foreign object damage 5. Grooved 6. Nicked 7. Punctured	13.0 2.0 19.0 11.0 0.5 4.0 15.0

TABLE XXXX. (Continued)

Component	Mode	Externally Caused	Occurrences Per 10 ⁶ Blade Hours
2. Spar-Twin Beam (Unidirectional "E" Glass)		1. Battle damage 2. Chipped 3. Dented 4. Foreign object damage 5. Grooved 6. Nicked 7. Punctured	31.0 2.0 50.0 29.0 0.5 4.0 36.0
3. Skin - Trailing Edge of Spar to Leading Edge of Spline		1. Battle damage 2. Bent 3. Broken 4. Buckled 5. Collapsed 6. Cut 7. Dented 8. Foreign object damage 9. Punctured 10. Torn	69.0 11.0 11.0 5.0 1.0 29.0 109.0 73.0 80.0 60.0
4. Trailing Edge Spline		1. Battle damage 2. Dented 3. Foreign object damage 4. Punctured	7.0 13.0 7.0 10.0

TABLE XXXX. (Continued)

Externally Caused		
Component	Mode	Occurrences Per 10 ⁶ Blade Hours
5. General	1. Overstressed, warped, sudden stop, overspeed, other	131.0
	Total External	825.0
	Total Blade	1658.0
Mean Time Between Removals		
Total Inherent	= 833	Maintenance Actions Per 10 ⁶ Blade Hours
MTBRI	= 1200	Hours
Total External	= 826	Maintenance Actions Per 10 ⁶ Blade Hours
MTBRE	= 1211	Hours
Total Blade	= 1659	Maintenance Actions Per 10 ⁶ Blade Hours
MTBRT	= 603	Hours
Mean Time To Removal		
Total Blade MTR	= 435	Hours
Total Inherent MTR =	498	Hours
Total External MTR =	400	Hours

TABLE XXXI. REPAIRABILITY ANALYSIS-CONFIGURATION IV

		Blade Removals - Inherent Causes			Maintenance Actions Per 10^6 Blade Hours					
Blade Component	Reason For Removal	Scrap	Repair	Scrap	D S Level	D S Repair	Scrap	Repair	Scrap	Depot Level Repair
1. Leading Edge Structure	1. Erosion and pitting of protective coating								440.0	
2. Spar-Twin Beam	1. Bonding separation 2. Crack 3. Delamination, crazing	20.0 1.0 2.0							28.0 1.0 2.0	
3. Honeycomb Core	1. Water contamination 2. Bonding separation			5.0	5.0					
4. Skin	1. Abrasion 2. Delamination 3. Crazing 4. Blisters 5. Bonding separation					18.0	36.0	40.0	24.0	50.0
5. Attach Point Bushings	1. Cracks 2. Wear 3. Corrosion					10.0	9.0	3.0		
6. Doublers	1. Bonding separation 2. Cracks 3. Corrosion								1.0 2.0 3.0	3.0 13.0 7.0

TABLE XXXXI. (Continued)

		Blade Removals - Inherent Causes - Continued					
Blade Component	Reason For Removal	Maintenance Actions Per 10 ⁶ Blade Hours					
		ORG Level	D S Level	Depot Level	Scrap	Repair	Scrap
7. Trailing Edge Spline	1. Cracks	1.0			1.0		
	2. Bonding separation	1.0			1.0		
	3. Delamination	2.0			3.0		
8. Trim Tab	1. Loose rivets		1.0				
	2. Bonding separation		4.0				
9. Counterweights	1. Loose			1.0			
	2. Corroded			2.0			
10. General	1. Excess vibration, out of adjustment, out of balance	21.0	8.0		27.0	13.0	
					49.0	15.0	5.0
						698.0	30.0
							36.0

TABLE XXXXI. (Continued)

		Blade Removals - External Causes		Maintenance Actions Per 10^6 Blade Hours						
Blade Component	Reason For Removal	ORG Level	D S Level	Scrap	Repair	Scrap	Repair	Depot Level	Scrap	Repair
1. Leading Edge Structure	1. Battle damage	3.0		5.0		5.0				
	2. Chipped				2.0					
	3. Dented			4.0				15.0		
	4. Foreign object damage				1.0			10.0		
	5. Grooved			0.5						
	6. Nicked				4.0					
	7. Punctured			3.0		12.0				
2. Spar Twin Beam	1. Battle damage	6.0		6.0		19.0				
	2. Chipped				2.0			2.0		
	3. Dented							50.0		
	4. Foreign object damage			5.0			7.0	18.0		
	5. Grooved			0.5					4.0	
	6. Nicked									36.0
	7. Punctured									
3. Skin Trailing Edge of Spar to Leading Edge of Spline	1. Battle damage							14.0	54.0	
	2. Bent								11.0	
	3. Broken									11.0
	4. Buckled									5.0
	5. Collapsed									1.0
	6. Cut							11.0	18.0	
	7. Dented							22.0	87.0	
	8. Foreign object damage							31.0	42.0	

TABLE XXXXI. (Continued)

		Blade Removals - External Causes - Continued				
Blade Component	Reason For Removal	Maintenance Actions Per 10 ⁶ Blade Hours				
		ORG Level	D S Level	Depot Level	Scrap Repair	Scrap Repair
3. Continued	9. Punctured 10. Torn		17.0 25.0	63.0 35.0		
4. Trailing Edge Spline	1. Battle damage 2. Dented 3. Foreign object damage 4. Punctured		1.0 1.0	6.0 12.0		
5. General	1. Overstressed		124.0			
		149.0		138.0	539.0	
Total Blade = 77% Repairable		198.0	15.0	143.0	1237.0	30.0
						36.0

**TABLE XXXII. MATH MODEL R/M INPUT VARIABLES -
CONFIGURATION IV**

Variable	Value
1. Aircraft Down Hours	4.3839 Down hours per flight hour
2. Aircraft Aborting Failure Rate	.015 Aborting failures per flight hour
3. Blade Mean Time Between Inherent Damage	1,200 Blade hours
4. Blade Retirement Life	5,000 Blade hours
5. % Damage Repaired On Aircraft, ORG Level	0.9 Percent
6. % Damage Repaired Off Aircraft, ORG Level	0 Percent
7. % Removed Blades Scrapped at ORG Level	12.0 Percent
8. % Removed Blades Sent to Direct Support	87.0 Percent
9. % Received Blades Repaired at Direct Support	85.0 Percent
10. % Received Blades Scrapped at Direct Support	10.0 Percent
11. % Received Blades Repaired at Depot	55.0 Percent
12. Maintenance Man-Hours to Inspect On Aircraft (ORG)	.25 Maintenance man-hours
13. Maintenance Man-Hours to Repair On Aircraft (ORG)	1.0 Maintenance man-hours
14. Maintenance Man-Hours to Repair Off Aircraft (ORG)	0.0
15. Maintenance Man-Hours per Blade Repair (Direct Support)	7.5 Maintenance man-hours
16. GSE Cost Per Repair (Direct Support)	\$84.10 per repair
17. GSE Cost Per Aircraft (Direct Support)	\$637.66 per aircraft
18. Parts/Material Cost (Direct Support)	\$66.00 per repair
19. Blade Overhaul Cost (Depot)	\$822.00 per blade

TABLE XXXIII. DESIGN FAILURE MODE AND EFFECT ANALYSIS - CONFIGURATION IV

Nomenclature	Function	Possible Failure Modes in Anticipated Environment	Effect of Failure Upon Assembly Function	Probable Symptom and Method of Detection
Leading Edge Structure	Provide airfoil contour	<u>Inherent:</u> <ul style="list-style-type: none"> 1. Erosion and pitting of protective coating. 2. Bonding separation, molded counterweight to carbon skin 3. Skin cracks, delamination <u>External:</u> <ul style="list-style-type: none"> 1. Battle damage 2. Cut, gashed, or torn 3. Dented 	<ul style="list-style-type: none"> 1. No mission effect. Repairable in the field. 2. Small bonding separations. No mission effect. Widespread bonding separation will affect blade balance. 3. No mission effect. Progressive deterioration if undetected. <ul style="list-style-type: none"> 1. Up to .50 cal. No mission effect. 2. Degradation in blade performance depending upon extent of damage. Possible blade unbalance. 3. No mission effect for minor dents. Severe dents may cause degradation in performance. 	<ul style="list-style-type: none"> 1. Visual detection. 2. Unbalanced blade. Detectable by coin tapping 3. Detectable visually. <ul style="list-style-type: none"> 1. Detect visually. 2. Noise and vibration. Detect visually. 3. Possible vibration. Detect visually.
Spar - Twin Beam (Unidirectional "E" Glass)	Primary structural member	<u>Inherent:</u> <ul style="list-style-type: none"> 1. Beam to core bonding separation 2. Elongation of bushing holes at blade attachment points 3. Cracks, delamination, crazing, of "E" glass <u>External:</u> <ul style="list-style-type: none"> 1. Battle damage 	<ul style="list-style-type: none"> 1. No mission effect for small unbonded areas. Undetected large areas can lead to deterioration in blade stiffness qualities. 2. Vibration will cause blade removal prior to any effect on structural capability. 3. Deterioration of structural capability if undetected. <ul style="list-style-type: none"> 1. Up to .50 cal. No mission effect. Greater than .50 cal. will result in degradation of structural capability depending on size and location. 	<ul style="list-style-type: none"> 1. Detect by tolerance check:possible vibration. 2. Noise and vibration. Detect by inspection. 3. Visual and possible vibration:by tolerance check. <ul style="list-style-type: none"> 1. Detect visually.

TABLE XXXIII. (Continued)

Nomenclature	Function	Possible Failure Modes in Anticipated Environment	Effect of Failure Upon Assembly Function	Probable Symptom and Method of Detection
Spar - Twin Beam (Unidirectional "E" Glass) (continued)	Primary structural member	External: 2. Cut, gashed or torn 3. Dented 4. Fractured	2. Degradation of structural capability depending upon size and location. 3. Minor dents. No mission effect. Large dents will result in decreased structural capability. 4. Loss of blade.	2. Detect visually. 3. Visual detection. 4. Loss of control.
Honeycomb Core	Provide stability for skin panel	Inherent: 1. Skin to core bonding separation 2. Water contamination External: 1. Punctured, bent, cut, or crushed	1. No effect for small areas. Possible deterioration in stiffness qualities for large areas. 2. Vibration or blade unbalance. 1. No effect for small areas. Decrease in blade stiffness characteristics for large areas.	1. Bucked or wrinkled skin. Detect by visual inspection or coin tap. Possible noise and vibration. 2. Blade unbalance, leakage or seepage. 1. Possible noise and vibration. Detect visually.
Skin (Carbon)	Provide airfoil surface contour and edgewise bending stiffness	Inherent: 1. Bonding separation A. Skin to beam B. Skin to T.E. spline 2. Blisters 3. Abrasion 4. Crazing 5. Delamination	1. No effect for small areas; large areas may reduce blade stiffness. 2. No effect for small areas if repaired. Progressive deterioration of skin laminates if undetected. 3. Progressive deterioration of skin laminates if undetected. 4. Same as 3 above. 5. Progressive deterioration and possible loss of skin strength if undetected.	1. Visual detection and coin tap. Possible noise and vibration. 2. Visual detection. 3. Visual detection. 4. Visual detection. 5. Visual detection.

TABLE XXXIII. (Continued)

Nomenclature	Function	Possible Failure Modes In Anticipated Environment	Effect of Failure Upon Assembly Function	Probable Symptom and Method of Detection
Skin (Carbon) Continued	Provide airfoil surface contour and edgewise bending stiffness	<u>External:</u> 1. Punctured, cut, torn, dented, scratched	1. No effect for small areas; large areas reduce blade strength.	1. Probable noise and vibration. Detect visually.
Attaching Point Bushings	Provide bearing surface for mounting bolts	<u>Inherent:</u> 1. Crack 2. Wear 3. Corrosion	1. No mission effect. 2. Performance deterioration. 3. No mission effect.	1. Visual inspection. 2. Noise and vibration. Detect visually. 3. Visual inspection.
		<u>External:</u> 1. Battle damage	1. Mission abort to loss of blade depending upon type and degree of damage.	1. Noise, vibration, loss of control. Detect by visual inspection.
External Built-up Doublers (Aluminum)	Provide greater cross-sectional area at root end attaching points	<u>Inherent:</u> 1. Bonding separation 2. Cracks 3. Corrosion	1. Progressive deterioration if undetected. 2. Deterioration of structural capability if allowed to propagate. 3. Possible origin of fatigue cracks if undetected.	1. Visual detection. Coin tapping. 2. Visual inspection. 3. Visual inspection.
		<u>External:</u> 1. Scratched, punctured, dented, cut, torn	1. Deterioration of functional capability.	1. Visual inspection.
Trailing Edge Spine	Provide edgewise blade stiffness	<u>Inherent:</u> 1. Bonding separation 2. Crack	1. No effect for separation under 6 inches. Greater than 6 inches will cause deterioration of edgewise stiffness characteristics. 2. Loss of edgewise stiffness if allowed to propagate.	1. Possible out of contour. Visual or coin tap inspection. Possible noise and vibration. 2. Visual inspection. Possible vibration.

TABLE XXXIII. (Continued)

Nomenclature	Function	Possible Failure Modes in Anticipated Environment	Effect of Failure Upon Assembly Function	Probable Symptom and Method of Detection
Trailing Edge Spline (Continued)	Provide edgewise blade stiffness	External: 1. Scratched, dented, crushed, punctured, cut or torn	1. Deterioration or loss of edgewise stiffness characteristics depending upon degree and location.	1. Noise, vibration; detect visually.
Trim Tab	Blade track adjustment	Inherent: 1. Loose rivets 2. Bonding separation	1. Possible loss of blade track. 2. Possible loss of blade track.	1. Noise, vibration; visual detection. 2. Noise, vibration; visual detection.
Counterweights - Spanwise and Chordwise Balance	Balance blade	External: 1. Bent, cracked, punctured	1. Possible loss of blade track.	1. Noise, vibration; visual detection.
Grip Pad and Drag Plate	Transfer blade loads to rotor head	Inherent: 1. Bonding separation 2. Cracks 3. Corrosion	1. Loss of blade balance if weights are separated. 2. Same as 1 above. 3. Possible source of fatigue cracks.	1. Visual inspection. 2. Visual inspection. 3. Visual inspection.
		External: 1. Battle damage	1. Loss of blade balance if weights are separated.	1. Vibration; visual inspection.

REPAIR PROCEDURES

1. LEADING EDGE POLYURETHANE RESTORATION

1. Clean and strip area to be restored using a rag saturated with methyl ethyl ketone.
2. Fill porous laminate substrates with a patching paste or filler.
3. Apply primer coat in accordance with instructions supplied with kit. Allow primer to dry at room temperature for not less than 1 hour. Primer coat may be sanded with 180 or 220 grit paper to promote adhesion and to provide smooth finish.
4. Mix and apply basecoat of polyurethane vehicle in accordance with instructions. Apply coating by brush or spray gun to achieve a dry mil thickness of 2 mils per coat.
5. Apply at 30 minute intervals to obtain a recommended basecoat minimum thickness of 6 mils.
6. Mix and apply final coat in accordance with instructions. The final coat should be applied with brush or spray gun to achieve a dry mil thickness of 2 mils per coat.
7. Apply at 30 minute intervals to obtain a recommended final coat thickness of 14 mils.
8. Allow to cure for minimum of 24 hours at 70 - 75°.

2. LEADING EDGE CARBON REPAIR

Foreign object damage to the leading edge not exceeding 2 inches in spanwise length and not extensive enough to have penetrated to the twin beam and honeycomb core is repairable. The damaged area would be replaced with a 6-inch-long prefabricated prescarfed section.

1. Using the prefabricated section as a template, clean an overlap area on the blade 4 inches larger than the prefabricated section.
2. Cut out the damaged area of the blade to allow the prefabricated section to be fitted into place.
3. Using the scarfing tool provided, scarf the skin adjacent to the cut-out area for mating with the prefabricated replacement.
4. Cut an overlay patch from the skin material 2 inches larger than the scarfed area.
5. Clean the repair area, the prefabricated replacement and the overlay patch by wiping with methyl-ethyl-ketone and applying primer.
6. Prepare adhesive and apply to the repair area and the inside of the prefabricated replacement section.
7. Position replacement section .
8. Apply adhesive to the inside surface of the overlay patch and to the outside of the repair area.
9. Position overlay patch and tape with masking tape.
10. Cover patch area with wax paper or Teflon sheet and position compression blanket over entire area. Inflate compression blanket to 15 PSI and leave in place for 8-hour cure period.
11. Remove compression blanket and finish patch by sanding edges to remove excess material and achieve a feathered edge.

3. LEADING EDGE BLEND REPAIR

A hollow aluminum alloy extrusion forms the leading edge of the blade. Nicks, dents or gouges in this aluminum leading edge or spar would be repairable within certain limits established for various areas of the spar. As an example, damage to the leading edge up to .250-inch deep would be repairable. All repairs would be made in accordance with the following instructions :

1. From the repair limitations figure, determine the maximum depth of damage that may be repaired in that area.
2. If the damage is repairable, use a single cut mill file to remove the damage, limiting the cleaning strokes to a span-wise motion. Do not file or blend in a chordwise direction.
3. Remove all file marks and blend the area, using #150 aluminum oxide abrasive cloth so that the depth of the repair is at least 0.002 inch deeper than the depth of the damage, but no deeper than the limits established for that area.
4. The width of the blend area must be 30 times the depth of the final rework.
5. Apply Alodine 1200 solution, specification MIL-C-5541, to the repaired area. Allow to remain on the surface for 2 to 4 minutes, wash with water and wipe dry.

4. TWIN BEAM REPAIR

The following repair procedure can be accomplished on the unidirectional fiberglass internal beams that have been damaged by a foreign object that penetrated the carbon skin.

The required repair materials, supplied in kit form, would include tapered premolded unidirectional patches, skin materials, a router and a router template.

1. Strip and clean the affected area and enough of the surrounding skin to afford a 4-inch overlap. Allow a 2-inch overlap for patches less than 1 square foot in area. Wipe down with methyl-ethyl-ketone (MEK).
2. Remove the skin from the damaged area to explore enough of the beam to allow routing and patching of the beam, by cutting through the skin with a sharp tool and applying heat to loosen the skin-to-beam and skin-to-core bond. Skin should be removed from a minimum of 4 inches around the damaged area.
3. Using a template and router, remove the damaged beam material to accept a tapered premolded beam patch.
4. Clean the tapered repair area of the beam by wiping with methyl-ethyl-ketone and applying primer.
5. Check the fit of the premolded patch to the repair area. Cut patch to proper width if necessary.
6. Select appropriate skin patch and trim to fit flush into the skin cut-out area.
7. Clean both sides of skin patch by wiping with methyl-ethyl-ketone and prime both sides.
8. Cut overlay patch to size and prepare for installation by wiping with methyl-ethyl-ketone and applying primer.
9. Prepare adhesive and apply first to the beam repair area and the tapered premolded patch. Position patch flush in the beam repair area.
10. Apply adhesive to the repaired beam and the skin patch; position skin patch flush in the cut-out area.

-
11. Apply adhesive to the outside surface of the skin patch, the surrounding overlap area and to the inside of the overlay patch.
 12. Cover the patch with scrim cloth trimmed to the outer edge of the patch.
 13. Position overlay patch over the patched area. Allow equal overlap on all sides.
 14. Cover the entire patch with wax paper or Teflon sheet and position compression blanket over entire area. Inflate compression blanket to 15 PSI and leave in place for 8-hour cure period.
 15. Remove compression blanket and finish patch by sanding edges to remove excess material and achieve a feathered edge.

5. FIBERGLASS SKIN REPAIR - PATCH

The following repair procedures can be accomplished for fiberglass skin damage such as abrasion, delamination, bonding separation, crazing and blisters. The repair procedure is not limited by size of affected area and has been successfully accomplished and flight tested at Sikorsky Aircraft. This procedure, with variation, is also applicable to external damage which penetrates the skin and extends into the honeycomb core. The repair procedure illustrated in Figures 59 through 72 was actually performed on a recent flight test article to repair extensive skin to honeycomb bonding separation which occurred due to damage to the trailing edge resulting from contact with a foreign object. All required repair materials including skin patches up to 1 square foot can be furnished in kit form. Skin material required for patches exceeding 1 square foot in area can be supplied in bulk form.

1. Strip and clean the affected area and enough of the surrounding skin to afford a 4-inch overlap. Allow a 2-inch overlap for patches less than 1 square foot in area. Wipe down with methyl ethyl ketone (M. E. K.).
2. Remove damaged skin by cutting around periphery of affected area with a sharp tool and applying heat to loosen the skin-to-core bond.
3. Select appropriate patch and trim to fit flush into cut-out area.
4. Prime both sides of patch and skin overlap area.
5. Prepare adhesive and apply to small separations between skin and core around periphery of cut-out area.
6. Apply adhesive to patch and position patch flush in cut-out area.
7. Apply adhesive to outside surface of patch and surrounding overlap area.
8. Cut overlay patch to size and prepare for installation by wiping with methyl ethyl ketone and applying primer.
9. Apply adhesive to surface of overlay patch and cover with scrim cloth. Trim scrim cloth to outer edge of patch.
10. Position overlay patch over patched area. Allow equal overlap on all sides.

11. Cover entire patch with wax paper or Teflon sheet and position compression blanket over entire area. Inflate compression blanket to 15 PSI and leave in place for 8-hour cure period.
12. Remove compression blanket and finish patch by sanding edges to remove excess material and achieve a feathered edge.

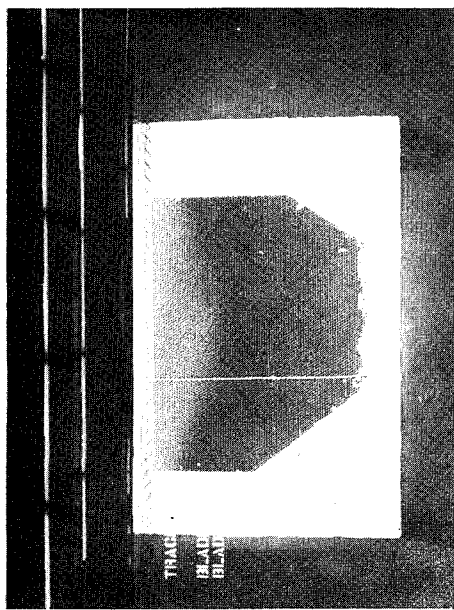


Figure 59. Remove Skin & Prepare Overlap Area.

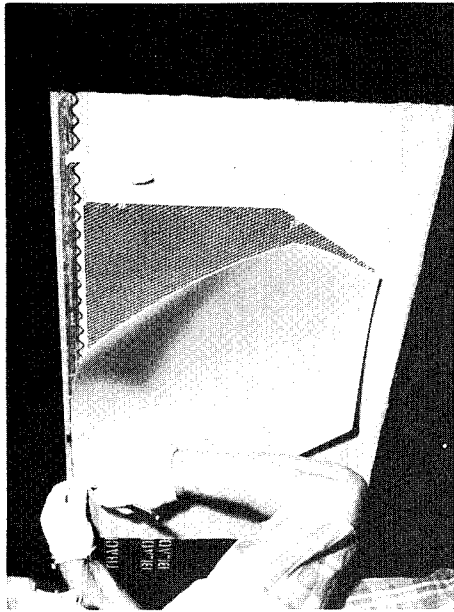


Figure 60. Trim Patch To Fit.

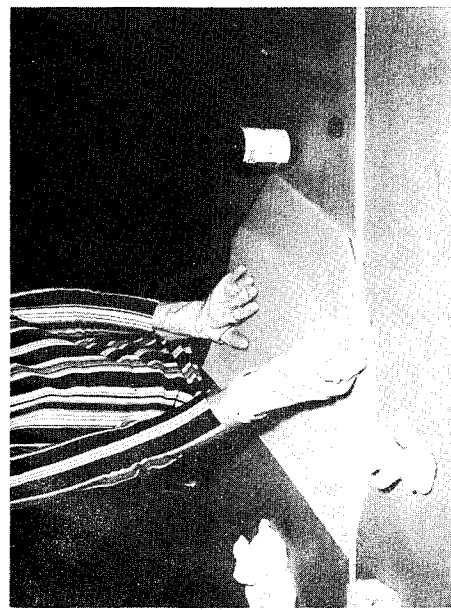


Figure 61. Prime Patch and Skin.

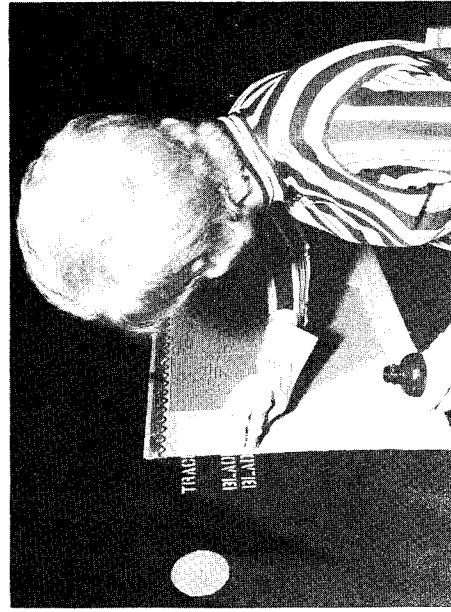


Figure 62. Prime Patch and Skin.

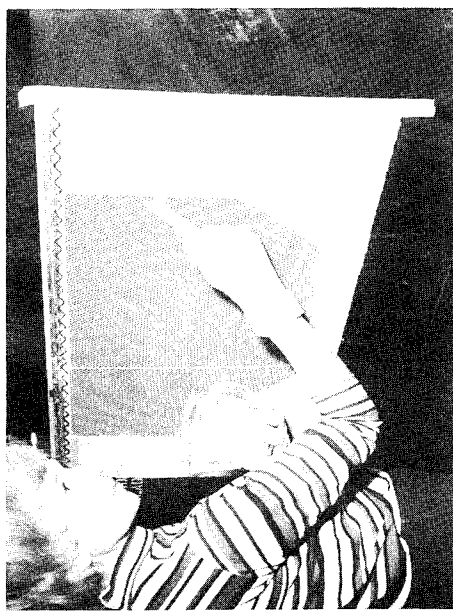


Figure 63. Fill Edge Separations.

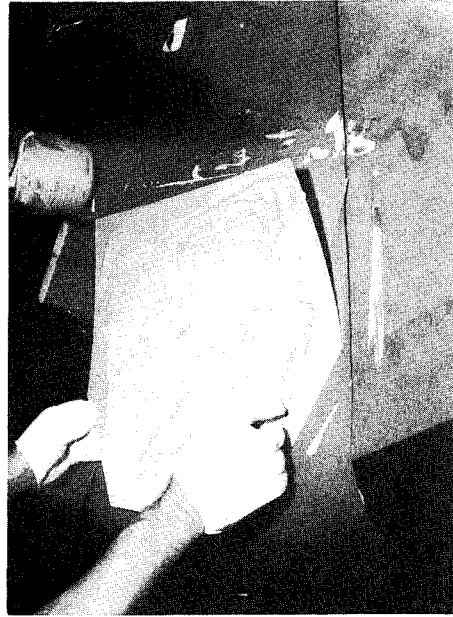


Figure 64. Apply Adhesive & Position Patch.

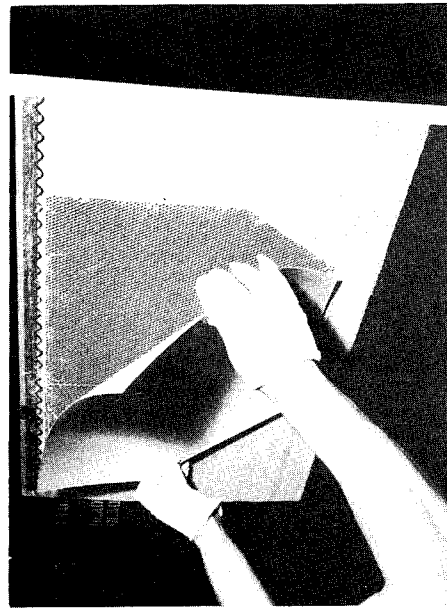


Figure 65. Apply Adhesive & Position Patch.

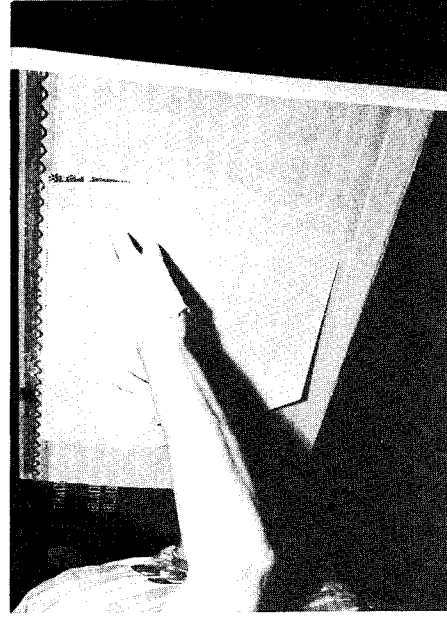


Figure 66. Apply Adhesive & Position Patch.

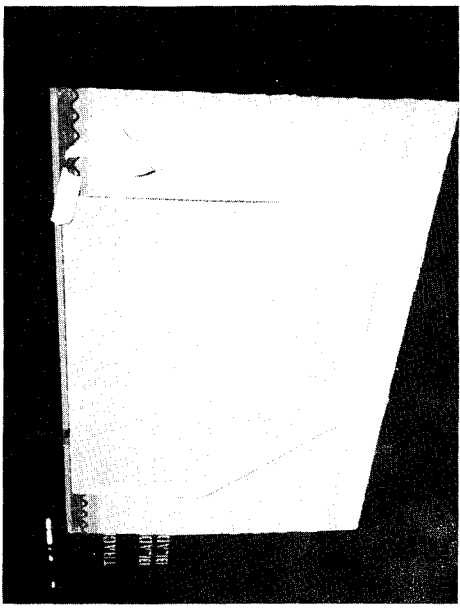


Figure 67. Positioned Patch.



Figure 68. Apply Adhesive.

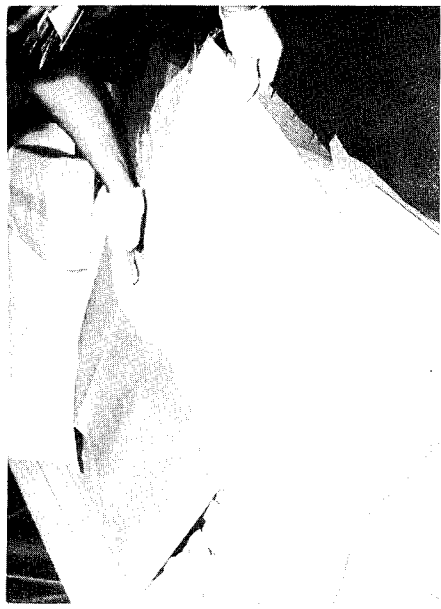


Figure 69. Apply Adhesive to Overlay and Position Scrim Cloth.



Figure 70. Position Overlay.

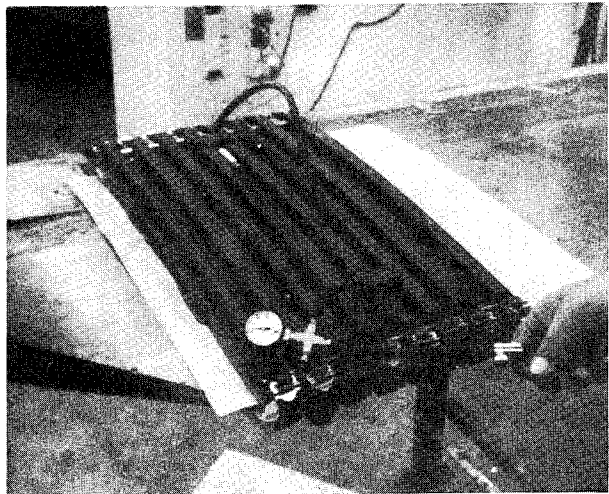


Figure 71. Install and Inflate Compression Blanket.

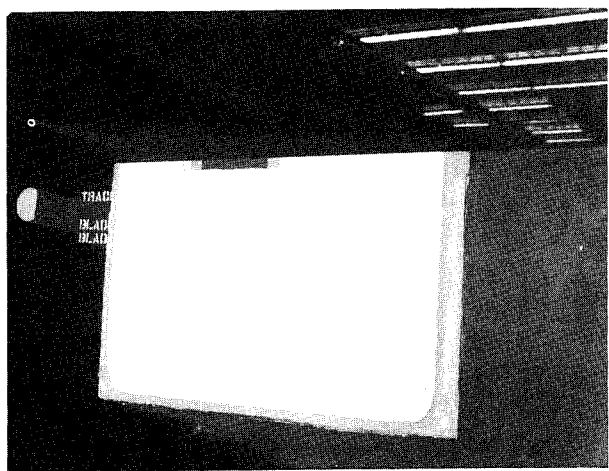


Figure 72. Finished Patch.

6. FIBERGLASS SKIN REPAIR - PLUG

The following repair procedure can be accomplished when a foreign object penetrates the fiberglass skin and honeycomb. Prefabricated skin/core sections of varying sizes would be furnished in kit form to replace damaged sections. Figures 73 through 84 illustrate this type of repair.

1. Strip and clean the affected area and enough of the surrounding skin to afford a 4-inch overlap. Allow a 2-inch overlap for patches less than 1 square foot in area.
2. Remove damaged skin by cutting around periphery of affected area with a sharp tool. Note: Wraparound template shall be used to align top and bottom holes.
3. Force a hacksaw blade through honeycomb and cut hole through blade, working alternately from top and bottom sides of blade.
4. Cut skin/core plug to fit hole.
5. Install skin/core plug and tape in position on top side.
6. Sand excess honeycomb on bottom side.
7. Remove plug, clean plug and hole with methyl-ethyl-ketone.
8. Cut two overlay patches to size and prepare for installation by wiping with methyl-ethyl-ketone and applying primer.
9. Prepare adhesive and apply to plug and hole.
10. Install plug.
11. Apply prepared adhesive to top of plug, overlap area of skin, and to one side of one patch.
12. Position overlay patch over patched area. Allow equal overlap on all sides.
13. Tape patch in position and cover with waxed paper or Teflon sheet.
14. Repeat Steps 11 through 13 for bottom side.
15. Position compression blanket over entire area. Inflate compression blanket to 15 PSI and leave in place for 8-hour cure period. Remove blanket and sand edges of patch to blend into blade contour.



Figure 73. Damaged Blade.

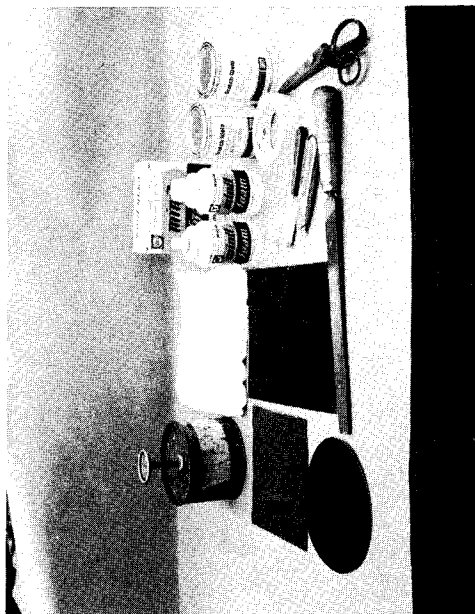


Figure 74. Repair Materials.

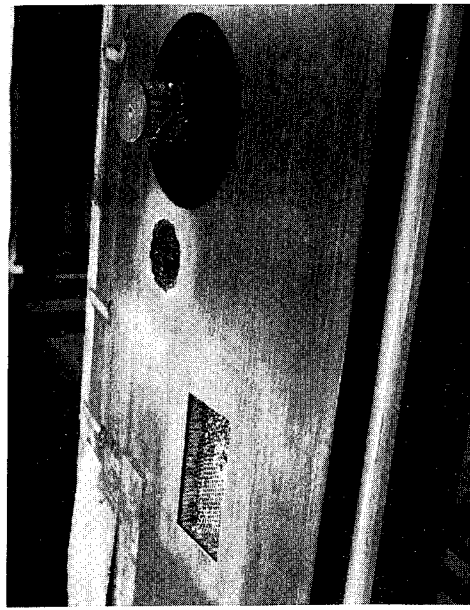


Figure 75. Replacement Ring.



Figure 76. Plug in Place.

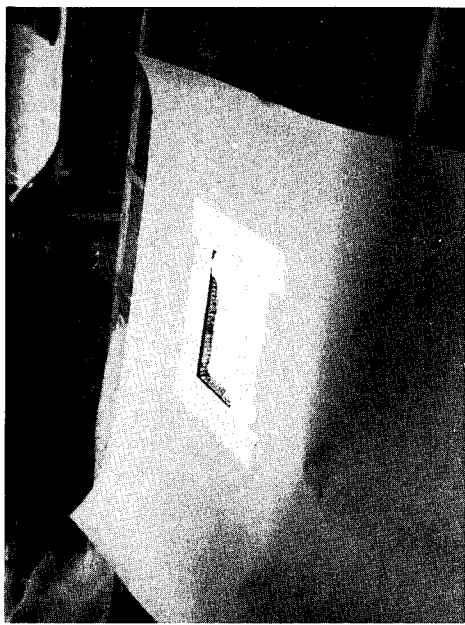


Figure 77. Apply Foam to Cavity.

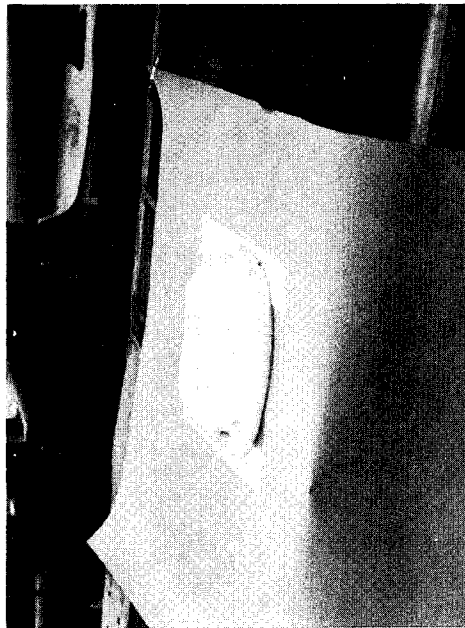


Figure 78. Expanded Foam.

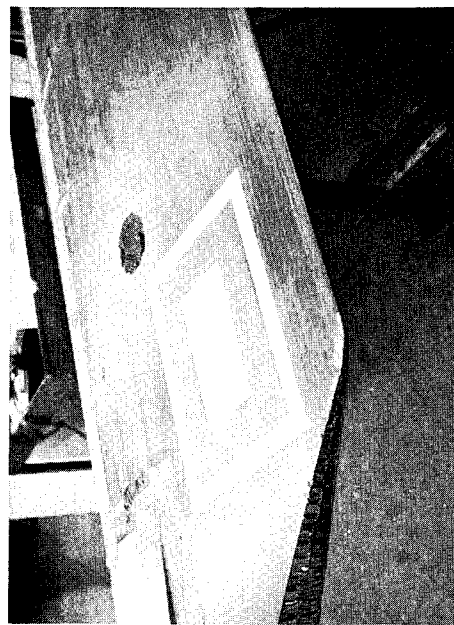


Figure 79. Foam Trimmed & Sanded to Contour.

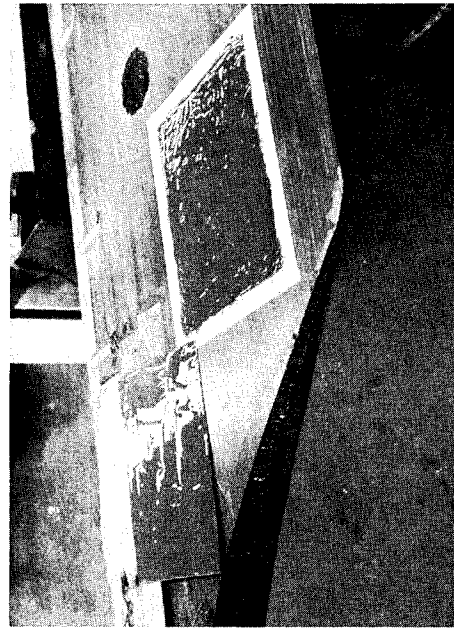


Figure 80. Apply Adhesive to Overlay & Plug.

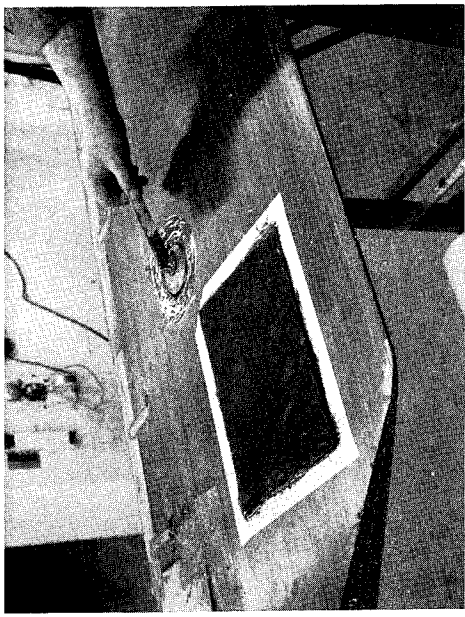


Figure 81. Apply Overlay - Apply Adhesive to Plug.

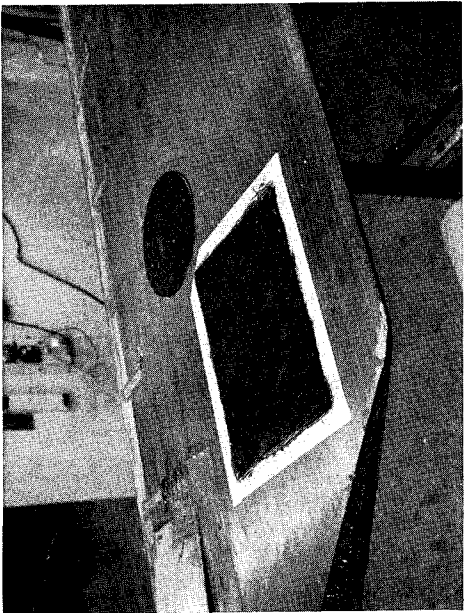


Figure 82. Apply Overlay to Plug.

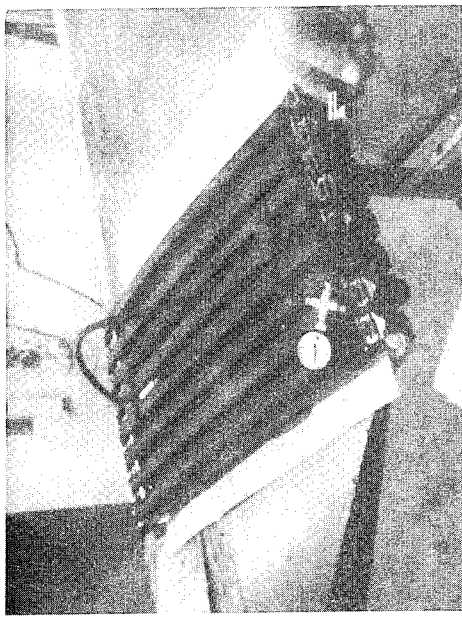


Figure 83. Apply Compression Blanket.



Figure 84. Finished Repair.

7. ATTACHING POINT BUSHING REPLACEMENT

Removal and replacement of worn, scored, corroded, or damaged attaching point bushings can be accomplished in the field since the subject blade will be manufactured with dual steel bushings (the outer steel bushing being adhesively bonded to the blade).

1. Press out damaged internal bushing using tool provided by the manufacturer.
2. Chill the inner steel replacement bushing in a solution of dry ice and methyl-ethyl-ketone (M.E.K.) for 3 minutes or until bubbling stops.
3. Wipe off replacement bushing and install into blade.

8. FIBERGLASS TRAILING EDGE SPLINE REPAIR

Delaminations and foreign object damage to the trailing edge spline are repairable. The damaged section would be replaced with a prefabricated prescarfed section.

1. Strip and clean the affected area and enough of the surrounding area to afford a 2-inch overlap chordwise and 4-inch spanwise.
2. Using the prefabricated prescarfed section as a template, lay out the area to be removed.
3. Using a hacksaw blade, cut out the affected area.
4. Fit the prefabricated section into the repair area.
5. Cut two overlay patches to size allowing the specified overlap.
6. Clean repair area of the trailing edge, prefabricated section and the two overlap patches by wiping with methyl-ethyl-ketone and applying primer.
7. Prepare adhesive and apply to top side of blade overlap area and one side of one overlay patch.
8. Position overlay patch and tape with masking tape.
9. Apply adhesive to the prefabricated section and fit into repair area.
10. Apply adhesive to one side of the second overlay patch and to the bottom side of the blade overlap area.
11. Position second overlay patch and tape with masking tape.
12. Cover patch areas with wax paper or Teflon sheet and position compression blanket over entire area. Inflate compression blanket to 15 PSI and leave in place for 8-hour cure period.
13. Remove compression blanket and finish patch by sanding edges to remove excess material and achieve a feathered edge.

APPENDIX III

COST-EFFECTIVENESS MODEL

The cost-effectiveness model computes the cost effectiveness of the UH-1 aircraft equipped with any candidate rotor blade design. The model has been programmed for the UNIVAC 1108 computer and is described by the following sections:

1. Input definition
2. Mission effectiveness analysis
3. Blade utilization and logistics analysis
4. Blade life-cycle cost analysis
5. Aircraft cost-effectiveness analysis
6. Mission analysis

A step-by-step description and output definition are given for Sections 2 through 5. An asterisk * is used to denote multiplication to avoid the ambiguous alphabetical symbol, x. Model input variables are parenthesized in the equations for further clarity.

1.1 GENERAL INPUT DEFINITIONS

<u>Symbol</u>	<u>Description</u>	<u>Units</u>
A_b	Blade set attrition	sets /FH
B	Installed blades per aircraft	
$BLCC_{UH}$	Baseline UH-1 blade life-cycle cost	\$
CB_{acq}	Single blade acquisition cost	\$
C_{cont}	Blade container cost	\$
C_{fuel}	Fuel and oil cost per pound of fuel consumed	\$/lb
CGR_{dep}	Replenishment GSE cost per repair, depot level	\$
CGR_{ds}	Replenishment GSE cost per repair, direct support level	\$
CGR_{off}	Replenishment GSE cost per off-aircraft repair, organizational level	\$
CGR_{on}	Replenishment GSE cost per on-aircraft repair, organizational level	\$
CGS_{dep}	GSE support cost per aircraft, depot level	\$
CGS_{ds}	GSE support cost per aircraft, direct support level	\$
CGS_o	GSE support cost per aircraft, organizational level	\$
C_m	Average mission capability	ton-knots
CMR_{ds}	Mean material cost per blade repair, direct support level	\$
CMR_{off}	Mean material cost per off-aircraft blade repair, organizational level	\$

<u>Symbol</u>	<u>Description</u>	<u>Units</u>
CMR _{on}	Mean material cost per on-aircraft blade repair, organizational level	\$
CO _{dep}	Blade overhaul cost, depot level	\$
CPOL _{UH}	Baseline UH-1 life-cycle fuel and oil cost	\$
CSH _{cont}	Empty blade container shipping cost from field to CONUS	\$
CSH _{fld}	Packaged blade shipping cost from CONUS to field	\$
CSHP _{dep}	Blade shipping preparation cost, depot level	\$
CSHP _{ds}	Blade shipping preparation cost, direct support level	\$
CSHP _o	Blade shipping preparation cost, organizational level	\$
CSH _{US}	Packaged blade shipping cost from field to CONUS	\$
DT	Aircraft down hours per flight hour	DH/FH
E _{mUH}	Baseline UH-1 mission effectiveness	ton-knots
FF	Average mission fuel flow	lb/FH
K _{inv}	Ratio of blade inventory spares to blade life-cycle replenishment spares	
L _a	Aircraft service life	FH
L _b	Blade scheduled retirement life	FH
LCC _{UH}	Baseline UH-1 life- cycle cost	\$
M _{inst}	Mean maintenance man-hours per blade installation	MMH

<u>Symbol</u>	<u>Description</u>	<u>Units</u>
MI_{dep}	Mean maintenance man-hours per blade receiving and inspection, depot level	MMH
MI_{ds}	Mean maintenance man-hours per blade inspection, direct support level	MMH
MI_{off}	Mean maintenance man-hours per off-aircraft blade inspection, organizational level	MMH
MI_{on}	Mean maintenance man-hours per on-aircraft damaged blade inspection, organizational level	MMH
M_{rem}	Mean maintenance man-hours per blade removal	MMH
M_{req}	Mean maintenance man-hours to requisition and obtain a replacement blade, organizational level	MMH
MR_{ds}	Mean maintenance man-hours per blade repair, direct support level	MMH
MR_{off}	Mean maintenance man-hours per off-aircraft blade repair, organizational level	MMH
MR_{on}	Mean maintenance man-hours per on-aircraft blade repair, organizational level	MMH
MS_{dep}	Mean maintenance man-hours per blade scrappage, depot level	MMH
MS_{ds}	Mean maintenance man-hours per blade scrappage, direct support level	MMH
MS_o	Mean maintenance man-hours per blade scrappage, organizational level	MMH
MTB_e	Blade mean time between external damage	FH

<u>Symbol</u>	<u>Description</u>	<u>Units</u>
MTB _i	Blade mean time between inherent damage	FH
PB _{ds}	Percent of damaged and removed blades sent to direct support	%
PBR _{dep}	Percent of received blades repaired at depot level	%
PBR _{ds}	Percent of received blades repaired at direct support level	%
PBR _{off}	Percent of damaged and removed blades repaired at organizational level	%
PBR _{on}	Percent of damaged blades repaired on aircraft	%
PBS _{ds}	Percent of received blades scrapped at direct support level	%
PBS _o	Percent of damaged and removed blades scrapped at organizational level	%
R _{civ}	Civilian maintenance personnel labor rate	\$ /hr
R _{mil}	Military maintenance personnel labor rate	\$ /hr
R _s	Aircraft mission abort failures per flight hour	maf/FH
T _m	Average mission flight time	FH
U _a	Aircraft annual utilization	FH

1.2 NONVARIABLE INPUTS

The following inputs described in Section 1.1 are assumed not to vary with rotor blade design:

<u>Customer Specified Input</u>	<u>Value</u>	<u>Contractor Specified Input</u>	<u>Value</u>
A _b	.0003	BLCC _{UH}	48455
B	2.	C _{fuel}	.02
C _{cont}	200.	CPOL _{UH}	53344
CSH _{cont}	45.	E _{mUH}	37.466
CSH _{fld}	130.	K _{inv}	.05263
CSHP _{dep}	70.	LCC _{UH}	1,585,000.
CSHP _{ds}	70.	MS _{ds}	.5
CSHP _o	70.	MS _o	.5
CSH _{US}	90.	U _a	500.
L _a	5000.		
M _{inst}	3.75		
MI _{dep}	2.5		
M _{rem}	3.75		
M _{req}	6.		
MS _{dep}	.5		
R _{civ}	12.00		
R _{mil}	4.00		

2.0 AIRCRAFT MISSION EFFECTIVENESS

The mission effectiveness of a single aircraft is the product of its mission availability, mission reliability, and mission capability.

2.1 Average daily utilization - FH/day

$$U_d = \frac{(U_a)}{365} \quad (28)$$

2.2 Average daily downtime - hr/day

$$T_d = (DT) * U_d \quad (29)$$

2.3 Mission availability

$$A_m = \frac{24 - T_d}{24} \quad (30)$$

2.4 Mission reliability

$$R_m = e^{-(R_s) * (T_m)} \quad (31)$$

2.5 Mission effectiveness

$$E_m = A_m * R_m * (C_m) \quad (32)$$

3.0 BLADE UTILIZATION AND LOGISTICS

The computation of blade life-cycle cost must reflect the maintenance, replenishment, inventory, and shipping burdens imposed by the rotor blade design. This analysis establishes the blade requirements of a single aircraft throughout its life cycle.

- 3.1 Blades inherently damaged. Based on aircraft retirement life and specified blade mean time between inherent damage.

$$BD_i = \frac{(B) * (L_a)}{(MTB_i)} \quad (33)$$

- 3.2 Blades externally damaged. Based on aircraft retirement life and blade mean time between external damage.

$$BD_e = \frac{(B) * (L_a)}{(MTB_e)} \quad (34)$$

- 3.3 Total blades damaged.

$$BD = BD_i + BD_e \quad (35)$$

- 3.4 Damaged blades repaired on aircraft. Based on a specified percentage.

$$BR_{on} = \frac{(PBR_{on}) * BD}{100} \quad (36)$$

- 3.5 Damaged blades removed from aircraft. All damaged blades not repaired on aircraft.

$$BD_{rem} = BD - BR_{on} \quad (37)$$

- 3.6 Removed blades repaired off aircraft, organizational level. Based on a specified percentage.

$$BR_{off} = \frac{(PBR_{off}) * BD_{rem}}{100} \quad (38)$$

- 3.7 Removed blades scrapped, organizational level. Based on a specified percentage.

$$BS_O = \frac{(PBS_O) * BD_{rem}}{100} \quad (39)$$

- 3.8 Removed blades sent to direct support. Based on a specified percentage.

$$B_{ds} = \frac{(PB_{ds}) * BD_{rem}}{100} \quad (40)$$

- 3.9 Damaged blades sent to depot from organizational level. Removed blades not scrapped, repaired at organizational level, or sent to direct support.

$$BO_{dep} = BD_{rem} - BR_{off} - BS_O - B_{ds} \quad (41)$$

- 3.10 Damaged blades repaired, direct support. Based on a specified percentage of blades received.

$$BR_{ds} = \frac{(PBR_{ds}) * B_{ds}}{100} \quad (42)$$

- 3.11 Damaged blades scrapped, direct support. Based on a specified percentage of blades received.

$$BS_{ds} = \frac{(PBS_{ds}) * B_{ds}}{100} \quad (43)$$

- 3.12 Damaged blades sent to depot from direct support. Blades received at direct support not scrapped or repaired.

$$BDS_{dep} = B_{ds} - BR_{ds} - BS_{ds} \quad (44)$$

- 3.13 Total damaged blades sent to depot.

$$B_{dep} = BO_{dep} + BDS_{dep} \quad (45)$$

- 3.14 Damaged blades repaired, depot. Based on a specified percentage of blades received.

$$BR_{dep} = \frac{(PBR_{dep}) * B_{dep}}{100} \quad (46)$$

- 3.15 Damaged blades scrapped, depot. Received blades not repaired.

$$BS_{dep} = B_{dep} - BR_{dep} \quad (47)$$

- 3.16 Total damaged blades scrapped, all levels.

$$BS = BS_O + BS_{ds} + BS_{dep} \quad (48)$$

- 3.17 Blades lost to attrition. Based on blade set attrition rate and aircraft retirement life.

$$B_{att} = (B) * (A_b) * (L_a) \quad (49)$$

3.18 Blades lost to scrappage and attrition.

$$B_{sa} = BS + B_{att} \quad (50)$$

3.19 Aircraft mean time between loss of blades to attrition - flight hours.

$$MTB_a = \frac{1}{(A_b)} \quad (51)$$

3.20 Aircraft mean time between inherent or external blade damage - flight hours.

$$MTB_d = \frac{1}{\frac{1}{(MTB_l)} + \frac{1}{(MTB_e)}} \quad (52)$$

3.21 Aircraft mean time between blade scrappage - flight hours.

$$MTB_s = \frac{MTB_d * BD}{BS} \quad (53)$$

3.22 Aircraft mean time between scrappage and attrition - flight hours.

$$MTB_{sa} = \frac{1}{\frac{1}{MTB_s} + \frac{1}{MTB_a}} \quad (54)$$

3.23 Aircraft mean time between scrappage, attrition, or blade retirement - flight hours. The time between scrappage or attrition may vary considerably from the mean, allowing some blades to reach their retirement lives. If blade retirement life exceeds aircraft retirement life, no blades are retired. If not, the following probability integral formula is used to estimate mean time including retirement:

$$MTB_{sar} = MTB_{sa} * (1 - e^{-\frac{(L_b)}{MTB_{sa}}}) \quad (55)$$

3.24 Blade replenishment spares. The sum of blades scrapped, retired, and lost to attrition.

$$B_{repl} = \frac{(B) * (L_a)}{MTB_{sar}} \quad (56)$$

3.25 Blades retired from service.

$$B_{ret} = B_{repl} - B_{sa} \quad (57)$$

- 3.26 Blades removed or installed. The sum of blades removed due to damage and blades retired.

$$B_{ri} = BD_{rem} + B_{ret} \quad (58)$$

- 3.27 Blades requisitioned from inventory. All removed blades not repaired at the organizational level.

$$B_{req} = B_{ri} - BR_{off} \quad (59)$$

- 3.28 Initial blade spares. Inventory blades either on hand or in the supply pipeline. Assumed to be proportional to life-cycle replenishment spares requirement.

$$B_{inv} = K_{inv} * B_{repl} \quad (60)$$

4.0 BLADE LIFE-CYCLE COST

This analysis computes blade contributions to the life-cycle cost of a single aircraft.

- 4.1 Blade contribution to aircraft flyaway cost. Based on the acquisition cost of installed blades.

$$C_{fly} = (B) * (CB_{acq}) \quad (61)$$

- 4.2 Blade contribution to initial spares cost. The cost of blades and containers in the spares inventory and shipping from CONUS to field.

$$C_{isp} = [(CB_{acq}) + (C_{cont}) + (CSH_{fld})] * B_{inv} \quad (62)$$

- 4.3 Blade contribution to replenishment spares cost. The cost of replenishment blades and shipping in recycled containers.

$$C_{rsp} = [(CB_{acq}) + (CSH_{fld}) + (CSH_{cont})] * B_{repl} \quad (63)$$

- 4.4 Cost of on-aircraft inspection for blade repairability, organizational level. Based on a specified mean MMH per damaged blade.

$$CI_{on} = (R_{mil}) * (MI_{on}) * BD \quad (64)$$

- 4.5 Cost of on-aircraft blade repairs, organizational level. Based on a specified mean MMH and material cost per blade repair.

$$CR_{on} = [(R_{mil}) * (MR_{on}) + (CMR_{on})] * BR_{on} \quad (65)$$

- 4.6 Cost of blade removal, organizational level. Based on mean MMH per blade removal.

$$C_{rem} = (R_{mil}) * (M_{rem}) * B_{ri} \quad (66)$$

- 4.7 Cost of off-aircraft inspection for blade disposition, organizational level. Based on mean MMH per damaged blade removed.

$$CI_{off} = (R_{mil}) * (MI_{off}) * BD_{rem} \quad (67)$$

- 4.8 Cost of off-aircraft repairs, organizational level. Based on a specified mean MMH and material cost per blade repair.

$$CR_{off} = [(R_{mil}) * (MR_{off}) + (CMR_{off})] * BR_{off} \quad (68)$$

- 4.9 Cost to requisition and obtain replacement blades, organizational level. Based on mean MMH per replacement blade.

$$C_{req} = (R_{mil}) * (M_{req}) * B_{req} \quad (69)$$

- 4.10 Cost of blade installation, organizational level. Based on mean MMH per blade installation.

$$C_{inst} = (R_{mil}) * (M_{inst}) * B_{ri} \quad (70)$$

- 4.11 Cost to dispose of scrap, organizational level. Based on mean MMH per blade scrappage.

$$CS_O = (R_{mil}) * (MS_O) * BS_O \quad (71)$$

- 4.12 Cost of shipping preparation, organizational level. Based on mean MMH per shipped blade.

$$CP_O = (CSHP_O) * BO_{dep} \quad (72)$$

- 4.13 Blade contribution to maintenance cost, organizational level.

$$\begin{aligned} CM_O = & CI_{on} + CR_{on} + C_{rem} + CI_{off} \\ & + CR_{off} + C_{req} + C_{inst} + CS_O + CP_O \end{aligned} \quad (73)$$

- 4.14 Cost of blade inspection, direct support level. Based on mean MMH per blade received.

$$CI_{ds} = (R_{mil}) * (MI_{ds}) * B_{ds} \quad (74)$$

- 4.15 Cost of blade repairs, direct support level. Based on a specified mean MMH and material cost per blade repair.

$$CR_{ds} = \left[(R_{mil}) * (MR_{ds}) + (CMR_{ds}) \right] * BR_{ds} \quad (75)$$

- 4.16 Cost to dispose of scrap, direct support level. Based on mean MMH per blade scrappage.

$$CS_{ds} = (R_{mil}) * (MS_{ds}) * BS_{ds} \quad (76)$$

- 4.17 Cost of shipping preparation, direct support level. Based on mean MMH per shipped blade.

$$CP_{ds} = (CSHP_{ds}) * BDS_{dep} \quad (77)$$

4.18 Blade contribution to maintenance cost, direct support level.

$$CM_{ds} = CI_{ds} + CR_{ds} + CS_{ds} + CP_{ds} \quad (78)$$

4.19 Cost of shipping blades to depot. Based on cost per shipped blade.

$$CSH_{dep} = (CSH_{US}) * B_{dep} \quad (79)$$

4.20 Cost of blade receiving and inspection, depot level. Based on MMH per blade received.

$$CI_{dep} = (R_{civ}) * (MI_{dep}) * B_{dep} \quad (80)$$

4.21 Cost of blade overhauls, depot level. Based on a specified mean cost per blade overhaul.

$$CR_{dep} = (CO_{dep}) * BR_{dep} \quad (81)$$

4.22 Cost to dispose of scrap, depot level. Based on mean MMH per blade scrappage.

$$CS_{dep} = (R_{civ}) * (MS_{dep}) * BS_{dep} \quad (82)$$

4.23 Cost of shipping preparation, depot level. Based on mean preparation cost per shipped blade.

$$CP_{dep} = (CSHP_{dep}) * BR_{dep} \quad (83)$$

4.24 Cost of shipping overhauled blades to field from depot. Based on mean cost per shipped blade.

$$CSHF_{dep} = (CSH_{fld}) * BR_{dep} \quad (84)$$

4.25 Blade contribution to maintenance cost, depot level.

$$\begin{aligned} CM_{dep} = & CSH_{dep} + CI_{dep} + CR_{dep} \\ & + CS_{dep} + CP_{dep} + CSHF_{dep} \end{aligned} \quad (85)$$

4.26 Total blade contribution to maintenance cost, all levels.

$$CM = CM_O + CM_{ds} + CM_{dep} \quad (86)$$

4.27 Replenishment GSE cost, organizational level. Based on specified mean GSE cost per repair and mean GSE support cost per aircraft.

$$CG_O = (CGR_{on}) * BR_{on} + (CGR_{off}) * BR_{off} + (CGS_O) \quad (87)$$

4.28 Replenishment GSE cost, direct support level. Based on specified mean GSE cost per repair and mean GSE support cost per aircraft

$$CG_{ds} = (CGR_{ds}) * BR_{ds} + (CGS_{ds}) \quad (88)$$

4.29 Replenishment GSE cost, depot level. Based on specified mean GSE cost per repair and mean GSE support cost per aircraft.

$$CG_{dep} = (CGR_{dep}) * BR_{dep} + (CGS_{dep}) \quad (89)$$

4.30 Total blade contribution to replenishment GSE cost, all levels.

$$CG = CG_o + CG_{ds} + CG_{dep} \quad (90)$$

4.31 Blade life-cycle cost. Blade contribution to aircraft life-cycle cost.

$$BLCC = C_{fly} + C_{isp} + C_{rsp} + CM + CG \quad (91)$$

5.0 AIRCRAFT COST EFFECTIVENESS

- 5.1 Aircraft fuel and oil cost. Based on average mission fuel flow and cost per pound of fuel.

$$CPOL = (C_{fuel}) * (FF) * (L_a) \quad (92)$$

- 5.2 UH-1 nonvariable life-cycle cost. UH-1 life-cycle cost less UH-1 POL and blade life-cycle costs.

$$LCC_{nv} = (LCC_{UH}) - (CPOL_{UH}) - (BLCC_{UH}) \quad (93)$$

- 5.3 Aircraft life-cycle cost. Based on UH-1 nonvariable life-cycle cost plus the candidate system POL and blade life-cycle costs.

$$LCC = LCC_{nv} + CPOL + BLCC \quad (94)$$

- 5.4 Aircraft cost effectiveness - ton-knots/\$. The ratio of mission effectiveness to life-cycle cost.

$$E_{ce} = \frac{E_m}{LCC} \quad (95)$$

- 5.5 Baseline UH-1 fleet effectiveness. The mission effectiveness of a fleet of 1000 UH-1 aircraft.

$$FE_{UH} = 1000 * (E_{mUH}) \quad (96)$$

- 5.6 Fleet effective cost. The life-cycle cost of a fleet of candidate aircraft where fleet size is adjusted to maintain the baseline fleet effectiveness of 1000 UH-1 aircraft.

$$FEC = \frac{FE_{UH}}{E_{ce}} \quad (97)$$

6.0 MISSION ANALYSIS

Improvements in blade producibility and repairability to reduce life-cycle cost may penalize weight or aerodynamic efficiency. These penalties are acceptable if overall cost effectiveness improves.

The impact of a blade design change on mission effectiveness depends on the requirements of the particular mission. For example, additional blade weight is a significant penalty only when gross weight is a mission constraint. Similarly, a penalty in rotor figure of merit will not be serious for a mission which is never power limited.

The utility role of the UH-1 demands that it operate throughout a wide range of conditions. This usage cannot be accurately represented by a single arbitrary design mission. To handle this situation, a Sikorsky simulation program was used to operate the UH-1 in a probabilistic mission environment to establish average overall productivity. One thousand individual mission sorties were simulated for each candidate blade configuration.

The mission environment used in the simulation was defined by probability distributions of the following parameters:

1. Takeoff pressure altitude
2. Ambient sea level air temperature (standard altitude lapse rate was assumed)
3. Required payload
4. Sortie radius
5. Percent of outbound payload carried inbound
6. Cover time per sortie
7. Takeoff hover power margin (fraction of HOGE power actually required)
8. Cruise elevation above takeoff

Probability distributions are shown in Figure 85. Altitude and temperature variations are taken from Reference 15. Sortie radius is distributed about a mean of 25 nautical miles. Takeoff power margin is based on zero-wind vertical takeoff being required 20% of the time. At the other extreme, favorable terrain or wind conditions are assumed to allow operation at higher weights than provided by adherence to the UH-1 cockpit placard criterion. This criterion, discussed in Reference 15, calls for a 3% N1 margin at 2-foot skid height, and corresponds to about 90% of HOGE power. Required payload is a demand function independent of capability. It averages 2150 pounds and exceeds the internal loading limit of 2420 pounds for 10% of the time. Cruise elevation averages 1500 feet above takeoff as defined in Reference 16.

Other inputs to the mission analysis include UH-1H rotor parameters, engine performance, parasite drag, basic operating weight, and constraints imposed by drive system rating, structural design gross weight, fuel capacity, and component life allowable speed envelope. Based on Reference 17, UH-1H parameters are:

Rotor Diameter: 48 ft

Total Blade Area: 84 ft²

Basic Operating Weight: 5387 lb

Engine: T53-L-13 rated at 1400 Military hp at SLS, with altitude/temperature and SFC performance per Lycoming Spec.
104.33

Drive System: 1100 hp flat rated

Red Line Speed: 130 kt indicated

Maximum Gross Weight: 9500 lb

Component Life Allowable Speed Envelope: References 17 and 18

Simulation of the UH-1H with existing blades in the established mission environment yielded the following results:

Average Takeoff Gross Weight: 7986 lb

Average Outbound Payload: 2051 lb

Average Cruise Speed: 120 knots true

Average Fuel Flow: 533 lb/flight/hr

Average Sortie Flight Time: 0.52 hr

Average Productivity: 50.3 ton-knots (outbound payload times
sortie radius over sortie time)

Percent of time takeoff limited by gross weight capability: 3.5%

Percent of time takeoff limited by available power: 1.6%

Percent of time cruise limited by available power: 0.1%

Percent of time cruise limited by component life speed
envelope: 99.9%

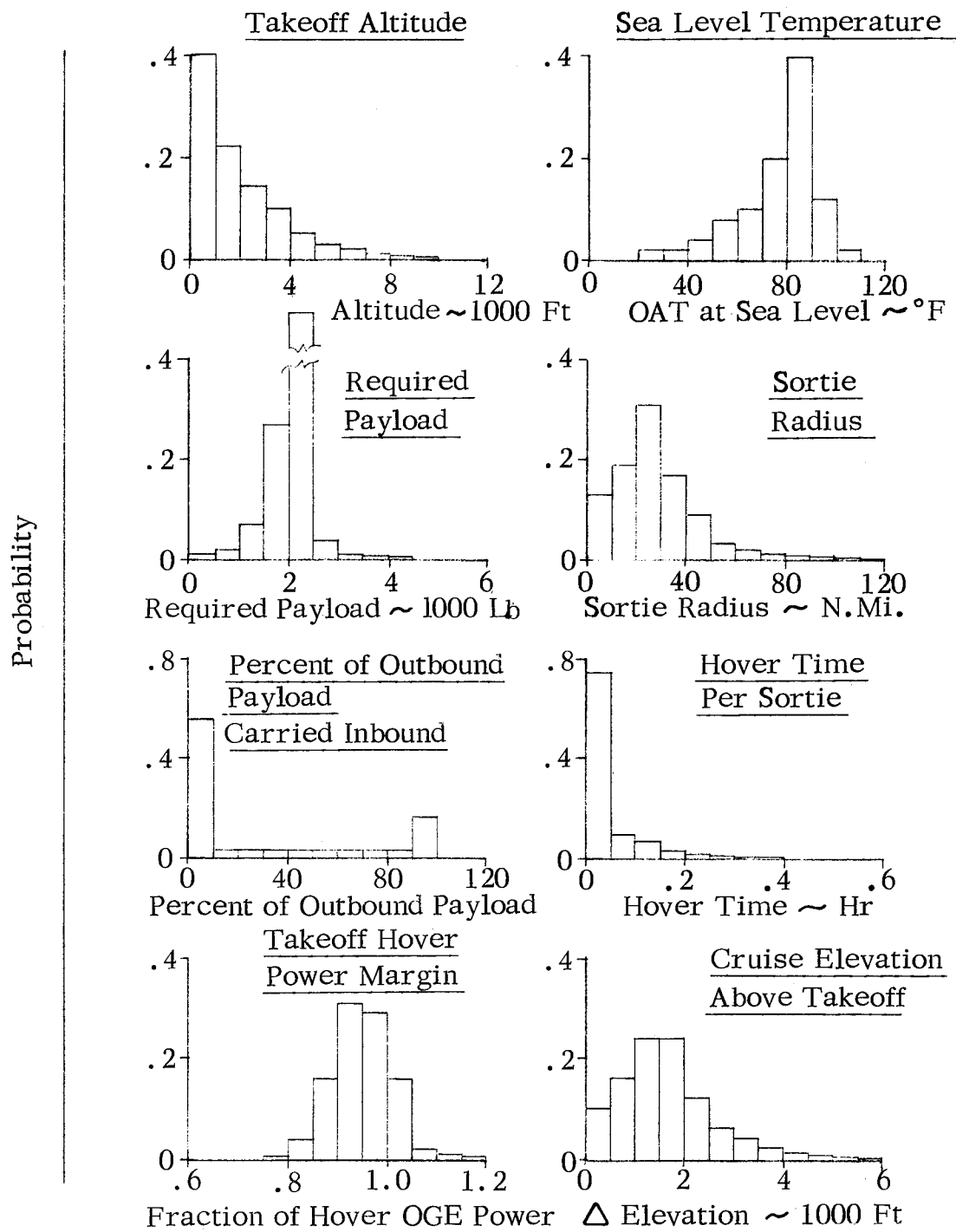


Figure 85. UH-1H Mission Environment.

APPENDIX IV
UH-1H BLADE DATA

TABLE XXXIV. UH-1 ROTOR BLADE DESIGN COST COMPARISONS

The following cost model values were supplied by the Government to standardize the various rotor blade comparisons. The current UH-1 rotor blade values are listed, together with values of the candidate blade that were considered relatively insensitive to variations in design. Where values of the candidate blade were not supplied, they were developed by the Contractor for use after approval by the Government Contracting Officer.

	<u>Current UH-1</u>	<u>Candidate</u>
Blade Life Hours	2500	-
Aircraft Life Hours	5000	Same
Aircraft Fleet Size	500-1000-2000	Same
Aircraft Attrition	Zero	Same
Blade Set Attrition	.0003/Flight Hr	Same
Time of Blade Initiation	Original Production	Same
Cost of One Blade	\$3000	-
Experience Curve Position	10,000 Blades	Same
Blade Spares Inventory	30% of Installed	-
% Inherent Damage	29.2%	-
% External Damage	70.8%	-
Blade Time Between Inherent Damage	547 Hours	-
Blade Time Between External Damage	400 Hours	Same
Repair Performance Degradation	Zero	Same
Cost Field, Org Mil Labor/Hr	4.00	Same
% Military Labor, Field	100%	Same
Field Overhead and Support Cost	Zero	Same
MMH Each Blade Removal	3.75	Same
MMH Disposition, Inspect	1.5	Same
MMH Repair, Field	-	-
Parts Material Cost/Repair (Fld)	\$5.00	-
GSE, Tooling Cost/Repair (Fld)	Zero	-
MMH Obtain Replacement Blade	3.0	Same
MMH Ops, Inventory, Requisition	3.0	Same
MMH Blade Installation	3.75	Same
% Field Repairs Require Removal	100%	-
% Removed Blades Scrapped, Org	30%	-
% Removed Blades Repaired, Org	12%	-
% Removed Blades to Depot Repair	58%	-
% Depot Received Blades Scrapped	68%	-
% Depot Received Blades Overhauled	32%	-
Shipping, 8000 Mi, Surface, Blade	\$90	Same

TABLE XXXIV. Continued

	Current UH-1	Candidate
Shipping, 8000 Mi, Surface, M-T Container	\$45	Same
Rotor Blade Container, Reuseable	\$200	Same
Preparation for Shipping, Field	\$70	Same
% Surface Shipping to CONUS	100%	Same
% Mil Air Shipping from CONUS	100%	Same
8000 Mi Mil Air Shipping	\$130	Same
% Civilian Labor, Depot	100%	Same
Composite Civilian Labor Cost, Hr	\$12	Same
Blade Overhaul Cost, Depot	\$925	-
Depot Overhaul and Support Cost	Zero	Same
MMH Receive, Unpack Depot	1.0	Same
MMH Inspect (100% of Rec'd), Depot	1.5	Same
MMH to Dispose of Scrap, Depot	.5	Same
Preparation for Shipping, Depot	\$70	Same
Shipping Containers Required	30% of Installed	-

NOTES:

- (a) Develop R&D, prototype and production candidate blade costs, determine learning curve equation, assume previous production of 10,000 units and establish cost at 10,000 unit for use in cost model and comparison with current UH-1 blade.
- (b) Conduct three separate cost runs for each fleet size, 500-1000 - 2000.
- (c) Aircraft utilization is 500 hours/year for 10 years, 5000 hour life.
- (d) Zero aircraft attrition permits the fleet size to remain constant throughout the analyses; replacing the blade sets at a rate of .0003/flight hour accounts for the new set of blades required as a result of attrition.
- (e) External damage is further characterized by the following rates:

Battle Damage	16.0%
Dent	25.4%
Foreign Object Damage	16.0%
Puncture	18.8%
Tear	8.0%
Overstress	15.8%

APPENDIX V COST EFFECTIVE COMPARISON USING MTBR OF 1063 HOURS

SUMMARY

Appendix V has been included to provide the R/M tabulations and the cost effective studies for Configuration V utilizing 1063 hours MTBR instead of 914 hours MTBR for the UH-1. With the higher MTBR, Configuration V saves $\$24.90 \times 10^6$ in fleet effective cost compared to the 1980 baseline blade. This represents only 5% less than the $\$26.22 \times 10^6$ saved with the original MTBR (page 249). This appendix also includes the rationale for use of ton-knots instead of ton-miles.

EQUIVALENCE OF MISSION TON-KNOTS AND LIFETIME TON-MILES

Mission ton-knots and lifetime ton-miles are equivalent measures of effectiveness. We have used mission ton-knots because its smaller magnitude is more convenient.

UH-1 effectiveness can be measured by total work performed. This work is expressed in ton-miles. However, work per mission is not an accurate measure since the number of lifetime missions varies with average mission time. The faster the average mission, the more lifetime work is delivered in a given useful life. For this reason, ton-miles per mission cannot be used.

Although mission ton-miles is not a valid measure of effectiveness, mission ton-miles per hour, or ton-knots, is, since it is equivalent to lifetime ton-miles. This equivalence can be illustrated with a simple example. Consider two helicopters, each capable of carrying 1000 pounds of payload for 20 miles under average mission conditions. One cruises at 100 knots, the other at 150 knots. Both deliver 10 ton-miles of work per mission, and on this basis have equal mission effectiveness. The faster helicopter, however, can fly more missions in a given 5000-hour service life. Ignoring mission turnaround time, the 100-knot helicopter delivers a lifetime work of 250,000 ton-miles ($1/2$ ton \times 20 miles \times 5000 hr life/.20 hr mission time). The 150-knot helicopter delivers 50% more work, or 375,000 ton-miles. This same 50% superiority for the faster helicopter is identified by comparing relative mission ton-knots, 75 versus 50. The smaller magnitude of the ton-knot values makes them a more convenient way to express overall effectiveness.

RELIABILITY ANALYSIS

Reliability analysis was performed to compare the baseline UH-1 Blade with Configuration V (timeframe 1980) using 1063 hours instead of 914 hours MTBR.

BASELINE MATH MODEL INPUT VARIABLES

Math model input variables for the baseline UH-1 blade were held constant with the exception of the MTBR used in the basic study. The MTBR value was changed from 914 hours to 1063 hours. The new MTBR of 1063 hours was apportioned to the external and inherent failure rates as follows:

Inherent	. 000230 = 4, 347 hours
External	. 000710 = 1, 408 hours
Total	. 000940 = 1, 063 hours

These new values were run in the math model to establish a new UH-1 baseline cost effectiveness value.

CONFIGURATION V MATH MODEL INPUT VARIABLES

New math model input variables were developed for Configuration V candidate blade using the reliability apportionment of Table XXXXV, the reliability analysis of Table XXXVI and the repairability analysis of Table XXXXVII, based upon the new 1063 hr MTBR for the baseline blade. The new math model R/M inputs are tabulated in Table XXXXVIII. These values were then run through the math model to establish the comparative cost effectiveness of Configuration V with the UH-1.

TABLE XXXV. RELIABILITY APPORTIONMENT-BASELINE UH-1
WITH 1063 HOUR MTBR

I. Inherent Damage		
Blade Component	Failure Mode	Frequency of Occurrence per 10 ⁶ Blade Hours
1. Spar	A. Bonding separates from core B. Elongation of bushing holes C. Cracks D. Abrasion strip separation E. Corrosion F. Pitted, abraded or eroded abrasion strip	3.0 9.0 11.0 16.0 10.0 <u>10.0</u> 59.0
2. Core (Aluminum)	A. Bonding voids B. Water contamination	18.0 <u>9.0</u> 27.0
3. Skin (Aluminum)	A. Unbonded at leading or trailing edge B. Corrosion C. Cracks	8.0 2.0 <u>27.0</u> 37.0
4. Retention Bushings	A. Cracks B. Wear C. Corrosion	9.0 8.0 <u>2.0</u> 19.0
5. Doublers (includes grip and drag plates)	A. Bonding separation B. Corrosion C. Cracks	4.0 2.0 <u>8.0</u> 14.0

TABLE XXXXV. (Continued)

I. Inherent Damage - (Continued)

Blade Component	Failure Mode	Frequency of Occurrence per 10 ⁶ Blade Hours
6. Trailing Edge Strip (Aluminum)	A. Bonding Separation B. Cracks	2.0 <u>7.0</u> 9.0
7. Trim Tab	A. Loose Rivets B. Unbonded	1.0 <u>3.0</u> 4.0
8. Counterweights	A. Loose B. Corroded	1.0 <u>1.0</u> 2.0
9. General		59.0
Total Inherent Damage		230.0
II. Total External Damage		710.0
III. Total Blade Damage		940.0

TABLE XXXVI. RELIABILITY ANALYSIS - CONFIGURATION V COMPARED TO BASELINE
UH - 1 BLADE WITH 1063 HOUR MTBR

Component	Mode	Inherent Causes		
				Occurrences Per 10 ⁶ Blade Hours
1. Leading Edge Structure	1. Erosion and pitting of protective coating			378.0
2. Spar-Twin Beam (Unidirectional "E" Glass)	1. Bonding separation 2. Crack 3. Delamination; crazing of "E" glass			41.0 2.0 3.0
3. Honeycomb Core (Nomex)	1. Water contamination 2. Bonding separation			9.0 23.0
4. Skin (Carbon)	1. Abrasion 2. Delamination 3. Crazing 4. Blisters 5. Bonding separation			15.0 31.0 34.0 21.0 43.0
5. Attaching Point Bushings	1. Cracks 2. Wear 3. Corrosion			9.0 8.0 3.0
6. Doublers; Grip and Drag Plate	1. Bonding separation 2. Cracks 3. Corrosion			3.0 13.0 6.0

TABLE XXXVI. (Continued)

Inherent Causes			
Component	Mode	Occurrences Per 10^6 Blade Hours	
7. T. E. Spline	1. Cracks 2. Bonding separation 3. Delamination	2.0 2.0 4.0	
8. Trim Tab	1. Loose rivets 2. Bonding separation	1.0 3.0	
9. Counterweights	1. Loose 2. Corroded	1.0 2.0	
10. General	Excess vibration, out of adjustment, unbalance	59.0	
	Total Inherent	716.0	
Externally Caused			
1. Leading Edge Structure	1. Battle damage 2. Chipped 3. Dented 4. Foreign object damage 5. Grooved 6. Nicked 7. Punctured	11.0 2.0 16.0 9.0 0.5 3.0 13.0	

TABLE XXXVI. (Continued)

		Externally Caused	
Component	Mode	Occurrences Per 10 ⁶ Blade Hours	
2. Spar-Twin Beam (Unidirectional "E" Glass)	1. Battle damage 2. Chipped 3. Dented 4. Foreign object damage 5. Grooved 6. Nicked 7. Punctured	27.0 2.0 43.0 25.0 0.5 3.0 31.0	
3. Skin - Trailing Edge of Spar to Leading Edge of Spline	1. Battle damage 2. Bent 3. Broken 4. Buckled 5. Collapsed 6. Cut 7. Dented 8. Foreign object damage 9. Punctured 10. Torn	59.0 9.0 9.0 4.0 1.0 25.0 94.0 63.0 69.0 52.0	
4. Trailing Edge Spline	1. Battle damage 2. Dented 3. Foreign object damage 4. Punctured	6.0 11.0 6.0 9.0	

TABLE XXXVI. (Continued)

Externally Caused			
Component	Mode	Occurrences Per 10^6 Blade Hours	
5. General	1. Overstressed, warped, sudden stop, overspeed, other	107.0	
	Total External	710.0	
	Total Blade	1426.0	
Mean Time Between Removals			
Total Inherent	= 716	Maintenance Actions Per 10^6 Blade Hours	
MTBRI	= 1397	Hours	
Total External	= 710	Maintenance Actions Per 10^6 Blade Hours	
MTBRE	= 1408	Hours	
Total Blade	= 1426	Maintenance Actions Per 10^6 Blade Hours	
MTBRT	= 701	Hours	

TABLE XXXVII. REPAIRABILITY ANALYSIS - CONFIGURATION V COMPARED TO BASELINE
UH-1 BLADE WITH 1063 HOUR MTBR

		Blade Removals - Inherent Causes			Maintenance Actions Per 10^6 Blade Hours		
Blade Component	Reason For Removal	Scrap Repair	D S Level	Depot Level	Scrap Repair	Scrap Repair	
1. Leading Edge Structure	1. Erosion and pitting of protective coating				378.0		
2. Spar-Twin Beam	1. Bonding separation 2. Crack 3. Delamination, crazing	17.0 1.0 1.0		24.0 1.0 2.0			
3. Honeycomb Core	1. Water contamination 2. Bonding separation		4.0	5.0	23.0		
4. Skin	1. Abrasion 2. Delamination 3. Crazing 4. Blisters 5. Bonding separation			15.0 31.0 34.0 21.0 43.0			
5. Attach Point Bushings	1. Cracks 2. Wear 3. Corrosion				9.0 8.0 3.0		
6. Doublers	1. Bonding separation 2. Cracks 3. Corrosion					1.0 12.0 6.0	

TABLE XXXVII. (Continued)

Blade Removals - Inherent Causes - (Continued)

Blade Component	Reason For Removal	Maintenance Actions Per 10^6 Blade Hours			
		ORG Level	D S Level	Depot Level	Scrap Repair Scrap Repair
7. T. E. Spline	1. Cracks	1.0		1.0	
	2. Bonding separation	1.0		1.0	
	3. Delamination	1.0		3.0	
8. Trim Tab	1. Loose rivets		1.0		
	2. Bonding separation		3.0		
9. Counterweights	1. Loose			1.0	
	2. Corroded			2.0	
10. General	Excess vibration, out of adjustment, out of balance	18.0	7.0		23.0 11.0
				40.0 14.0 4.0 602.0	25.0 31.0

TABLE XXXVII. (Continued)

Blade Removals - External Causes

Blade Component	Reason for Removal	Maintenance Actions Per 10^6 Blade Hours			
		ORG Level	D S Level	Depot Level	Scrap Repair
1. Leading Edge Structure	1. Battle damage	2.0		4.0	5.0
	2. Chipped			2.0	
	3. Dented	3.0		13.0	
	4. Foreign object damage	1.0		8.0	
	5. Grooved	0.5			
	6. Nicked			3.0	
	7. Punctured	2.0		11.0	
2. Spar-Twin Beam	1. Battle damage	5.0		5.0	17.0
	2. Chipped			2.0	
	3. Dented			43.0	
	4. Foreign object damage	5.0		6.0	14.0
	5. Grooved	0.5			
	6. Nicked			3.0	
	7. Punctured			31.0	
3. Skin-Trailing Edge of Spar to Leading Edge of Spline	1. Battle damage			12.0	47.0
	2. Bent				9.0
	3. Broken				9.0
	4. Buckled				4.0
	5. Collapsed				1.0
	6. Cut				
	7. Dented				
	8. Foreign object damage			27.0	36.0

TABLE XXXVII. (Continued)

Blade Removals - External Causes - (Continued)

Blade Component	Reason for Removal	Maintenance Actions Per 10^6 Blade Hours			
		ORG Level	D S Level	Depot Level	Scrap Repair Scrap Repair Scrap Repair
3. Continued	9. Punctured 10. Torn		12.0 22.0	57.0 30.0	
4. T. E. Spline	1. Battle damage 2. Dented 3. Foreign object damage 4. Punctured		1.0 1.0	5.0 10.0 6.0 9.0	
5. General	Overstressed	107.0			
		128.0	117.0	465.0	
Total Blade = 78% Repairable		168.0	14.0	121.0	1067.0
				25.0	31.0

TABLE XXXVIII. MATH MODEL R/M INPUT VARIABLES -
CONFIGURATION V COMPARED TO BASELINE
UH-1 BLADE WITH 1063 HOUR MTBR

Variable	Value
1. Aircraft Down Hours	4.3839 Down hours per flight hour
2. Aircraft Aborting Failure Rate	.015 Aborting failures per flight hour
3. Blade Mean Time Between Inherent Damage	1,397 Blade hours
4. Blade Retirement Life	5,000 Blade hours
5. % Damage Repaired On Aircraft, ORG Level	1.0 Percent
6. % Damage Repaired Off Aircraft, ORG Level	0 Percent
7. % Removed Blades Scrapped at ORG Level	12.0 Percent
8. % Removed Blades Sent to Direct Support	88.0 Percent
9. % Received Blades Repaired at Direct Support	87.0 Percent
10. % Received Blades Scrapped at Direct Support	10.0 Percent
11. % Received Blades Repaired at Depot	55.0 Percent
12. Maintenance Man-Hours to Inspect On Aircraft (ORG)	.25 Maintenance man-hours
13. Maintenance Man-Hours to Repair On Aircraft (ORG)	1.0 Maintenance man-hours
14. Maintenance Man-Hours to Repair Off Aircraft (ORG)	0.0
15. Maintenance Man-Hours per Blade Repair (Direct Support)	7.5 Maintenance man-hours
16. GSE Cost Per Repair (Direct Support)	\$84.10 per repair
17. GSE Cost Per Aircraft (Direct Support)	\$637.66 per aircraft
18. Parts/Material Cost (Direct Support)	\$66.00
19. Blade Overhaul Cost (Depot)	\$822.00 per blade

COST-EFFECTIVENESS EVALUATION

The revised MTBR criterion - from 914 to 1063 hours for the baseline UH-1 blade - does not significantly alter the study conclusions. The increase in MTBR reduces the number of damaged blades by about 14%, so the benefits of blade repairability are reduced slightly. True blade expendability, where the cost of repairing damaged blades at depot is greater than the cost of replacing them with new blades, is still not achieved.

With the higher MTBR the Configuration V blade design saves \$24. 90 million in fleet effective cost compared to the 1980 baseline blade. This is only 5% less than the \$26. 22 million saved with the original MTBR. The cost of replacing a damaged blade with a new one is still higher than the cost of repairing it at depot (these costs are unaffected by MTBR), so true expendability is still not achieved. The Configuration V blade can be considered more expendable than before, however, since the fewer number of damaged blades means that elimination of all depot repair incurs a net fleet cost penalty of only \$33, 000 compared to \$66, 000 with the original MTBR.

Figure 86 compares the sensitivity of aircraft cost effectiveness to blade acquisition cost for the two MTBR criteria. The impact on both the 1980 baseline blade and the Configuration V blade is shown. Overall cost effectiveness is slightly improved by the increased MTBR, but the relative position of the two blade configurations remains about the same. Figure 87 shows the cost effectiveness blade acquisition cost trends for the new MTBR criterion with and without depot repair. These trends can be compared to those in Figure 53 for the original MTBR criterion.

The impact of the increase in MTBR on the benefits provided by the Configuration V blade design is summarized as follows:

<u>Improvement relative to 1980 baseline blade</u>		
	MTBR = 914	MTBR = 1063
Blade life-cycle cost	- \$27, 669	- \$26, 342
Aircraft life-cycle cost (including fuel)	- \$27, 680	- \$26, 352
Fleet effective cost	- \$26, 220, 000	- \$24, 900, 000

Tables XLIX and L present the detailed cost effectiveness information for the 1980 baseline and Configuration V blades, respectively, under the new MTBR criterion. These compare to Tables XXI and XXIX for the same blades under the original MTBR criterion.

1980 - With Depot Repair

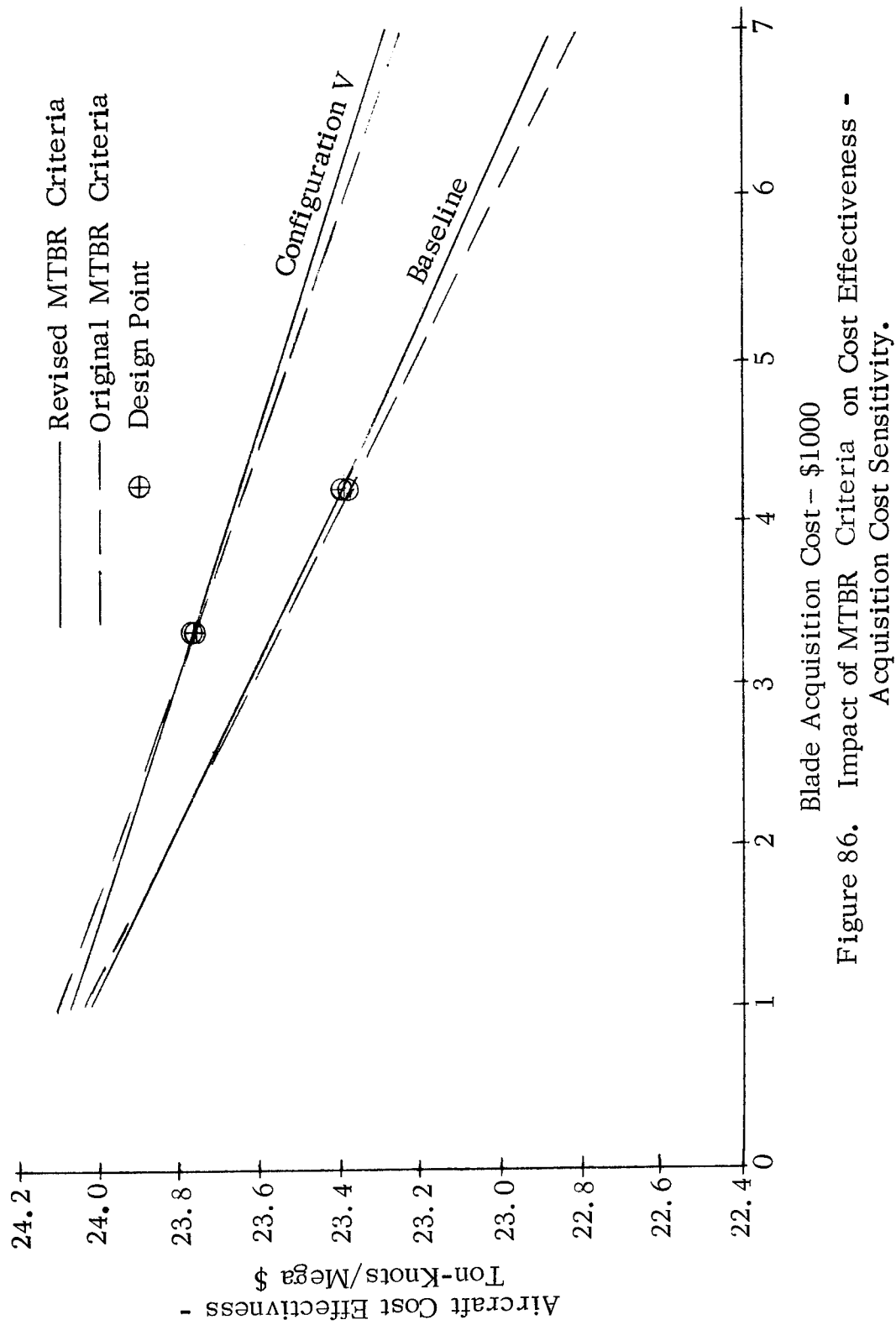


Figure 86. Impact of MTBR Criteria on Cost Effectiveness - Acquisition Cost Sensitivity.

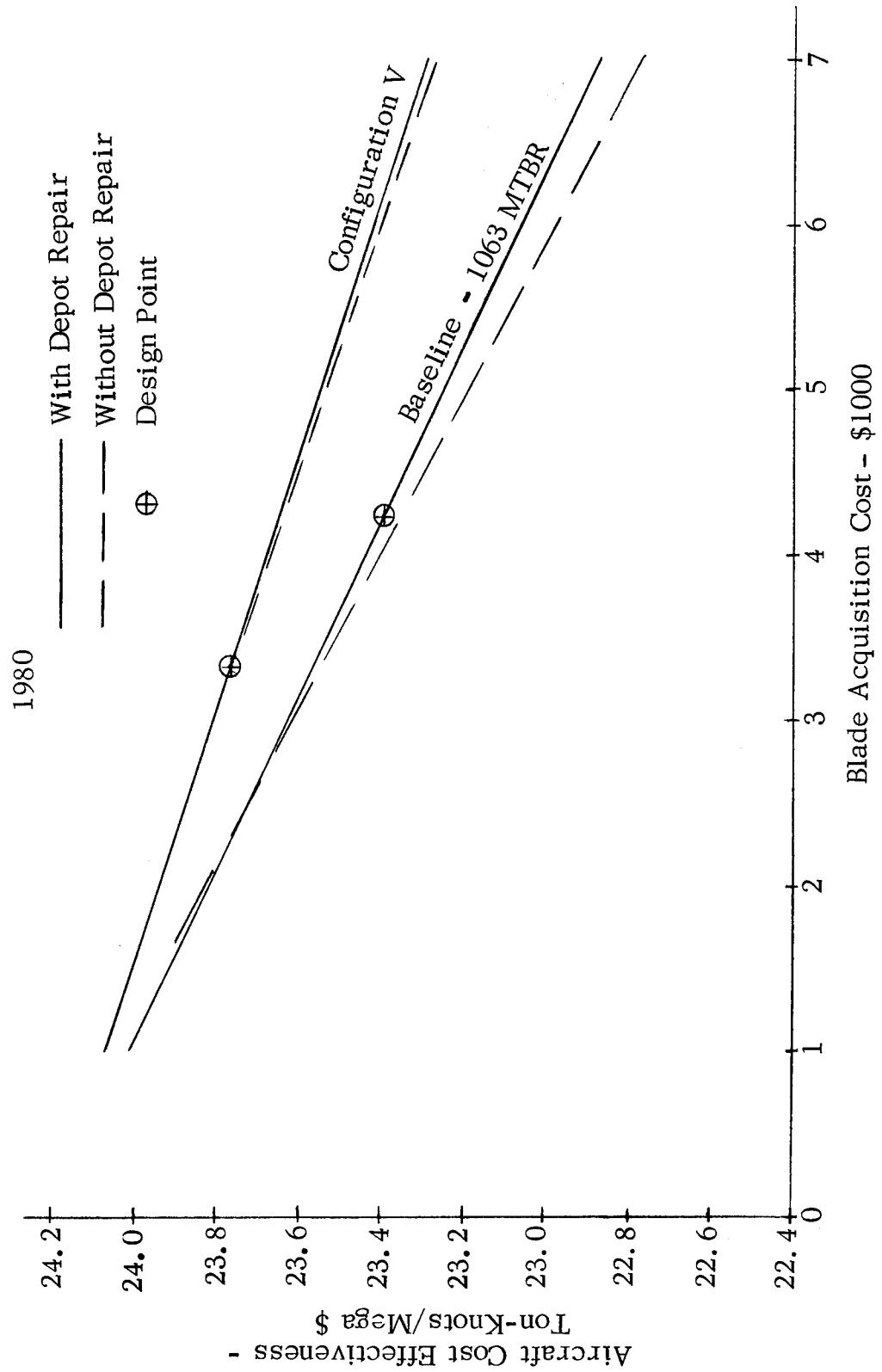


Figure 87. Impact of Blade Acquisition Cost • Baseline • 1063 MTBR.

TABLE XLIX. COST EFFECTIVE SUMMARY - 1063 MTBR
BASELINE CONFIGURATION - 1980

Aircraft Mission Effectiveness	37.466 ton-knots
Aircraft Life-Cycle Cost	\$1,601,476
Aircraft Cost Effectiveness	23.395 ton-knots/mega \$
Fleet Effective Cost Fleet size adjusted to maintain fleet effectiveness of 1000 base- line UH-1 aircraft	1,601.48 mega \$
Life-Cycle Fuel and Oil Cost	\$53,344
<u>Blade Contribution To:</u>	
Flyaway cost	\$ 8,417
Initial spares cost	\$ 2,771
Replenishment spares cost	\$ 46,023
Organizational level maintenance cost	\$ 840
Direct support level maintenance cost	\$ 523
Depot level maintenance cost	\$ 3,379
Replenishment GSE cost	\$ 0
Blade Life-Cycle Cost	\$ 61,953
<u>Life-Cycle Blades:</u>	
Damaged	9.40 Blades
Repaired at the organizational level	0 "
Repaired at the direct support level	1.13 "
Repaired at the depot level	1.75 "
Retired on schedule	0.97 "
Replenished by new spares	10.50 "
<u>Expendability</u>	
Scraping blades normally sent to depot for overhaul yields the following:	
Aircraft cost effectiveness	23.349 ton-knots/megadollars
Fleet effective cost	1604.64 megadollars

**TABLE L. COST EFFECTIVE SUMMARY - 1063 MTBR
CONFIGURATION V - 1980**

Aircraft Mission Effectiveness	37.431 ton-knots
Aircraft Life-Cycle Cost	\$1,575,124
Aircraft Cost Effectiveness	23.764 ton-knots/mega \$
Fleet Effective Cost	1,576.58 mega \$
Fleet size adjusted to maintain fleet effectiveness of 1,000 baseline UH-1 aircraft	
Life-Cycle Fuel and Oil Cost	\$53,336
Blade Contribution To:	
Flyaway cost	\$ 6,668
Initial spares cost	\$ 1,371
Replenishment spares cost	\$ 22,482
Organizational level maintenance cost	\$ 1,195
Direct support level maintenance cost	\$ 1,555
Depot level maintenance cost	\$ 329
Replenishment GSE cost	\$ 2,011
Blade Life-Cycle Cost	\$ 35,611
Life-Cycle Blades:	
Damaged	14.26 Blades
Repaired at the organizational level	0.14 "
Repaired at the direct support level	10.81 "
Repaired at the depot level	0.20 "
Retired on schedule	0.30 "
Replenished by new spares	6.41 "
Expendability	
Scraping blades normally sent to depot for overhaul yields the following:	
Aircraft cost effectiveness	23.759 ton-knots/megadollars
Fleet effective cost	1576.91 megadollars

APPENDIX VI

PLAN FOR FUTURE HARDWARE EVALUATION

INTRODUCTION

In compliance with the requirements of Contract DAAJ02-71-C-0046, this appendix presents the plan for a hardware evaluation of an expendable UH-1H blade. In view of Sikorsky Aircraft's experience and test facilities as related to articulated rotors, it is more practical to evaluate expendable blade concepts on the Sikorsky S-61 helicopter. This is considered reasonable because the expendable concept should be applied to any helicopter application. A proposal to evaluate an expendable S-61 main rotor blade can be submitted upon request.

The selected design was Configuration V, which was found to be the most cost-effective blade for 1980. This design consists of an all composite twin-beam structure fabricated in two half sections. A development program, prior to the Plan for Future Hardware, would be required to develop the advanced process for fabrication.

This appendix includes the development program for the pultrusion process, blade design and fabrication, ground tests, whirl tests, flight tests and operational suitability for field service of Configuration V. Costs and schedule are also included for the Plan for Future Hardware.

DEVELOPMENT PROGRAM

Before the Plan for Future Hardware Evaluation is started, a development period is required for the pultrusion process.

The first phase would be to fabricate simple flat sheets to determine if the .020 inch to .030 inch bias cloth on the trailing edge truss of Configuration V can be processed successfully with present dies. Problems may arise with die fouling or freezing which may require die modifications or resin system changes. Two investigations will be made of fabrication, one for material @ $\pm 45^\circ$ orientation and another with conventional 90° cross weave. Each type would be fabricated for test evaluation. Sufficient material would be run through the experimental die to give an indication of possible future production problems, such as progressive die fouling, unpredictable jamming or other complications, so that these can be properly taken into account before proceeding.

The second phase would be to proceed with tooling for a partial section of the truss fairing. This step would be used to check out the ability to flow the skins together properly in the final webbed shape selected, to

determine what warp or distortion problems occur, and to provide sample sections for test evaluation.

The third phase would be to produce the final production fairing section. This would involve the design and procurement of a full-scale die configuration suitable for production. A number of trailing edge fairings would be produced for test evaluation using this die. There would be some flexibility in the tooling to allow for changes in wall thicknesses, material composition, and distribution of webs.

The fourth phase would be an expansion of Phases I through III, i. e., the fabrication of the twin-beam spar. The spar beam is a solid section and will not be as complex as the web section. However, combining this component with the truss will require additional dies and mandrels and some development. Several sections would be fabricated and then subjected to quality control for inspection of dimensional tolerances, straightness, bowing, contouring, etc. Several specimens would also be evaluated by structural testing. Work would continue during this phase until the parts can meet the minimum specifications of strength and dimensional requirements. This development time for fabrication of sections and subsequent structural test evaluation should be approximately 1-1/2 years.

PLAN FOR FUTURE HARDWARE

The plan is for fabricating a total of 8 full blade assemblies of Configuration V. Four of these assemblies will be used for fatigue structural tests. Each one of the four will serve as two test specimens, one inboard and one outboard, resulting in a total of four inboard and four outboard test specimens. A total of four full blade assemblies will be utilized for whirl and flight tests.

In addition, an equal number of UH-1 blades will be subjected to the same structural, whirl and flight tests to obtain a valid comparison with the new blade.

Figure 88 shows the phases of the program which would cover a period of two years. The cost breakdown through flight test is shown below.

Cost Breakdown

Engineering - - - -	\$800,000
Manufacturing - - - -	\$884,000
Materials and - - - -	\$116,000
Direct Cost	
	<u>\$1,800,000</u>

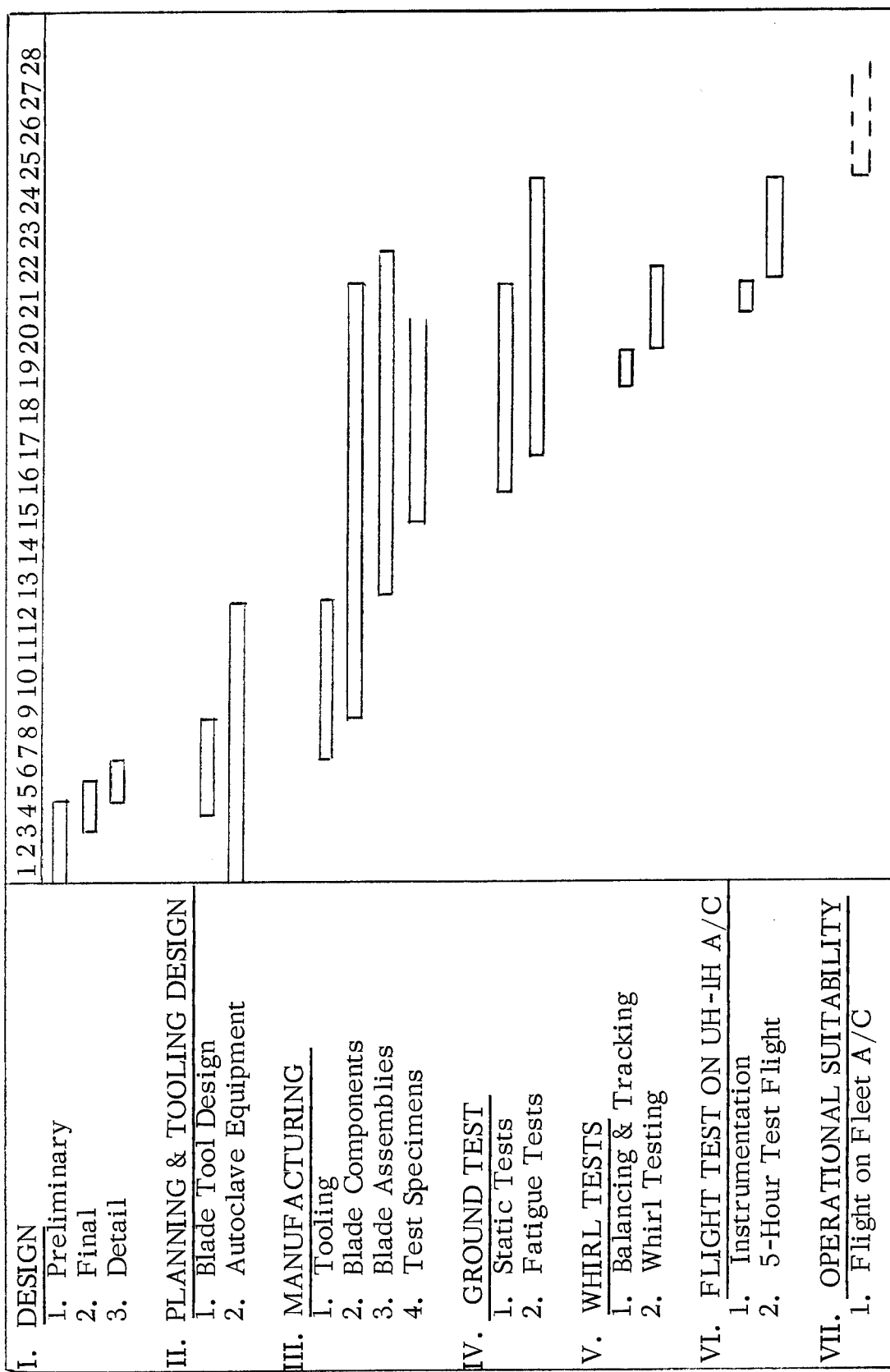


Figure 88. Plan for Future Hardware Evaluation.

DESIGN AND FABRICATION

Detail and assembly drawings will be prepared and released to Purchasing and Manufacturing for procurement of materials and fabrication of in-house portions of the blade. In addition, manufacturing and design engineers will support the subcontractor responsible for the fabrication of the blade half section by the pultrusion process. Design and material specifications will be developed to provide high quality components.

The upper and lower tool molds will be machined from aluminum castings. Machining will be accomplished on a tape controlled milling machine and the finished tool surface will be machined to within .005 inch of the required aerodynamic contour. The root end of the mold would be contoured to accommodate the enlarged attachment area of the blade. Dies for the root doublers and forging drag plates would be procured for fabrication and for later assembly onto the blade.

The half blade pultrusion assembly (which includes the fiberglass spar, trailing edge truss with combinations of carbon and fiberglass, the leading and trailing edge carbon doubler and spline) would be inspected by quality control upon completion of each part. A short section would be cut from each end for examination by Materials and Processing personnel and for additional test evaluation. The mass distribution of each half would also be prechecked prior to applying counterweights to minimize any balancing problems which may occur after assembly.

The finished root end doublers and drag plate would be placed in their respective mold, and each half blade section would be placed in position over the doublers. The leading edge counterweight consisting of elastomer containing lead shot would be cast in place using a retaining tool. The honeycomb core and the foam-in-place would next be assembled in the blade. A routing tool which fits on the mold will then be used to cut the assembly to the chordline. The mass distribution of the two machined blade halves will then be determined and corrections made to the leading edge counterweights.

The two blade halves will then be joined by structural adhesive. A polyurethane erosion coating will then be applied to the leading edge, and tip weights will then be added to adjust the blade spanwise balance. The final blade assembly will be inspected using ultrasonic coin tap, visual, and dynamic balance techniques.

Throughout the blade fabrication process, Engineering and Manufacturing Engineering will revise and update the manufacturing operations plan. At the completion of the fabrication effort, a complete set of

operation sheets, with all modifications, will be compiled and evaluated to establish a firm manufacturing base.

STRUCTURAL TEST PLAN

Full-scale blade specimens of Configuration V and specimens of the present UH-1 baseline production blade will be laboratory tested to provide comparison of the expendable and production blades and to verify structural integrity for flight testing of the expendable blade. This is accomplished by overstress fatigue testing of these full-scale blade specimens to

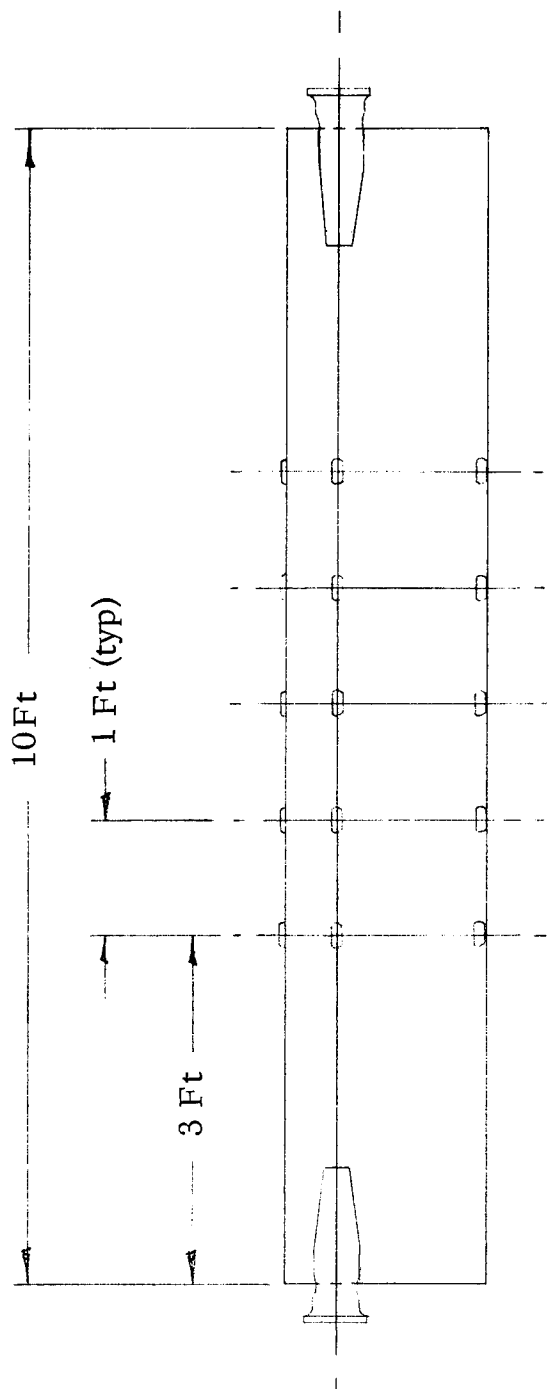
1. Establish mean strength
2. Verify rotor blade design analysis
3. Determine rotor blade failure modes
4. Determine rotor blade fail-safe characteristics

Overstress fatigue testing is conducted on eight representative specimens of both the Sikorsky Aircraft designed expendable main rotor blade and the production UH-1 main rotor blade: four outboard specimens of both configurations, representing the most highly stressed outboard blade section, and four inboard specimens of both configurations, representing the hub-to-blade attachment area or root end.

The specimens are fabricated from four full-scale blades of both configurations by separating the test portions from the full-scale blades and modifying the specimen ends to accept load fittings compatible with the fatigue testing equipment. See Figures 89 and 90.

Both configurations are tested to avoid interpretation of any differences in mean strength which may occur, as a result of differences in test techniques, differences in handling of mean strength data, of systematic error, i. e., a difference in the mean strength between blades tested now and blades tested in the original substantiation several years ago.

Overstress relates the blade specimen test stress level to the aircraft blade operating stress level. The blade specimen test level is higher than the analytically predicted blade mean strength stress level and is much higher than the blade operating stress level. Testing at an overstress level determines the mean strength of the blade in a reasonable time frame by initiating a crack or accumulating the number of cycles



Bending Strain Gages at Each Location Along the Spar

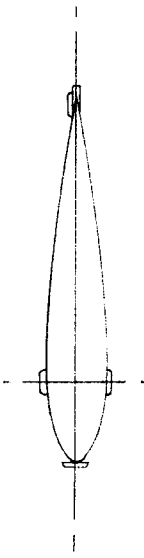
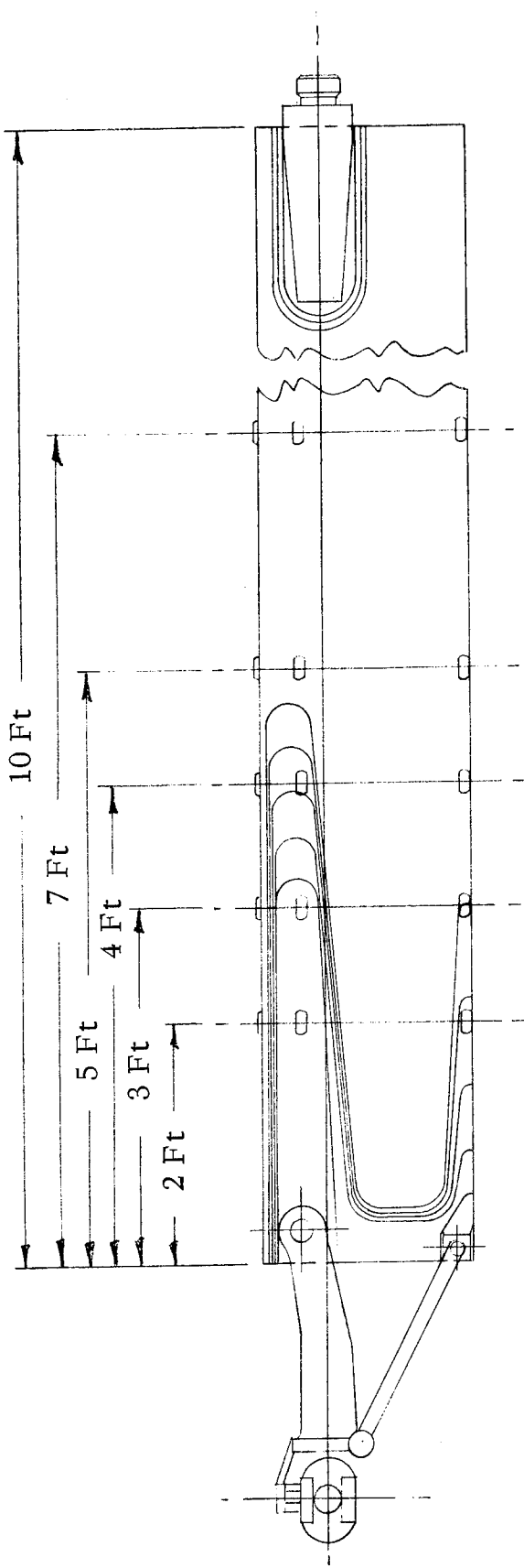


Figure 89. Outboard Specimen.



Bending Strain Gages At Each Location Along the Spar & Root End

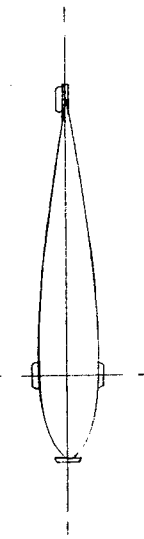


Figure 90. Inboard Specimen.

that is predetermined to be a runout. If a runout occurs, subsequent test specimens will be tested at a higher stress level to initiate a crack. If the specimen does not separate, crack propagation testing is conducted by applying stresses representative of normal aircraft blade operating conditions and measuring crack length. Crack propagation testing of the specimen shall be discontinued after 25 hours.

The outboard specimen is tested as a resonant pin-pin beam. An axial load is mechanically applied to simulate centrifugal force. By orienting the specimen at a particular angle with relation to the plane of the pins that support the specimen, blade edgewise and flatwise stresses are obtained. The specimen is mechanically forced to vibrate at a frequency close to its natural frequency, resulting in vibratory stress caused by deflection of the specimen. The closer the forcing frequency is to the natural frequency of the specimen, the greater the beam deflection and resulting stress. Required stress levels are obtained by increasing the forcing frequency.

The root end specimen is tested as a cantilevered beam. An axial load, mechanically applied, simulates centrifugal force. By orienting the specimen at a particular angle with relation to the direction of the applied load, blade edgewise and flatwise stresses are obtained.

Both the outboard and the root end specimens are instrumented in selected areas to measure strains. Edgewise and flatwise strains will be measured.

Each specimen is tested at a constant stress level, and strength data is presented in the form of a stress-cycle (S-N) plot. See Figure 91.

An S-N curve shape for the applicable material is drawn through the test data points. Aircraft blade operating stresses are related to this curve to determine the structural reliability of the blade. See Figure 92.

Crack propagation data will be presented in the form of a real time plot of stress vs. aircraft flight time. See Figure 93.

A static rap test establishes the edgewise and flatwise natural frequency of the blade. A strain-gaged blade is hung vertically and struck with a mallet in each of the three (edgewise, flatwise, and torsional) directions. The output of the respective strain gages determines the three respective natural frequencies. See Figure 94.

ROTOR SYSTEM WHIRL TESTS

Comparison rotor whirl tests of the expendable and standard UH-1 blades

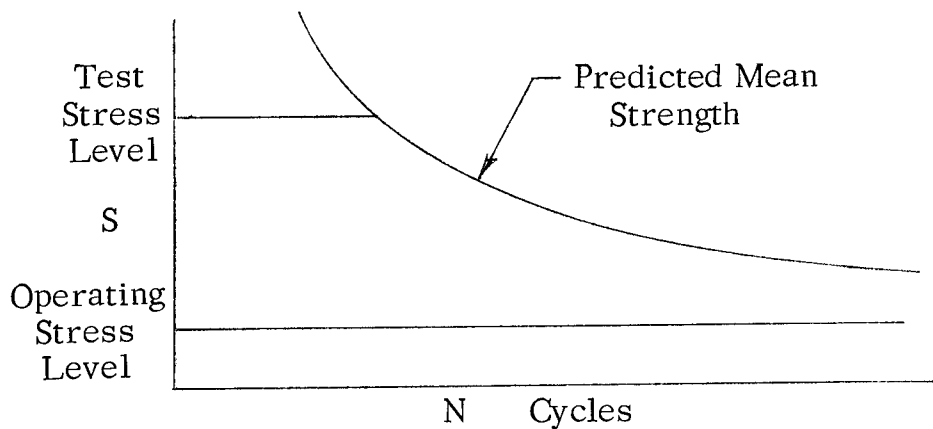


Figure 91. Stress Level of Operation.

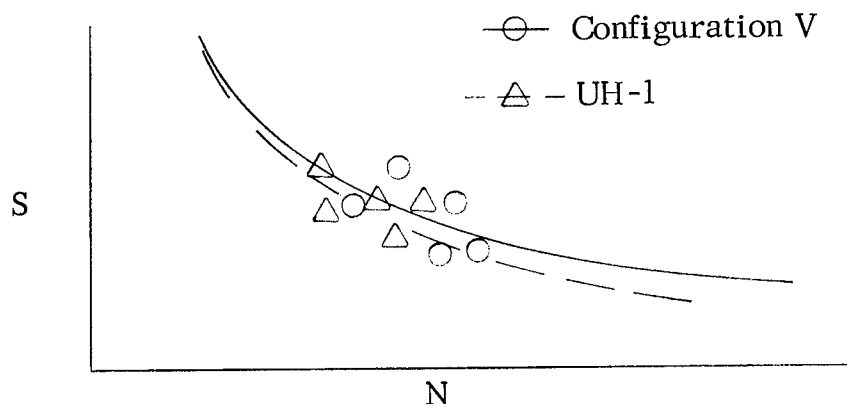


Figure 92. S-N Strength Data.

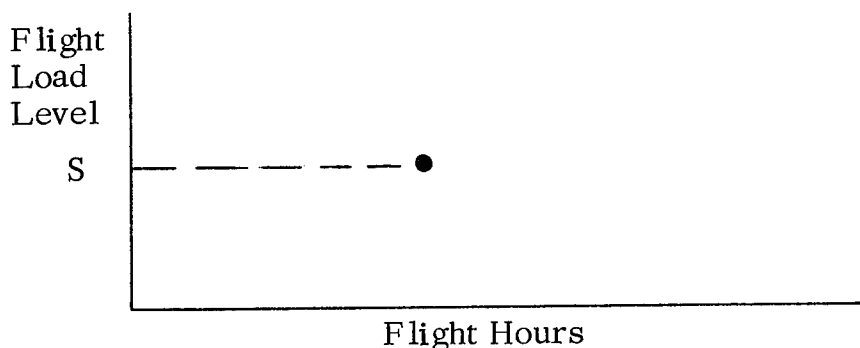


Figure 93. Crack Propagation.

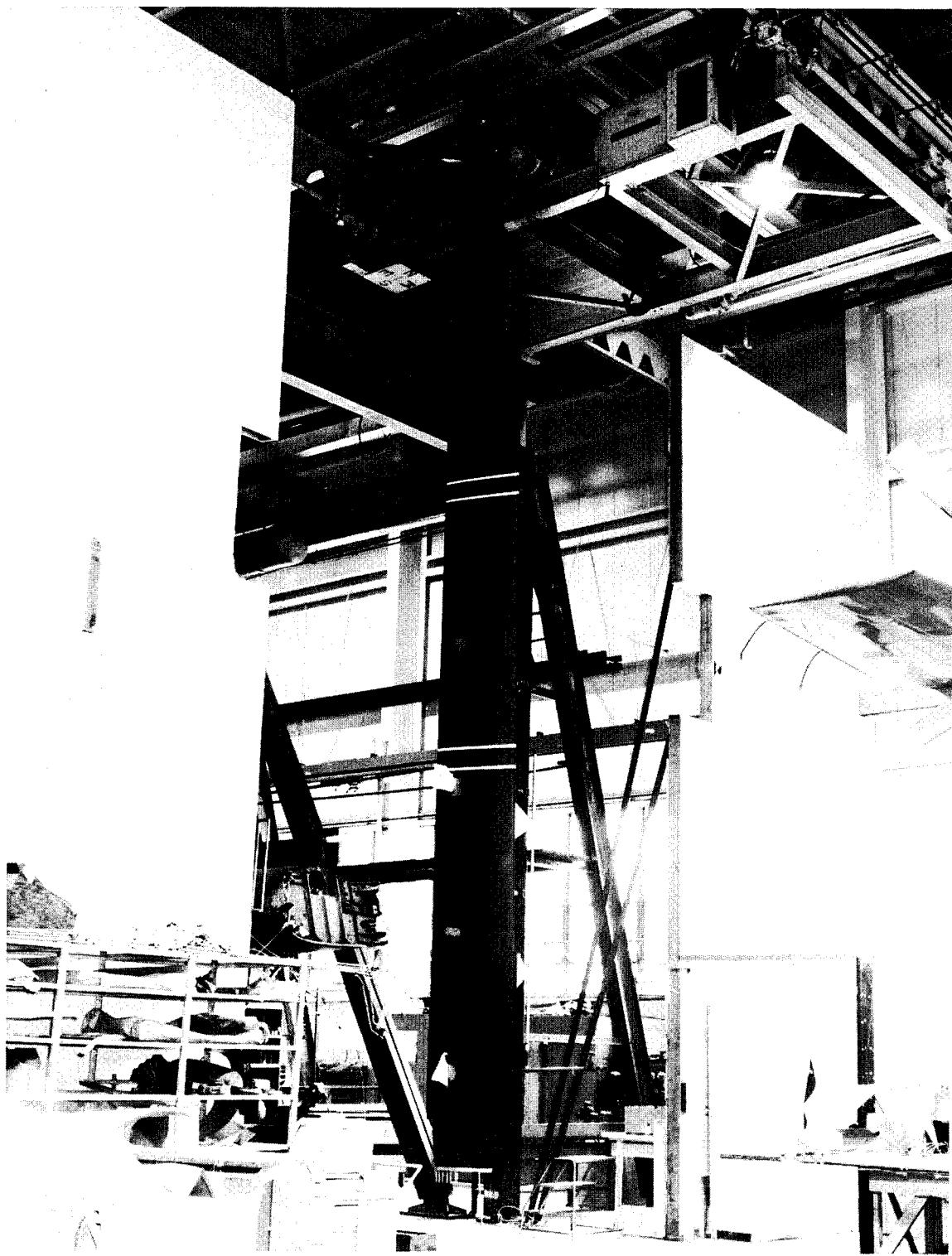


Figure 94. Static Rap Test For Blade Frequency.

verify equal hover performance, aerodynamic and aeroelastic predictions of stability, and provide adequate endurance validation for flight testing. The rotor whirl tests consist of the following:

1. Aerodynamic and dynamic balance adjustments to provide identical tracking characteristics in flight.
2. Comparative hover performance tests of the expendable blades and standard UH-1 blades to demonstrate equal performance.
3. Stress and motion surveys to validate design predictions of stress levels and frequency response.
4. Thirty hours of endurance at conditions simulating anticipated flight loads.
5. Dynamic checkout of blade instrumentation prior to flight testing.
6. A 1-minute rotor overspeed test at 110% of limit power off rotor speed.

Aerodynamic and dynamic balancing is accomplished on the Sikorsky 2000 HP Main Rotor Test Stand by adjusting the blade pitching moment and track characteristics alike on the expendable blades. Aerodynamic balancing consists of adjusting the trailing edge trim tabs to match the blade pitching moments at low angles of attack. Dynamic balancing entails matching the blade pitching moments and track at high collective pitch angles by chordwise adjustments to tip weights. The blade pitch-moments are obtained by measuring the steady loads in the rotor head rotating control rods. Track measurements are obtained using a Chicago Aerial Electronic Blade Tracker.

Comparative hover performance tests on the expendable and standard UH-1 blades are performed on the 30-foot-high Sikorsky 2,000 HP Main Rotor Test Stand to demonstrate equal lift capability. Rotor thrust, power, blade angle and pitching moment data are obtained at tip Mach numbers corresponding to 90%, 100% and 110% of normal rotor speed for both blade types from zero thrust to the maximum attainable thrust as limited by the structural or geometric limits. To keep wind effects to a minimum, data are obtained when the wind velocity does not exceed 5 knots. Following correction of the data to sea level standard conditions (59°F , 29.92 inches Hg, and zero wind), the results are presented as comparison plots for each tip Mach number. Figures 95 and 96 show the Test Stand and Thrust/Performance comparisons.

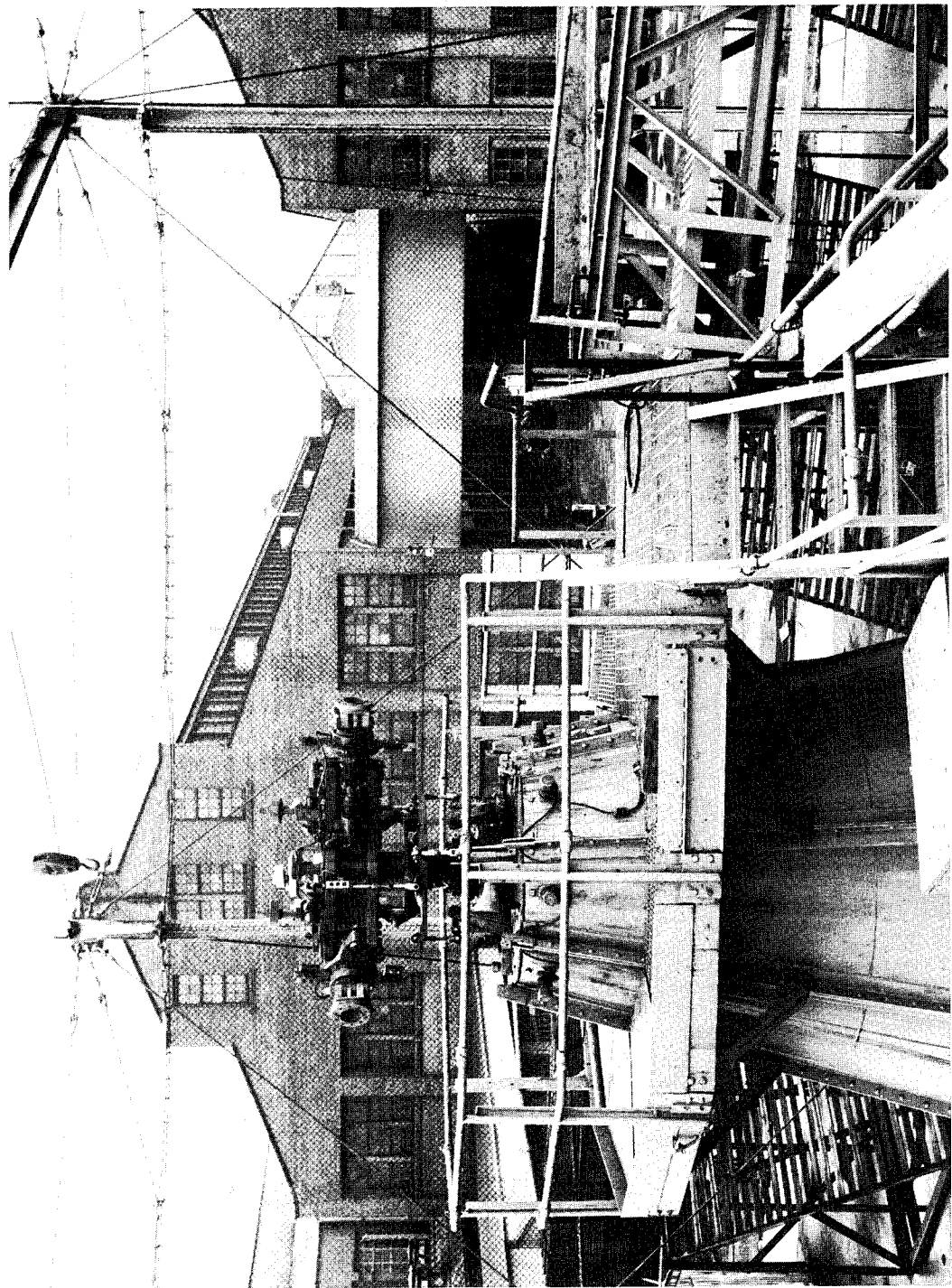


Figure 95. 2000 HP Main Rotor Test Stand.

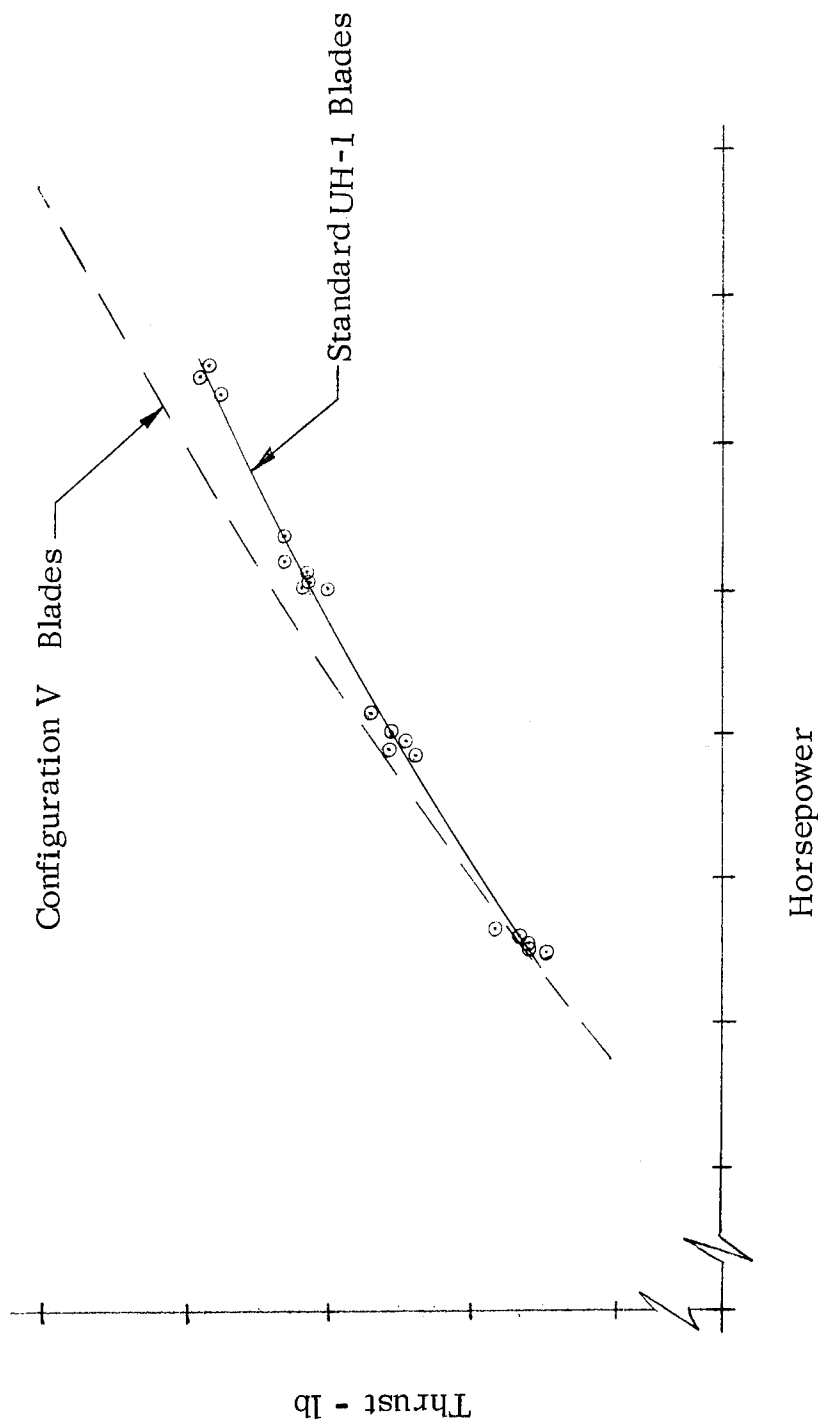


Figure 96. Rotor Hover Performance Comparison,
Configuration V vs Standard Blades.

Stress measurements obtained throughout the rotor operating range as functions of rotor speed, rotor thrust, and blade flapping validate design stress levels and natural frequency response throughout the entire operating range to verify design criteria. The data are acquired on magnetic tape to facilitate data reduction and analysis.

Thirty hours of endurance testing at 8000 pounds of thrust and blade flapping loads simulating anticipated flight loads provides adequate assurance of structural integrity prior to flight tests.

The final whirl test consists of a 1-minute overspeed run at 110% of the limit power off to demonstrate safe operation at maximum autorotative rotor speed. Following the whirl tests and prior to flight tests, the blades are inspected to verify that no defects resulted from the whirl tests.

5-HOUR FLIGHT EVALUATION

A 5-hour flight test will be conducted for hardware evaluation of the expendable UH-1 main rotor blade. Flight tests of the Sikorsky-designed expendable main rotor blades will determine the structural airworthiness of the blades and investigate the effect of the new component on general aircraft handling and vibration characteristics. Blade stress and motion data will be obtained throughout the established aircraft operating envelope with vibration and handling qualities data obtained simultaneously with the structural measurements. Principal measurements will also be obtained on selected main rotor components to provide safety of flight and to evaluate the influence of the new component on stresses and loads in other areas of the rotor system. The flight tests will be conducted at the Sikorsky test facility, Stratford, Connecticut, at altitudes ranging from ground level to approximately 3,000 feet density altitude. A bailed UH-1 and pilot will be required for the flight test program.

The test rotor blade will be extensively instrumented using strain gages (approximately 30) to determine the stress distribution and blade response characteristics. Chordwise and normal bending stresses will be measured at several blade stations including the root end attachment area and approximately five additional spanwise locations. Stress levels will also be recorded on the structural trailing edge of the blade and torsional stresses measured at the 30% and 75% blade radius stations. A typical Sikorsky main rotor blade strain gaged to recorded edgewise, flatwise and torsional stresses is illustrated in Figure 97. Additional main rotor instrumentation will include blade motions, control loads, drag brace load, shaft bending, and edgewise and flatwise stresses on the hub/sleeve assembly. Aircraft attitude, control positions, vibration levels and load factor will also be recorded along with pertinent cockpit data (airspeed, rotor speed, altitude, etc.) which are necessary to document the flight conditions.

The structural characteristics of the expendable blade will be primarily evaluated at the maximum aircraft allowable gross weight at both the forward and aft center-of-gravity extremes. An initial hovering flight will be conducted at light gross weight followed by subsequent flight testing at the maximum gross weight condition. The heavy weight testing will require a gradual buildup in forward speed until maximum forward speed is achieved. During this phase, selected parameters will be monitored by telemetry to provide safety of flight. A cursory check of blade stress will also be conducted at the aircraft basic design gross weight to verify that the maximum blade stress levels occur at the alternate gross weight configuration. No extreme altitude or envelope type tests are planned for this evaluation.

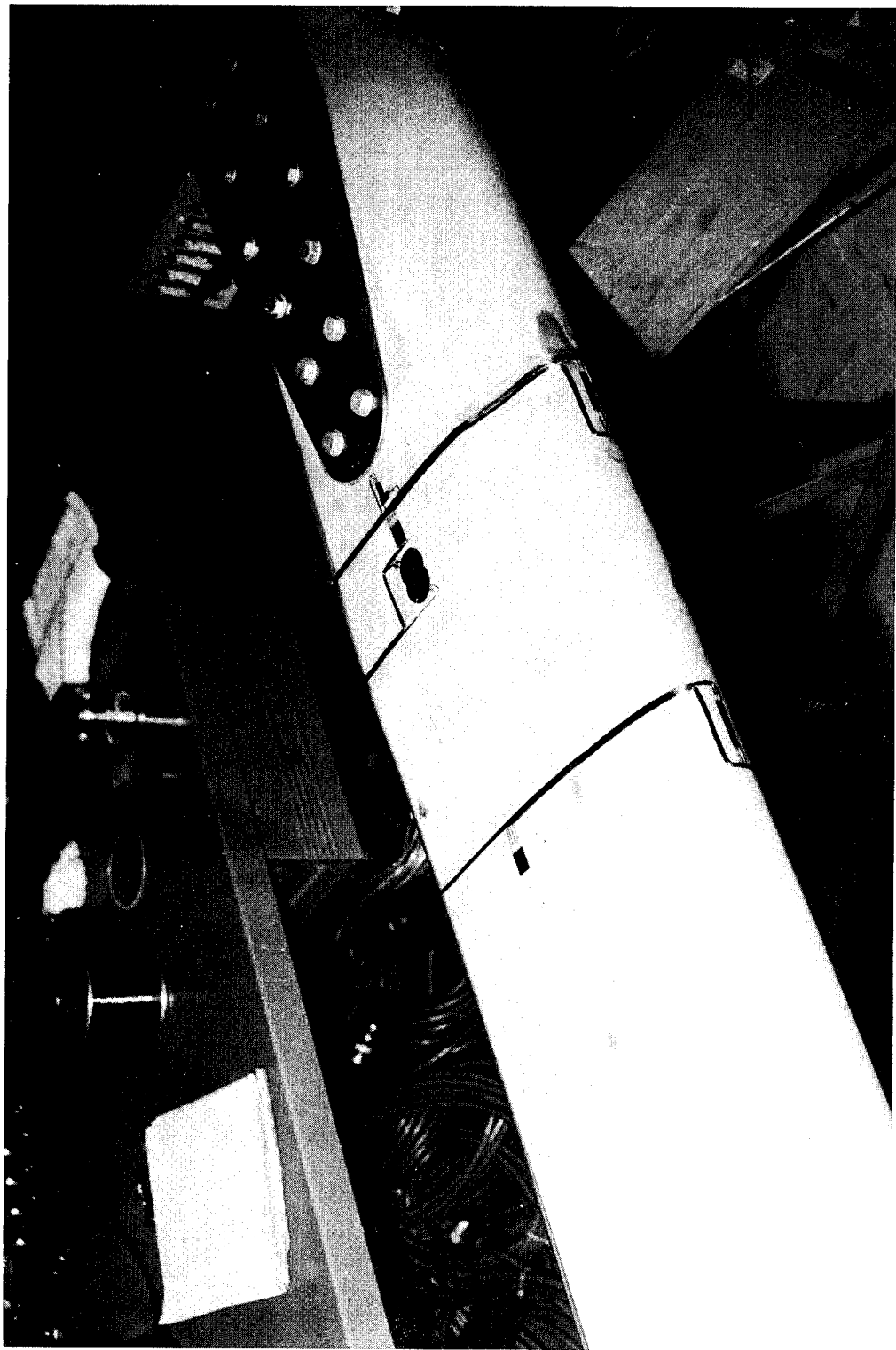


Figure 97. Typical Strain Gaged Blade.

Test data will be acquired at maximum gross weight for the following flight conditions:

1. Rotor engagement.
2. Hovering flight including sideward flight, rearward flight, control reversals, hover turns and rotor speed sweeps.
3. Level flight to V_{max} at various rotor speeds.
4. Normal maneuvering and control reversals within the approved operating flight envelope.
5. Partial power descents at three airspeeds and two rates of descent.
6. Autorotations at three airspeeds at normal, maximum and minimum approved power-off rotor speeds.
7. Takeoff, climbs, climbing turns, and final approach and landing.

The cursory check of blade stresses at the aircraft design gross weight will be limited to but will not necessarily include all of items 1, 2, 3, and 7 above.

DESIGN REPORTS

Three technical reports will be prepared for this study: Blade Loads Report, Stress Report and Test Report. The Blade Loads Report will summarize all the aerodynamic loads subjected to the blade throughout the aircraft flight spectrum. The Stress Report will present a detail stress analysis of all blade components for the most critical aircraft maneuvers. It will also present a blade life calculation for the flight spectrum established in the Blade Loads Report. The Test Report would include all the results of structural ground testing and the stability and handling qualities from flight testing.

OPERATIONAL SUITABILITY EVALUATION

A 2-year field service evaluation of the expendable main rotor blade is required to demonstrate component reliability and maintainability. Following substantiation of the expendable blade, environmental testing under actual field service conditions is proposed. Field service experience will be obtained by installing 6 sets of blades on operational UH-1H helicopters operating under normal field conditions. Inspection of the blades would be conducted daily and the findings reported in field service reports. The reports should specify the operating environment, effects of erosion by sand, dust, rain, and describe any damage incurred, along with the procedures for repairing the damaged blade. The damage and repair data should include but not be limited to:

1. Time to damage
2. Type of damage
3. Description of repair procedure
4. Man-hours required for inspection, repair, and checkout of component
5. Problems encountered with repaired components

The inspection procedure should be continued for 2 years from time of delivery, with the environment of the blade being varied as much as possible.

After the first year, an evaluation will be made of the expendable blade to determine feasibility of incorporation into production. Vigilance will still be maintained on the blades installed for the 2-year period.

CONTINGENCIES

1. A total of eight UH-1H blade assemblies should be supplied for structural and whirl test evaluation.
2. UH-1H rotor head components and assemblies should be supplied as required for ground tests.
3. A bailed UH-1 helicopter and qualified test pilot are required for the program.
4. If a qualified pilot is not provided with the aircraft, Sikorsky test pilots will be used. However, additional costs will be required to qualify two Sikorsky pilots at an off-site facility.
5. Sikorsky personnel can support the test aircraft; however, appropriate manuals and handbooks have to be provided, preferably before the test program commences.

RECOMMENDATIONS

It is recommended, as a first phase, that a development program for the pultrusion process of manufacturing a one-piece cover be started immediately. In addition to supplying the ground work for the 1980 twin beam concept, the process is also applicable to Configuration VI, the aluminum spar with the automated cover. It is further recommended that the expendable blade concept be evaluated on a Sikorsky S-61 helicopter. This program would evaluate the cost, reliability, repairability and the aeromechanics of the twin-beam expendable blade concept.

DISTRIBUTION

Director of Defense Research & Engineering	1
Assistant Chief of Staff for Force Development, DA	1
Deputy Chief of Staff for Logistics, DA	1
United States Army, Pacific	1
Chief of Research & Development, DA	3
Army Aviation Systems Command	2
Hq, Army Air Mobility Research & Development Laboratory	2
Systems Research Integration Office, AMRDL	1
Ames Directorate, Army Air Mobility Research & Development Laboratory	2
Eustis Directorate, Army Air Mobility Research & Development Laboratory	45
Langley Directorate, Army Air Mobility Research & Development Laboratory	2
Lewis Directorate, Army Air Mobility Research & Development Laboratory	2
Army Aviation Systems Test Activity	2
Army R&D Group (Europe)	2
Army Scientific & Technical Information Team (Europe)	1
Army Advanced Materiel Concepts Agency	1
Army Coating & Chemical Laboratory	1
Army Land Warfare Laboratory	1
Army Human Engineering Laboratories	2
Army Natick Laboratories	1
Army Ballistic Research Laboratories	1
Army Research Office	1
Army Materials & Mechanics Research Center	6
Army Plastics Technical Evaluation Center	1
Army Materiel Systems Analysis Agency	1
USACDC Aviation Agency	2
USACDC Transportation Agency	1
Edgewood Arsenal	1
Army Command & General Staff College	1
Army Aviation Test Board	2
Army Arctic Test Center	1
Army Agency for Aviation Safety	1
Army Field Office, AFSC	1
Air Force Flight Test Center	1
San Antonio Air Materiel Area	1
Air Force Materials Laboratory	4
Air Force Flight Dynamics Laboratory	5
Aeronautical Systems Division, AFSC	2
Naval Air Systems Command	13
Chief of Naval Research	3
Naval Research Laboratory	1
Naval Safety Center	1
Naval Air Rework Facility	1
Naval Air Test Center	1
Naval Air Development Center	3
Naval Weapons Laboratory	1
Naval Ship Research & Development Center	3
Marine Corps Liaison Officer, Army Transportation School	1
U.S. Coast Guard	1
Transportation Systems Center	1
NASA Headquarters	1
Ames Research Center, NASA	3
Langley Research Center, NASA	2

Lewis Research Center, NASA	1
Manned Spacecraft Center, NASA	1
Scientific & Technical Information Facility, NASA	2
Department of Transportation Library	1
Eastern Region Library, FAA	1
Federal Aviation Administration, Washington	3
Civil Aeromedical Institute, FAA	1
Bureau of Aviation Safety, National Transportation Safety Board	1
Government Printing Office	1
Defense Documentation Center	12

Unclassified

Security Classification

DOCUMENT CONTROL DATA - R & D*(Security classification of title, body of abstract and indexing annotation must be entered when the overall report is classified)*

1. ORIGINATING ACTIVITY (Corporate author) Sikorsky Aircraft Division of United Aircraft Stratford, Connecticut		2a. REPORT SECURITY CLASSIFICATION Unclassified
3. REPORT TITLE EXPENDABLE MAIN ROTOR BLADE STUDY		
4. DESCRIPTIVE NOTES (Type of report and inclusive dates) Final Report		
5. AUTHOR(S) (First name, middle initial, last name) John A. Longobardi Everett Fournier		
6. REPORT DATE April 1973	7a. TOTAL NO. OF PAGES 298	7b. NO. OF REFS 18
8a. CONTRACT OR GRANT NO. DAAJ02-71-C-0046	9a. ORIGINATOR'S REPORT NUMBER(S) USAAMRDL Technical Report 72-47	
b. PROJECT NO. 1F1622205A11901	9b. OTHER REPORT NO(S) (Any other numbers that may be assigned this report) Sikorsky Engineering Report 50748	
10. DISTRIBUTION STATEMENT Approved for public release; distribution unlimited.		
11. SUPPLEMENTARY NOTES	12. SPONSORING MILITARY ACTIVITY Eustis Directorate, U.S. Army Air Mobility Research and Development Laboratory, Fort Eustis, Virginia	
13. ABSTRACT This report presents Sikorsky's study of expendable blade designs applicable to the Army's UH-1H helicopter with its teetering rotor system. The program included design, reliability, maintainability and cost analysis studies. Reliability and maintainability parameters were developed which were subsequently inserted into cost model equations to determine life cycle cost comparisons of the new blade designs with the present UH-1H blade. More than fifteen configurations were investigated and reduced to six viable blade designs. They included aluminum, steel, and composite configurations. The study covered two time frames: 1972 and 1980. The results showed that a low-cost aluminum extrusion (Configuration I) with a fiberglass composite skin was the most cost effective for 1972. The 1980 time frame showed that an all-composite blade (Configuration V) was the most cost effective. The report also includes field repair procedures for the leading candidate blades developed. A simulated field repair was performed demonstrating the feasibility of composite/honeycomb repair. Also included is a future plan for hardware evaluation outlining the major phases in a development program for the most cost effective blade for the 1980 time frame.		

Unclassified

Security Classification

14. KEY WORDS	LINK A		LINK B		LINK C	
	ROLE	WT	ROLE	WT	ROLE	WT
UH-1H Helicopter Expendable Blades Repairable Blades Cost Effective Blades Field Repairable Blades Semirigid Teetering Rotor System High Modulus Composite Blades Automation of Blade Production						